Geohydrology, Geochemistry, and Ground-Water Simulation-Optimization of the Central and West Coast Basins, Los Angeles County, California

By Eric G. Reichard, Michael Land, Steven M. Crawford, Tyler Johnson, Rhett R. Everett, Trayle V. Kulshan, Daniel J. Ponti, Keith J. Halford, Theodore A. Johnson[1], Katherine S. Paybins, *and* Tracy Nishikawa

5025-32

[1] Water Replenishment District of Southern California

U.S. DEPARTMENT OF THE INTERIOR
GALE A. NORTON, *Secretary*

U.S. GEOLOGICAL SURVEY
Charles G. Groat, *Director*

CONTENTS

FIGURES

TABLES

CONVERSION FACTORS, VERTICAL DATUM, AND ABBREVIATIONS

CONVERSION FACTORS

Multiply	By	To obtain
acre	0.004047	square kilometer
foot (ft)	0.3048	meters
acre foot (acre-ft)	1,233.	cubic meter
cubic foot (ft^3)	0.02832	cubic meter
gallon (gal)	3.785	liter
inch (in.)	0.3048	meters
mile (mi)	1.609	kilometers
square mile (mi^2)	2.590	square kilometer

Temperature in degrees Celsius (^{o}C) may be converted to degrees Fahrenheit (^{o}F) as follows:

$$^oF = 1.8\ ^oC + 32.$$

VERTICAL DATUM

Sea level: In this report, "sea level" refers to the National Geodetic Vertical Datum of 1929 (NGVD of 1929)—a geodetic datum *derived* from a general adjustment of the first-order level nets of both the United States and Canada, formerly called Sea Level Datum of 1929.

Altitude, as used in this report, refers to distance above or below sea level.

ABBREVIATIONS

^{o}C	degrees Celcius
δ	delta
GIS	Geographic Information System
mg/L	milligrams per liter
NIU	Newport Inglewood Uplift
pCi/L	picocuries per liter
per mil	parts per thousand, as used with delta (δ) notation
pmc	percent modern carbon
PVC	polyvinyl chloride
RMSE	root mean square error
SMCL	Secondary Maximum Contaminant Level
SS	sum-of-square error
TDS	total dissolved solids
TU	tritium unit

μg/L   micrograms per liter

μS/cm   microsiemens per centimeter at 25°C

UTM   Universal Transverse Mercator

VSMOW   Vienna Standard Mean Ocean Water

yr   year

Organizations

LACDPW   Los Angeles County Department of Public Works

USGS   U.S. Geological Survey

WRDSC   Water Replenishment District of Southern California

WELL-NUMBERING SYSTEM

      Wells are identified and numbered according to their location in the rectangular system for the subdivision of public lands. Identification consists of the township number, north or south; the range number, east or west; and the section number. Each section is divided into sixteen 40-acre tracts lettered consecutively (except I and O), beginning with "A" in the northeast corner of the section and progressing in a sinusoidal manner to "R" in the southeast corner. Within the 40-acre tract, wells are sequentially numbered in the order they are inventoried. The final letter refers to the base line and meridian. In California, there are three base lines and meridians; Humboldt (H), Mount Diablo (M), and San Bernardino (S). All wells in the study area are referenced to the San Bernardino base line and meridian (S) Well numbers consist of 15 characters and follow the format 004S012W005H05S. In this report, well numbers are abbreviated and written 4S/12W-5H5. Wells in the same township and range are referred to only by their section designation, 5H5. The following diagram shows how the number for well 4S/12W-5H5 is derived.
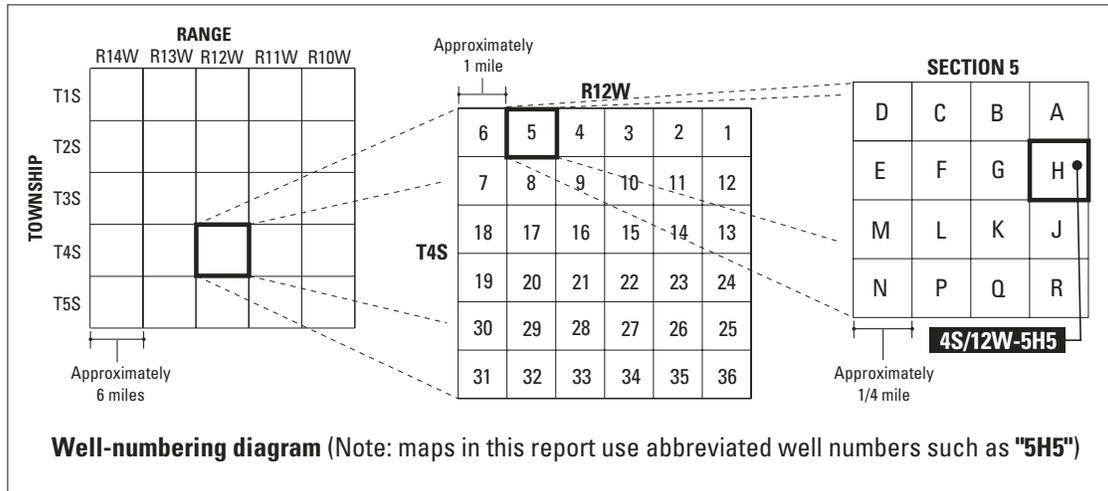
Well-numbering diagram (Note: maps in this report use abbreviated well numbers such as **"5H5"**)

Geohydrology, Geochemistry, and Ground-Water Simulation-Optimization of the Central and West Coast Basins, Los Angeles County, California

By Eric G. Reichard, Michael Land, Steven M. Crawford, Tyler Johnson, Rhett R. Everett, Trayle V. Kulshan, Daniel J. Ponti, Keith J. Halford, Theodore A. Johnson, Katherine S. Paybins, *and* Tracy Nishikawa

ABSTRACT

Historical ground-water development of the Central and West Coast Basins in Los Angeles County, California through the first half of the 20th century caused large water-level declines and induced seawater intrusion. Because of this, the basins were adjudicated and numerous ground-water management activities were implemented, including increased water spreading, construction of injection barriers, increased delivery of imported water, and increased use of reclaimed water. In order to improve the scientific basis for these water management activities, an extensive data collection program was undertaken, geohydrological and geochemical analyses were conducted, and ground-water flow simulation and optimization models were developed.

In this project, extensive hydraulic, geologic, and chemical data were collected from new multiple-well monitoring sites. On the basis of these data and data compiled and collected from existing wells, the regional geohydrologic framework was characterized. For the purposes of modeling, the three-dimensional aquifer system was divided into four aquifer systems—the Recent, Lakewood, Upper San Pedro, and Lower San Pedro aquifer systems. Most pumpage in the two basins is from the Upper San Pedro aquifer system.

Assessment of the three-dimensional geochemical data provides insight into the sources of recharge and the movement and age of ground water in the study area. Major-ion data indicate the chemical character of water containing less than 500 mg/L dissolved solids generally grades from calcium-bicarbonate/sulfate to sodium bicarbonate. Sodium-chloride water, high in dissolved solids, is present in wells near the coast. Stable isotopes of oxygen and hydrogen provide information on sources of recharge to the basin, including imported water and water originating in the San Fernando Valley, San Gabriel Valley, and the coastal plain and surrounding hills. Tritium and carbon-14 data provide information on relative ground-water ages. Water with abundant tritium (greater than 8 tritium units) is found in and downgradient from the Montebello Forebay and near the seawater barrier projects, indicating recent recharge. Water with less than measurable tritium is present in, and downgradient from, the Los Angeles Forebay and in most wells in the West Coast Basin. Water from several deep wells was analyzed for carbon-14. Uncorrected estimates of age for these samples range from 600 to more than 20,000 years before present. Chemical and isotopic data are combined to evaluate changes in chemical character along flow paths emanating from the Montebello and Los Angeles Forebays.

A four-layer ground-water flow model was developed to simulate steady-state ground-water conditions representative of those in 1971 and transient conditions for the period 1971–2000. Model results indicate increases in ground-water storage in all parts of the study area over the simulated thirty-year period. The model was used to develop a three-dimensional ground-water budget and to assess impacts of two alternative future (2001–25) ground-water development scenarios—one that assumes continued pumping at average current rates and a second that assumes increasing pumping from most wells in the Central Basin. The model simulates stable or slightly increasing water levels for the first scenario and declining water levels (25 to 50 ft in the Central Basin) in the second scenario. Model sensitivity to parameter values and to the assumed Orange County boundary condition was evaluated. Particle tracking was applied to simulate advective transport of water from the spreading ponds, the coastline, and the seawater injection barriers. Particle tracking results indicate that most flow within the Upper San Pedro aquifer system occurs within about 20 percent of the total aquifer system thickness and that virtually all water injected into the seawater barrier projects has flowed inland.

The simulation model was linked with optimization to identify the least-cost strategies for improving hydraulic control of seawater intrusion in the West Coast Basin by means of increased injection and (or) in-lieu delivery of surface water. For the base-case optimization analysis, assuming constant ground-water demand, in-lieu delivery was determined to be most cost effective. Several sensitivity analyses were conducted with the optimization model. Raising the imposed average water-level constraint at the hydraulic-control locations resulted in non-linear increases in cost. Systematic varying of the relative costs of injection and in-lieu water yielded a trade-off curve between relative costs and injection/in-lieu amounts. Changing the assumed future scenario to one of increasing Central Basin pumpage caused a small (7-percent) increase in the computed costs of seawater intrusion control.

INTRODUCTION

Background

Water use and water needs have been very closely tied to the development of greater Los Angeles, from its agricultural origins through its subsequent urbanization. As stated by Mendenhall (1905b) "...the story of the growth of this region becomes a story of the utilization and application of its available waters." Since the first water wells were drilled about 150 years ago, ground water has been a significant component of water supply in the region. In the Central and West Coast Basins (fig. 1), which are the focus of this report, ground-water development through the first half of the 20th century resulted in large water-level declines and associated problems such as seawater intrusion. This led to the adjudication of the basins in the early 1960s and the initiation of ground-water management activities including injection, spreading, pumping restrictions, and delivery of surface water to replace some pumping. Ground water currently supplies about one third of the water supply for the 4 million people who live in the Central and West Coast Basins.

Sound management of the ground-water resources of the Central and West Coast Basins requires understanding of the geohydrology and geochemistry of the region. The first regional assessment of ground-water conditions in the Los Angeles coastal area was completed by Mendenhall (1905a,b,c). A series of reports by Poland and co-workers (Piper and Garrett, 1953; Poland and others, 1956; Poland and others, 1959) provided a detailed description of the geology, geohydrology, and ground-water chemistry of the area. A series of reports by the California Department of Water Resources (1961, 1962, 1966) presented an analysis of the regional geohydrology, including explicit delineation of aquifers. The Central and West Coast Basins are within the Los Angeles Geologic Basin. Overviews of the geology and tectonic history of the Los Angeles Basin were provided by Yerkes and others (1965) and Wright (1991).
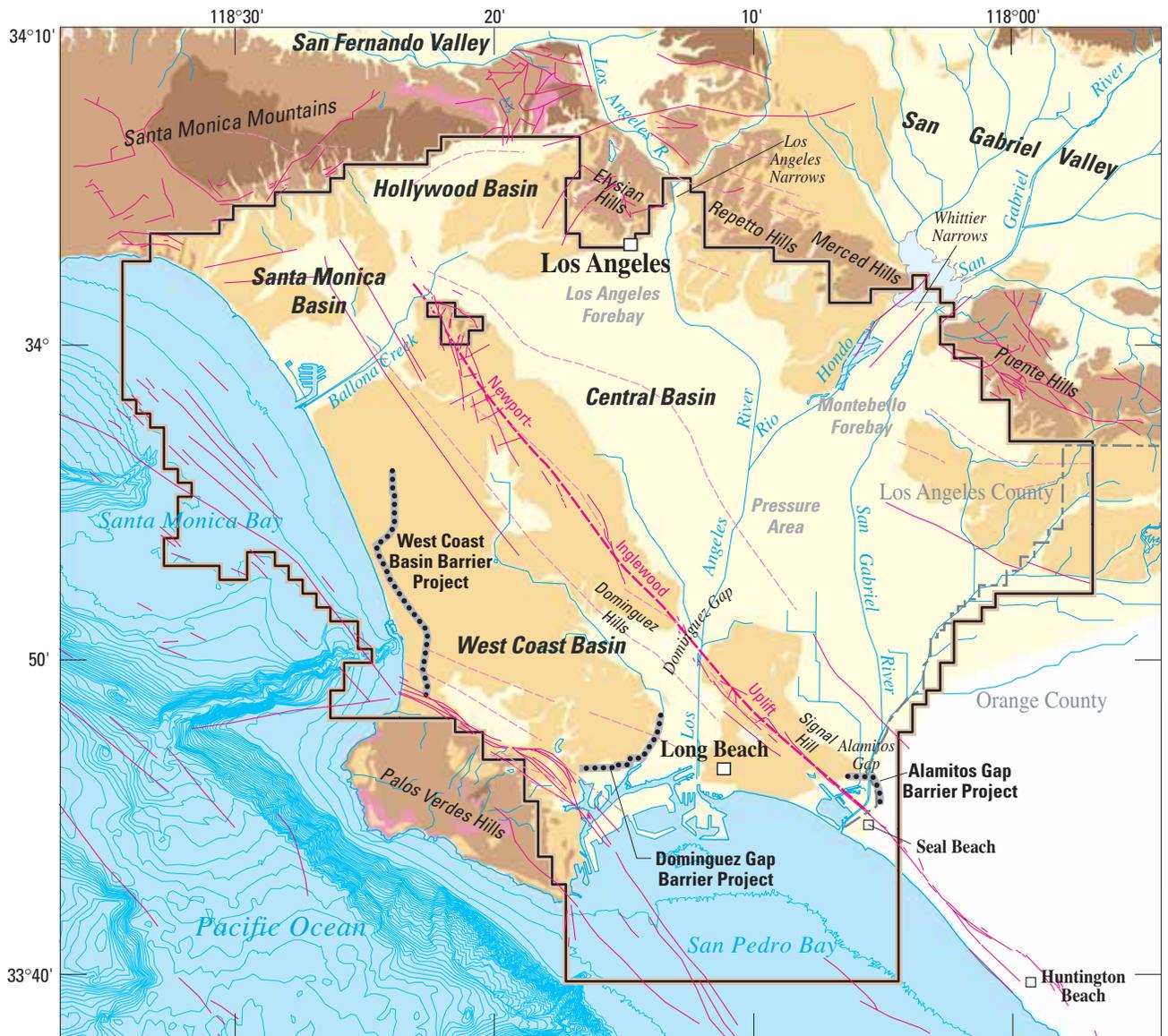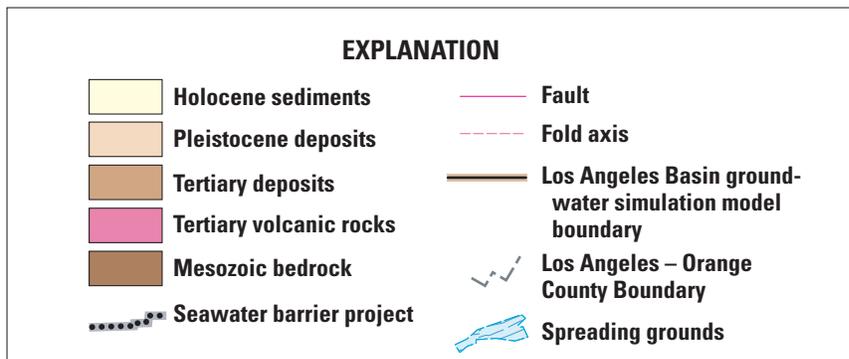
Figure 1. Surface geology of the study area, Los Angeles County, California.

Although numerous studies have been conducted on specific ground-water issues in the Central and West Coast Basins, there has been no regional assessment of the regional geohydrology and geochemistry since the work of the California Department of Water Resources in the 1960s and no development of a three-dimensional computer simulation model of the multi-aquifer ground-water system.

Purpose and Scope

The objectives of the work described in this report were to characterize the three-dimensional regional ground-water flow system and geochemistry in the Central and West Coast Basins and to develop and apply appropriate models for evaluating ground-water management issues in the Central and West Coast Basins in Los Angeles County, California. This work was conducted by the U.S. Geological Survey (USGS) during 1995–2002 in cooperation with the Water Replenishment District of Southern California (WRDSC). The report describes data compilation and new data collection, provides an overview of the geologic/hydrogeologic frameworks and the ground-water flow system, details the regional geochemistry, documents the development of a regional ground-water simulation model, and describes the use of the model and its linkage with optimization methods to evaluate alternative water-management strategies.

Description of Study Area

The study area, shown in figure 1, lies within the coastal part of the greater Los Angeles metropolitan area. The study area is bounded by the Santa Monica Mountains to the north; the Elysian, Repetto, Merced, and Puente Hills to the northeast; Orange County to the southeast; and the Pacific Ocean (Santa Monica Bay and San Pedro Bay) and the Palos Verdes Hills to the west and southwest. The study area incorporates the four coastal ground-water basins in Los Angeles County: the Central Basin, the West Coast Basin, the

Hollywood Basin, and the Santa Monica Basin (California Department of Water Resources, 1961). The total onshore area covered by these four basins is about 480 mi^2. All four basins are considered generally in this report; however, the focus is on the Central and West Coast Basins.

The study area is drained by three main rivers; the Los Angeles River, the San Gabriel River, and the Rio Hondo (fig. 1). The Los Angeles River, which drains the San Fernando Valley to the north, enters the study area through the Los Angeles Narrows. The San Gabriel River and Rio Hondo, which drain the San Gabriel Valley to the northeast, enter the study area through the Whittier Narrows. The areas downstream from the Los Angeles Narrows and the Whittier Narrows are known as the Los Angeles Forebay and the Montebello Forebay, respectively. As described later, these forebay areas were delineated by the California Department of Water Resources (1961) as areas where surface water could freely percolate into the ground-water system. The non-forebay part of the Central Basin, where such percolation is more restricted, is referred to as the Pressure Area.

Acknowledgments

DATA COMPILATION AND NEW DATA COLLECTION

A major component of this study was developing a Geographic Information System (GIS) for the study area. The GIS, which is a spatially relational database, serves as a tool for combining data and geographic features from a variety of sources. It also provides a mechanism for analyzing combinations of data, visualizing the data, and interfacing the data with other applications, including a ground-water model. The GIS can store features and attributes of the ground-water system, analyze data between spatial layers, and display data in the form of maps and graphics. Details of the GIS are in Appendix I.

Development of the GIS enabled the compilation and coordinated analysis of the existing data for the study area. However, despite the abundance of existing data, it was necessary to collect new data to significantly improve the understanding of the regional ground-water flow system. Most existing data (collected prior to this investigation) for the study area are collected from production wells with large screened intervals. The two major data-collection tasks in this study have been the drilling and logging of multiple-well monitoring sites and conducting water-quality sampling and analysis.

This report incorporates data collected at 24 new multiple-well monitoring sites (fig. 2A). The spatial distribution of the sites encompasses the Montebello Forebay, the Whittier area, the Los Angeles Forebay, the Pressure Area of the Central Basin, and the West Coast Basin. Each multiple-well site consists of four to six polyvinyl chloride (PVC) monitoring wells installed at different depths in the same drill hole. Perforated intervals of the different wells are isolated from one another by low-permeability bentonite grout. Considerable data have been collected from each monitoring site. The cuttings were logged as the well was drilled. Two to four cores were collected during the drilling of each site and were analyzed for hydraulic properties. Geophysical and temperature logs were conducted at each well. Water levels were measured regularly and water-quality samples were collected and analyzed.

The data collected from these monitoring sites provide information on the vertical variability of hydraulic properties, water levels, and water quality at each site. This depth-dependent information is needed to improve the characterization of the three-dimensional ground-water system. A compilation of data collected from the monitoring sites is provided by Land and others (2002). A summary of construction information for these sites is in Appendix II

GEOLOGIC FRAMEWORK

The current understanding of the structural and tectonic history of the Los Angeles Basin has been described by Wright (1991); he summarizes and builds on a considerable body of previous work, including the seminal work of Yerkes and others (1965). The Los Angeles Basin is at the northern end of the Peninsular Ranges geomorphic province. Structurally, the Peninsular Ranges province is characterized by fault zones that trend northwest to west-northwest. The Los Angeles Basin is of considerable geologic interest as an area of major oil-production and active seismicity.

The study area of this report lies within the central and southwestern structural blocks of the Los Angeles Basin. The Central and Hollywood ground-water basins are within the central block, and the West Coast and Santa Monica ground-water basins (fig. 2) are within the southwestern block. The Newport-Inglewood Uplift (NIU) is a northwest-trending zone that separates the central and southwestern blocks (fig.1). The NIU extends from Beverly Hills southeast to Newport Beach in southern Orange County. The fault zone can be projected at least 45 mi southward offshore (Wright, 1991). The NIU is a series of en echelon anticlinal folds and discontinuous faults. It is characterized by wrench-style deformation, which is inferred to be predominantly right-lateral strike slip (Harding, 1973; Yeats, 1973). Total displacement along the NIU is estimated to be less than 2 mi (Hill, 1971).
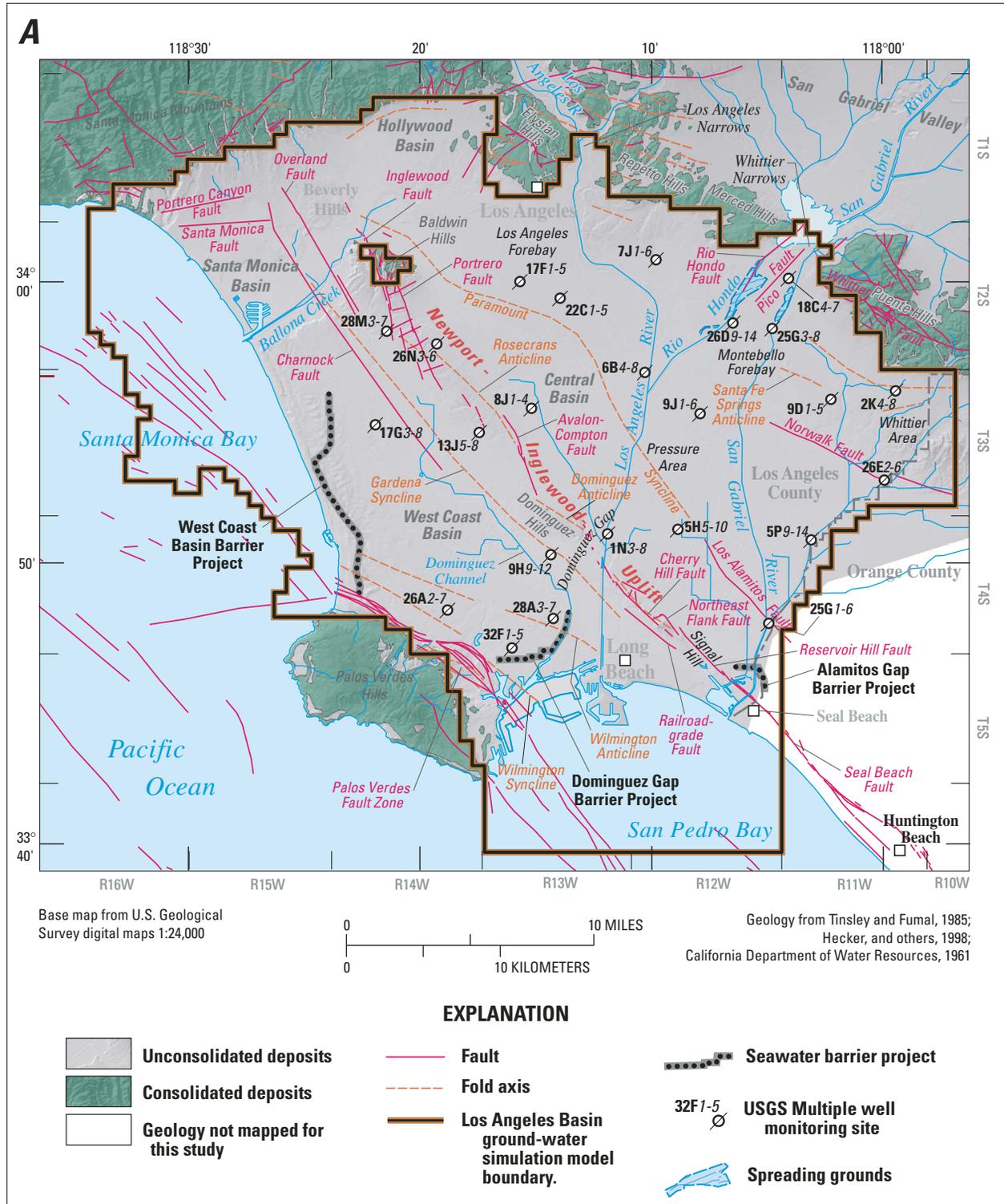
Figure 2. Location of U.S. Geological Survey wells (*A*) and geohydrologic-section lines, wells with geophysical logs, and geologic structures (*B*) in the study area, Los Angeles County, California.
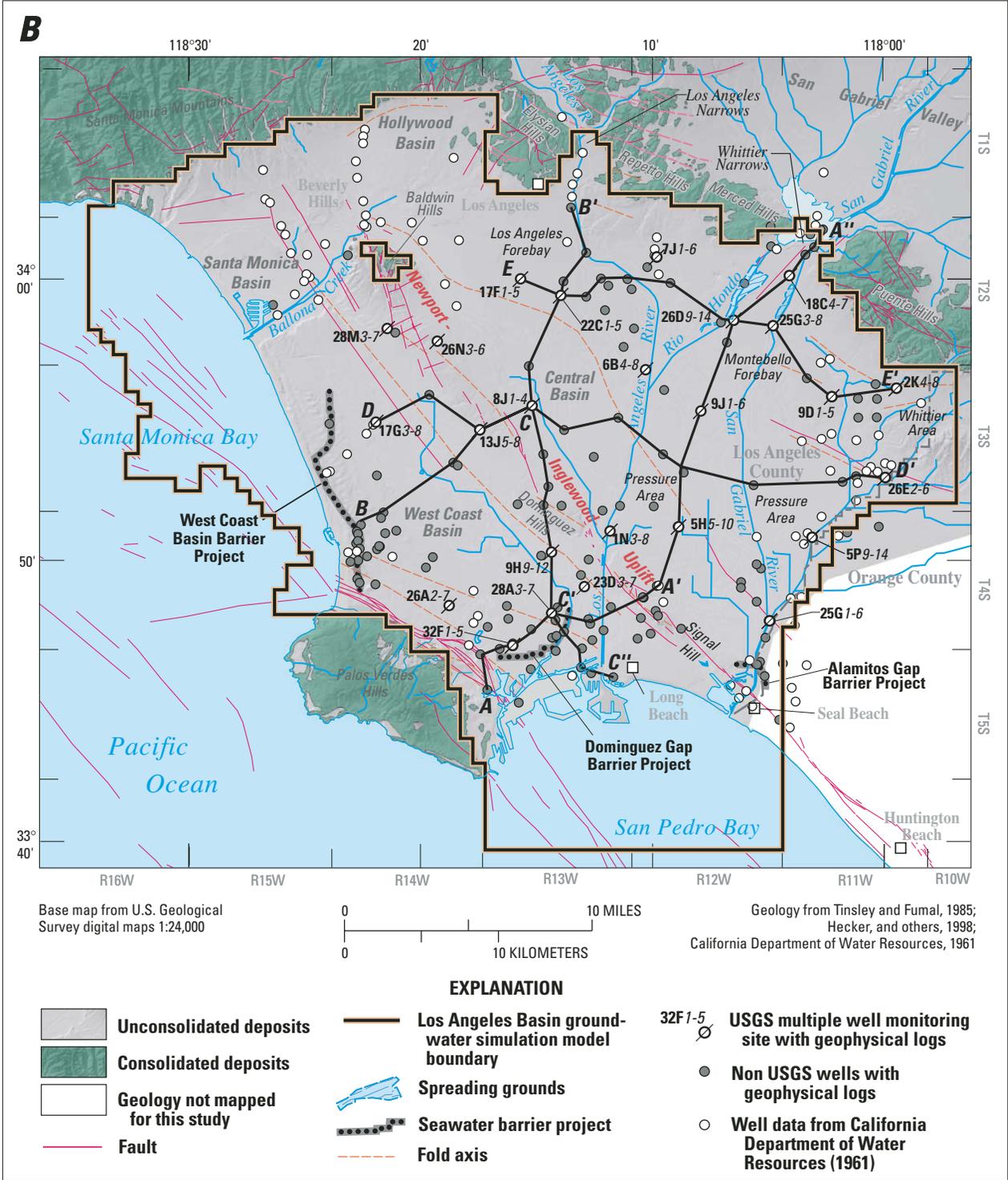
Figure 2.—Continued.

The faults and folds of the NIU include Beverly Hills, Baldwin Hills, Inglewood Fault, Portrero Fault, Rosecrans Anticline, Avalon-Compton Fault, Dominguez Anticline, Cherry Hill Fault, Railroad Grade Fault, Northeast Flank Fault, Reservoir Hill Fault, and Seal Beach Fault (fig. 2). Wright (1991) excludes Beverly Hills from the NIU, considering them to be a part of the Santa Monica Fault system. Yerkes and others (1965) stated that oil field data indicate middle Miocene displacement along the NIU and noted that the "arching and erosion of marine upper Pleistocene and of younger nonmarine strata in the hills along the zone, and numerous seismic shocks,...attest to continuing activity." The NIU has been considered to approximately coincide with the boundary between western basement Catalina Schist and eastern basement granitic rocks (California Department of Water Resources, 1961; Yerkes and others, 1965). Wright (1991) stated that this distinction between the eastern basement and western basement material is less clearly defined.

Yerkes and others (1965) divided the geologic and structural evolution of the Los Angeles Basin into five phases: (1) predepositional phase, (2) prebasin phase of deposition, (3) basin inception phase, (4) principal phase of subsidence and deposition (upper Miocene to lower Pleistocene), and (5) basin disruption (upper Pleistocene to Holocene). Biddle (1991) stated that recent research has begun to address the underlying processes, but that the five phases of Yerkes and others (1965) have generally remained valid. Of main relevance to the geohydrology are phases 4 and 5. Subsequent research has incorporated new understanding of the effects of plate tectonics on the formation of the Los Angeles Basin. During Phase 4, much of the present form of the current Los Angeles Basin was established (Yerkes and others 1965). Wright (1991) described the multiple tectonic mechanisms at work during this period.

Blake (1991) detailed the complexities of the nomenclature for Pliocene sediments in the subsurface of the Los Angles Basin. He described the Pico Formation in the Los Angeles Basin as upper Pliocene to upper Pleistocene deposits containing "lower middle bathyal to neritic deposits" (fig. 3). Poland and others (1956, 1959) defined the Pico formation in hydrostratigraphic terms; the lower and middle divisions consist of sandstone, siltstone, and claystone and the upper division of "semi-consolidated sand, silt, and clay of marine origin." This hydrostratigraphic unit, which is referred to as the Pico unit throughout this report, does not necessarily correlate to the Pico formation as defined biostratigraphically in Blake (1991).

Also deposited in the Palos Verdes Hills area during the early Pleistocene were the Lomita Marl, Timms Point Sand, and San Pedro Sand members of the San Pedro Formation. In this area, which contains the type section of the San Pedro Formation described by Woodring and others (1946), the San Pedro Formation unconformably overlies the lower Pliocene and Miocene deposits. In contrast, the San Pedro Formation conformably overlies Pliocene deposits on the south margins of the Puente Hills. Poland and others (1956, 1959) described the San Pedro Formation in the subsurface as including virtually all Pleistocene strata of predominantly marine origin that overlie the Pico hydrostratigraphic unit. Ponti (1989) stated that the subsurface San Pedro Formation is middle to upper part of the lower Pleistocene in age and appears to conformably overlie the Pico Formation in the southwest part of the Los Angeles Basin. Yerkes and others (1965) described the San Pedro Formation as consisting of marine silt, sand, and gravel deposited at moderate to shallow depths. Blake (1991) states that the San Pedro Formation represents a transition from inter-neritic deposits to nonmarine deposits. In this report, two hydrostratigraphic units are identified in the San Pedro Formation: a lower San Pedro unit that was deposited in deep water and includes local turbidite deposits and an upper San Pedro unit that apparently was deposited in shallower water and consists of packages of regressional sequences.

AGE	FORMATION	AQUIFER	AQUIFER SYSTEMS	MODEL LAYER
HOLOCENE	ACTIVE DUNE SAND	SEMIPERCHED	RECENT AQUIFER SYSTEM	1
		GASPUR		
UPPER PLEISTOCENE	OLDER DUNE SAND	BALLONA	**Upper Aquifer Systems**	2
	LAKEWOOD FORMATION (California Dept. of Water Resources, 1961)	EXPOSITION ARTESIA	LAKEWOOD AQUIFER SYSTEM	
	(UNNAMED UPPER PLEISTOCENE, Poland and others 1956, 1959)	GARDENA GAGE (200 FOOT SAND)		
LOWER PLEISTOCENE	*SAN PEDRO FORMATION*	HOLLYDALE JEFFERSON LYNWOOD (400 FOOT GRAVEL) SILVERADO	UPPER SAN PEDRO AQUIFER SYSTEM **Lower Aquifer Systems**	3
		SUNNYSIDE LOWER SAN PEDRO	LOWER SAN PEDRO AQUIFER SYSTEM	4
UPPER PLIOCENE	*PICO FORMATION*		**Pico unit**	

Modified from California Department of
Water Resources, 1961; Ponti, 1989

EXPLANATION

Lower Aquifer Systems { **Aquifer systems grouping for geochemical analysis**

Figure 3. Geologic formations, aquifers, aquifer systems, and model layers in the Central and West Coast Basins, Los Angeles County, California.

Yerkes and others (1965) described Phase 5 of basin development in the Los Angeles Basin as being characterized by tectonic uplift and erosion during the mid-Pleistocene, resubmergence and marine deposition during the late Pleistocene, and uplift and alluvial deposition from the late Pleistocene to the Holocene. Davis and others (1989) described this as a period of compressional shortening. Ponti (1989) used aminostratigraphic techniques to determine that, in the southern part of the West Coast Basin, most of the apparent disruption during this period was the result of eustatic sea-level changes rather than tectonic activity. During the late Pleistocene, shallow-water marine sediments [referred to as unnamed upper Pleistocene deposits by Poland and others (1956, 1959)] including the Palos Verdes Sand of Woodring and others (1946), as well as nonmarine fluvial, alluvial, and eolian sediments were deposited. These late Pleistocene deposits are referred to collectively by the California Department of Water Resources (1961) as the Lakewood Formation. Yerkes and others (1965) characterized the upper Pleistocene deposits as consisting of marine terrace deposits, nonmarine terrace cover in the southwestern block (West Coast Basin), and nonmarine fluvial and lagoonal deposits in the central block (Central Basin). An angular unconformity exists between the middle part of the upper Pleistocene Lakewood formation and the underlying San Pedro Formation in some locations.

Late Pleistocene and Holocene sediments were deposited in canyons incised into the Pleistocene deposits during sea-level low stands (Yerkes and others, 1965; Ponti, 1989). Gaps (including the Dominguez and Alamitos Gaps) were cut into the rising hills along the NIU, and channels were cut into the emerged sea bottom. When sea level rose again, these entrenched channels and gaps were filled with sequences of fluvial, lagoonal, and estuarine deposits. The California Department of Water Resources (1961) stated that the incising of the channels occurred during sea level low stand during the most recent glacial period (60,000 yr before present to 15,000 yr before present), and that the channels were then filled with Holocene deposits as sea levels rose. The basal part of these channel deposits is coarse grained and very permeable. Away from the channels in alluvial-fan and flood-plain depositional environments, thin layers of sand and silty sand were deposited (Yerkes and others,

1965). Ponti (1989) suggested that several stages of cutting and filling occurred during both Pleistocene and Holocene time and that the basal zone contains restricted marine deposits as well as fluvial deposits. Although all the deposits above the Lakewood Formation will be referred to as recent deposits in the remainder of this report, it is important to keep in mind that some of these deposits are likely of Pleistocene age.

HYDROGEOLOGIC FRAMEWORK

The first characterizations of the aquifers in the Los Angeles coastal basins were completed by Poland and co-workers (Poland and others, 1956, 1959). The California Department of Water Resources (1961) built on the work of Poland and further analyzed the ground-water flow system. Identified aquifers are shown in the stratigraphic column in figure 3. Cross sections developed by the California Department of Water Resources (1961) were, for the most part, based on drillers' logs.

One goal of the current study was to develop new sections utilizing geophysical logs along with ancillary information, including geochemical data. About 150 geophysical logs were compiled and digitized (fig. 2B). Five cross sections, *A–A", B–B', C–C", D–D',* and
E–E' (figs. 2B and 4) were developed for this study. The sections were chosen to include new USGS monitoring sites and to cover as much of the Central and West Coast Basins as possible. Only electrical resistivity logs are shown in figure 4; however, spontaneous potential (SP), natural gamma ray, caliper, and geologic logs of drill cuttings also were evaluated where available. For this study, aquifers were grouped into four aquifer systems: the Recent, Lakewood, Upper San Pedro, and Lower San Pedro aquifer systems (fig. 3). The Pico unit also is shown and is defined as a non-transmissive zone that underlies the lower San Pedro aquifer system. Factors considered in defining the aquifer systems include unconformities, lithology, depositional characteristics, geochemistry, and vertical water-level differences. Considerable emphasis was placed on the characteristics of the geophysical logs.

EXPLANATION

Figure 4

Geologic age — **Aquifer system**

Holocene — Recent

Pleistocene — Lakewood / Upper San Pedro / Lower San Pedro

Pliocene — Pico unit

——?— — **Geologic contact** – Dashed where approximately located, queried where uncertain

Fault – Dashed where acts as partial barrier to ground-water flow, queried where uncertain

USGS multiple-well monitoring site

18C4-7 — Abbreviated well number

Well casing

Screened interval

Electric log

→ Increasing resistivity

Non USGS well

28D1 — Abbreviated well number

Well casing

Electric log

→ Increasing resistivity

Figure 4. Geohydrologic sections *A–A'', B–'B', C–C'', D–D',* and *E–E',* in the study area, Los Angeles Country, California (lines of sections are shown in figure 2B).
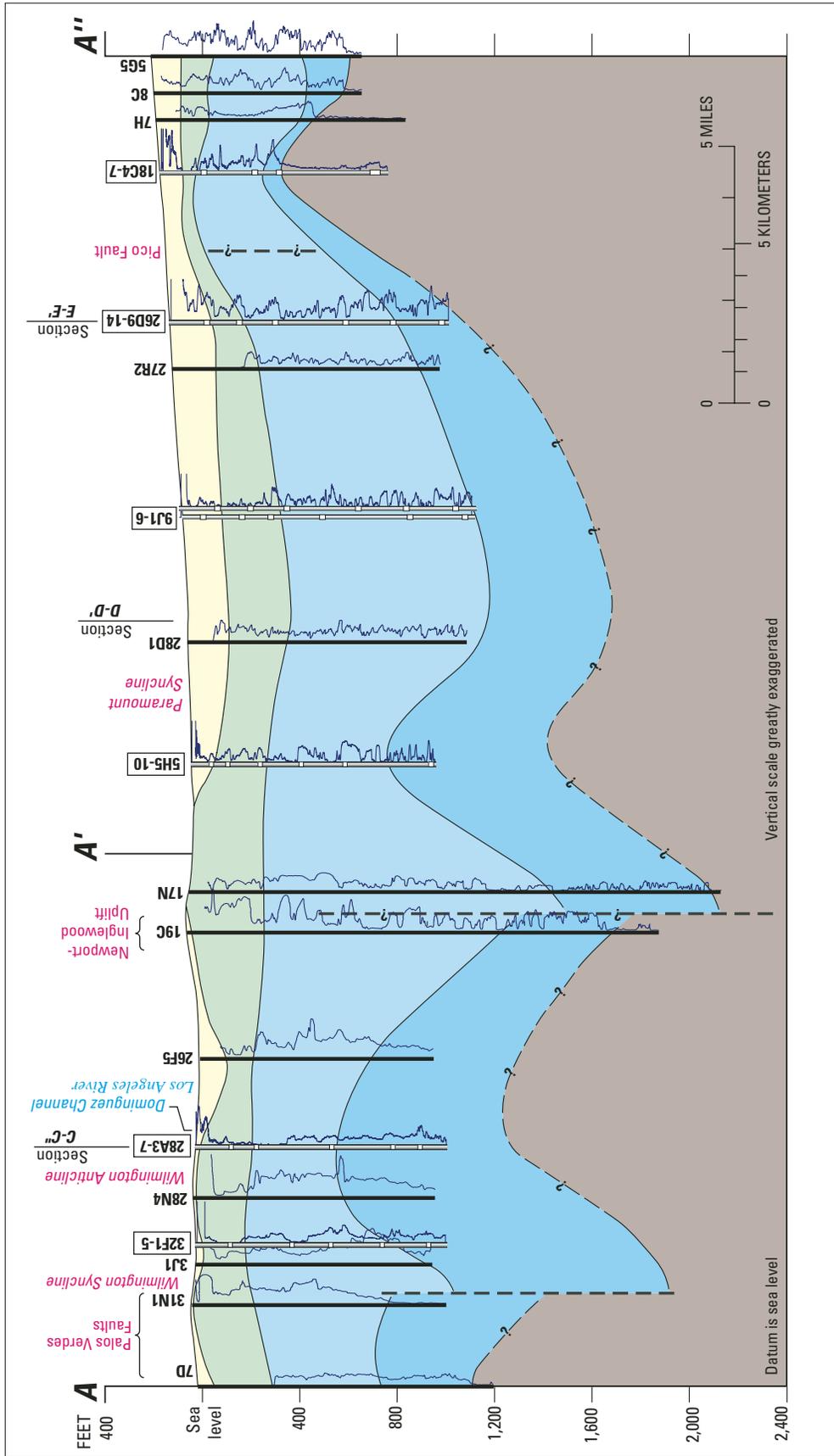
Figure 4. —Continued.
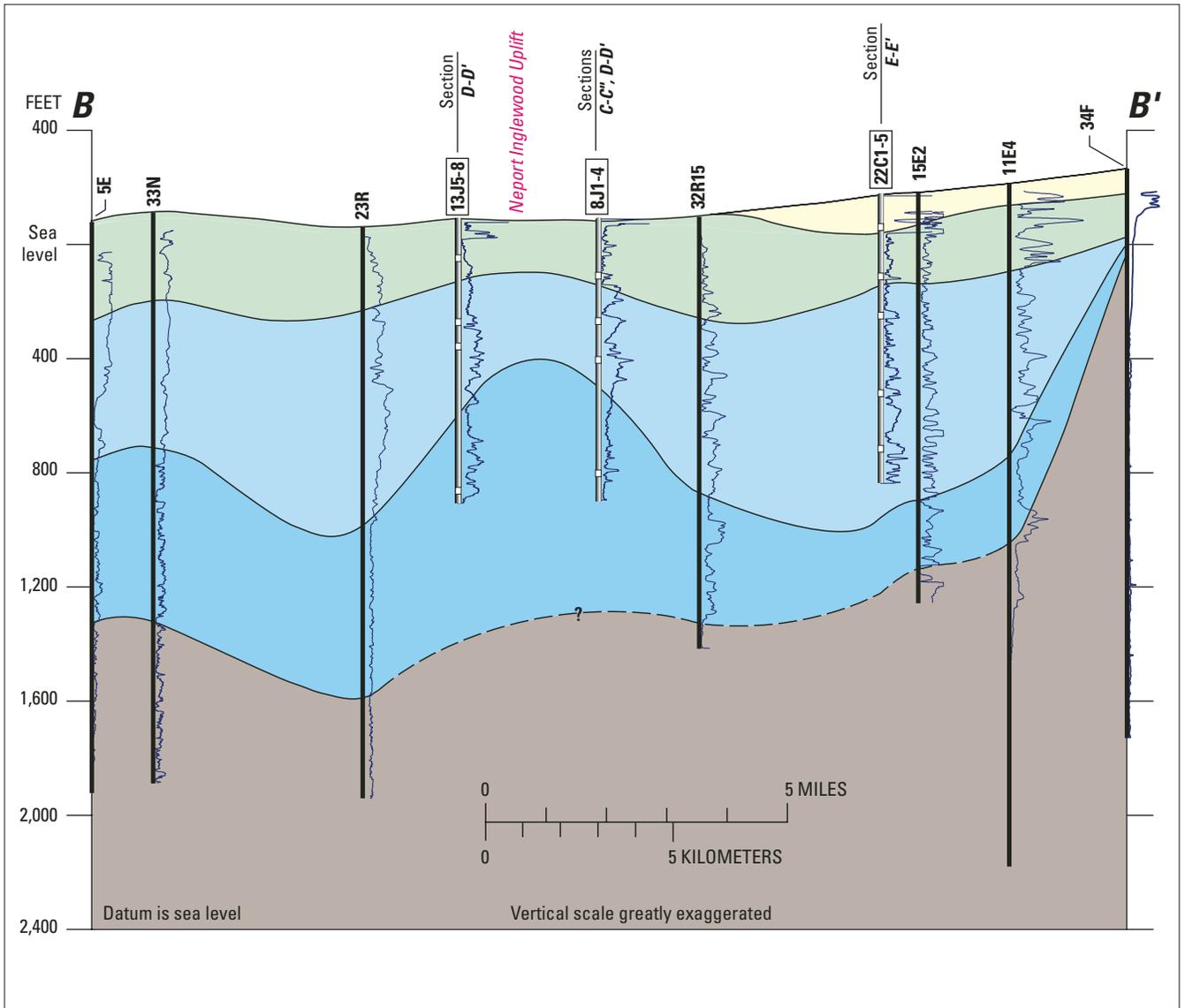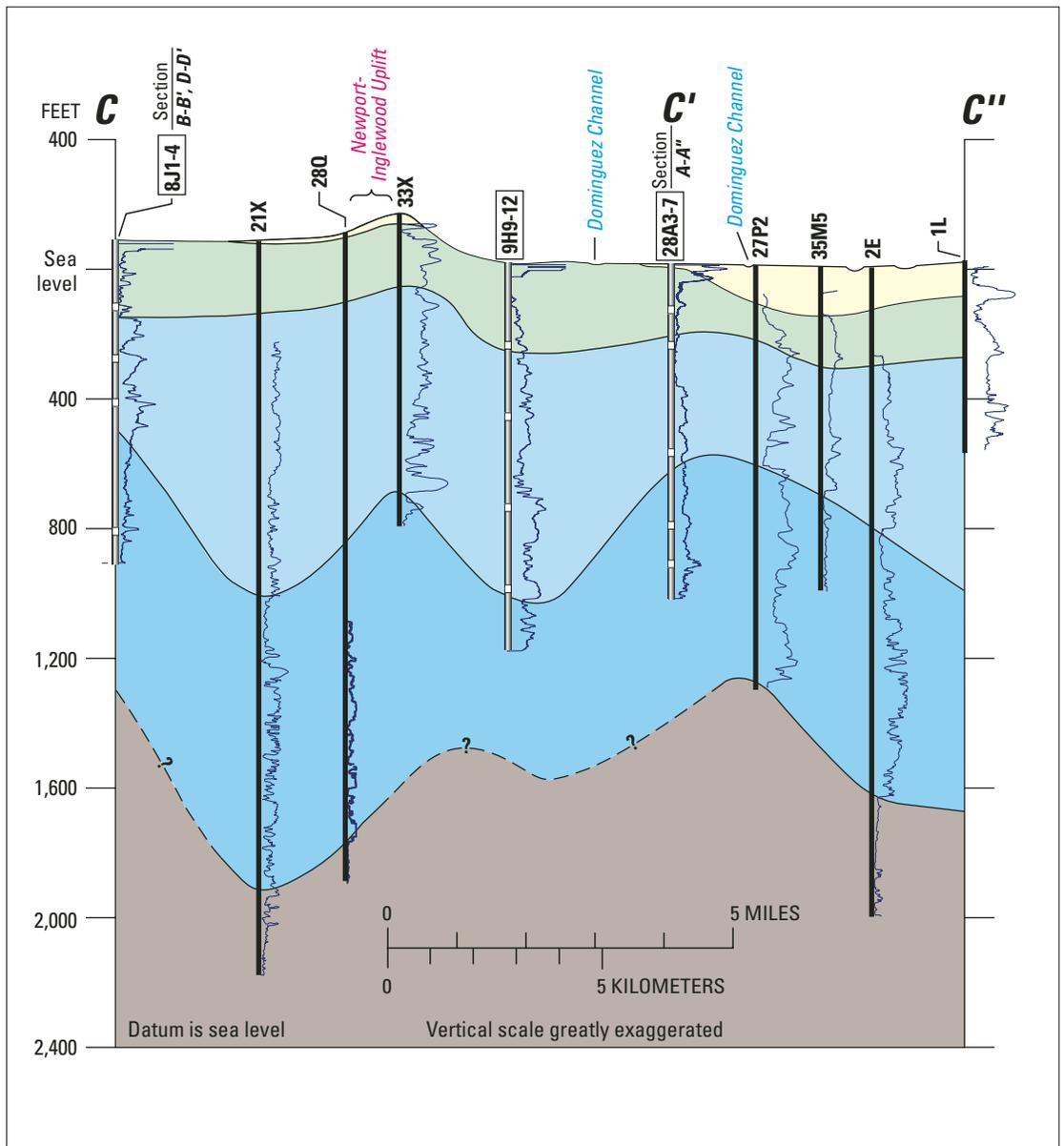
Figure 4.—Continued.
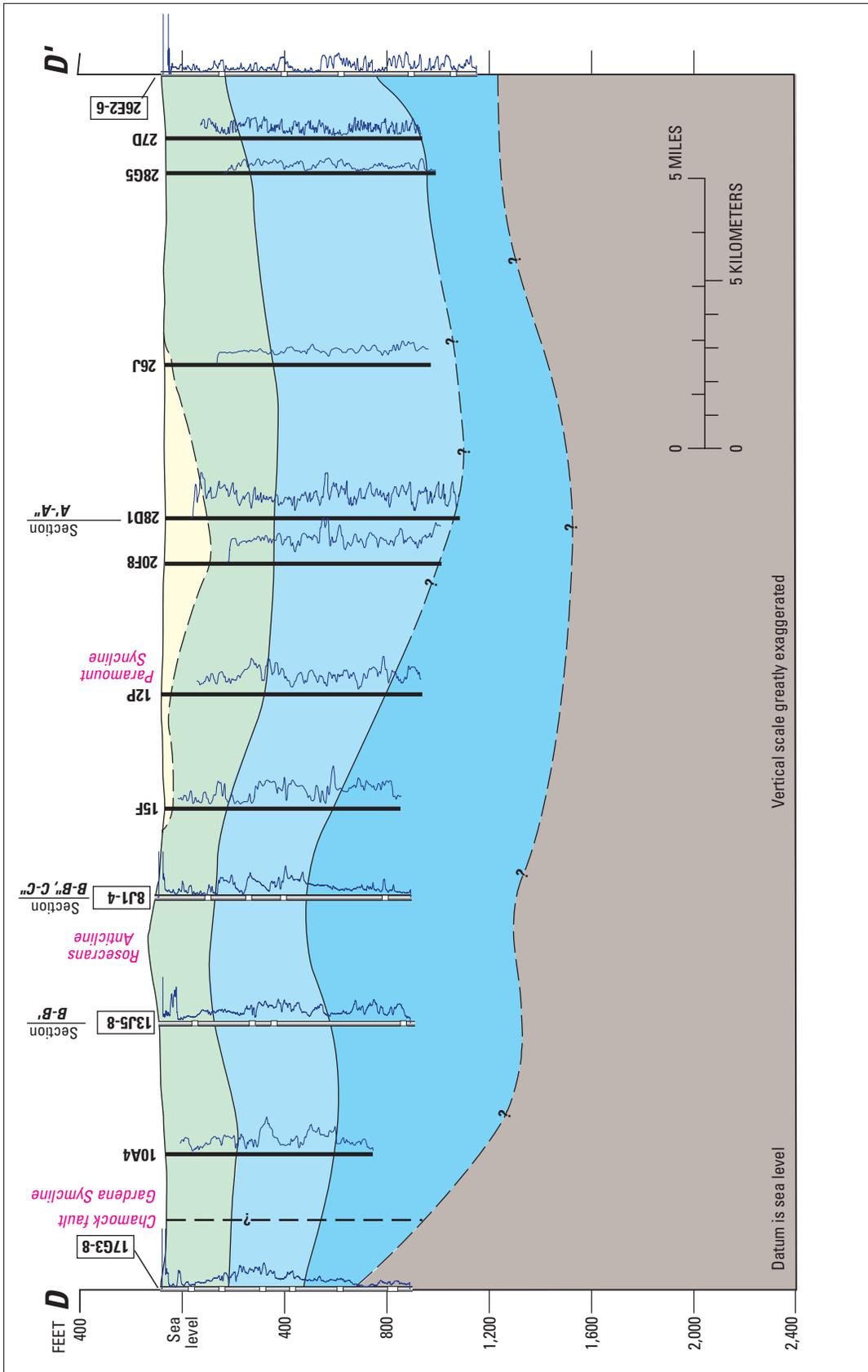
Figure 4.—Continued.
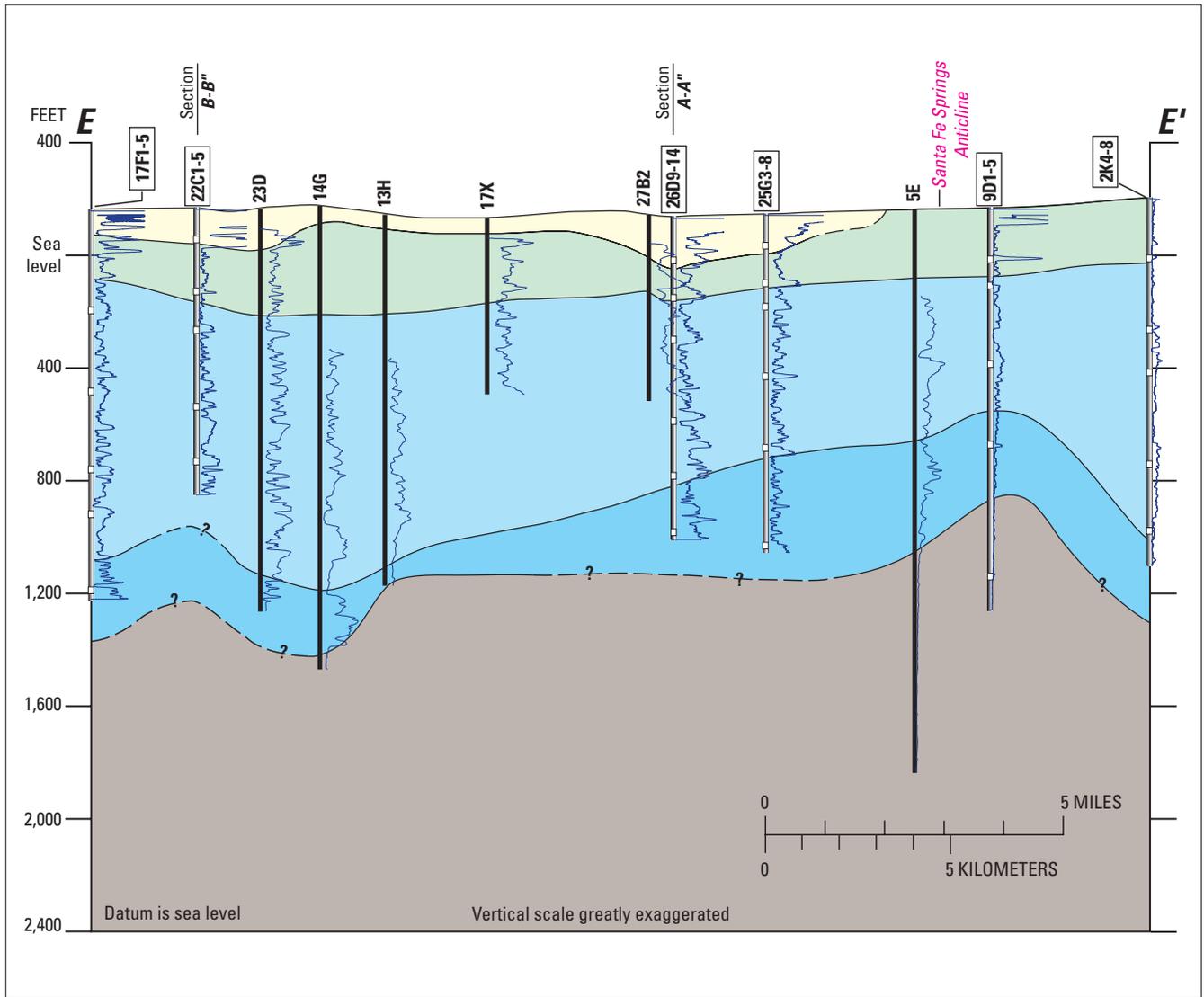
Figure 4.—Continued.

Figure 4.—Continued.

Recent Aquifer System

The geohydrologic units that compose the Holocene (Recent) age deposits of the Recent aquifer system include the semiperched aquifer, the Bellflower aquiclude, the Gaspur aquifer, and the Ballona aquifer (California Department of Water Resources, 1961). Although these geohydrologic units are referred to in this report as consisting of Holocene-age deposits, some of these units consist of deposits of Pleistocene age. The semiperched aquifer is a relatively thin layer of coarse sand and gravel near the land surface; it consists of alluvial sediments and, in parts of the West Coast Basin, marine deposits that may include the late Pleistocene Palos Verdes Sand. Because of low yields and poor water quality, little water is pumped from the semiperched aquifer. Except in parts of the Montebello and Los Angeles Forebay areas, this semiperched zone is separated from the underlying aquifers by a zone of lower permeability materials referred to as the Bellflower aquiclude. The Bellflower aquiclude is very heterogeneous and includes all of the fine grained sediments that extend from the ground surface or from the base of the semiperched aquifer, down to the underlying aquifer (California Department of Water Resources, 1961).

The coarse, basal zone of the Recent aquifer system is called the Gaspur aquifer. The California Department of Water Resources (1961) defined the extent of the Gaspur aquifer to be limited to two lobes in the Montebello and Los Angeles Forebays merging near the city of Downey and extending along the current Los Angeles River channel through the Dominguez Gap to the ocean. In the forebay areas, the Gaspur aquifer is nearly all sand and gravel. Hydraulic conductivities have been reported as high as 800 ft/d (California Department of Water Resources, 1961).

Although the Ballona aquifer, which extends along the western part of the Ballona Creek channel in the Santa Monica Basin, also consists of Holocene (Recent) deposits, it is not explicitly included in the Recent aquifer system in the model developed for this study. The Ballona aquifer is the stratigraphic equivalent of the Gaspur aquifer and may have been deposited by the Los Angeles River system (including, perhaps, the downstream reaches of the Rio Hondo and San Gabriel River) when it flowed out into Santa Monica Bay. The yield of the Ballona aquifer is quite variable and the Ballona aquifer is not a major source of water supply.

Delineating the Recent aquifer system can be difficult because parts of its deposits are unsaturated and geophysical information is not dependable. However, the basal Gaspur aquifer is indicated by a high-resistivity zone in some of the logs. There also tends to be an SP shift and an increase in the natural gamma emission below the Gaspur aquifer. The Gaspur aquifer is typically 40 to 50 ft of coarse pebbly sand. Depth to the base of the Gaspur ranges from close to land surface to 175 ft below land surface. Geologic logs indicate oxidized conditions at shallow depths that may indicate Pleistocene deposition. The Holocene deposits were likely laid down rapidly and underwent little oxidation. The uppermost Pleistocene deposits, in contrast, likely were deposited more slowly and subjected to oxidation. The use of a surficial geology map developed by John Tinsley (U.S. Geological Survey, written commun., 1997) helped determine, when other sources of evidence were not conclusive, whether or not Holocene deposits were present.

Lakewood Aquifer System

The main aquifers of the Lakewood aquifer system are the Exposition, Artesia, Gardena, and Gage aquifers (fig. 3). Generally, the Lakewood aquifer system is a heterogeneous unit dominated by sandy silts and silty sands interbedded with sands that become coarser and thicker near the base of the aquifer system. Gamma logs from many wells show the alternating lithologies in the upper part of the Lakewood aquifer system; the lower coarse-grained units typically are indicated by decreases in gamma emissions. Because deposition of the Lakewood Formation was controlled by sea-level fluctuations, pre-existing topography, and, to a lesser extent, subsidence or uplift, the Lakewood aquifers have varying thicknesses and degrees of sorting. The entire Lakewood aquifer system ranges in thickness from 150 to 400 ft.

Sediments within the Exposition and Artesia aquifers in the upper part of the Lakewood Formation (fig. 3) are considered to have been deposited contemporaneously. The Exposition aquifer is associated with the Los Angeles River and the Artesia aquifer with the San Gabriel River (California Department of Water Resources, 1961). The Exposition aquifer is very heterogeneous and characterized by discontinuous sand and gravel zones separated by silt and clay lenses. The Artesia aquifer consists of coarse gravel, coarse to fine sand, and interbedded silts and clays. The age of parts of both aquifers may be similar to deposits that form the Gaspur aquifer (California Department of Water Resources, 1961). The Exposition and Artesia aquifers commonly are poorly defined or absent.

The Gardena and Gage aquifers are at the base of the Lakewood Formation (fig. 3). The Gage aquifer was referred to by Poland and co-workers(1956, 1959) as the 200-foot sand—although, as noted by California Department of Water Resources (1961) and confirmed during this study, the depth to the base of the Lakewood aquifer system can be considerably deeper than 200 ft in the Central Basin (fig. 4). The Gardena aquifer consists of coarse deposits of probable fluvial origin that are inset into the dominantly shallow-water deposits that compose the Gage aquifer. The Gage aquifer consists of sand and gravel with lenses of sandy silt, silty clay, and clay. In this study, the Gage and Gardena aquifers were viewed as a single but complex aquifer system that is a source for water supply in some parts of the study area.

Upper San Pedro Aquifer System

The Upper San Pedro aquifer system incorporates the Hollydale, Jefferson, Lynwood, and Silverado aquifers (fig. 3). An angular unconformity exists between the Lakewood Formation and the underlying San Pedro Formation. The boundary between the Lakewood aquifer system and the Upper San Pedro aquifer system is identified on most geophysical logs by a shift in the SP log and a change in the character of both the gamma and resistivity logs. Large resistivity spikes, with accompanying SP shifts and decreases in natural gamma emission, coincide with the coarse-grained productive aquifers within the Upper San Pedro system. The Upper San Pedro aquifer system thins toward the margins of the forebays and at

structural highs such as those along the NIU. This thinning is presumed to result, in part, from mid-Pleistocene emergence (as sea level declined) and subsequent erosion. In the Los Angeles Forebay area, the Upper San Pedro aquifer system appears to be finer grained overall than elsewhere in the basin.

The Hollydale and Jefferson aquifers are the uppermost aquifers within the Upper San Pedro aquifer system. The California Department of Water Resources (1961) defines the areal extent of both aquifers to be limited to the Central Basin. Neither aquifer is considered an important source of water supply. The Hollydale aquifer is presumed to contain fluvial deposits in the northern part of the basin—in the Los Angeles and Montebello Forebays—and shallow marine deposits in the southern part. The underlying Jefferson aquifer was defined strictly on the basis of drillers' logs and is considered to be generally fine grained (California Department of Water Resources, 1961). Individual units correlative with the Hollydale and Jefferson aquifers are definable only locally.

The Lynwood aquifer is an important source of water. It is believed to consist of continental deposits in the forebay area and shallow marine deposits to the south and west. The Lynwood aquifer is seen on many resistivity logs as upward-coarsening sequences as indicated by upward-increasing resistivities.

The Silverado aquifer is in the lower part of the Upper San Pedro aquifer system (fig. 3) and produces the most water in the study area. In its type area, in Long Beach, the Silverado aquifer has been correlated to the marine San Pedro Sand by Poland and others (1956, 1959). In some areas the Silverado aquifer is associated with sediment deposited by the ancestral Rio Hondo and San Gabriel River systems (California Department of Water Resources, 1961). Overall, the aquifer system appears to be of mixed origin, with nonmarine deposits consisting of sand and gravel that are interbedded with silt and clay, and marine deposits characterized by blue-gray sand, gravel, silt, and clay, along with shells and wood fragments. The Silverado aquifer merges with overlying aquifers in the forebay areas. It also merges with both overlying and underlying aquifers near Santa Monica Bay (California Department of Water Resources, 1961). In many wells, the resistivity log for the Silverado aquifer indicates a fining-upward package.

Lower San Pedro Aquifer System

The Lower San Pedro aquifer system includes the Sunnyside aquifer (also referred to as the Lower San Pedro aquifer). The upper part of this system tends to be characterized by alternating fine-grained and coarse-grained zones. The fine-grained zones tend to pinch out or disappear near the forebay margins, such as at USGS Pico Rivera-1 (2S/11W-18C4–7) and 1S/13W-34F (fig. 4A,B). The coarsest part of the aquifer system generally is at the base and is as much as 100 ft thick. The Lower San Pedro aquifer system becomes very shallow and merges with the Upper San Pedro aquifer system in both the Los Angeles and Montebello Forebay areas. Most of the geophysical logs compiled in this study do not reach the base of the Lower San Pedro aquifer system. The total thickness of the Lower San Pedro aquifer system is as at least 600 ft in the center of the Central Basin. The typical resistivity-log signature of the Lower San Pedro aquifer system can be seen at the USGS Lakewood-1 (4S/12W-5H5–10) monitoring site at depths greater than 790 ft (fig. 4A).

Pico Unit

Underlying these four aquifer systems is the Pico hydrostratigraphic unit. On resistivity logs, the unit is characterized by a flat, low-resistivity signature. Resistivity within the Pico unit in some zones (generally 10 ft thick or less) is higher than that in some of the overlying units. This high resistivity may reflect thin zones of higher consolidation and (or) better water quality.

Analysis of Hydraulic Conductivities

Laboratory estimates of saturated vertical hydraulic conductivity were made from 48 cores taken at the USGS monitoring sites (Land and others, 2002, table 33). These values give some indication of the range of vertical hydraulic conductivities in the aquifer systems. Cores were generally taken in finer grained material; good recovery was not possible in the coarsest materials. Vertical hydraulic conductivity values ranged from less than 2.8×10^{-5} to 8 ft/d with a geometric mean of 2.7×10^{-2} ft/d. The vertical hydraulic conductivity estimates can be categorized by

the lithologic description of the drill cuttings for that interval. The geometric mean vertical hydraulic conductivity of cores taken in materials described as predominantly clay, silt, and sand was 3.9×10^{-3} ft/d, 1.0×10^{-2} ft/d, and 1.0×10^{-1} ft/d, respectively.

Slug tests were conducted at 69 USGS wells (Land and others, 2002, table 32). The estimated hydraulic conductivities, computed for two assumed values of specific storage (1.0×10^{-4} and 1.0×10^{-6} ft^{-1}), ranged from 11 to 27 ft/d in the Recent aquifer system (2 wells), 1 to 140 ft/d in the Lakewood aquifer system (15 wells), 3 to 70 ft/d in the Upper San Pedro aquifer system (34 wells), 1.5 to 65 ft/d in the Lower San Pedro aquifer system (16 wells), and 0.1 to 8 ft/d in the Pico unit (2 wells). An assumption in the slug-test analysis is that the imposed stress affects the entire perforated interval of the well. In general, the slug tests appear to underestimate hydraulic conductivities relative to those computed from multi-well aquifer tests (for example, Attachment 2, table C, California Department of Water Resources, 1961). Complete discussion of the procedures and analyses used for the slug tests is provided by Land and others (2002).

REGIONAL GROUND-WATER FLOW SYSTEM

Sources and Movement of Water

The ground-water system is recharged by direct precipitation, irrigation return, stream recharge, runoff from the surrounding uplands, artificial recharge of water through spreading grounds, injection of water in the seawater-barrier wells, and underflow from adjacent basins. Recharge from streams is limited because most of the streams are concrete lined. The Los Angeles River is lined throughout the study area except just upstream from where it enters San Pedro Bay. The San Gabriel River is lined except in the upper parts of the Montebello Forebay and near the Alamitos Gap, and the Rio Hondo is lined throughout the study area. The study area is hydraulically linked to three adjacent basins: the San Fernando Valley to the north, the San Gabriel Valley to the northeast, and the Orange County Basin to the southeast.

Under current conditions, most recharge occurs in the Montebello Forebay. This recharge includes artificial recharge in spreading ponds adjacent to the Rio Hondo and the San Gabriel Rivers and within the stream channels (fig. 1). Even before the artificial-recharge program began, the Montebello Forebay was a major recharge area because of the unconfined conditions and the presence of the San Gabriel River and Rio Hondo. No artificial recharge is conducted within the Los Angeles Forebay. The California Department of Water Resources (1961) stated that, because of its more highly urbanized conditions, natural recharge in the Los Angeles Forebay has been less than that in the Montebello Forebay.

Before significant ground-water development began, ground water moved from the forebay areas (and from the Santa Monica Mountains on the northwest) south and west toward the Santa Monica and San Pedro Bays. Water moved laterally outward and vertically downward to underlying confined aquifers. The water eventually discharged either in wetlands or offshore.

The NIU is a major structural feature that acts as a partial barrier to ground-water flow between the Central and West Coast Basins. Other faults (fig. 2) in the study area also appear to have hydraulic effects. Poland and others (1959) stated that faults in the Los Angeles area affect ground-water flow because of displacement of units and cementation within fault zones. The degree to which different faults affect flow in different aquifers is uncertain. The ground-water simulation model developed as part of this study has been used to test hypotheses regarding the permeability effects of faults. The California Department of Water Resources (1961) discussed the hydraulic effects of faults (and other structures) within the NIU, including the Rosecrans Anticline and the Inglewood, Portrero, Avalon-Compton, Cherry Hill, and Northeast (NE) Flank, Reservoir Hill, and Seal Beach Faults (fig. 2). Bawden and others (2001) used interferometric synthetic aperture radar (InSAR) to correlate seasonal land deformation with ground-water pumpage. Their results clearly showed a discontinuity in land deformation across the southern part of the NIU. Because the NIU affects interflow between the Central and West Coast Basins, considerable effort has been directed at quantifying the ground-water flow rates across it. (Montgomery Watson, 1993). Further discussion of flow across the NIU is provided later as part of the water-budget analysis of the ground-water modeling section of this report.

In addition to the NIU, Poland and others (1959) noted water-level discontinuities associated with the Charnock and Overland Faults in the West Coast Basin (fig. 2). In the Central Basin, the Pico, Rio Hondo, and Los Alamitos Faults may restrict flow in the aquifers in Pleistocene sediments (California Department of Water Resources, 1961). In the Santa Monica Basin, the Santa Monica and Portrero Canyon Faults potentially restrict ground-water flow in Pleistocene formations (Wright, 1991; Pratt and others, 1998). As can be seen in figure 2, there are numerous other faults in the study area that may affect ground-water flow. In addition, there likely are unmapped faults that are affecting ground-water movement.

Ground-Water Development

The first water wells were drilled in the mid-1800s, and by the early 1900s there were more than 4,000 wells in the study area (Mendenhall, 1905a,b,c). Poland and others (1959) reported the presence in 1895 of a flowing well 2 mi north of Signal Hill that had water levels 80 ft above land surface. Mendenhall (1905a,b,c) reported many flowing wells in the area. At that time, approximately 30 percent of the area was under flowing artesian conditions.

Historical quantities of pumping, injection, and spreading in the Central and West Coast Basins are shown in figure 5. Note in figure 5 that pumpage for 1935–57 is from the California Department of Water Resources (1962), whereas that for 1961–2000 was reported to the Water Masters and published in 2000 by Water Replenishment District of Southern California (WRDSC).
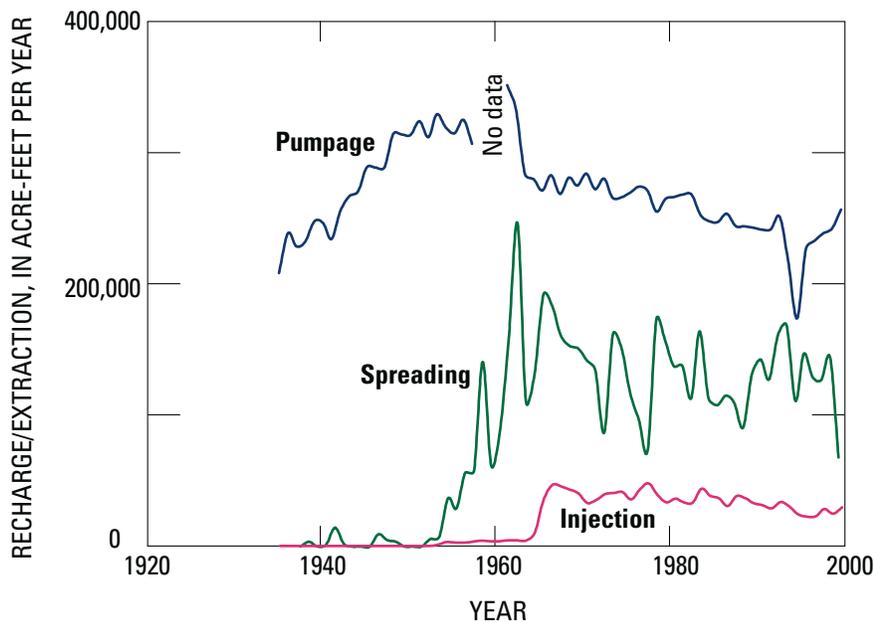
Figure 5. Historical pumpage, injection, and spreading of water in the Central and West Coast Basins, Los Angeles County, California.

From 1900 to 1930, pumpage increased considerably owing to increasing urban demand, lack of surface-water supplies, and development of the deep well turbine (Poland and others, 1959). By the 1920s, water levels were below sea level throughout much of the West Coast Basin. The entire ground-water flow system had changed dramatically; ground water no longer discharged into wetlands or offshore. Instead, seawater began moving inland in aquifers from both Santa Monica Bay and San Pedro Bay. By the 1940s elevated chloride owing to seawater intrusion was noted in all coastal areas (Poland and others, 1959, Pl. 16). The continuing trend through the 1950s was one of increasing pumpage (fig. 5) coupled with a shift from agricultural to urban water use. The increase in ground-water pumpage led to further declines in water levels. In many ground-water basins, large ground-water-level declines are accompanied by land subsidence. Poland and others (1959, p. 145) stated that ground-water withdrawals likely caused some subsidence in the West Coast Basin, but that it was not possible to quantitatively distinguish between subsidence strictly caused by ground-water pumping

and subsidence caused by tectonic effects and to hydraulic connection to oil-producing areas. More recently, the InSAR work of Bawden and others (2001) showed significant seasonal land-surface oscillation in parts of the Central Basin that correlates with seasonal pumping patterns. They also saw evidence of possible longer term land-surface changes between 1993 and 1999.

Paralleling the increasing ground-water pumping were two important surface-water developments: importation of water via pipelines and use of surface water for artificial recharge. Importation of water began in 1913 when water from Owens Valley was first delivered to the area via the Los Angeles Aqueduct. In 1948, Colorado River water was first delivered to the area via the Colorado Aqueduct. In the late 1930s, spreading of local runoff in ponds in the Montebello Forebay began. In the early 1950s, imported water began to be used for this spreading. Also in the 1950s, well injection of imported water at what is now the West Coast Basin Barrier Project (fig. 2) began on an experimental basis; the principal goal of this injection was to create a hydraulic barrier to seawater intrusion.
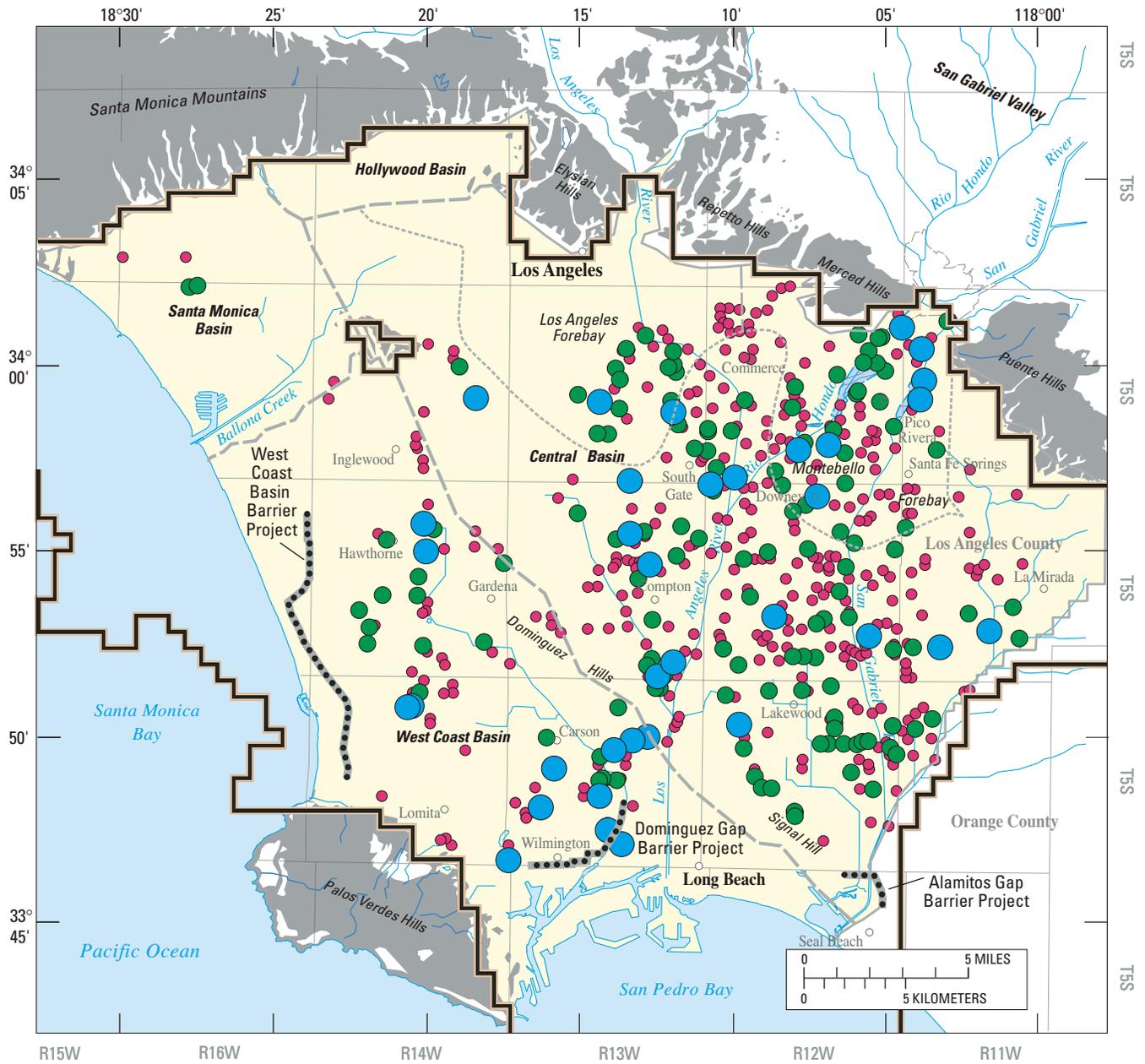
Figure 6.   Ground-water production in the study area in water year 2000, Los Angeles County, California.
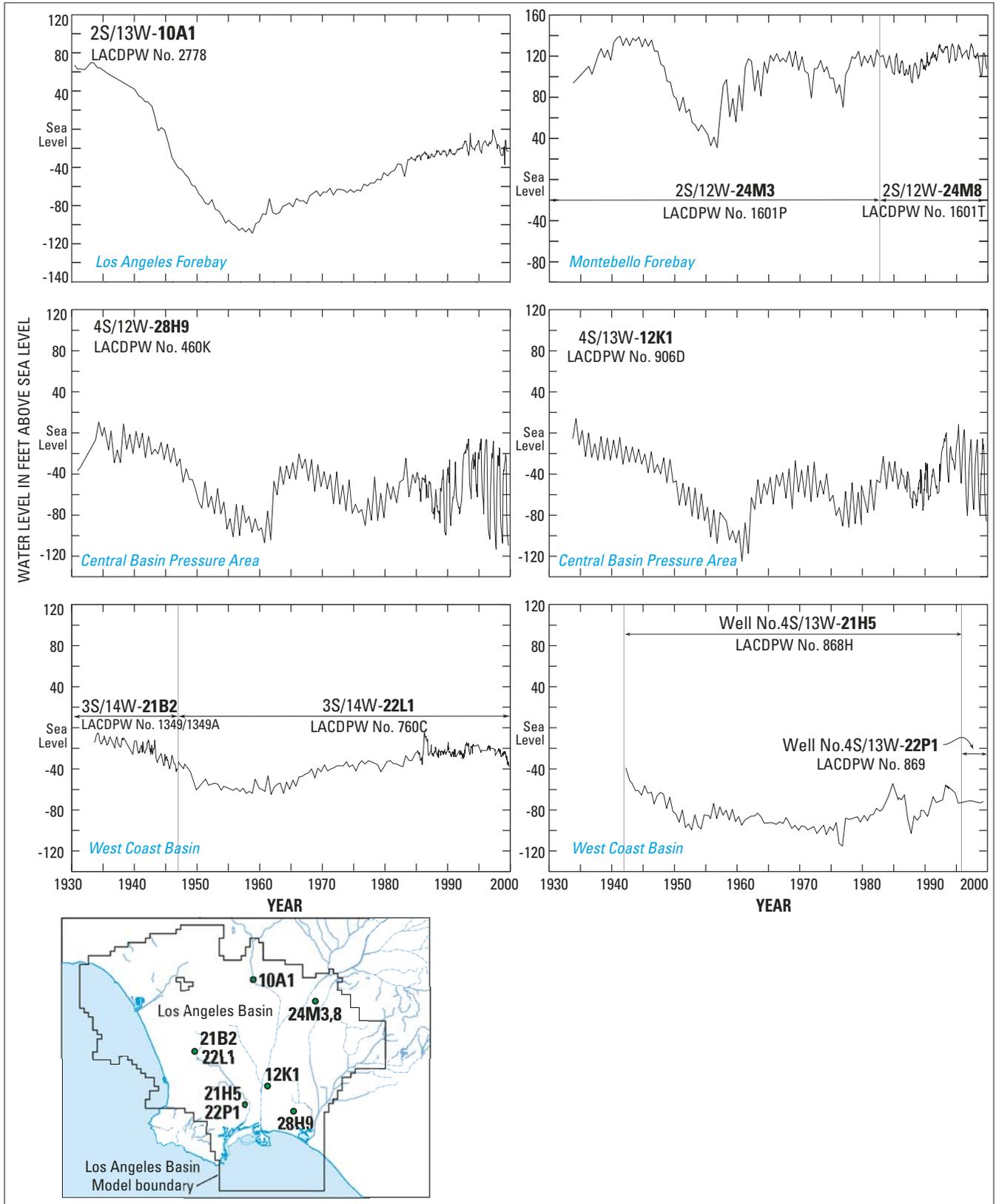
Figure 7. Long-term hydrographs of water levels at selected wells in study area, Los Angeles County, California.

The continuing depletion of ground-water storage eventually led to the adjudication of both the Central and West Coast Basins in the early 1960s. The WRDSC was formed in 1959 to protect and manage ground water in the two basins. The dramatic changes that occurred after the basins were adjudicated are illustrated in figure 5. In particular, there were large decreases in pumpage and large increases in injection and spreading rates. The pumpage decreases reflect the increasing direct use of imported water. The injection and spreading increases reflect the construction of new facilities (the Alamitos Gap Barrier Project in 1965 and the Dominguez Gap Barrier Project in 1971) and the increasing use of imported and reclaimed water. Reclaimed water began to be used for spreading in the 1960s and for injection at the West Coast Basin Barrier Project in the 1990s. An additional source of imported water, the State Water Project, became available in the 1970s.

The distribution of pumpage for water year 2000 is shown in figure 6. It can be seen from figure 6 that there is a greater density of active production wells in the Central Basin relative to the West Coast Basin and that there are several local areas of concentrated pumpage throughout the study area.

Long-term hydrographs for key wells monitored by Los Angeles County are shown in figure 7. The hydrographs clearly show the long-term declines though the mid-1950s, the differing patterns of post-adjudication recovery in different parts of the study area, and the change in annual and seasonal trends in parts of the Central Basin Pressure Area since the mid-1990s.

GEOCHEMICAL ANALYSIS

Introduction

Water-Quality Network

Ground-water samples were collected from 170 wells at 78 ground-water sites from August 1995 to May 2001 (fig. 8). Additional chemical data from the California Department of Health Services Title-22 monitoring program (California Department of Health Services, 1998), the Los Angeles County Department of Public Works Hydrologic Report (Los Angeles County Department of Public Works, 1998), and the Water Replenishment District Regional Groundwater Monitoring Report (Water Replenishment District of Southern California, 2000) were compiled.

Construction and Well Selection

The ground-water quality network includes 24 multiple-well monitoring sites (Appendix II), 20 existing observation wells, and 38 existing production wells. Nearly all samples were collected from the Central and West Coast ground-water basins; a few samples were from adjacent ground-water basins. The multiple-well monitoring sites consist of four to six wells installed at various depths within a single borehole and vertically sealed using bentonite grout (fig. 9).

Existing observation and production wells were incorporated into the monitoring network to help meet additional water-quality data-collection needs. Observation wells sampled as part of this study are screened over relatively short intervals, typically 10 to 40 ft, to provide information from a single water-bearing unit. These 20 wells are constructed of 2- or 4-inch-diameter PVC or galvanized steel. Existing production wells sampled as part of this study were designed for municipal water supply. Production wells were selected for sampling on the basis of location and limited perforated range (commonly less than 100 ft). Unlike observation wells, some of these wells have a screened interval that is open to several water-bearing units; consequently, water from these wells is a mixture of water from those units.

Data Collection and Purpose

Water-quality samples were collected using a portable submersible pump or at a spigot near the production well head. Water-level depth, specific conductance, pH, temperature, dissolved oxygen, and alkalinity were recorded during the collection process. To assess general water-quality conditions and study the chemical character of the ground water, samples were analyzed for major ions, nutrients, and trace elements. To study the source and movement of ground-water recharge through the basin, samples were analyzed for the stable isotopes of deuterium (^{2}H) and oxygen-18 (^{18}O). To estimate the residence time of water in the ground, samples were analyzed for the radioisotopes tritium (^{3}H) and carbon-14 (^{14}C). Data-collection procedures, well identification and construction, and other information from the monitoring network utilized in this report are presented by Land and others (2002).
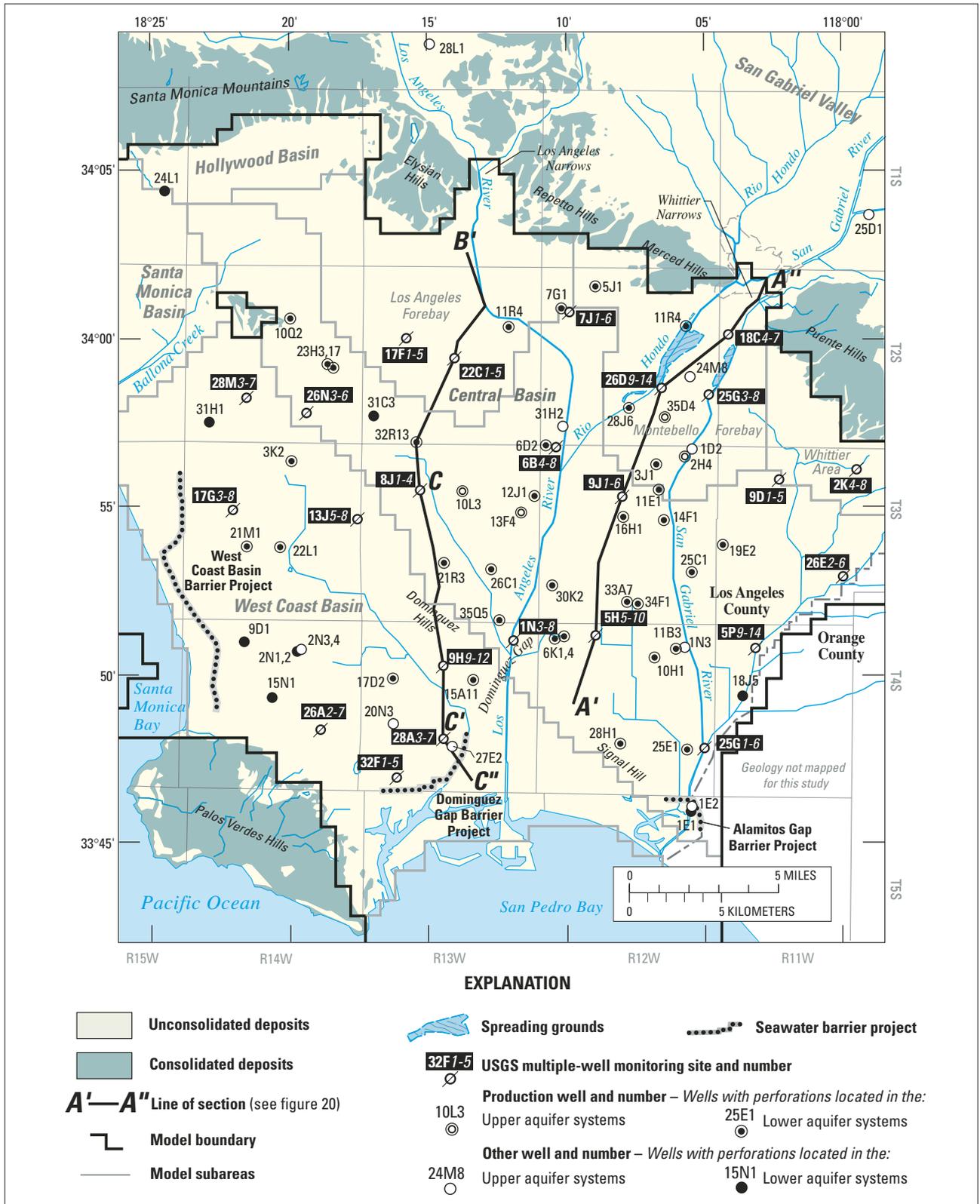
Figure 8. Location of ground-water sampling sites and geochemical flow path cross sections in the study area, Los Angeles County, California.

Well vault as it appears on surface

View from top of typical borehole

Borehole
(top of hole approximately 12 inches in diameter)

Well vault

#3 #2 #4 #5
#1

Grout

Sand

Grout

Sand

Grout

Sand

Grout

Sand

Grout

DEPTH, IN FEET BELOW LAND SURFACE

0

100

200

300

400

500

Well casing
(2 inches in diameter)

600

Well screen
(20 feet in height)

700

Sand

Borehole
(bottom of hole approximately 8 inches in diameter)

800

Native Soil

Grout

Total depth 897 feet

900

Horizontal scale greatly exaggerated.

Drill method: hydraulic mud rotary

Figure 9.   Components of typical USGS multiple-well monitoring site.

For the purpose of evaluating the regional ground-water quality and geochemical conditions, data collected from wells are divided into three groups following the model-layer hydrostratigraphy: the Upper aquifer systems, which include the Recent and Lakewood aquifer systems; the Lower aquifer systems, which include the Upper San Pedro and Lower San Pedro aquifer systems; and the Pico unit (fig. 3).

Discussion of much of the geochemical data is grouped by subareas with emphasis on the USGS multiple-well monitoring sites. In the Central Basin, the subareas and the multiple-well monitoring sites associated with them, are the Montebello Forebay (Pico Rivera-1, Pico Rivera-2, and Rio Hondo-1), Los Angeles Forebay (Huntington Park-1 and Los Angeles-1), Pressure Area near the forebays (Willowbrook-1, South Gate-1, Commerce-1, and Downey-1), Pressure Area distal to the forebays (Inglewood-2, Lakewood-1, Cerritos-1, and Long Beach-1 and -2), and Whittier Area (Whittier-1 and Santa Fe Springs-1). In the West Coast Basin, the subareas and the multiple-well monitoring sites associated with them are the interior margin (Gardena-1 and Carson-1) and coastal margin (Hawthorne-1, Wilmington-1, and Wilmington-2).

Ground-Water Quality

In general, the quality of most water in the study area is suitable for industrial and public supply. Dissolved-solids concentrations are low throughout most of the aquifers, often less than 500 mg/L (table 1). Concentrations are lower, and less variable, in water sampled from wells in the Central Basin compared with the West Coast Basin. Similarly, chloride concentrations are low throughout most of the freshwater aquifers, commonly less than 50 mg/L. In several areas, however, particularly shallow units and coastal regions, dissolved-solids concentrations exceed 500 mg/L and sulfate concentrations exceed 500 mg/L. Water is generally under sub-oxic or slightly reducing conditions. In some portions of the basin, manganese and iron concentrations exceed the drinking-water limit. In water from deeper or distal wells (on the basis of field observations), hydrogen sulfide gas is inferred to be present.

Dissolved-solids concentrations, commonly referred to as total dissolved solids (TDS), ranged from 181 to more than 12,000 mg/L (fig. 10A). Water throughout much of the Central and West Coast Basins contains less than 500 mg/L TDS. In general, TDS concentrations decrease with increasing depth and with increasing distance from forebay areas. In some areas—such as the Whittier Area, near the Palos Verdes Hills, and especially along the coast—dissolved solids concentrations exceed 1,000 mg/L in wells perforated in both the Upper and Lower aquifer systems.

In figure 10B, the median value for TDS is lower for water in the Central Basin than for the West Coast Basin and lower for water in the Lower aquifer systems than for the Upper aquifer systems. The median value for TDS in water from wells in the Upper aquifer systems of the Central Basin is 443 mg/L. Most water in the first quartile of this group is not located in the forebay areas, but is similar to native water in the Montebello (225-300 mg/L) and Los Angeles (275–350 mg/L) Forebays (Poland, 1956). Upgradient from the study area in the San Gabriel and San Fernando Valleys, water in shallow monitoring wells 1S/11W-25D1 and 1N/13W-28L1 contained relatively low TDS concentrations, 392 and 331 mg/L, respectively.

The median value for TDS in water from wells perforating the Lower aquifer systems of the Central Basin is 359 mg/L (fig. 10B). Some of the lowest observed TDS concentrations in the study area occur in the Central Basin Pressure Area, particularly in the Lower aquifer systems near Lakewood and Long Beach, where concentrations are as low as 181 mg/L (4S/12W-5H5). High outlying concentrations in wells in the Central Basin represent water sampled from wells in the Whittier Area (3S/11W-2K4 and 2K5) or near the coast (5S/12W-1E1, 4S/12W-25G5).

Table 1. Composition of selected waters in the study area, Los Angeles County, California

[USGS, U.S. Geological Survey; µS/cm, microsiemens per centimeter; <, less than; —, no data]

	Gardena-1 (3S/14W-13J8)	Lakewood-1 (4S/12W-5H10)	Huntington Park-1 (2S/13W-22C2)	Rio Hondo-1 (2S/12W-26D12)	Carson-1 (4S/13W-9H10)	Long Beach-1 (4S/12W-25G3)	Hawthorne-1 (3S/14W-17G5)	Wilmington-1 (4S/13W-28A6)	Pico Rivera-1 (2S/11W-18C4)	Commerce-1 (2S/12W-7J1)	Seawater[2]	San Gabriel River[3]	State Project	Colorado River
Specific conductance, µS/cm at 25°C	1,665	1,133	581	764	392	317	939	4,430	582	21,700	50,000	528	446	1,070
pH	7.3	7.4	7.8	7.5	8.2	8.8	7.8	7.6	8.0	7.5	—	7.5	8.1	8.3
Temperature, °C	22	21	20	19	24	22	25	22	23	22	—	—	—	14[5]
Dissolved oxygen, in mg/L	5	.4	.5	.3	.2	<.1	.2	.1	.05	<.1	—	—	—	10[5]
Alkalinity as CaCO$_3$, in mg/L	161	195	178	146	169	119	442	142	284	503	116	88	75	130
Residue on evaporation, in mg/L	1,160	739	363	484	230	209	549	2,703	370	12,820	34,500	331	246	679
MAJOR IONS, in mg/L														
Calcium	150	143	59	75	32	4	34	282	8	183	410	43	20	81
Magnesium	37	14	14	14	7	.0	21	96	3	144	1,350	12	12	30
Sodium	87	52	40	62	42	66	143	457	119	4,284	10,500	41	48	101
Potassium	5.4	4.5	3.4	4.0	2.4	.7	14	13	4.7	45	390	5.5	2.7	4.3
Chloride	370	210	22	69	21	12	50	1,209	4	7,071	19,000	51	64	87
Fluoride	.30	.16	.47	.45	.26	.66	.24	<.10	.31	.19	1.30	.21	.13	.35
Sulfate	53	44	82	121	<.1	15	1	288	5	4	2,700	77	40	292
Bromide	1.0	1.4	.11	.11	.078	.018	.11	4.6	.011	44	67	—	.21	.083
Iodide	.009	.089	.004	.020	.027	.009	.077	.79	.005	9.4	.060	—	—	.001[5]
Silica as SiO$_2$	29	24	22	22	22	20	34	26	30	31	6.4	—	14	8.6
NUTRIENTS, in mg/L														
Ammonia as N	.090	.50	<.020	<.020	.37	.17	2.4	2.2	2.0	27	—	.95	—	—
Nitrite plus nitrate as N	2.0	<.050	.11	2.9	<.050	<.050	<.050	.12	<.050	.029	—	2.17	1.92	.75
Orthophosphate as P	1.2	.21	.28	.028	.026	1.6	.22	.10	2.6	.86	.39	.39	—	—

Table 1. Composition of selected waters in the study area, Los Angeles County, California—Continued

	Shallow[1]		Forebay[1]		Native[1]		Coastal[1]		Pico unit[1]		Surface water		Imported water[4]	
	Gardena-1 (3S/14W-13J8)	Lakewood-1 (4S/12W-5H10)	Huntington Park-1 (2S/13W-22C2)	Rio Hondo-1 (2S/12W-26D12)	Carson-1 (4S/13W-9H10)	Long Beach-1 (4S/12W-25G3)	Hawthorne-1 (3S/14W-17G5)	Wilmington-1 (4S/13W-28A6)	Pico Rivera-1 (2S/11W-18C4)	Commerce-1 (2S/12W-7J1)	Seawater[2]	San Gabriel River[3]	State Project	Colorado River
TRACE ELEMENTS, in µg/L														
Barium	100	337	70	64	39	1	34	121	15	621	20	53	—	93[5]
Boron	117	91	133	202	102	88	486	221	603	6,532	4,500	200	160	124
Iron	5	145	<3	<10	7	<10	38	17	36	1,049	3	561	—	<10[5]
Lithium	14	—	<4	<4	5	5	12	—	34	148	170	—	—	—
Manganese	54	442	9	17	18	12	72	51	40	157	2	79	—	<3[5]
Strontium	1,200	1,331	470	476	369	25	415	3,688	122	4,227	7,975	—	—	918[5]
ISOTOPES														
Deuterium, in per mil	-42	-52	-47	-60	-47	-57	-46	-78	-65	-34	0	—	—	-98[5]
Oxygen-18, in per mil	-6.5	-7.8	-7.2	-8.4	-7.3	-8.6	-7.1	-9.8	-9.6	-5.9	0	—	—	-12.1[5]
Tritium, in TU	1.0	2.4	<.1	8.2	<.1	<.1	<.1	19	<.1	.3	—	—	—	11[5]

[1]From 'Geologic, hydrologic, and water-quality data from multiple-well monitoring sites in the Central and West Coast Basins, Los Angeles County, California' by Land, Everett, and Crawford, 2002, U.S. Geological Survey Open-File Report 01-277.

[2]From 'Study and interpretation of the chemical characteristics of natural water, 3d ed' by Hem, 1989, U.S. Geological Survey Water-Supply Paper 2254.

[3]From Los Angeles County Public Works, Watershed Management Division, Storm Water Quality Monitoring Report (http://www.ladpw.org/wmd/). Mean concentrations for the San Gabriel River (S14) Mass Emission Site, 1994–2000, accessed April 2002.

[4]Mean concentration for State Project [Devil's Canyon Afterbay (1974–2001)] and Colorado River water [Lake Mathews Headworks (1942–2001)], Hsiao Chiu Wang, Metropolitan Water District, written commun., 2002.

[5]USGS unpublished data (http://waterdata.usgs.gov/nwis/); sample collected at the Metropolitan Water District, West Basin, Cross-connection #37 on March 17, 1999 (Station ID: 334921118134101).
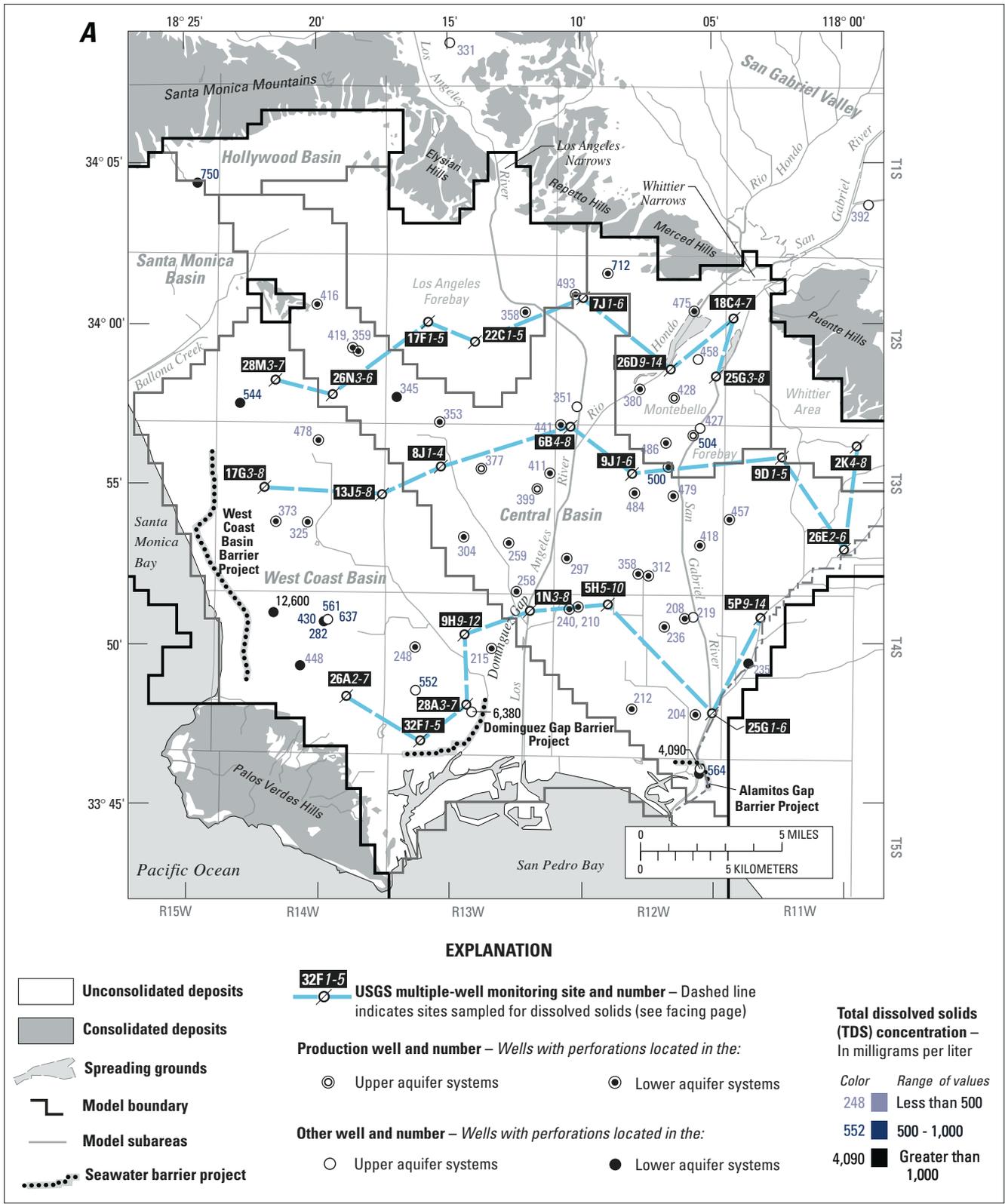
Figure 10. Distribution of dissolved-solids concentrations from sampled ground water (*A*) and boxplot of concentrations in ground water from the Upper and Lower aquifer systems, in the Central and West Coast Basins (*B*), Los Angeles County, California.

A, continued

Inglewood-1
-28M3-7

M7	921
M6	624
M5	861
M4	--
M3	4,340

Inglewood-2
-26N3-6

N6	--
N5	293
N4	1,480
N3	1,640

Los Angeles-1
-17F1-5

F5	641
F4	462
F3	377
F2	373
F1	351

Huntington Park-1
-22C1-5

C5	--
C4	658
C3	466
C2	353
C1	341

Commerce-1
7J1-6

J6	384
J5	556
J4	504
J3	457
J2	486
J1	12,200

Rio Hondo-1
26D9-14

D14	341
D13	355
D12	467
D11	450
D10	446
D9	280

Pico Rivera-1
18C4-7

C7	577
C6	649
C5	307
C4	362

Upper / Lower / Pico unit

Pico Rivera-2
25G3-8

G8	524
G7	503
G6	547
G5	494
G4	523
G3	455

EXPLANATION

USGS mulitple-well monitoring site and abbreviated number –

Name on top is common name

Boundary between Upper and Lower aquifer systems, where present

Well perforation

Boundary between Lower aquifer systems and Pico unit, where present

Aquifer systems grouping for geochemical analysis

-- No data

Hawthorne-1
-17G3-8

G8	2,060
G7	558
G6	484
G5	564
G4	765
G3	879

Gardena-1
-13J5-8

J8	977
J7	325
J6	324
J5	369

Willowbrook-1
-8J1-4

J4	347
J3	332
J2	319
J1	311

South Gate-1
-6B4-8

B8	413
B7	477
B6	447
B5	--
B4	308

Downey-1
-9J1-6

J6	811
J5	519
J4	529
J3	482
J2	344
J1	211

Santa Fe Springs-1
-9D1-5

D5	--
D4	771
D3	826
D2	781
D1	--

La Mirada-1
-26E2-6

E6	492
E5	429
E4	326
E3	264
E2	359

Whittier-1
-2K4-8

K7	669
K6	678
K8	1,490
K5	2,390
K4	2,540

Total dissolved-solids (TDS) concentration –
In milligrams per liter

Color	Range of values
248	Less than 500
552	500 - 1,000
4,090	Greater than 1,000

Lomita-1
-26A2-7

A7	--
A6	1,110
A5	686
A4	715
A3	844
A2	300

Wilmington-2
-32F1-5

F5	9,760
F4	1,990
F3	335
F2	1,370
F1	515

Wilmington-1
-28A3-7

A7	789
A6	2,470
A5	1,720
A4	787
A3	490

Carson-1
-9H9-12

H12	574
H11	320
H10	230
H9	206

Long Beach-2
-1N3-8

N8	1,190
N7	840
N6	293
N5	248
N4	280
N3	200

Lakewood-1
-5H5-10

H10	610
H9	256
H8	278
H7	247
H6	206
H5	181

Long Beach-1
-25G1-6

G6	742
G5	1,630
G4	232
G3	196
G2	208
G1	202

Cerritos-1
-5P9-14

P14	278
P13	274
P12	278
P11	308
P10	263
P9	282

Figure 10.—Continued.

B

Figure 10.—Continued.

In the West Coast Basin, the median value for TDS in water from wells perforating the Upper aquifer systems is 843 mg/L (fig. 10B). All of these wells exceed the Secondary Maximum Contaminant Level (SMCL) of 500 mg/L for TDS set by the U.S. Environmental Protection Agency (U.S. Environmental Protection Agency, 1996). The median value for TDS in the Lower aquifer systems of the West Coast Basins is 534 mg/L. In general, TDS concentrations are lower in the interior part of the basin near the NIU, and appear to increase toward the coast. Most wells in the first quartile of this group cluster near Dominguez Gap (fig. 10A)(such as 4S/13W-9H9; 207 mg/L). High outlying values in the West Coast Basin group are commonly found for wells located near the coast, such as 4S/14W-9D1 and 4S/13W-27E2. Water from all wells at Inglewood-1 and Lomita-1 monitoring sites exceed the SMCL.

Dissolved-solids measurements from the Pico unit are limited and vary with respect to depth and location. For example, in the relatively shallow portion of the Pico unit, wells 2S/11W-18C4 and 4S/13W-1N3 yield relatively fresh water (362 and 200 mg/L, respectively) (fig. 10B). In the relatively deeper portion of the Pico unit, however, wells 2S/12W-7J1 and 2S/14W-28M3 yield relatively saline water (12,200 and 4,340 mg/L, respectively). These results are consistent with earlier observations in the basin (Piper and Garrett, 1953; Zielbauer and others, 1962).

General Chemical Character

The major-ion data for all ground-water samples collected for this study are summarized in the trilinear diagrams in figure 11. Piper and Garrett (1953) used trilinear diagrams to study the occurrence of native, blended, and contaminated ground water in earlier investigations of the Los Angeles area. The diagram shows the relative contribution of major cations and anions (on a charge equivalent basis) as a percentage of the total ion content of the water (Piper, 1944). In this report, the dominant cation and anion species are used to describe the chemical character—or hydrochemical facies (Knobel and others, 1998)—of a water sample. Where no one species exceeds 50 percent, the first and second most abundant ions are given for description purposes. For example, water from well 4S/13W-28A6 is termed a sodium/calcium-chloride type.

Major ion data in figure 11A is grouped according to TDS concentrations. Water containing more than 1,000 mg/L TDS is characterized principally by sodium and chloride ions. Water containing dissolved solids from 500 mg/L to 1,000 mg/L displays a mixed composition, typically a calcium-bicarbonate or calcium/sodium-bicarbonate/chloride character. Water containing less than 500 mg/L TDS shows the broadest range of chemical composition, collectively a calcium-bicarbonate/sulfate to calcium-bicarbonate to sodium-bicarbonate character. Of this group, water dominated by sodium and bicarbonate ions is located away from the forebay area and generally is lower in TDS.

Major ion data in figure 11B is grouped according to depth. Distinct ground-water compositions are not always exclusive to a particular aquifer system, or region. In general, wells yielding water of calcium-bicarbonate or calcium-bicarbonate/sulfate composition are perforated in the Upper aquifer systems or are located in or near the forebay areas. Wells yielding water of calcium/sodium-bicarbonate or sodium-bicarbonate composition typically are perforated in the Lower aquifer systems or are located away from areas of recharge. Wells perforated in the Pico unit, with the exception of 2S/12W-7J1 (Commerce-1; see fig. 11C), also yielded water of sodium-bicarbonate composition. Wells yielding water of sodium-chloride composition are located near the coast and are perforated in the Upper or Lower aquifer systems.

Central Basin

Historically, the main sources of water in the Montebello Forebay were the San Gabriel River and Rio Hondo, subsurface flow through the Whittier Narrows, and local precipitation. Water currently utilized for spreading consists of seasonally varying proportions of local runoff, imported water [Colorado River and (or) State Water Project], and, increasingly, reclaimed water. Values for dissolved solids in the Montebello Forebay are considerably higher now than during the 1930s and 1940s (typically less than 300 mg/L; Poland and others, 1956, 1959), suggestive of the long-term effects of artificial-recharge operations.
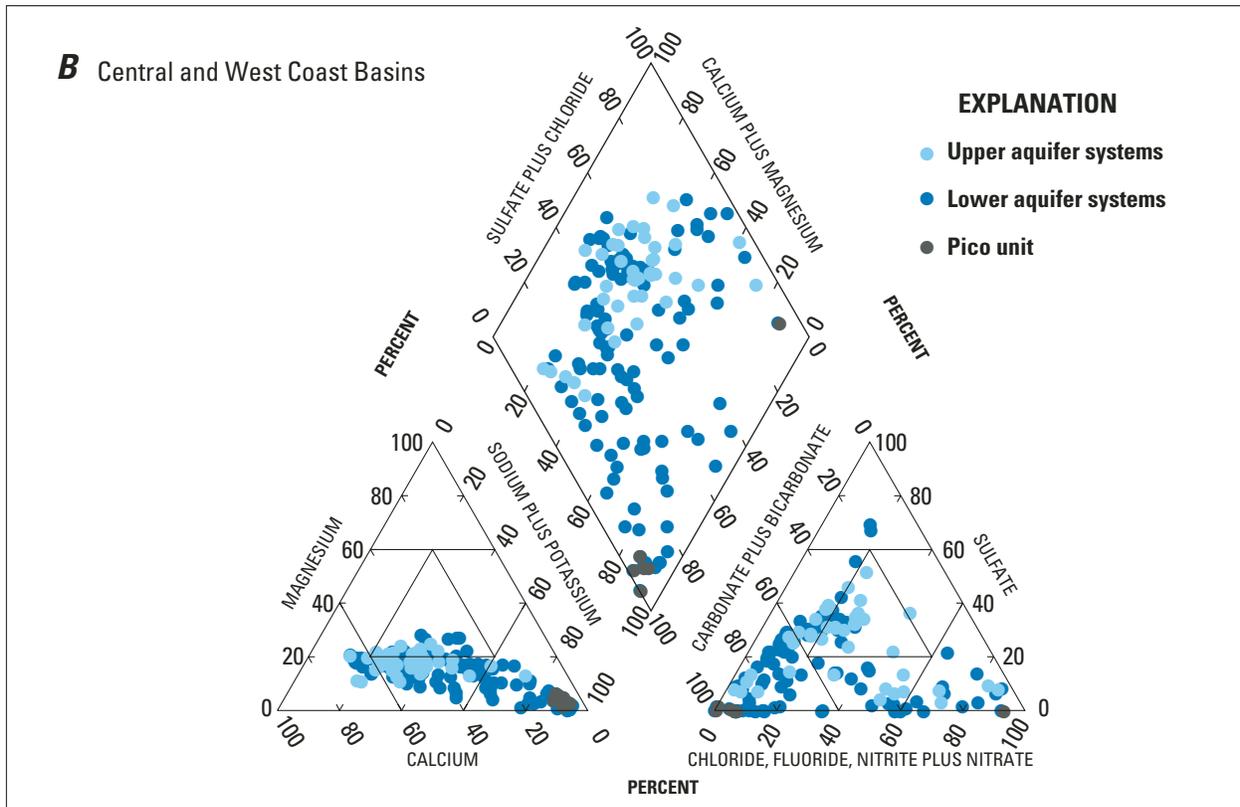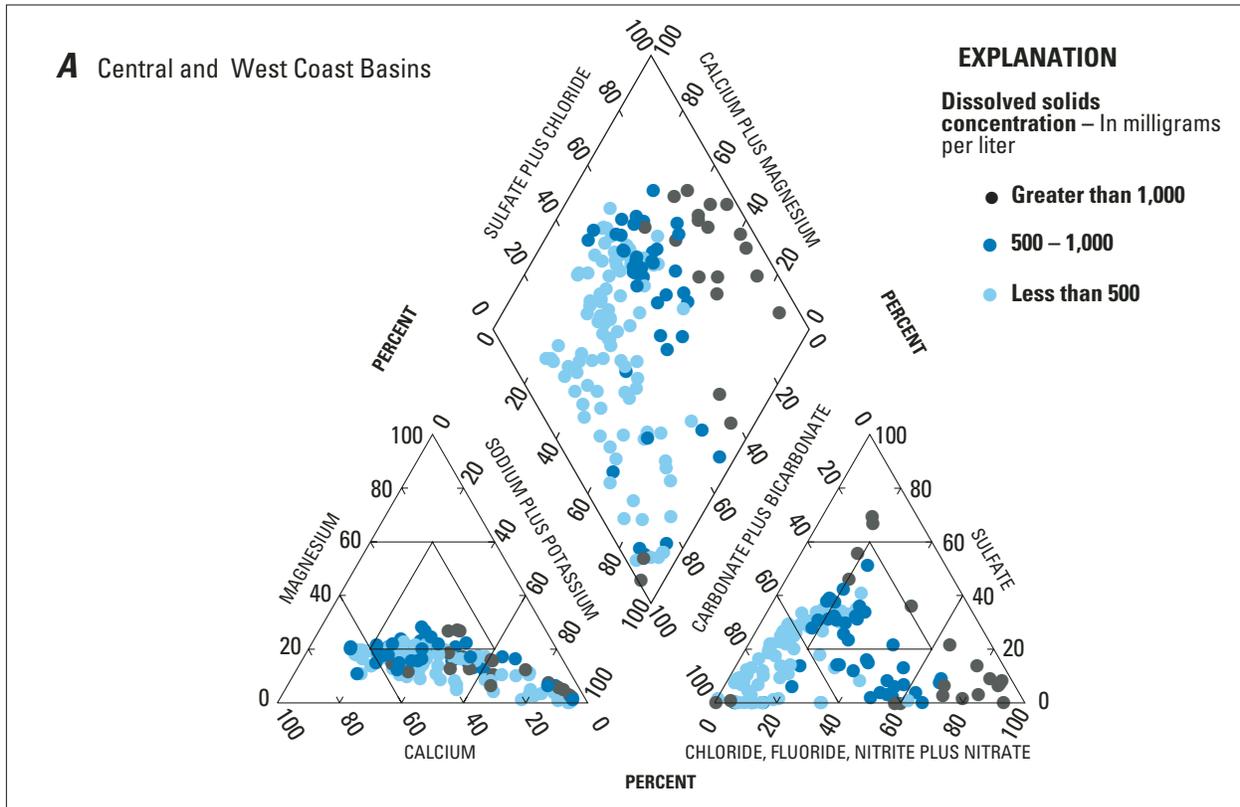
Figure 11. General chemical character of ground water sampled in the Central and West Coast Basins with grouping by total dissolved solids concentration (*A*), grouping by aquifer systems (*B*), and labelling of selected wells (*C*), Los Angeles County, California.

C

STATE WELL NUMBERS FOR SELECTED WELLS SHOWN IN FIGURES 11A AND B

A. 2S/14W-31H1
B. 3S/14W-13J5
C. 3S/14W-13J6
D. 3S/14W-13J7
E. 3S/14W-13J8
F. 3S/14W-21M1
G. 3S/14W-22L1
H. 4S/13W-15A11
I. 4S/13W-28A3
J. 4S/13W-28A4
K. 4S/13W-32F3
L. 4S/13W-9H9
M. 4S/13W-9H10
N. 4S/13W-9H11
O. 4S/14W-15N1
P. 4S/14W-2N1
Q. 4S/14W-2N2

1. 2S/11W-18C4
2. 2S/11W-18C5
3. 2S/12W-26D9
4. 2S/12W-31H2
5. 2S/13W-11R4
6. 2S/13W-17F1
7. 2S/13W-17F2
8. 2S/13W-17F5
9. 2S/13W-22C2
10. 2S/13W-22C4
11. 2S/13W-31C3
12. 3S/11W-19E2
13. 3S/11W-2K4
14. 3S/11W-2K7
15. 3S/12W-14F1
16. 3S/12W-6B4
17. 3S/12W-6B6
18. 3S/12W-6B7
19. 3S/12W-9J1
20. 3S/12W-9J3
21. 3S/12W-9J4
22. 3S/12W-9J5
23. 3S/13W-10L3
24. 3S/13W-8J1
25. 3S/13W8J2
26. 4S/12W-25E1
27. 4S/12W-25G1
28. 4S/12W-25G2
29. 4S/12W-25G3
30. 4S/12W-25G5
31. 4S/12W-28H1
32. 4S/12W-5H9
33. 4S/12W-5H10

Figure 11.—Continued.

Data from the Pico Rivera-1 and Rio Hondo-1 (2S/11W-18C4–7 and 2S/12W-26D9–14, respectively) monitoring sites show significant differences in chemical character with depth (fig. 11). Calcium-bicarbonate/sulfate type water, common in the Upper aquifer systems, was not observed in parts of the Lower aquifer systems or the Pico unit. In other parts of the Lower aquifer systems, such as 2S/11W-18C5 (307 mg/L TDS), calcium-bicarbonate water is present (fig. 11). Farther downgradient, water yielded by 2S/12W-26D9 (280 mg/L TDS, the lowest observed value in the Montebello Forebay) grades to a calcium/sodium-bicarbonate composition. Water from well 2S/11W-18C4 (362 mg/L TDS) had a strongly sodium-bicarbonate character typical of most water from the Pico unit.

As noted earlier, the Los Angeles Forebay differs from the Montebello Forebay in that there is no artificial ground-water recharge program in place. Changes in chemical character, though more subtle, occur with depth and reflect this difference. Water from the Lower aquifer systems (wells 2S/13W-17F2, 2S/13W-22C2) has a calcium-bicarbonate character and is relatively low in TDS (373, 353 mg/L, respectively); in deeper parts (well 2S/13W-11R4) water has a calcium/sodium-bicarbonate character. Water observed at these locations resembles native water of the Los Angeles Forebay as described by Poland and others (1956, 1959) in terms of overall chemical composition and range of dissolved solids. In contrast, relatively shallow monitoring wells at the Los Angeles-1 (2S/13W-17F5; 641 mg/l TDS) and Huntington Park-1 (2S/13W-22C4; 658 mg/L TDS) sites indicate calcium-bicarbonate/chloride and calcium-bicarbonate/sulfate water, respectively, is present. A possible explanation for these differences might be a long-term shift or degradation in the water quality of the Los Angeles River.

In the Central Basin Pressure Area, calcium/sodium-bicarbonate water is commonly present downgradient of the Los Angeles Forebay (wells 3S/13W-8J2, 3S/13W-10L3, 2S/13W-31C3, and 2S/12W-31H2) but is limited to a few deep wells downgradient of the Montebello Forebay (3S/12W-6B4, 3S/12W-9J1). This water is relatively low in TDS (211–377 mg/L) and is quite similar to native water described by Poland (1959). Most wells sampled downgradient from the Montebello Forebay yielded calcium-bicarbonate/sulfate water (3S/12W-6B6–7, 3S/12W-9J3–5, 3S/12W-14F1, and 3S/11W-19E2) containing 447–529 mg/L TDS (fig. 10A, 11).

In the Whittier Area, data collected from the Whittier-1 monitoring site indicate water is generally higher in dissolved solids than elsewhere in the Central Basin; TDS values increase significantly with depth (see fig. 10A). The chemical character within the Lower aquifer systems grades with depth from mixed cation-bicarbonate (3S/11W-2K7) to sodium-sulfate (3S/11W-2K4). This sulfate-rich water was not observed elsewhere in the study area.

Further downgradient in the Central Basin Pressure Area, nearly all wells sampled, especially those at the Lakewood-1 (4S/12W-5H59) monitoring site, contained water that ranges from a calcium-bicarbonate to calcium/sodium-bicarbonate to sodium-bicarbonate composition. Calcium-rich water from this group differs from the calcium-rich water in (or near) the Montebello Forebay in that dissolved sulfate and dissolved solids are relatively low. Additionally, the ratio of calcium to sodium generally decreases with depth. Monitoring wells (4S/12W-25G1–3) at the Long Beach-1 site and a few nearby production wells (4S/12W-25E1 and 4S/12W-28H1) perforating Lower aquifer systems yielded sodium-bicarbonate water that was notably warm, tan-yellow colored, and among the lowest in TDS (196–212 mg/L).

In the Central Basin Pressure Area, water in parts of the Upper aquifer systems is distinguished as having a calcium-chloride character. At well 4S/12W-5H10 (Lakewood-1 #6; 610 mg/L TDS) (fig. 10A), this composition likely results from local recharge to the Upper aquifer systems. In comparison, a similar chemical character at well 4S/12W-25G5 (Long Beach-1 #5; 1,630 mg/L TDS) is attributed to an influx of seawater or other brine water.

West Coast Basin

The chemical character of water in the West Coast Basin varies considerably with respect to depth and distance from the coast. In the interior of the West Coast Basin, as in the Central Basin, TDS content generally decreases with depth. Calcium/sodium-chloride water from Gardena-1 (3S/14W-13J8), perforating the Upper aquifer systems, contained 977 mg/L TDS. Data collected from wells at the Gardena-1 and Carson-1 (3S/14W-13J7, 4S/13W-9H11, respectively) monitoring sites indicate that the top part of the Lower aquifer systems contains calcium-bicarbonate water, also low in TDS (325 and 320 mg/L, respectively) (fig. 10A). The chemical composition of this water is similar to that of several upgradient wells (especially at the Willowbrook-1 site) across the NIU. At greater depths in the Lower aquifer systems, the composition of water shifts from calcium/sodium-bicarbonate (4S/13W-9H10 and 4S/13W-13J6) to sodium-bicarbonate (4S/13W-9H9 and 4S/13W-17D2). The sodium-bicarbonate character of water from Gardena-1 #1 (3S/14W-13J5) in the lower San Pedro Aquifer system is distinguished from other deep water by a moderate sulfide odor and significant concentrations of dissolved ammonia 5.8 mg/L as N), indicating reducing ground-water conditions. This water is similar to native water across the NIU (3S/13W-8J1) but differs from deep water in the Los Angeles Forebay (2S/13W-11R4 and 2S/13W-17F1).

The chemical character of water near the coast is influenced by the variety of water sources, including the ocean and the seawater-barrier projects. Wells sampled within approximately 4 mi of the coast had TDS ranging from 282 to more than 12,600 mg/L. Of these, water from wells 4S/14W-2N1–2, and -15N1; 3S/14W-21M1 and -22L1; 2S/14W-31H1; and 4S/13W-32F3 is calcium/sodium-bicarbonate to sodium-bicarbonate in character with TDS ranging from 282 to 544 mg/L. The sodium-bicarbonate water noted in well 4S/14W-15N1 (Upper San Pedro Aquifer system) is similar to native water observed locally in the Silverado aquifer by Poland (1959). Most other wells near the coast yield water that is primarily comprised of sodium and chloride ions and typically exceeds 1,000 mg/L TDS. At the USGS Wilmington-1 monitoring site, however, wells 4S/13W-28A3 and -28A4, perforated in the Lower aquifer systems, yielded sodium-chloride type water, but with only 490 and 787 mg/L TDS, respectively (fig. 10A).

Dissolved Chloride

Dissolved chloride in ground water is generally unreactive and attributable to both natural and anthropogenic processes. Chloride concentrations in water from sampled wells ranged from 4 to more than 7,000 mg/L (fig. 12). Chloride concentrations correlate strongly ($R^2 = 0.98$) with TDS and are higher in wells near the coast, near uplifted basin margins, and in selected shallow wells. The SMCL for chloride is 250 mg/L (U.S. Environmental Protection Agency, 1996).

In the Central Basin, the median chloride value for water in the Upper aquifer systems is about 60 mg/L. In the Lower aquifer systems the median value is 30 mg/L. Relatively higher chloride water is present in a pair of wells in the Whittier Area (3S/11W-2K4 and -2K5; 280 and 240 mg/L, respectively) (fig. 12).

In the West Coast Basin the median chloride values for the Upper and Lower aquifer systems are 300 and 95 mg/L, respectively. Near the coast, water from wells 4S/13W-27E2 and -32F5, and 4S/14W-9D1 contain significant dissolved chloride (3,200, 5,200, and 6,800 mg/L, respectively). A two-part mixture between native West Coast Basin ground water (table 1) and seawater yields partial seawater compositions of 17, 27, and 35 percent for these wells. However, there may be other sources of high-chloride water besides seawater—including water from shallow or semi-perched aquifers (Piper and Garrett, 1953), water from applied irrigation (Izbicki, 1991), water from fine-grained marine deposits, and water from the dissolution of evaporite minerals. Chemical data for some of these sources are given in table 1.

Figure 12. Dissolved-chloride concentration in ground water sampled in the study area, Los Angeles County, California.
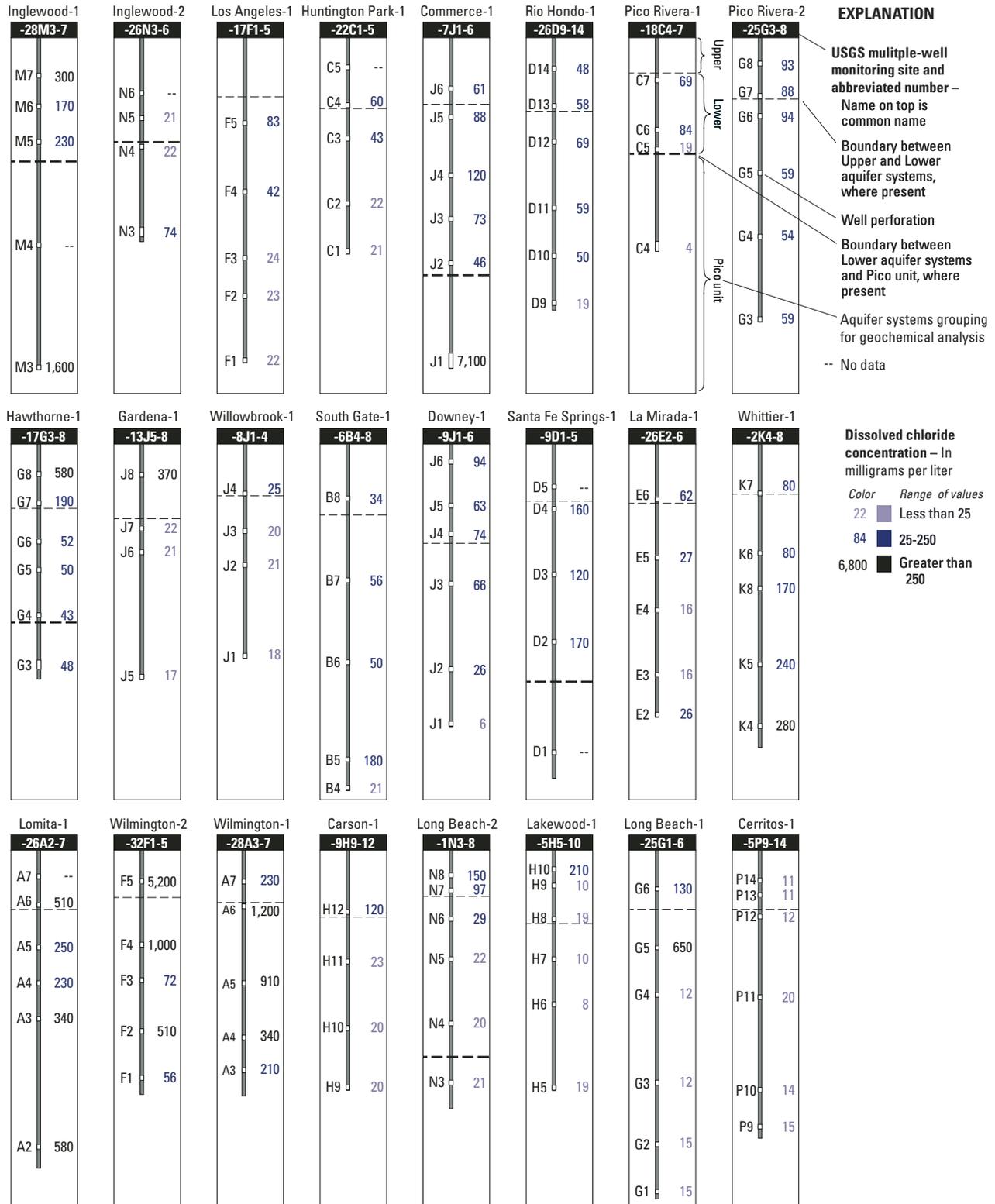
Figure 12.—Continued.

Dissolved Oxygen

Dissolved oxygen is supplied to the ground-water system by the infiltration of recharge water and by the movement of air throughout the unsaturated zone above the water table (Hem, 1992). Surface water may contain significant dissolved oxygen, depending on the temperature and, to a lesser extent, source. Decomposable organic material (especially peat or lignite) is abundant in coastal aquifers and will react, in the presence of certain bacteria, with dissolved oxygen in the ground water (Hem, 1992). In the Central and West Coast Basins, dissolved-oxygen concentrations range from less than measurable to almost 6 mg/L; 80 percent of the values are less than 1 mg/L (fig. 13).

The median value for dissolved oxygen in the Upper aquifer systems of the Central Basin is 0.3 mg/L. In most of the Central Basin, including the Los Angeles Forebay, concentrations decrease with depth and (or) with increasing distance downgradient (fig. 13). In and near the Montebello Forebay, however, dissolved-oxygen concentrations appear to increase with depth. For example, dissolved oxygen in most water collected from the Upper aquifer systems is low (less than 1 mg/L). Such concentrations have been attributed to the rapid microbial oxidation of nutrient-rich reclaimed wastewater (Leenheer and others, 2001) that currently averages about one-third of the artificially spread water. In contrast, dissolved oxygen is much higher in parts of the Lower aquifer systems (2S/12W-25G35) and near the Montebello Forebay (3S/12W-6B5 and -9J2 and 3S/11W-19E2) (fig. 13). Artificial recharge containing a greater percentage of imported water during the 1960s may account for these higher concentrations. In the distal part of the Central Basin Pressure Area, dissolved oxygen is usually low or less than measurable (3S/13W-26N5 and 4S/12W-5H6).

Dissolved-oxygen concentrations in the West Coast Basin are much less variable than those in the Central Basin. The median value for water in the Upper and Lower aquifer systems is 0.1 mg/L; most wells contain concentrations that are less than measurable. High outlying values are associated with water from relatively shallow wells and may result from the infiltration of local precipitation (3S/14W-13J8, 2S/14W-28M7) or from the injection of imported water (4S/13W-28A7) along the coast (fig. 13).

Dissolved Sulfate

Sulfate, unlike chloride, is not conservative and is controlled by redox conditions in the ground-water system. Dissolved sulfate in ground water is commonly attributed to dissolution of evaporites (for example, gypsum) or oxidation of pyrite minerals. Dissolved-sulfate concentrations exceeding 250 mg/L are an aesthetic concern (U.S. Environmental Protection Agency, 1996) and occur in 7 percent of all wells sampled during this study (fig. 14). Locally, sources of high-sulfate water include seawater, applied irrigation water, and imported Colorado River water (table 1).

Dissolved-sulfate concentrations range from less than measurable (0.1 mg/L) to 1,300 mg/L (fig 14). In the Central Basin, the median value for sulfate is 110 mg/L in the Upper aquifer systems and 74 mg/L the Lower aquifer systems; concentrations do not always decrease with increasing depth. Sulfate concentrations generally decrease away from the forebays. In distal parts of the Central Basin Pressure Area, the decrease in sulfate concentrations is abrupt (see, for example, 2S/14W-26N5, 3S/13W-8J1, and 4S/12W-5H7, and -1N4) because little or no artificially recharged water is present. Very low or less than measurable sulfate in the study area is also consistent with sulfate reduction, a microbially mediated process that occurs in the absence of dissolved oxygen (Piper, 1953; Drever, 1988). The reduction of dissolved sulfate significantly influences water quality in portions of the study area.

Very high values of sulfate in the Central Basin were measured in water from wells at several depths in the Whittier Area (3S/11W-2K45, -2K8) (fig. 14). Near the Alamitos Gap Barrier Project, seawater may be a source of high sulfate to well 4S/12W-25G5. Other locations that exceed the SMCL (250 mg/L) include a shallow monitoring well at Downey-1 (3S/12W-9J6) and at the Long Beach-2 site along the Los Angeles River (4S/13W-1N78), near the NIU.

THIS PAGE INTENTIONALLY LEFT BLANK
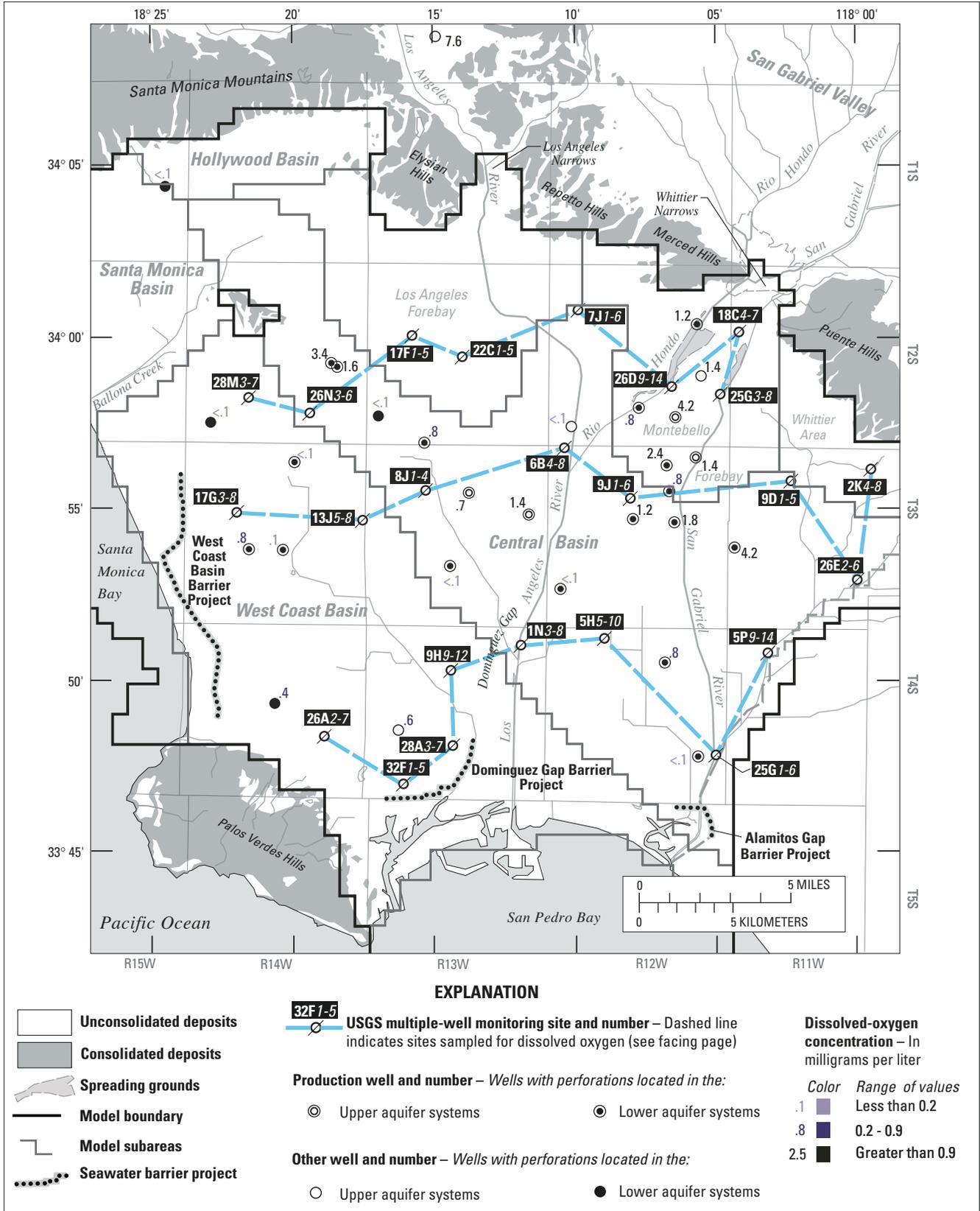
Figure 13. Dissolved-oxygen concentrations in ground water sampled in the study area, Los Angeles County, California.

Inglewood-1 -28M3-7
M7 3.4
M6 .2
M5 .1
M4 --
M3 <.1

Inglewood-2 -26N3-6
N6 --
N5 <.1
N4 <.1
N3 <.1

Los Angeles-1 -17F1-5
F5 2.6
F4 .5
F3 --
F2 .4
F1 .4

Huntington Park-1 -22C1-5
C5 --
C4 1.3
C3 1.7
C2 .5
C1 .2

Commerce-1 -7J1-6
J6 5.7
J5 4.8
J4 .6
J3 .3
J2 <.1
J1 <.1

Rio Hondo-1 -26D9-14
D14 .3
D13 .3
D12 .3
D11 .9
D10 .6
D9 .2

Pico Rivera-1 -18C4-7
C7 .3
C6 .2
C5 .2
C4 .1

Pico Rivera-2 -25G3-8
G8 .1
G7 .2
G6 .1
G5 3.5
G4 3.3
G3 2.5

Upper / Lower / Pico unit

EXPLANATION

USGS mulitple-well monitoring site and abbreviated number –
Name on top is common name
Boundary between Upper and Lower aquifer systems, where present
Well perforation
Boundary between Lower aquifer systems and Pico unit, where present
Aquifer systems grouping for geochemical analysis

< Less than
-- No data

Dissolved oxygen concentration –
In milligrams per liter (mg/L)

Color	Range of values
.1	Less than .2
.9	.2 - .9
2.5	Greater than .9

Hawthorne-1 -17G3-8
G8 .2
G7 <.1
G6 .2
G5 .2
G4 <.1
G3 <.1

Gardena-1 -13J5-8
J8 6.0
J7 .8
J6 .5
J5 <.1

Willowbrook-1 -8J1-4
J4 .2
J3 .4
J2 .2
J1 .1

South Gate-1 -6B4-8
B8 .2
B7 .3
B6 4.1
B5 2.5
B4 .2

Downey-1 -9J1-6
J6 .2
J5 .2
J4 .2
J3 3.2
J2 3.3
J1 .2

Santa Fe Springs-1 -9D1-5
D5 --
D4 <.1
D3 <.1
D2 --
D1 --

La Mirada-1 -26E2-6
E6 .3
E5 .2
E4 .1
E3 <.1
E2 .1

Whittier-1 -2K4-8
K7 1.2
K6 .9
K8 .6
K5 .6
K4 .5

Lomita-1 -26A2-7
A7 --
A6 .1
A5 <.1
A4 <.1
A3 --
A2 .2

Wilmington-2 -32F1-5
F5 <.1
F4 <.1
F3 <.1
F2 <.1
F1 <.1

Wilmington-1 -28A3-7
A7 <.2
A6 .2
A5 <.2
A4 .2
A3 .2

Carson-1 -9H9-12
H12 .2
H11 .3
H10 .2
H9 <.1

Long Beach-2 -1N3-8
N8 .4
N7 .6
N6 .8
N5 <.1
N4 .2
N3 <.1

Lakewood-1 -5H5-10
H10 .2
H9 .3
H8 .2
H7 .2
H6 <.1
H5 <.1

Long Beach-1 -25G1-6
G6 .1
G5 .5
G4 .5
G3 <.1
G2 .1
G1 <.1

Cerritos-1 -5P9-14
P14 .2
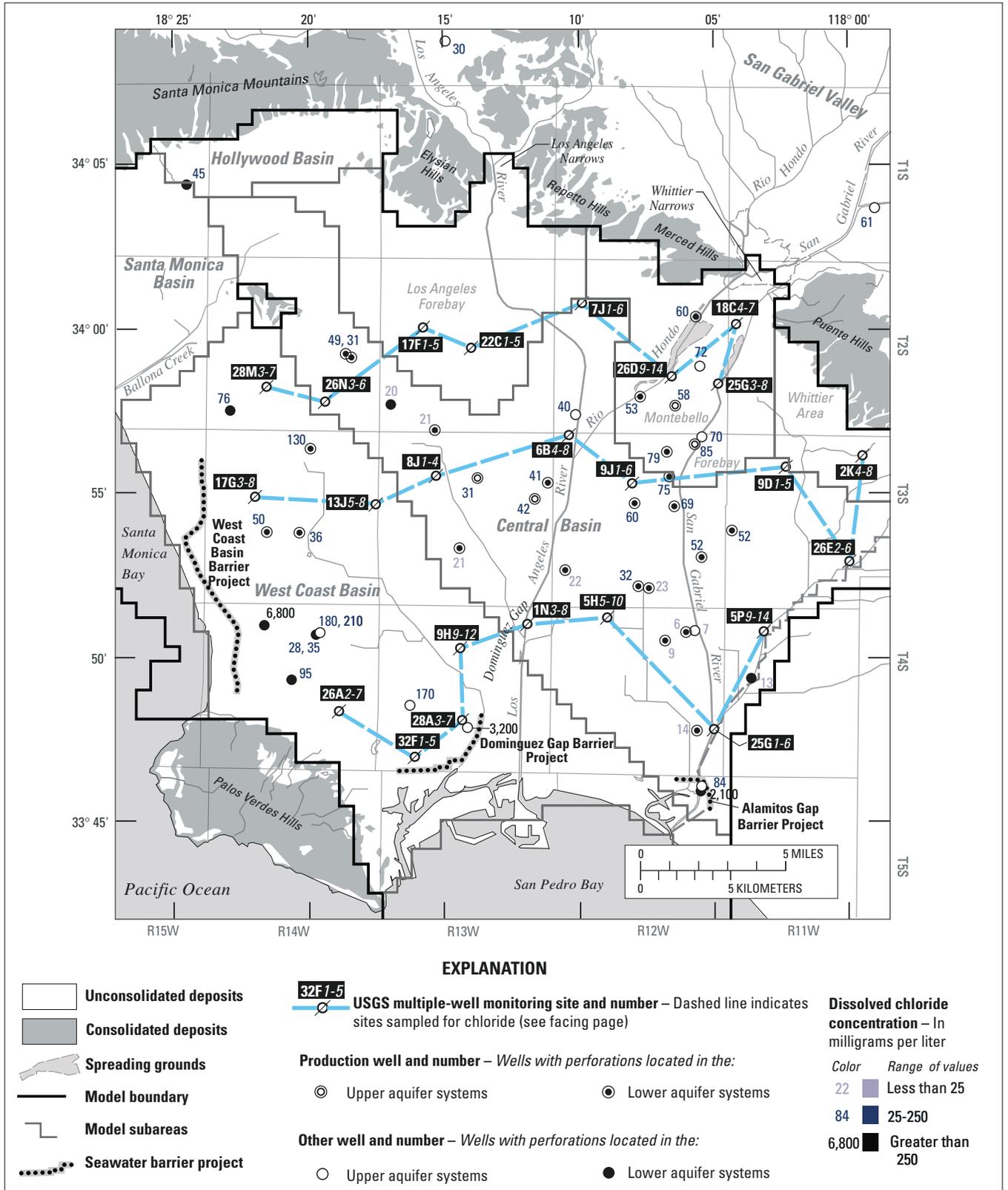P13 .2
P12 .3
P11 .6
P10 .2
P9 .2

Figure 13.—Continued.

Figure 14. Dissolved sulfate concentrations in ground water sampled in the study area, Los Angeles County, California.
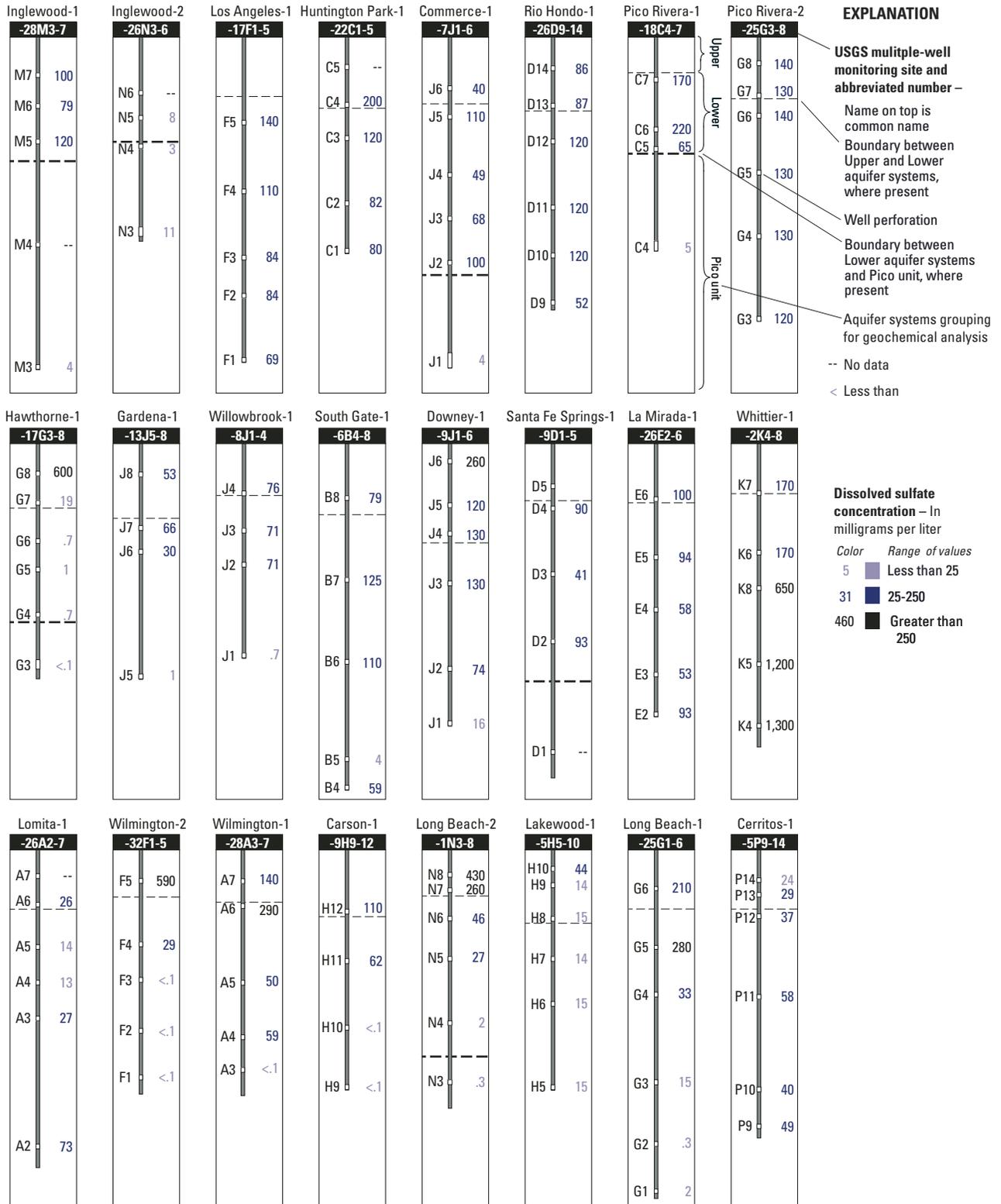
Figure 14.—Continued.

Sulfate concentrations are relatively low throughout most of the West Coast Basin, with median values of 100 and 14 mg/L in the Upper and Lower aquifer systems, respectively. Concentrations vary considerably in the Upper aquifer systems and, along the coast, exceed the SMCL (250 mg/L) in water from wells 3S/14W-17G8, 4S/14W-9D1, and 4S/13W-27E2. In the Lower aquifer systems, less than measurable sulfate concentrations occur in water from several wells (3S/14W-17G3 and 4S/13W-9H9, -28A3, and -32F3). A rotten egg odor, presumed to be hydrogen sulfide gas, was observed in water outgassing from these and other wells in deep parts of the study area. Sulfide, generated as a product of sulfate reduction, also is indicative of strongly reducing ground-water conditions.

Dissolved Manganese

Dissolved manganese in the study area generally is present as Mn^{+2} and controlled by the redox condition of the ground water (Hem, 1992). Concentrations range from less than 1 g/L to more than 1,000 g/L. About 40 percent of the sampled wells yielded water exceeding the SMCL, which is set, for aesthetic reasons, at 50 g/L (U.S. Environmental Protection Agency, 1996).

The median value for manganese in the West Coast Basin (72 g/L) was higher than in the Central Basin (30 g/L). The median value for the Upper aquifer systems (76 g/L) was higher than in the Lower aquifer systems (26 g/L). The data indicate a general pattern of increasing concentrations along flowpaths. Relatively low (less than 5 g/L) concentrations of manganese were found in the forebay areas and in Lower aquifer systems wells several miles downgradient from the Montebello Forebay. Low manganese concentrations are expected under oxic conditions. Relatively high (greater than 50 g/L) concentrations of manganese were found in most water from the Upper aquifer systems outside the forebays and in the Lower aquifer systems along the coast, in the Whittier area, and in the southeast part of the Central Basin Pressure Area. Higher concentrations are expected in the absence of dissolved oxygen prior to the reduction of iron-oxidized minerals (Berner, 1981). Particularly high manganese concentrations were measured in water

from several wells in the Central Basin (4S/12W-5H8, 3S/11W-26E5, and 4S/11W-25G5) and the West Coast Basin (3S/14W-17G8 and -13J6, and 2S/14W-28M5) (fig. 8).

Dissolved Iron

Iron, like dissolved oxygen and sulfate, is not conservative in the ground-water flow system. Dissolved iron in ground water is controlled by pH and redox conditions and is dependent on iron-bearing minerals in the aquifer (Hem, 1992). In the study area, concentrations ranged from less than 3 g/L to more than 1,000 g/L. The SMCL for dissolved iron is set at 300 g/L (U.S. Environmental Protection Agency, 1996).

Iron exceeded the limit in only 6 percent of all measured samples. These samples were collected from wells near the coast (4S/13W-27E2 and 4S/14W-2N4), in deep portions of the Whittier area (3S/11W-2K4–5), or in the Pico unit (2S/14W-28M3 and -26N3, and 2S/12W-7J1) (fig. 8).

The median value for iron in wells sampled in the West Coast Basin was 38 g/L; concentrations generally were more variable in the Upper aquifer systems than in the Lower aquifer systems. The median value in the Central Basin was 22 g/L; higher concentrations (30–300 μg/L) were found in portions of the Upper aquifer systems.

Isotopic Composition of Ground Water

Isotopes help yield interpretations that may not be apparent from traditional chemical or hydrologic data. In this study, isotopes were used to evaluate the source of ground-water recharge, ground-water movement, and relative residence time of water within the aquifer systems in the study area.

Deuterium and Oxygen-18

Oxygen-18 and deuterium (hydrogen-2) are stable isotopes of oxygen and hydrogen. These isotopes are heavier than the common oxygen and hydrogen isotopes (oxygen-16 and hydrogen-1, respectively) and, as a result, show slightly different physical and chemical behavior.

The isotopic composition of water is measured as a ratio (for example, oxygen-18/oxygen-16 or deuterium/hydrogen) and is expressed in terms of per mil (parts per thousand) differences (delta oxygen-18, $\delta^{18}O$, or delta deuterium, δD) from the international standard composition of ocean water, known as Vienna Standard Mean Ocean Water (VSMOW) (Gonfiantini, 1984). Differences are computed as:

$$\{(Ratio_{sample}/Ratio_{VSMOW}) - 1\} \cdot 1,000$$

By convention, VSMOW has δD and $\delta^{18}O$ values equal to 0.0 per mil. Water that has an isotopic ratio less than VSMOW will have a negative δD value and is depleted in deuterium relative to the ocean-water standard.

The δD values for all wells sampled in the study area are shown in figure 15. δD values ranged from -34 per mil (near the West Coast Basin barrier project) to -88 per mil (near the Alamitos Gap Barrier Project). Isotopically light water (δD more negative than -50 per mil) was generally observed in the eastern half of the study area; isotopically heavy water (δD less negative than -50 per mil) was observed in the western half of the study area. Isotopic fractionation and mixing are two processes that affect the stable-isotope composition of ground water.

Changes to δD and $\delta^{18}O$ of water as a result of isotopic fractionation typically occur prior to recharge. When water evaporates or condenses, slight differences in mass preferentially cause more of the lighter isotopes to partition into the less dense phase. These changes do not readily occur in low-temperature ground-water systems. Changes to δD and $\delta^{18}O$ of water as a result of mixing require two or more isotopically distinct sources of water. δD and $\delta^{18}O$ are conservative in mixing; a binary mixture will therefore produce an isotopic composition proportional to each source.

Since most precipitation in the study area originates from evaporation of seawater, δD and $\delta^{18}O$ values of precipitation are linearly correlated and can be plotted along a line referred to as the meteoric water line (Craig, 1961). In figure 16A, as one moves up the meteoric water line, one moves from isotopically lighter water (more negative δD and $\delta^{18}O$) to isotopically heavier water (less negative δD and $\delta^{18}O$). The isotopic composition of samples relative to each other and to the meteoric water line provides information on source and evaporative effects of the water (Mazor, 1991; Izbicki, 1996).

The isotopic composition of precipitation is highly variable and dependent on meteorological factors including—air mass source, temperature, elevation, proximity to the coast, and rainout effects (Williams and Rodini, 1997; Kendall and McDonnell, 1998). Large, short-term variations in the isotopic composition of precipitation (which becomes ground-water recharge) are eventually dampened by dispersion within the ground-water system yielding a well-averaged composition that relates to a particular source of recharge (Clark and Fritz, 1997). On a regional scale, water condensing at cooler temperatures (or higher elevations) is isotopically lighter then water condensing at warmer temperatures (or lower elevations).

In figure 16A, δD and $\delta^{18}O$ data for sampled wells indicate that a range of isotopic compositions is present in both ground-water basins. Most ground water ranges from -37 to -64 per mil δD. Imported Colorado River and State Project water sampled as part of this study has a lighter isotopic composition (about -100 and -73 per mil δD, respectively) and plots substantially below the meteoric water line (fig. 16A) due to extensive evaporation (Williams and Rodini, 1997).

Central Basin

In the Central Basin, δD for water in sampled wells ranged from -34 to -88 per mil (fig. 16). Most samples having an isotopic composition that plots above the meteoric line cluster into two groups of values based on geographic regions within the basin. These differences indicate that, historically, separate sources of recharge have existed for each forebay in the Central Basin.
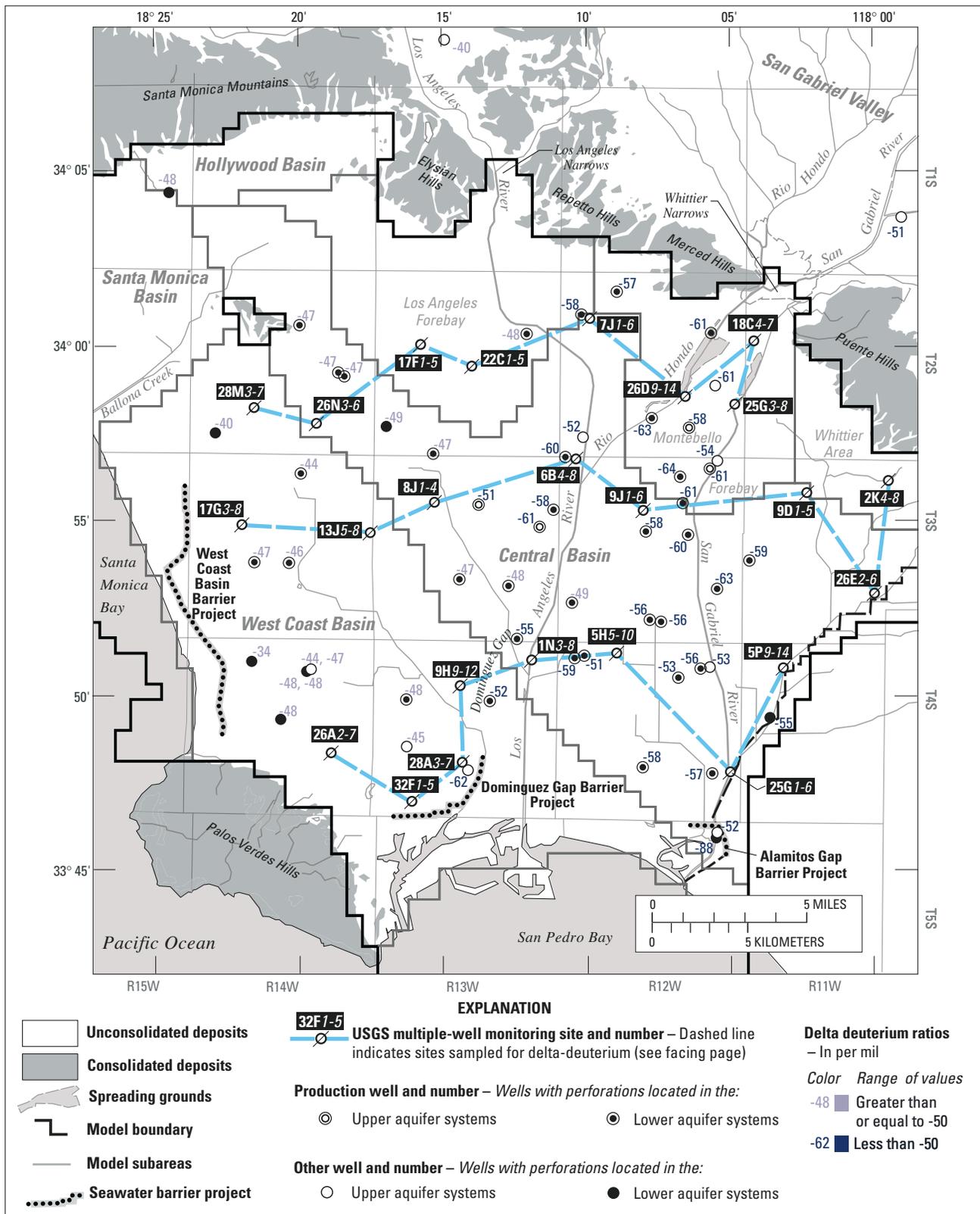
Figure 15. Delta-deuterium values in ground water sampled in the study area, Los Angeles County, California.
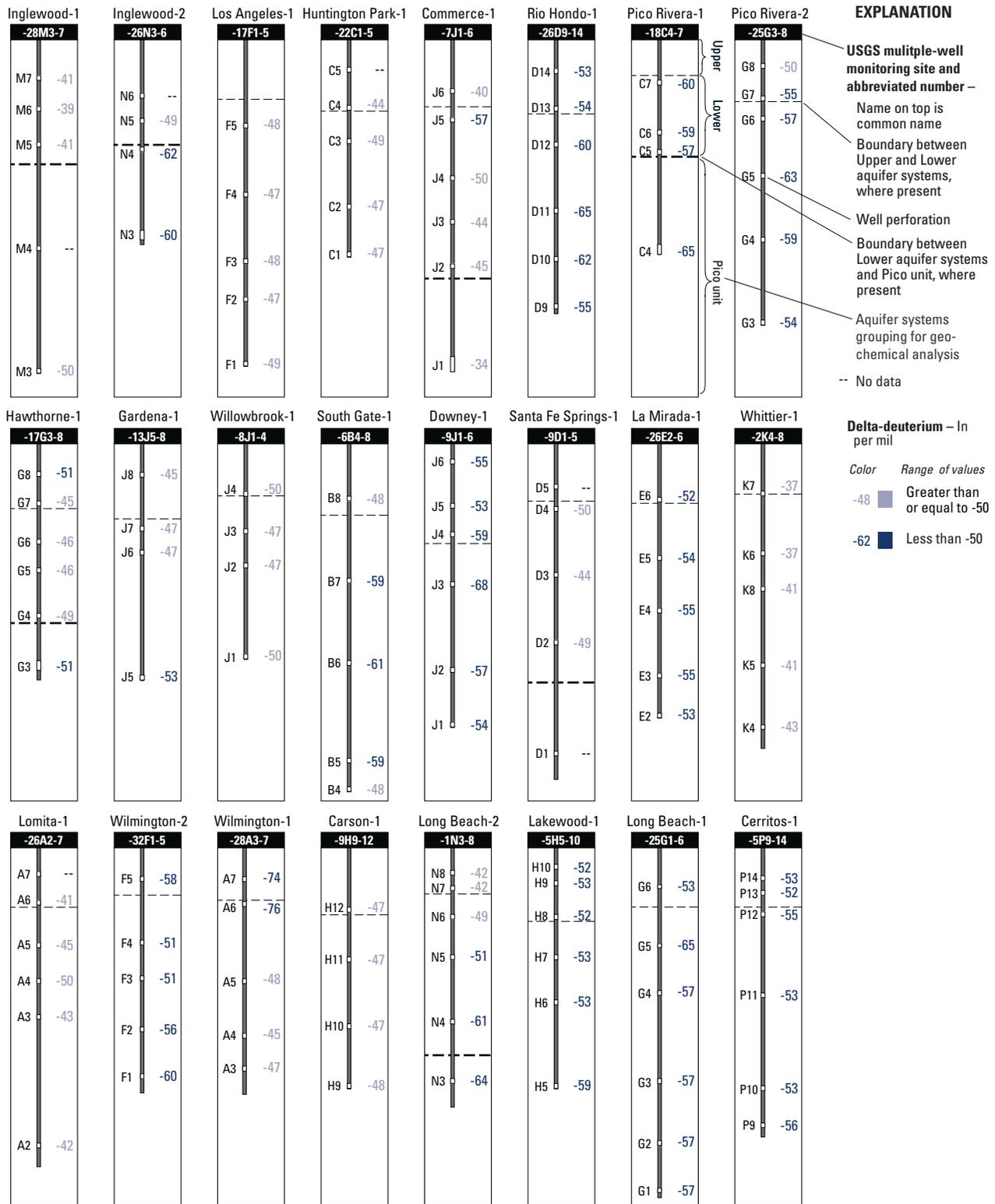
Figure 15.—Continued.
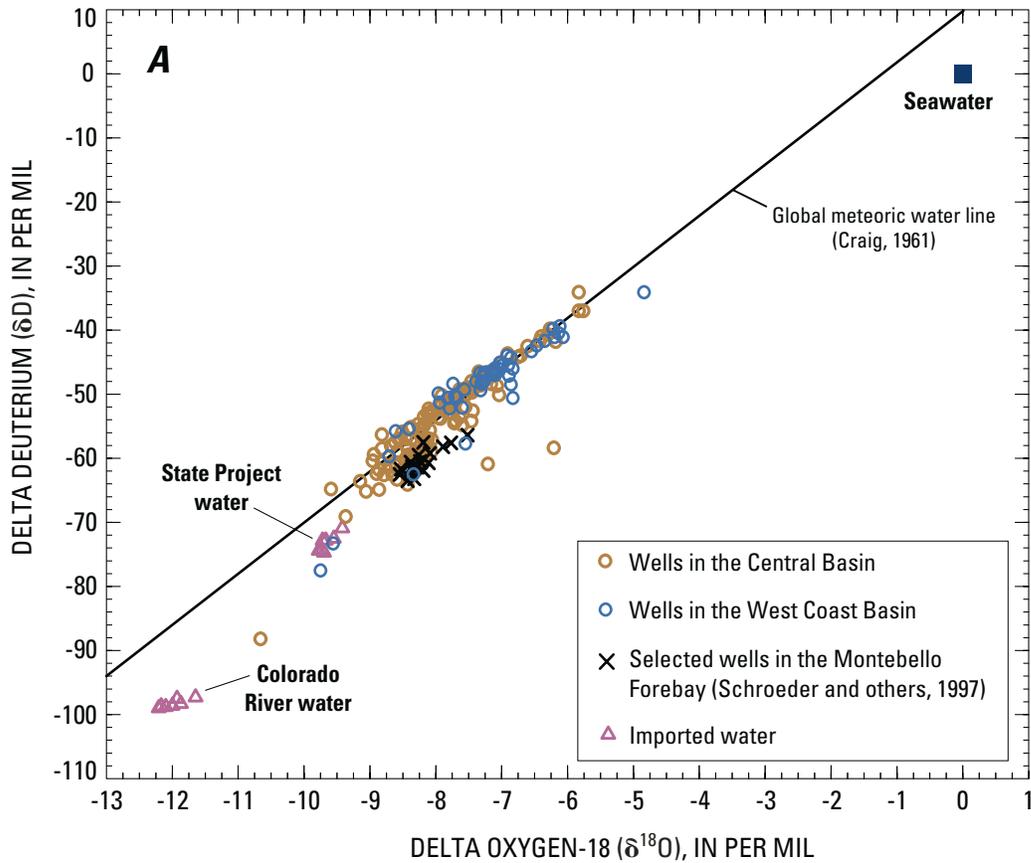
Figure 16. Delta deuterium as a function of delta oxygen-18 in ground water sampled in the study area (*A*), in the Central Basin (*B*), in the West Coast Basin (*C*), Los Angeles County, California.
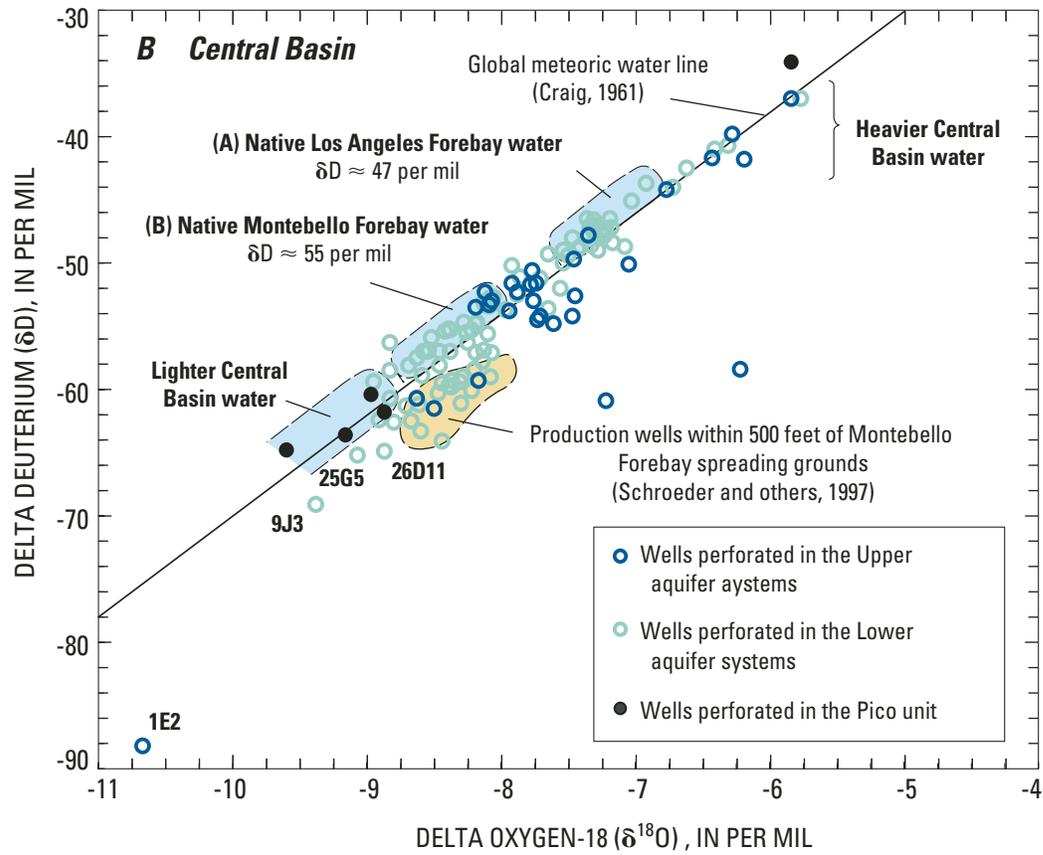
Figure 16.—Continued.
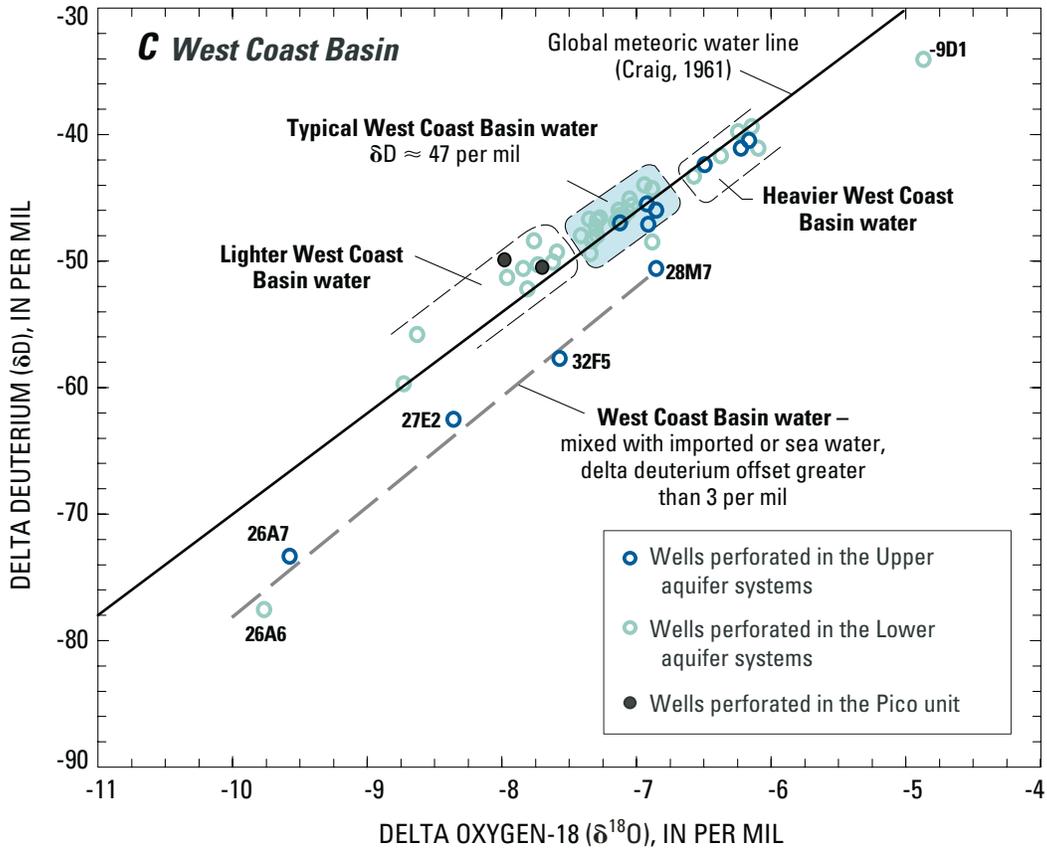
Figure 16.—Continued.

One group of samples plots above the meteoric water line at about -47 per mil δD (fig. 16*B*) and is associated with wells located within the Los Angeles Forebay (2S/13W-17F3–4, -22C1, and -22C2), near the Los Angeles Forebay (2S/14W-23H3, 2S/13W-32R13, 3S/12W-6B4, and -6B8, and 2S/12W-7J2), and downgradient of the Los Angeles Forebay (3S/13W-8J2, -21R3, and -26C1, 3S/12W-30K2, 2S/14W-26N5,). Water in this group originates as precipitation falling on the lower lying hills of the San Fernando Valley (feeding the Los Angeles River) and is a source of recharge and underflow to the Los Angeles Forebay. This water occurs throughout the western half of the Central Basin, primarily in the Lower aquifer systems; extensiveness in the Upper aquifer systems is uncertain.

A second group of samples plots above the meteoric water line at about -55 per mil δD (fig. 16*B*) and is associated with numerous wells perforated in the Lower aquifer systems throughout the distal part of the Central Basin Pressure Area (4S/12W-28H1, -25G2, -5H6, and -10H1, 4S/11W-5P10, and 3S/11W-26E3) and in a few deep wells near the Montebello Forebay (2S/11W-18C5, 2S/12W-26D9, and 3S/12W-9J1). Water in this group originates as precipitation falling on the relatively higher San Gabriel Mountains and is a source of recharge and underflow to the Montebello Forebay. This water also is present in some wells perforated in the Upper aquifer systems in the distal part of the Central Basin Pressure Area (4S/13W-1N3, 4S/12W-5H9, and 4S/11W-5P13).

In addition to these two main groups, other sets of samples in the Central Basin have an isotopic composition that plots above (or near) the meteoric water line. Isotopically heavy water (from -36 to -43 per mil δD) present in wells 4S/13W-1N7–8 (near the Dominguez Gap area) and 2S/12W-7J6 (near Commerce) (fig. 15) is attributed to local precipitation in the coastal plain and surrounding hills. In general, this water seems to be limited to shallow portions of the Central Basin, although it is present at all monitored depths at the Whittier-1 monitoring site (3S/11W-2K4–8; fig. 16*B*). Isotopically light water (less than -60 per mil δD) in a few wells perforated in the Lower aquifer systems or Pico unit (2S/14W-26N4, 2S/11W-18C4, 4S/13W-1N4, and 4S/12W–5H5) is depleted by -6 to -11 per mil δD and chemically distinct from samples collected from overlying wells at the

same location. These isotopic values are consistent with recharge during cooler conditions during the late Pleistocene (Clark and Fritz, 1997). Water that plots between the Los Angeles and the Montebello forebay groups (fig. 16*B*) may result from a combination of recharge from these sources (for example, wells 4S/13W-1N5–6 and 4S/12W-6K4; between the Montebello Forebay and Whittier Area (wells 3S/11W-9D2 and -9D4).

Most samples in the Central Basin with isotopic compositions that plot below the meteoric water line and contain less than -50 per mil δD are associated with wells proximal to the Montebello Forebay. Within the Montebello Forebay, values for the Upper and Lower aquifer systems cluster at about -55 and -61 per mil δD, respectively (fig 15). Many wells in the Lower aquifer systems have an isotopic composition (fig. 16*A*) that is nearly identical to that of several wells within 500 ft of the Montebello Forebay spreading grounds (Schroeder and others, 1997).

In the study area, the extent to which a sample is offset below the meteoric water line often reflects the degree of mixing of native and artificially recharged water. For example, the distinct isotopic composition of water from wells 3S/12W-9J3, 4S/11W-25G5, and 2S/12W-26D11 in the Central Basin (fig. 8) can be explained by substantial mixing with an imported source of water. This mixing is evident in water from well 5S/12W-1E2 because only imported Colorado River water is injected at the nearby Alamitos Gap Barrier Project. Recharge to this well (assuming a two-component mixture) is estimated to be approximately 25 percent native Central Basin water and 75 percent imported Colorado River water.

West Coast Basin

In the West Coast Basin, δD values for water in sampled wells ranged from -34 to -76 per mil. Many samples from the Lower aquifer systems (for example, 4S/13W-9H11 and 3S/14W-13J7 and -17G5) and a few from the Upper aquifer systems (4S/13W-9H12 and 3S/14W-17G7) plot above the meteoric water line at about -47 per mil δD (shaded area, fig 16*C*). This range of δD and $\delta^{18}O$ is typical of most native ground water in the West Coast Basin. The similarity in isotopic composition between this group and water in the Los Angeles Forebay suggests they share the same source of recharge.

Relatively heavy water, which plots near the meteoric water line (-39 to -43 per mil δD; fig. 16C), is present in selected wells located near the coast (2S/14W-31H1), close to the Newport-Inglewood Uplift near Baldwin Hills (3S/14W-13J8 and 2S/14W-28M5–7), and near Palos Verdes Hills (4S/14Q-26A2–3, and -26A6) (fig. 15). Recharge of precipitation in the coastal plain and surrounding hills is the likely source of this isotopically heavy water. δD values as heavy as -32 per mil have been measured in shallow ground water at a monitoring site on the Palos Verdes Hills (T. Johnson, Water Replenishment District of Southern California, written commun., 1999).

Another source of isotopically heavy water in the basin is seawater (0 per mil δD). The heaviest water sampled in the West Coast Basin was in well 4S/14W-9D1 (about -34 per mil δD). Given the high chloride concentration (6,800 mg/L), an isotopic composition depleted by more than 3 per mil δD below the meteoric water line, and proximity to the coast, seawater appears to be a significant source (about 30 percent) of water to this well.

Injection of imported water along the West Coast Basin and Dominguez Gap Barrier Project is an important source of recharge to the West Coast Basin. The effect of this recharge is evident in the isotopic composition of water from wells 4S/13W-27E2, -28A6, and -28A7, 2S/14W-28M7 and 4S/13W-32F5. Mixing of imported and native West Coast Basin water yields very light water that plots below the meteoric water line fig. 16C). For example, deuterium measured in water from well 4S/13W-28A6 (-76 per mil δD) suggests a source of recharge composed of at least 60 percent imported water.

Relatively light water, which plots above the meteoric water line (-48 to -60 per mil δD; fig. 16C), indicates another distinct source of recharge in part of the West Coast Basin. At least two explanations are possible. First, some of this water may have recharged under cooler climatic conditions in the Los Angeles

Forebay. For example, water from two wells perforating the Pico unit (3S/14W-17G3 and 2S/14W-28M3) is chemically distinct and is isotopically light relative to overlying water commonly found in the Lower aquifer systems (fig. 16C). This range (about -51 per mil δD) and pattern also is evident in water from a few deep wells within the Lower Aquifer systems (3S/14W-13J5 and -17G4 and 4S/14W-2N1) (figs. 8, 15). Second, some of this water may have recharged through the Montebello Forebay. The isotopic composition of water from wells 4S/13W-32F1–2 (relative to overlying water; fig. 16C)) is too light to be explained by climate change alone and, moreover, is identical to the composition of natural recharge originating from the Montebello Forebay (fig. 16B). Movement of water from the Central Basin through the Dominguez Gap to these wells is supported by isotopically light water from upgradient well 4S/13W-1N4 (-61 per mil δD) (fig. 15). It appears that this water may be limited to deep parts of the Lower aquifer systems downgradient from the Dominguez Gap.

Tritium

Radioisotopes, such as tritium, can be used to estimate the age of water in the ground. To distinguish water that was recharged relatively recently from older water, samples were analyzed for tritium content. Tritium is a naturally occurring unstable isotope of hydrogen that decays by beta-particle emission into helium-3 (half-life of 12.4 years). Because tritium is part of the water molecule and is affected only by radioactive decay, it serves as a natural tracer for identifying (that is, age dating) recently recharged waters (Michel, 1989). Tritium is present—in varying concentrations—in seawater, precipitation, surface water, and recycled wastewater. In this investigation, tritium values are presented as absolute concentrations in tritium units (TU); one TU is equivalent to a $^3H/^1H$ ratio of 10^{-18}, or an equal activity of 3.19 picoCuries per liter of pure water.

Prior to 1952, the tritium concentration in precipitation in coastal southern California was about 2 TU (Izbicki, 1996). Assuming that water recharging the Los Angeles coastal basin prior to 1952 had a tritium concentration of 2 TU or less, the tritium in that same ground water would have decayed to a concentration less than 0.1 TU (less than measurable in this study) by 2000. Beginning in 1952, significant quantities of tritium were released into the atmosphere from the testing of hydrogen bombs, reaching a maximum in 1963 (fig. 17). Owing to enrichment in water vapor across the continental land mass, the tritium concentration in precipitation for the Colorado River Basin—water that was subsequently imported for spreading and injection—is higher than in precipitation originating in coastal southern California (Michel, 1989). Also, because of the time required to transport Colorado River water, the concentration of tritium entering the ground-water systems lags the values shown in figure 17 (Michel and Schroeder, 1994).

Tritium values in water from wells sampled as part of this study range from less than measurable to 31 TU, and are categorized in figure 18. Water with very low, or less than measurable, tritium content is interpreted as "older" water recharged prior to 1952. Water with tritium content greater than 1.0 TU is interpreted as "recent" water recharged after 1952. Water with relatively high tritium content (greater than 8 TU) has a significant portion of recharge that occurred around the peak period of weapons testing (fig. 17). Water with moderate tritium content (1.0 to 8 TU) is interpreted as recent but not necessarily attributable to recharge during any specific period after 1952. Interpreting tritium analyses is complicated by the potential mixing of older and younger water, by the potential leakage of younger water into deep wells through well bores (Mazor, 1991; Izbicki, 1996), and by values that could be attributed to either side of the 1963 peak (fig. 17).

Central Basin

In the Central Basin, tritium values commonly ranged from less than measurable to as high as 31 TU.

Recent water occurs extensively in the Upper and Lower aquifer systems within the Montebello Forebay and for several miles downgradient in the surrounding Central Basin Pressure Area near wells 2S/12W-7J5, 3S/13W-13F4, -3S/12W-14F1, and -25C1 (figs. 8, 18). Recent water also is present in wells near the Alamitos Gap Barrier Project (4S/12W-1E2) and along Los Angeles River near the Dominguez Gap (4S/13W-1N78). The shaded area in figure 18 shows the approximate extent of recent water in the Lower aquifer systems.

Significant concentrations of tritium (greater than 8 TU) occur within the Montebello Forebay, but concentrations were generally highest in wells downgradient in the Central Basin Pressure Area. Near the spreading grounds along the San Gabriel River, abundant tritium is present in water at all monitored zones (2S/12W-25G3–8; Pico Rivera-2). Near the South Gate-1 monitoring site, water containing abundant tritium extends to a depth 1,340 ft below land surface (3S/12W-6B5; 17 TU). These data, which are consistent with stable isotope, chemical, and temperature data, show recently recharged water is present in the Lower aquifer system. However, tritium values at a few locations in or near the Montebello Forebay (2S/12W-26D9 and 3S/12W-9J1 and -6B4) suggest that the age of water in other deep portions of the Lower aquifer systems (as well as the Pico unit) exceeds 50 years.

The highest tritium concentration (31 TU) was observed in water from well 3S/12W-9J3 (fig. 18), possibly corresponding to water recharged near the peak period of weapons testing. The maximum tritium concentration (decay-corrected to 1996, when the sample was collected) in water recharged during this period is estimated to be 110 TU; this, however, does not account for dispersion within the ground-water system. Efforts to obtain a more refined estimate of age, through the coupled measurement of tritium and helium-3, suggest that most water to this well was recharged during 1968 (R. Anders, U.S. Geological Survey, written commun., 2001).
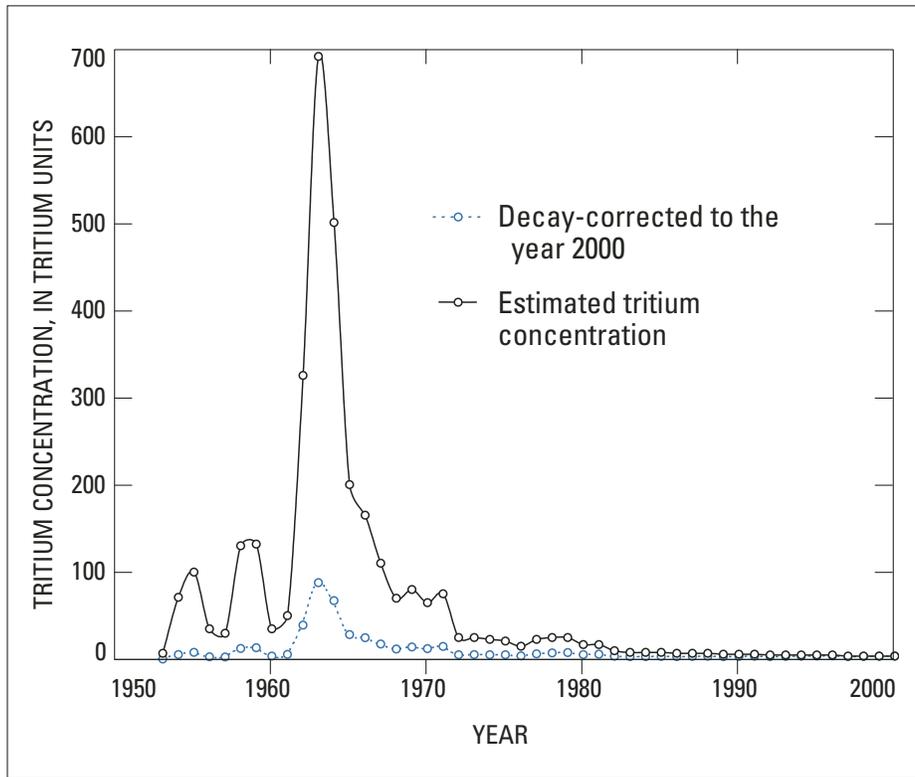
Figure 17. Estimated tritium activities in precipitation, Los Angeles County, California (from Michel, 1989).

THIS PAGE INTENTIONALLY LEFT BLANK
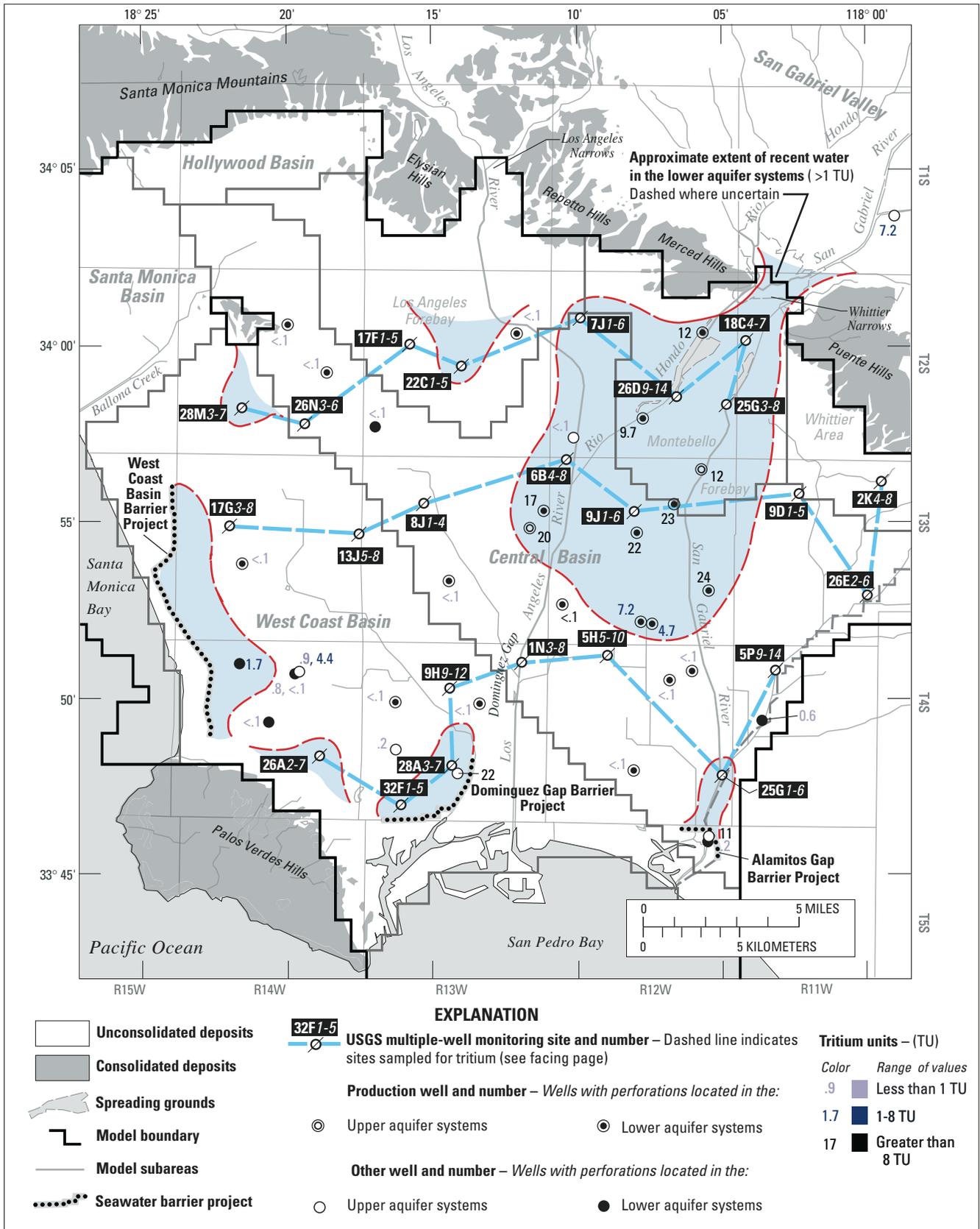
Figure 18. Tritium concentration in ground water sampled in the study area, Los Angeles County, California. Blue areas show approximate extent of recent water (greater than 1TU) in the Lower aquifer systems; dashed where uncertain.

Inglewood-1 **-28M3-7**
M7 1.6
M6 .3
M5 <.1
M4 --
M3 <.1

Inglewood-2 **-26N3-6**
N6 --
N5 <.1
N4 <.1
N3 <.1

Los Angeles-1 **-17F1-5**
F5 .1
F4 .1
F3 .2
F2 <.1
F1 <.1

Huntington Park-1 **-22C1-5**
C5 --
C4 .6
C3 1.3
C2 <.1
C1 <.1

Commerce-1 **-7J1-6**
J6 <.1
J5 19
J4 2.4
J3 .2
J2 <.1
J1 --

Rio Hondo-1 **-26D9-14**
D14 7.2
D13 8.1
D12 8.1
D11 13
D10 18
D9 .1

Pico Rivera-1 **-18C4-7**
C7 15
C6 12
C5 4.4
C4 <.1
Upper
Lower

Pico Rivera-2 **-25G3-8**
G8 8.4
G7 9.1
G6 8.4
G5 18
G4 17
G3 8.4
Pico unit

Hawthorne-1 **-17G3-8**
G8 18
G7 1.0
G6 <.1
G5 <.1
G4 <.1
G3 <.1

Gardena-1 **-13J5-8**
J8 1.0
J7 .1
J6 .3
J5 .3

Willowbrook-1 **-8J1-4**
J4 .1
J3 <.1
J2 <.1
J1 <.1

South Gate-1 **-6B4-8**
B8 <.1
B7 14
B6 25
B5 17
B4 <.1

Downey-1 **-9J1-6**
J6 16
J5 5.0
J4 18
J3 31
J2 5.6
J1 .1

Santa Fe Springs-1 **-9D1-5**
D5 --
D4 <.1
D3 .4
D2 <.1
D1 --

La Mirada-1 **-26E2-6**
E6 .1
E5 <.1
E4 <.1
E3 <.1
E2 <.1

Whittier-1 **-2K4-8**
K7 <.1
K6 <.1
K8 .1
K5 <.1
K4 <.1

Lomita-1 **-26A2-7**
A7 --
A6 .2
A5 .4
A4 .3
A3 .5
A2 3.1

Wilmington-2 **-32F1-5**
F5 17
F4 1.4
F3 <.1
F2 <.1
F1 <.1

Wilmington-1 **-28A3-7**
A7 12
A6 19
A5 1.0
A4 <.1
A3 <.1

Carson-1 **-9H9-12**
H12 .1
H11 <.1
H10 <.1
H9 .1

Long Beach-2 **-1N3-8**
N8 3.8
N7 5.0
N6 <.1
N5 <.1
N4 <.1
N3 <.1

Lakewood-1 **-5H5-10**
H10 2.0
H9 <.1
H8 .5
H7 <.1
H6 <.1
H5 <.1

Long Beach-1 **-25G1-6**
G6 .3
G5 26
G4 .1
G3 <.1
G2 <.1
G1 <.1

Cerritos-1 **-5P9-14**
P14 <.1
P13 <.1
P12 <.1
P11 <.1
P10 <.1
P9 <.1

Figure 18.—Continued.

Tritium values indicate that water from wells in the Los Angeles Forebay and surrounding Central Basin Pressure Area is older water. In sharp contrast to the Montebello Forebay, only one well in the Los Angeles Forebay (2S/13W-22C3), and none of the wells downgradient to the west (2S/14W-10Q2), to the south (3S/13W-8J3), or along the NIU (3S/13W-21R3) contains recent water (greater than 1 TU) ([fig. 18](#)). In the southeast part of the Central Basin Pressure Area, older water is typically present in both aquifer systems. Less than measurable tritium in water from wells 3S/12W-30K2, 4S/12W-5H7 and -10H1, 4S/11W-5P11, and 3S/11W-9D2 approximates a boundary beyond which recent water is absent. An exception is made for abundant tritium observed in water from wells 5S/12W-1E2 and 4S/12W-25G5 (11 and 26 TU, respectively). The source of this water (based on δD values) is attributed to injection at the Alamitos Gap Barrier Project.

West Coast Basin

In the West Coast Basin, tritium values ranged from less than measurable to 22 TU ([fig. 18](#)). Most wells, especially those in the Lower aquifer systems, contain water with low or less than measurable tritium concentrations. For example, low tritium values highlight the predominance of older water along the interior of the basin (2S/14W-28M5, 3S/14W-13J7, 4S/13W-9H11, -15A11, and -17D2) ([fig. 18](#)). Older water also is present in many deeper wells (3S/14W-17G6 and 4S/13W-32F3 and -28A4) along the coast, which suggests that the Lower aquifer systems do not contain significant recharge from the barrier projects at these locations.

Recent water in the West Coast Basin is generally limited to areas along the coast and to the Upper aquifer systems ([figs. 8](#), [18](#)). Near the coast, water in the Lower aquifer systems from well 4S/14W-9D1 may contain a small fraction of recently intruded seawater (1.7 TU). Farther inland, water from the West Coast Basin Barrier Project may be reaching well 4S/13W-1N2, along with a plume of saline water. The highest tritium value observed in the West Coast Basin (22 TU) was in water from well 4S/13W-27E2, and is attributed to injection of imported water at the Dominguez Gap Barrier Project. High tritium (greater than 8 TU) also is associated with other wells located near the barrier projects (3S/14W-17G8 and 4S/13W-28A7 and -32F5). Near the NIU, moderate tritium values in relatively shallow wells (2S/14W-28M7 and 3S/14W-13J8) may reflect recent recharge from local precipitation.

Carbon-14

Samples from selected wells were analyzed for carbon-14 to further distinguish the relative age of older water in the basin. Carbon-14 is a naturally occurring unstable isotope of carbon with a half-life of 5,730 years that can be used to estimate ground-water age (since time of recharge) up to about 20,000 years (Gat and Gonfiantini, 1981). Carbon-14 data are reported as percent modern carbon (pmc) by comparing carbon-14 activities with the specific activity of National Bureau of Standards oxalic acid; 12.88 disintegrations per minute per gram of carbon in the year 1950 equals 100 percent modern carbon (Izbicki and others, 1998). Like tritium, significant quantities of carbon-14 were released into the atmosphere from the testing of hydrogen bombs. As a result, very recent water may contain carbon-14 in excess of 100 pmc. Unlike tritium, carbon-14 is not part of the water molecule; rather it is introduced into the ground-water system through plant respiration, decay of organic matter in soils, and dissolution of minerals and, as such, is subject to reactions that occur between dissolved constituents and the aquifer matrix (Fontes, 1985).

Samples for which carbon-14 activity was determined ranged from 1 to 123 pmc ([fig. 19](#)); most are from wells perforated in the Lower aquifer systems. Ground-water ages (corresponding to measured carbon-14 activity) discussed in this report are apparent ages (recharge, in years before present) and relative to water in well 2S/11W-18C5, which contains 90 pmc. These estimates are not corrected for reactions within the aquifer, and therefore they may not reflect the true age of the water. In other words, the apparent age given by the carbon-14 value represents the maximum age possible for the ground water. Based on work in an adjacent coastal basin (Izbicki, 1996), use of uncorrected carbon-14 values may overestimate the groundwater age by 20 to 50 percent.

THIS PAGE INTENTIONALLY LEFT BLANK
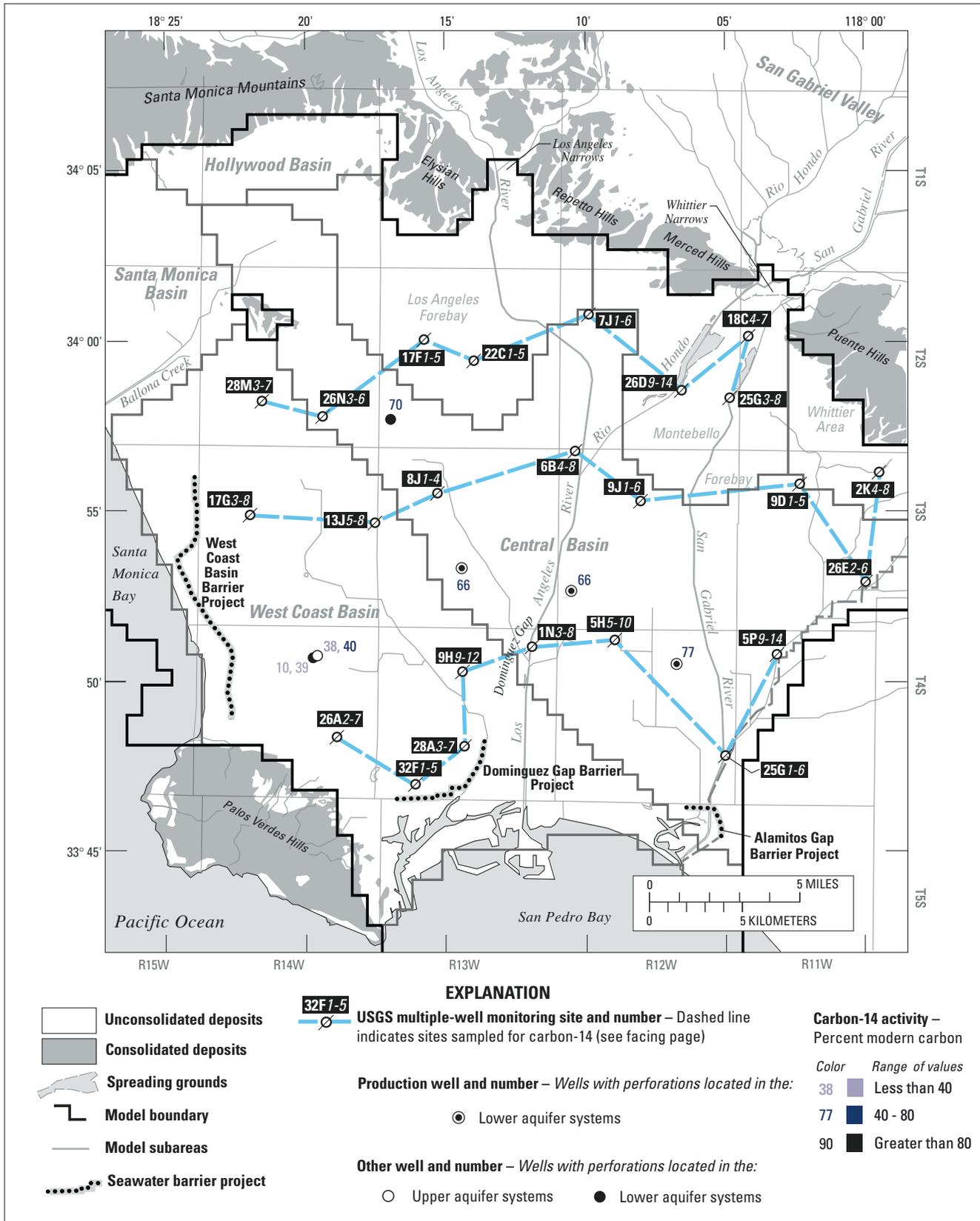
Figure 19. Carbon-14 activities in sampled ground water in the study area, Los Angeles County, California.

Inglewood-1
-28M3-7
M7 --
M6 --
M5 53
M4 --
M3 --

Inglewood-2
-26N3-6
N6 --
N5 --
N4 --
N3 --

Los Angeles-1
-17F1-5
F5 --
F4 76
F3 --
F2 82
F1 53

Huntington Park-1
-22C1-5
C5 --
C4 --
C3 --
C2 84
C1 84

Commerce-1
-7J1-6
J6 --
J5 --
J4 --
J3 57
J2 28
J1

Rio Hondo-1
-26D9-14
D14 --
D13 --
D12 96
D11 --
D10 83
D9 35

Pico Rivera-1
-18C4-7
C7 --
C6 --
C5 90
C4 2

Pico Rivera-2
-25G3-8
G8
G7
G6 --
G5 --
G4 111
G3 93

EXPLANATION

USGS mulitple-well monitoring site and abbreviated number –

Name on top is common name

Boundary between Upper and Lower aquifer systems, where present

Well perforation

Boundary between Lower aquifer systems and Pico unit, where present

Aquifer systems grouping for geochemical analysis

-- No data

(Pico Rivera-1: Upper, Lower, Pico unit)

Hawthorne-1
-17G3-8
G8 --
G7 --
G6 16
G5 10
G4 8
G3 3

Gardena-1
-13J5-8
J8 --
J7 --
J6 65
J5 9

Willowbrook-1
-8J1-4
J4 --
J3 --
J2 68
J1 16

South Gate-1
-6B4-8
B8 --
B7 --
B6 --
B5 94
B4 48

Downey-1
-9J1-6
J6 --
J5 --
J4 --
J3 123
J2 86
J1 74

Santa Fe Springs-1
-9D1-5
D5 --
D4 --
D3 --
D2 --
D1 --

La Mirada-1
-26E2-6
E6 --
E5 --
E4 22
E3 53
E2 20

Whittier-1
-2K4-8
K7 --
K6 --
K8 15
K5 15
K4 15

Carbon-14 activity –
Percent modern carbon

Color	Range of values
2	Less than 40
57	40 - 80
90	Greater than 80

Lomita-1
-26A2-7
A7 --
A6 --
A5 --
A4 --
A3 --
A2 --

Wilmington-2
-32F1-5
F5 --
F4 --
F3 14
F2 5
F1 3

Wilmington-1
-28A3-7
A7 --
A6 --
A5 --
A4 44
A3 30

Carson-1
-9H9-12
H12 --
H11 56
H10 44
H9 28

Long Beach-2
-1N3-8
N8 --
N7 --
N6 --
N5 22
N4 4
N3 1

Lakewood-1
-5H5-10
H10 --
H9 72
H8 59
H7 61
H6 54
H5 8

Long Beach-1
-25G1-6
G6 --
G5 61
G4 53
G3 24
G2 30
G1 31

Cerritos-1
-5P9-14
P14 --
P13 59
P12 57
P11 34
P10 46
P9 56

Figure 19.—Continued.

The apparent ages corresponding to carbon-14 activities, grouped according to tritium content, for selected wells in the study area are shown in table 2. Water containing less than 1 TU contains carbon-14 with an activity of 1 to 84 pmc. This is predominantly older water with an apparent age between several thousand to several hundred years before present. Uncorrected carbon-14 data from four wells perforating the Pico unit (1 to 7 pmc) suggest that recharge is on the order of 20,000 years before present.

Water containing more than 1 TU and carbon-14 values exceeding 89 pmc is recent water (table 2). Water containing more than 1 TU and carbon-14 values less than 90 pmc may result from a mixture of recent and older water, or significant dissolution of aquifer material. In both circumstances, an apparent age cannot be accurately assigned.

Central Basin

Carbon-14 values in the Central Basin ranged from 1 to 123 pmc (fig 19). The median value in the Lower aquifer systems is 56 pmc. Carbon-14 values are high in the forebay areas and generally decrease with depth and distance downgradient. In the Montebello Forebay area several wells yielded recent water (greater than 1 TU) with carbon-14 values greater than 80 pmc. The highest carbon-14 value in the Central Basin was observed in water from 3S/12W-9J3 (123 pmc; also the highest tritium concentration) and is consistent with recent (bomb influenced) water. Similarly, carbon-14 values for wells 3S/12W-6B5 and 2S/12W–25G3–4 (94, 93, and 111 pmc, respectively) illustrate the vertical extent of this very recent water. However, carbon-14 in water from well 2S/12W-26D9 (35 pmc) indicates that much older water (about 7,700 years in table 2) is present in deep portions of the Montebello Forebay.

In the Los Angeles Forebay, carbon-14 activity is greater than 80 pmc in a few wells (2S/13W-17F2, and -22C1–2) perforated in the Lower aquifer systems. This is older water (less than 1 TU) with an apparent age of about 600 to 800 years (table 2). The carbon-14

value for water from another well, 2S/13W-17F1 (53 pmc), in the Los Angeles Forebay, indicates a substantial increase in apparent age (4,400 years) with depth in the Lower aquifer systems.

Downgradient wells from the Los Angeles Forebay in the Central Basin Pressure Area (3S/13W-8J2 and -21R3, 3S/12W-30K2, and 2S/13W-31C3) yielded water with carbon-14 values (66 to 70 pmc) corresponding to an apparent age range of about 2,100 to 2,600 years (fig. 19; table 2). Much farther downgradient, very old water (about 20,000 years) is present in wells in the Lower aquifer systems (4S/13W-1N4 and 4S/12W-5H5). Water from this part of the basin does not contain any significant fraction of recent water (fig. 18) and is considered to be representative of native water.

In the Whittier area, water from the three lower wells at the Whittier-1 site (3S/11W-2K4, 5, and 8) has the same carbon-14 values (15 pmc), possibly as a result of deep circulation to the Lower aquifer systems.

West Coast Basin

In the West Coast Basin, carbon-14 values ranged from 2 to 65 pmc for water in the Lower aquifer systems (fig. 19). The median carbon-14 value is 28 pmc–substantially less than that in the Central Basin–and values generally decrease with depth and toward the coast. These data are consistent with a long travel times for water moving from the forebays, across the NIU, to the coast. For example, carbon-14 values from deeper wells in the Lower aquifer systems at the USGS Gardena-1 (9 and 65 pmc) monitoring site are similar to values at USGS Willowbrook-1 (16 and 68 pmc) (fig. 19). Furthermore, carbon-14 and stable isotope (fig. 15) data at these two sites do not show that the Newport-Inglewood Uplift greatly impedes flow between the basins in this area. In contrast, chemistry and stable-isotope data from the USGS Inglewood-1 and USGS Inglewood-2 sites are very different from each other, indicating that the NIU acts as a significant barrier between these locations.

Table 2. Carbon-14 and apparent-age for selected wells sampled, Los Angeles County, California

[Carbon-14: measured activity. Apparent age: the maximum in years before present since recharged. Assumes an initial activity of 90 percent modern carbon during recharge—not corrected for reactions within the aquifer matrix. Basin: C, Central; W, West Coast. Aquifer or unit: Pico, Pico unit; LSP, Lower San Pedro; USP, Upper San Pedro; Lake, Lakewood]

Measured carbon-14 (pmc)	Apparent age (years before present)	Basin	Aquifer System or unit	State well No.
Water containing less than 1 tritium unit				
1	37,000	C	Pico	4S/13W-1N3
2	33,000	C	Pico	2S/11W-18C4
3	29,000	W	LSP	4S/13W-32F1
3	29,000	W	Pico	3S/14W-17G3
4	25,000	C	LSP	4S/13W-1N4
5	24,000	W	USP	4S/13W-32F2
7	21,000	C	Pico	2S/12W-7J1
8	20,000	W, C	LSP	3S/14W-17G4, 4S/12W-5H5
9	19,000	W	LSP	3S/14W-13J5
10	18,000	W	USP, LSP	3S/14W-17G5, 4S/14W-2N1
14	15,000	W	USP	4S/13W-32F3
15	15,000	C	USP	3S/11W-2K4, -2K5, -2K8
16	14,000	W	USP	3S/14W-17G6
16	14,000	C	LSP	3S/13W-8J1
20	12,000	C	LSP	3S/11W-26E2
22	12,000	C	USP	3S/11W-26E4, 4S/13W-1N5
24	11,000	C	USP	4S/12W-25G3
28	9,800	W	USP	4S/13W-9H9
28	9,500	C	LSP	2S/12W-7J2
30	9,200	W	LSP	4S/13W-28A3
30	9,100	C	LSP	4S/12W-25G2
31	8,800	C	LSP	4S/12W-25G1
34	8,000	C	USP	4S/11W-5P11
35	7,700	C	LSP	2S/12W-26D9
38	7,200	W	USP	4S/14W-2N3
39	7,000	W	USP	4S/14W-2N2

Measured carbon-14 (pmc)	Apparent age (years before present)	Basin	Aquifer System or unit	State well No.
44	6,000	W	USP	4S/13W-9H10
44	5,800	W	LSP	4S/13W-28A4
46	5,500	C	LSP	4S/11W-5P10
48	5,100	C	LSP	3S/12W-6B4
53	4,400	C	LSP	2S/13W-17F1, 3S/11W-26E3
53	4,400	W	LSP	2S/14W-28M5
53	4,400	C	USP	4S/12W-25G4
54	4,200	C	USP	4S/12W-5H6
56	3,900	W	USP	4S/13W-9H11
56	3,900	C	LSP	4S/11W-5P9
57	3,800	C	LSP, USP	2S/12W-7J3, 4S/11W-5P12
59	3,500	C	Lake	4S/12W-5H8
61	3,200	C	USP	4S/12W-5H7
65	2,600	W	USP	3S/14W-13J6
66	2,600	C	USP	3S/12W-30K2, 3S/13W-21R3
68	2,300	C	USP	3S/13W-8J2
70	2,100	C	USP	2S/13W-31C3
72	1,800	C	Lake	4S/12W-5H9
74	1,600	C	USP	3S/12W-9J1
76	1,300	C	USP, Lake	2S/13W-7F4, 4S/11W-9P13
77	1,300	C	USP	4S/12W-10H1
82	800	C	USP	2S/13W-17F2
84	600	C	USP	2S/13W-22C1–2
Water containing more than 1 tritium unit				
40	Mixture[1]	W	Lake	4S/14W-2N4
61	Mixture[1]	C	USP	4S/12W-25G5
83	Mixture[1]	C	USP	2S/12W-26D10
86	Mixture[1]	C	USP	3S/12W-9J2
90	Recent	C	LSP	2S/11W-18C5
93	Recent	C	LSP	2S/12W-25G3
94	Recent	C	USP	3S/12W-6B5
96	Recent	C	USP	2S/12W-26D12
111	Recent	C	USP	2S/12W-25G4
123	Recent	C	USP	3S/12W-9J3

[1]Mixture of recent (less than 50 years before present) and older water.

Water from well 4S/14W-2N3–4 contained 38 and 40 pmc, respectively, indicating water of significant age is present in the Upper aquifer systems (table 2). However, water from well 4S/14W-2N4 also contained 4.4 TU. This water is a mixture of recent water (possibly from injection at the West Coast Basin Barrier Project) (fig. 18) and possibly very old ground water. Very old water is present in water from wells near the coast (3S/14W-17G4 and 4S/13W-32F1; 8 and 3 pmc, respectively) and corresponds to an apparent age on the order of 20,000 years. Water in both of these wells has a slight to strong measurable color and odor.

Integrated Geochemical Analysis of the Regional Ground-Water Flow System

To further evaluate movement of water within the study area and to better understand changes in the ground-water flow system, aspects of the chemistry and isotope data are integrated along two cross sections of the Los Angeles basin (fig. 20). The section lines shown in figure 8 were modified from geohydrologic sections (fig. 2) to approximate ground-water flowpaths from the forebays prior to development of the basin.

The chemical character of ground water changes as it moves downgradient from the forebay as a result of water-mineral interactions and mixing within an aquifer system. Primary controls on the degree of change depend on (1) sources of recharge, (2) mineral assemblages derived from weathering and from mountains surrounding the study area, and (3) residence time of the ground water. Some of the processes and water-mineral interactions that affect the ground-water chemistry along the section lines shown in figure 20 are summarized in table 3. Redox processes (not shown) that affect ground-water chemistry involve manganese, nitrogen, and molecular oxygen.

A geohydrologic section emanating from the Montebello Forebay and extending into the Central Basin Pressure Area is shown in figure 20*A*. Relatively fresh water is present throughout the section. Tritium (greater than or equal to 1 TU) in water, along with chemical and isotopic data, shows that artificial spreading of water in the Montebello Forebay recharges the ground-water system at significant depths and distances from the spreading facilities. Data indicate that the Upper aquifer systems typically contain recent water spanning a range of chemical character owing to multiple sources of artificial recharge. In the Lower aquifer systems, this water, away from the Montebello Forebay, is also shown in well 3S/12W–33A7. Although stable-isotope data indicate that the bulk of recharge to this well is native water originating from the San Gabriel Valley, the presence of moderate tritium (7.2 TU) (fig. 18) suggests a component of ground water having recharged less than 50 years ago. Some of the recent water occurring in the Lower aquifer systems— specifically the Lower San Pedro aquifer system (2S/11W-18C5)—may also be related to underflow through the Whittier Narrows.

A geohydrologic section emanating from the Los Angeles Forebay and extending across the NIU into the West Coast Basin is shown in figure 20*B*. Recent water is yielded by two wells in the Los Angeles Forebay (2S/13W-17F5 and -22C4) and a few wells near the coast. This reflects the limited recharge in the Los Angeles Forebay (in comparison with the Montebello Forebay) and the effects of injection at the Dominguez Gap Barrier Project. Older water is yielded by deep wells of the Los Angeles Forebay, shallow and deep wells downgradient along section *C'–B'*, and wells near the interior of the West Coast Basin. Carbon-14 data show that apparent ground-water ages generally increase with depth and distance away from the forebay. Furthermore, carbon-14 data show significant differences in the relative ages of water within the Lower aquifer systems.
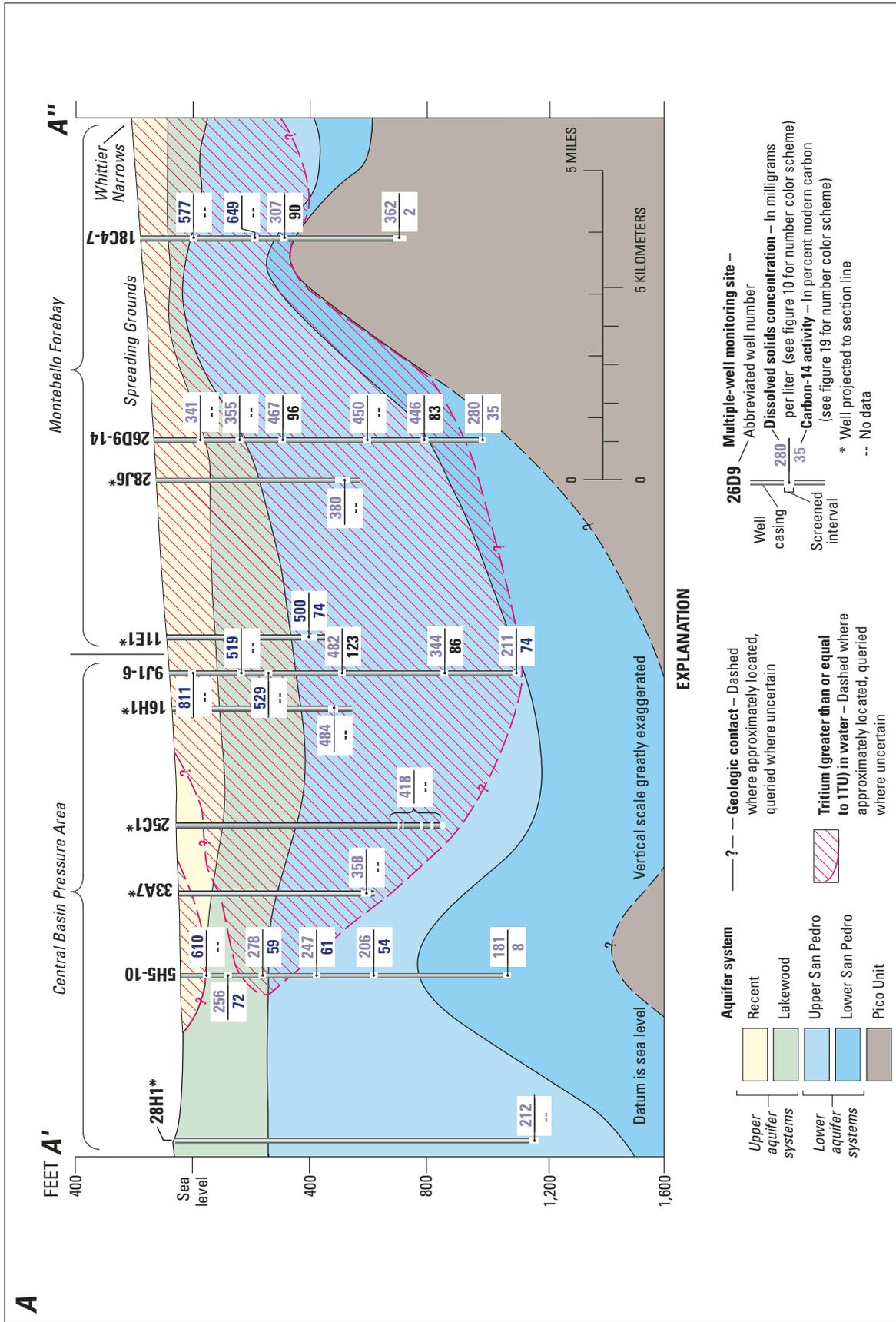
Figure 20. Dissolved-solids concentration, measurable tritium activity, and carbon-14 activity in ground water from wells sampled along geohydrologic sections *A'–A''*(A)and *C'–B'*(B), Los Angeles County, California.

Figure 20.—Continued.

To clarify the source and movement of recharge waters in the study area, oxygen-18 and deuterium were plotted, and then grouped by available tritium concentrations. As shown in figure 21, nearly all waters that have very low, or less than measurable, tritium plot above the meteoric water line. This older water in the study area originates, predominantly, from the San Fernando Valley (about -47 per mil δD) and the San Gabriel Valley (about -55 per mil δD). This water is similar to "native fresh waters of good chemical quality" described by Piper and Garrett (1953).

All recent water in figure 21 that has significant tritium (greater than 8 TU) plots below the meteoric water line. Most points cluster at about –61 per mil δD, are chemically distinct, and show the influence of artificially recharged water. The extent to which a sample is offset below the meteoric water line largely reflects the relative proportion of native water that has mixed with artificially recharged water. The effect of this mixing is evident in water from well 5S/12W-1E2 since only imported Colorado River water is injected at the nearby Alamitos Gap Barrier Project. Assuming only a two-component mixture, recharge to this well (based on δD values) consists of 25 percent native Central Basin water and 75 percent imported Colorado River water.

In figure 21, water from a few wells has moderate tritium values (1 to 8 TU) and varied isotopic composition. Few regional generalizations can be drawn from this group, as differences likely reflect a combination of local hydrologic factors. For example, values for wells 4S/14W-9D1 and 4S/14W-2N4 could result from a mixture of seawater, imported water, and (or) native water (fig. 8). Values for other wells associated with this group may indicate recently recharged native water in the Dominguez Gap (4S/13W-1N8) and Whittier Narrows (2S/11W-18C5) areas.

Table 3. Processes and reactions controlling water quality along geohydrologic sections A'–A'' and C'–B', Los Angeles County, California

Process	Reaction	Note
1. Sulfate reduction	$2CH_2O + SO_4^{-2} \rightarrow H_2S + 2HCO_3^{-2}$	Requires organic material (generalized as CH_2O)in aquifer; mediated by sulfate-reducing bacteria
2. Cation exchange	$2Na^+ + Ca\text{–clay} \rightarrow Ca^{+2} + Na_2\text{–clay}$	Exchange of dissolved calcium (or magnesium) in water for sodium on clay minerals
3. Calcite precipitation	$HCO_3^- + Ca^{+2} \rightarrow CaCO3 + H^+$	Precipitation of minerals that remove ions from the water
4. Evaporite dissolution	$NaCl(s) \rightarrow Na^+ + Cl^-$ $CaSO_4(s) \rightarrow Ca^{+2} + SO_4^{-2}$	Salts from areas of ground-water discharge, lagoons, or semi-perched aquifers
5. Iron cycling	Oxidation/reduction, dissolution	Iron-hydroxides; iron-silicates; pyrite
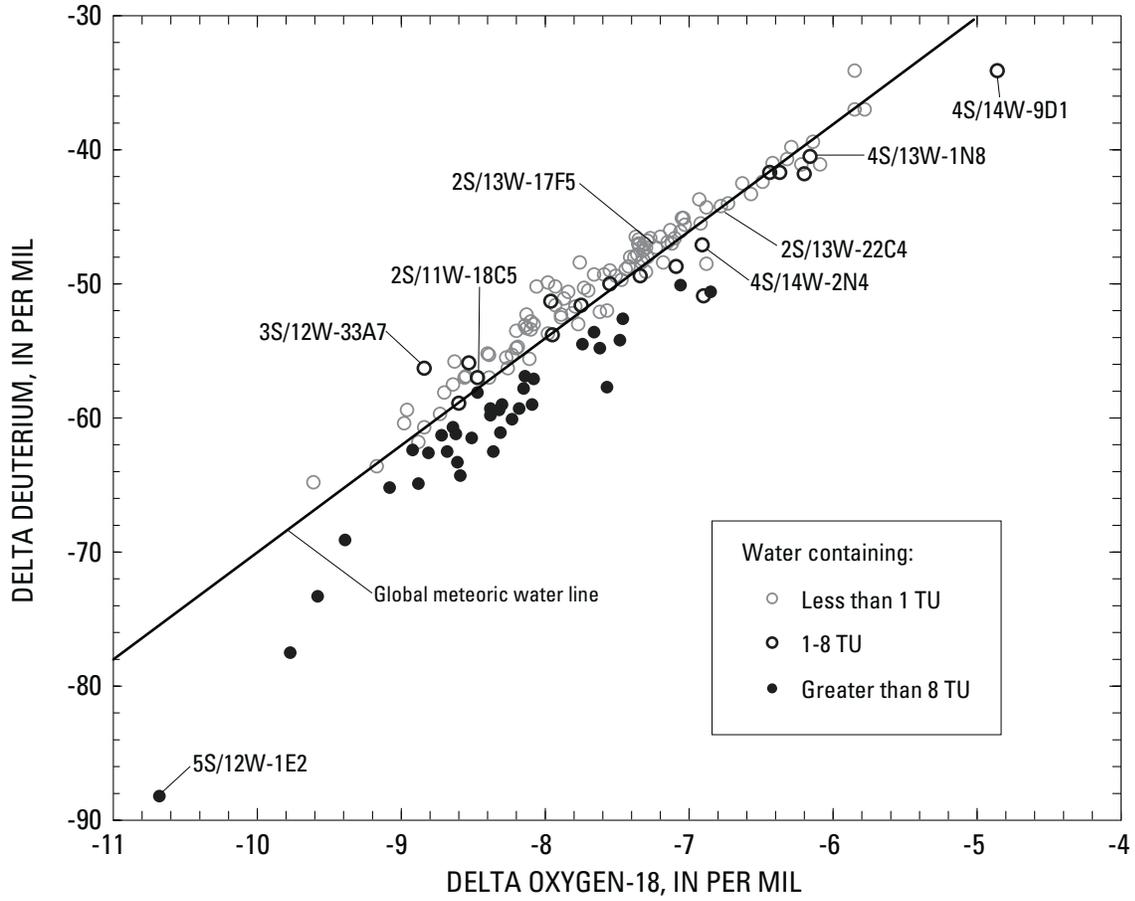
Figure 21. Delta deuterium as a function of delta oxygen-18, grouped by tritium concentration in ground water sampled in the study area, Los Angeles County, California.

DEVELOPMENT OF A GROUND-WATER SIMULATION MODEL

A ground-water simulation model was developed to synthesize the understanding of the three-dimensional geohydrologic system and to serve as a tool to evaluate alternative ground-water management strategies. The model covers the entire study area, including parts offshore. The grid for the model is shown in figure 22. The model uses the USGS MODFLOW program (McDonald and Harbaugh, 1988; Harbaugh and Mc Donald, 1996). The uniform finite-difference grid consists of 4,480 cells, each 0.5 mi by 0.5 mi. The model includes separate layers for the four main aquifer systems described earlier (fig. 3). The extent of layer 1, representing the Recent aquifer system, is limited and is based on the extent of the Gaspur aquifer. First, a steady-state model was run to approximate conditions in water year 1971. A 30-year transient case (1971–2000) was then simulated using yearly stress periods.

Required model inputs include boundary conditions, elevation of aquifer-system bases, hydraulic conductivities, storage properties of the aquifer systems, vertical conductance between aquifer systems, conductance across faults, recharge, and pumpage. Layer 1 was modeled as unconfined (a Type 1 layer in MODFLOW) with layer base, specific yield, and hydraulic conductivity specified. Layers 2–4 were modeled as confined/unconfined (Type 3 layers in MODFLOW) with layer top, layer base, confined storage coefficient, specific yield, and hydraulic conductivity specified. Re-wetting was allowed for layers 1 through 3 (layer 4 did not go dry in any of the simulations).

Boundary Conditions

The model-boundary conditions are no-flow along the boundary with Tertiary deposits to the north and northeast (the Santa Monica Mountains and the Elysian, Repetto, Merced, and Puente Hills) and to the southwest (the Palos Verdes Hills) (figs. 1, 22). Within the model domain, the Baldwin Hills also are modeled as no-flow cells. For layer 1 (fig. 22A) no-flow boundaries are used to represent the estimated areal extent of the Gaspur aquifer. General-head boundaries were used at the Los Angeles and Whittier Narrows to represent ground-water underflow from San Gabriel and San Fernando Valleys. These general-head boundaries were applied using average measured water levels over the simulation period at wells along these boundaries (well 1S/13W-14E3 for the Los Angeles Narrows and wells 2S/11W-5L1 and -6G2 for the Whittier Narrows; these water levels are quite constant over the simulation period) (fig. 23). The general-head-boundary conductance specified in MODFLOW for the cells at these two boundaries is 0.3 ft^2/s. Time-varying specified head boundaries were used at the Los Angeles–Orange County boundary in the Central Basin to represent ground-water underflow to and from the Orange County ground-water basin (note, the model boundary actually extends from 0.5 to 3 miles into Orange County). The specified-head boundaries were set on the basis of measured water levels over the simulation period at wells 3S/11W-35J3, 4S/11W-4K1, -19R1, and 5S/11W-7C1 (fig. 23). Values used for these wells are the averages of the annual minimum and maximum levels. Water levels at these wells are assumed to represent conditions in model layer 3 (fig. 22C). Comparable water levels for layers 2 and 4 (layer 1 is not active at this boundary) were estimated on the basis of relative heads at the USGS multiple-well monitoring sites La Mirada-1, Cerritos-1, and Long Beach-1. The implications of applying this boundary condition are discussed and tested later.
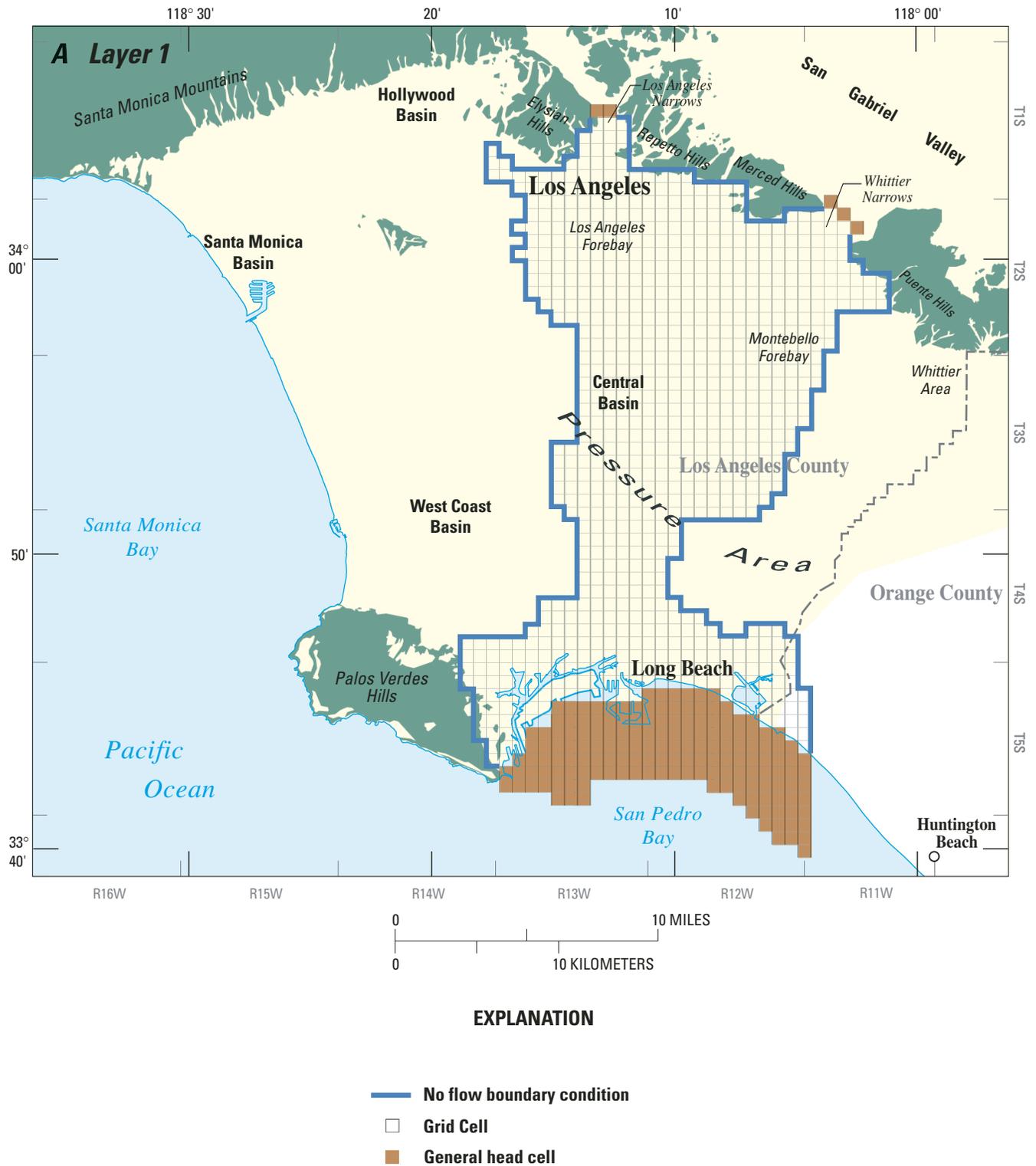
Figure 22. Model grid and boundary conditions for the ground-water simulation model for layer 1, Recent aquifer system (*A*); layer 2, Lakewood aquifer system (*B*); and layers 3 and 4, Upper San Pedro and Lower San Pedro aquifer systems (*C*), Los Angeles County, California.

Figure 22.—Continued.

Figure 22.—Continued.

Figure 23. Wells used for water-level calibration and head-dependant boundary conditions for ground-water simulation model, Los Angeles County, California.

All offshore cells in the uppermost layer (either layer 1, or layer 2 where layer 1 is not present) are set as general-head boundaries to simulate the impact of the overlying seawater. At the outermost offshore cells, general-head boundaries are specified for all layers. For all these offshore general-head boundaries, a freshwater-equivalent head based on the bathymetry is specified. This equivalent head is a very simplified way to account for the impacts of the higher density seawater. It is computed as the bathymetric depth multiplied by 0.025, the relative density difference between seawater and freshwater. The general-head-boundary conductance values specified in MODFLOW for the outermost offshore cells were 0.006 ft^2/s (for layer 1 and for layers 2-4 in the Santa Monica Bay) and 0.003 ft^2/s (for layers 2-4 in the San Pedro Bay) (fig. 22). Given the average modeled thickness of these cells (ranging from 100 to 540 ft), these conductance values imply average hydraulic conductivity values at these outermost offshore boundaries that range from about 0.25 to 2.5 ft/day. General-head-boundary conductance values of 0.0001 ft^2/s were specified for the interior ocean cells in the uppermost active layer. Assuming an average vertical distance of about 60 ft between these cells and the overlying ocean, these conductance values imply average vertical hydraulic conductivity values at these interior ocean boundaries of about 0.0001 ft/day. The underlying Pico unit (fig. 3) is considered to be a no-flow boundary. Faults were incorporated into the model using the horizontal-flow barrier package for MODFLOW (Hsieh and Freckleton, 1993).

Model-Layer Elevations

Elevations of the bases of the four aquifer systems were determined from the hydrostratigraphy analyses described earlier in this report. These elevation values were specified in the model (fig. 24) and were used to estimate hydraulic conductivity, storage coefficient, and vertical conductance; to apportion pumpage and injection between model layers; and to determine which water-level wells to use for each layer in the calibration process. Surfaces of

model layer elevations were developed by using the GIS to interpolate and extrapolate from the elevations determined at individual wells.

Geophysical logs from about 160 wells, including 24 USGS monitoring sites, along with about 90 lithologic logs included in cross sections presented by the California Department of Water Resources (1961) were used to develop the model layer elevations. Depths to the base of the four aquifer systems were determined at individual wells. Discussion of the criteria used in this analysis is included in the earlier section on "Hydrogeologic Framework." In addition to these physical wells, 21 artificial well locations were used for simple extrapolations of the elevation of each layer to the edges of the model boundary that were consistent with topography and bathymetry.

To construct a grid to interpolate the surface of the base of the four aquifer layers, a separate griding program, Surfer 7 (Golden Software, 1999), was used. Kriging was chosen as the interpolating algorithm for the lower three layers because of the flexibility in adjusting the variogram and the fact that kriging allows anisotropy, or weighting in divergent directions, in its calculations. A summary of the kriging results is in Appendix IV. In layer 3 the estimated angle of anisotropy was about 180 degrees (north-south); no anisotropy was applied in layers 2 or 4. A variogram was established for each layer by adjusting the sill, correlation length, and nugget effect. Because of its limited extent, the Recent aquifer system was interpolated using a simple radial basis function. No anisotropy was used in the interpolation of the grid.

A grid surface was produced and exported back into the GIS, converted into polygon coverages, and incorporated into the model input. The top of layers 2–4 also is the base of the layer above it. Where layer 1 is not active (fig. 22A), the top of layer 2 is taken to be 75 ft below land surface. For numerical stability in modeling, the base of each model layer was required to be a minimum depth below the base of the overlying layer (or land surface for layer 1). These minimum depths were 100 ft for layer 1, 125 ft for layer 2 and 75 ft for layers 3 and 4.
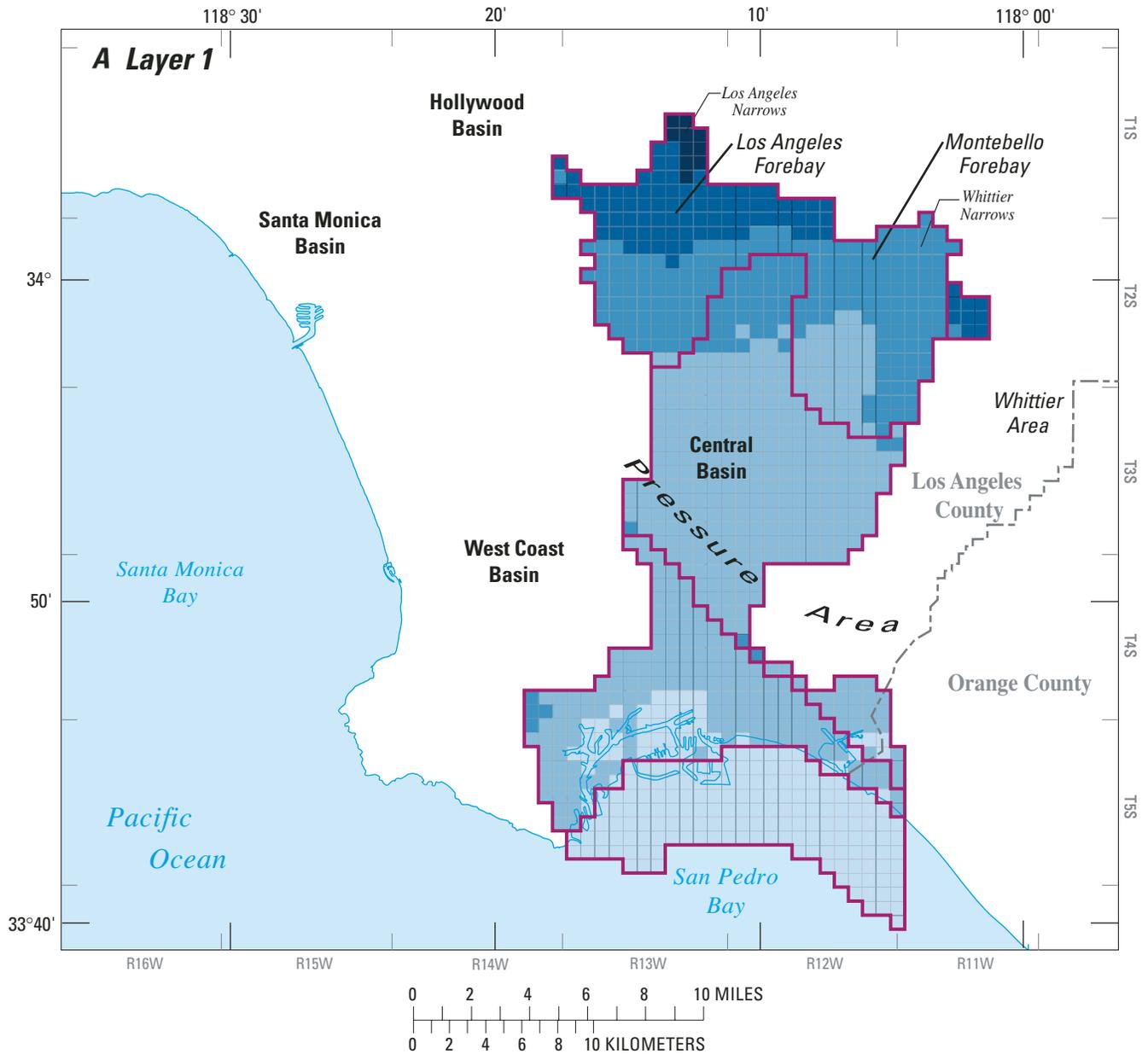
Figure 24. Elevation of base of layers 1-4 of the ground-water simulation model: Recent aquifer system (*A*), Lakewood aquifer system (*B*), Upper San Pedro aquifer system (*C*), and Lower San Pedro aquifer system (*D*), Los Angeles County, California.

Figure 24.—Continued.

C Layer 3

Los Angeles Narrows

Whittier Narrows

Hollywood Basin

Santa Monica Basin

Los Angeles Forebay

Montebello Forebay

Whittier Area

Central Basin

Pressure

Los Angeles County

West Coast Basin

Santa Monica Bay

Area

Orange County

Pacific Ocean

San Pedro Bay

EXPLANATION

Elevation of base of layer – In feet above or below sea level

200 - 300	⁻300 - ⁻200

200 - 300

100 - 200

0 - 100

⁻100 - 0

⁻200 - ⁻100

⁻300 - ⁻200

⁻400 - ⁻300

⁻500 - ⁻400

⁻600 - ⁻500

⁻700 - ⁻600

⁻800 - ⁻700

⁻900 - ⁻800

⁻1,000 - ⁻900

⁻1,100 - ⁻1,000

⁻1,200 - ⁻1,100

⁻1,300 - ⁻1,200

⁻1,400 - ⁻1,300

⁻1,500 - ⁻1,400

⁻1,600 - ⁻1,500

Figure 24.—Continued.

D Layer 4

Hollywood Basin

Santa Monica Basin

Los Angeles Narrows

Whittier Narrows

Los Angeles Forebay

Montebello Forebay

Whittier Area

Central Basin

Los Angeles County

West Coast Basin

Pressure

Area

Santa Monica Bay

Orange County

Pacific Ocean

San Pedro Bay

118° 30'   20'   10'   118° 00'

34° 00'

50'

33°40'

T1S

T2S

T3S

T4S

T5S

R16W   R15W   R14W   R13W   R12W   R11W

0   2   4   6   8   10 MILES

0   2   4   6   8   10 KILOMETERS

EXPLANATION

Elevation of base of layer – In feet above or below sea level

200 - 300	-300 - -200	-800 - -700	-1,300 - -1,200
100 - 200	-400 - -300	-900 - -800	-1,400 - -1,300
0 - 100	-500 - -400	-1,000 - -900	-1,500 - -1,400
-100 - 0	-600 - -500	-1,100 - -1,000	-1,600 - -1,500
-200 - -100	-700 - -600	-1,200 - -1,100	

Figure 24.—Continued.

Hydraulic Properties

Initial estimates of hydraulic conductivities for each layer were calculated by summing the component transmissivities presented by the California Department of Water Resources (1961) for the relevant aquifers in each model layer ([fig. 3](#)) and dividing by the layer thicknesses. The resulting hydraulic conductivities were smoothed by computing the mean value within a three-by-three cell neighborhood around each cell. These values were modified during calibration. The final model-calibrated values used in the model are shown in [figure 25](#). Hydraulic conductivity values range from 13 to 800 ft/d for layer 1, 0.1 to 130 ft/d for layer 2, 0.6 to 140 ft/d for layer 3 and 1.0 to 50 ft/d for layer 4. Note, in the model calibration, upper bounds of 800, 150, 150, and 50 ft/d were fixed for layers 1–4, respectively.

The vertical conductance (V_{cont}) between the aquifers was computed by applying equation 51 of McDonald and Harbaugh (1988, p. 5–13). The vertical hydraulic conductivity for each model layer was computed as a fraction of the horizontal conductivity. The applied fractions range from 0.10 in the forebay areas to 0.0005 between layers 2 and 3 in the inland part of the West Coast Basin. The very small values for these ratios reflect the fact that within the thick aquifer systems that make up the model layers, the horizontal conductance is dominated by the horizontal hydraulic conductivity of the continuous coarse-grained deposits, and the vertical conductance is dominated by the vertical hydraulic conductivity of the fine-grained materials. Resulting values for vertical conductance in the model are shown in [figure 26](#). V_{cont} values range from 8×10^{-6} to 0.22 /day between layers 1 and 2, 7×10^{-7} to 7×10^{-2} /day between layers 2 and 3, and 2×10^{-6} to 4×10^{-2} /day between layers 3 and 4.

The specific-yield values used for layer 1, which are shown in [figure 27](#), were based, in part, on the work of the California Division of Water Resources (1934, pl. F), which mapped specific yield in the coastal Los Angeles area as ranging from 0.15 to 0.23. Specific yield values used for layer 1 range from 0.075 to 0.25 (as shown in [figure 27A](#), specific yield values of .075 were applied to layer 1 cells outside of the forebay areas). For layers 2–4, a specific storage value of 5.0×10^{-6}/ft for layer 2 and 2.0×10^{-6}/ft for layers 3–4 was multiplied by aquifer thickness to obtain the confined storage coefficients for each layer. The resulting storage coefficient values, shown in [figure 27B–D](#) range from .0006 to .003 in layer 2, .00015 to .0018 in layer 3, and .00015 to .0016 in layer 4. A constant specific yield of 0.075 was assigned to layers 2–4.

Conductances across the faults were specified in the horizontal-flow-barrier package in MODFLOW. These conductance values are referred to as hydraulic characteristics (Hsieh and Freckleton (1993). Initially, hydraulic characteristics for all faults were set at high values (1.0×10^{-5}/sec) that did not restrict flow. These values were modified during model calibration and are listed in [table 4](#). Final values applied for hydraulic characteristics range from 5.0×10^{-10} to 1.0×10^{-5} /sec.

Areal Recharge

It is assumed that areal recharge occurs in the uppermost active model layer. Areal recharge represents the combined effects of mountain-front recharge on the perimeter of the model domain and direct precipitation, return flow from irrigation such as lawn watering, and other distributed sources (for example, leakage from pipes) within the interior of the model domain. Because most parts of the major rivers are lined with concrete, river recharge/discharge is not simulated in the model. Recharge through the unlined channels of the Rio Hondo and San Gabriel River in the upper Montebello Forebay (Central Basin) is accounted for as part of the artificial spreading operations. Note that the potential hydraulic effects of the short unlined sections of the San Gabriel and Los Angeles Rivers near the San Pedro Bay are not simulated in the model.
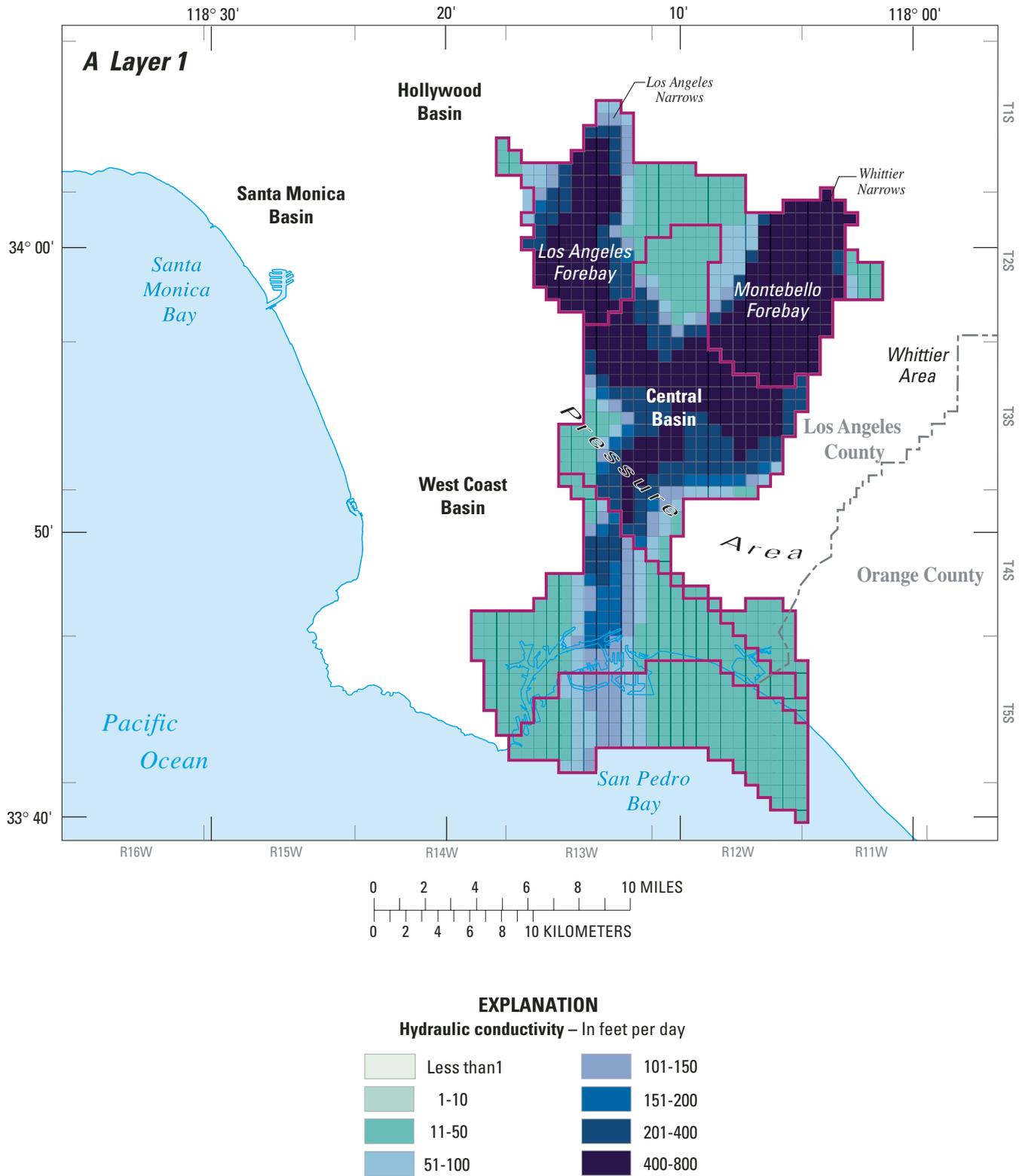
Figure 25. Hydraulic conductivities for layers 1–4 of the ground-water simulation model: Recent aquifer system (A), Lakewood aquifer system (B), Upper San Pedro aquifer system (C), and Lower San Pedro aquifer system (D), Los Angeles County, California.

B *Layer 2*

EXPLANATION

Hydraulic conductivity – In feet per day

Less than 1	101-150
1-10	151-200
11-50	201-400
51-100	400-800

Figure 25.—Continued.

C Layer 3

EXPLANATION

Hydraulic conductivity – In feet per day

Less than1	101-150
1-10	151-200
11-50	201-400
51-100	400-800

Figure 25.—Continued.

D *Layer 4*

Hollywood Basin

Santa Monica Basin

Los Angeles Narrows

Los Angeles Forebay

Whittier Narrows

Montebello Forebay

Whittier Area

Central Basin

West Coast Basin

Pressure Area

Los Angeles County

Orange County

Santa Monica Bay

Pacific Ocean

San Pedro Bay

0 2 4 6 8 10 MILES

0 2 4 6 8 10 KILOMETERS

EXPLANATION

Hydraulic conductivity – In feet per day

Less than 1	101–150
1–10	151–200
11–50	201–400
51–100	400–800

Figure 25.—Continued.
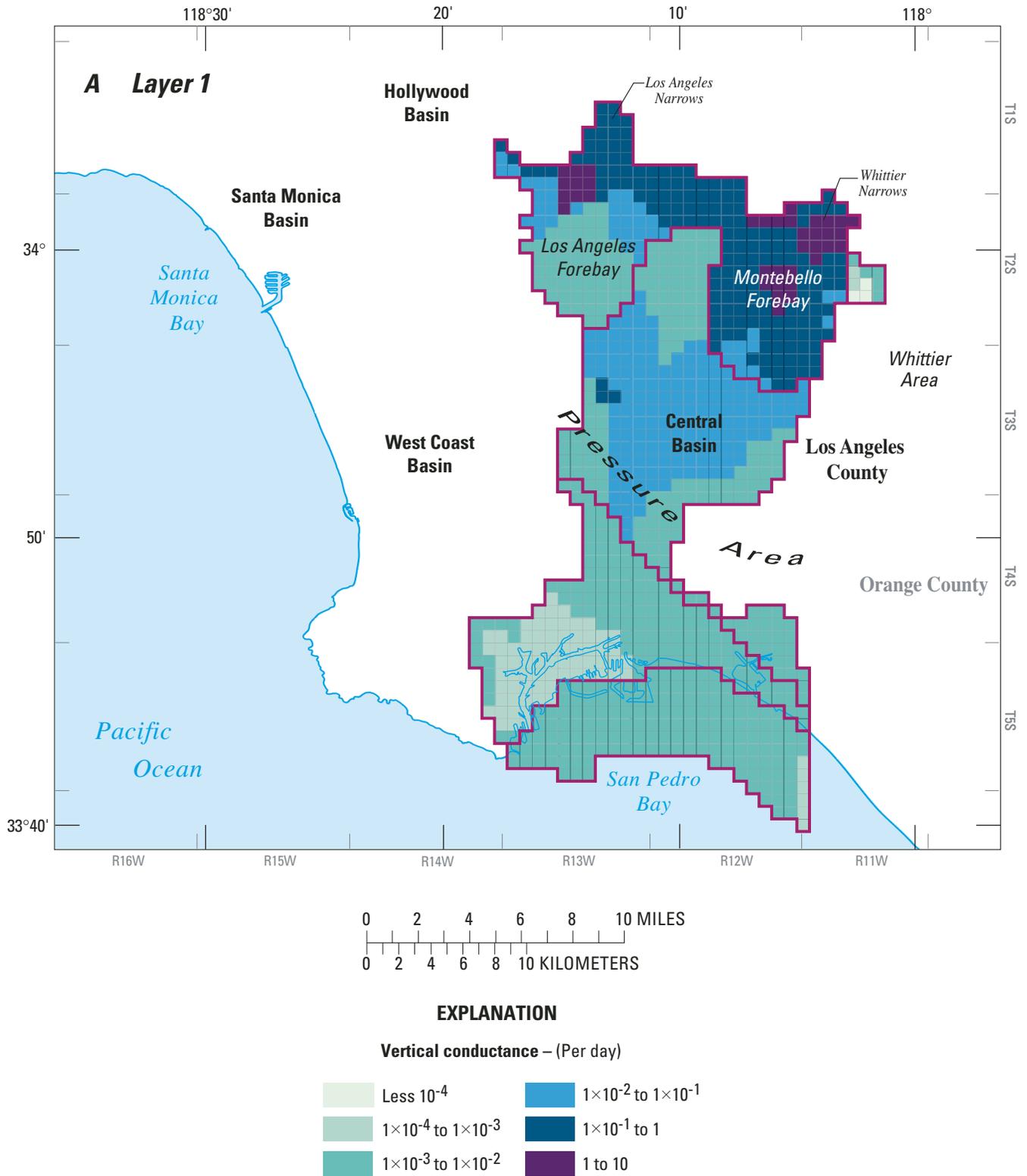
Figure 26. Vertical conductances for the ground-water simulation model: between layers 1 and 2, Recent and Lakewood aquifer systems (*A*); between layers 2 and 3, Lakewood and Upper San Pedro aquifer systems (*B*); and between layers 3 and 4, Upper San Pedro and Lower San Pedro aquifer systems (*C*), Los Angeles County, California.
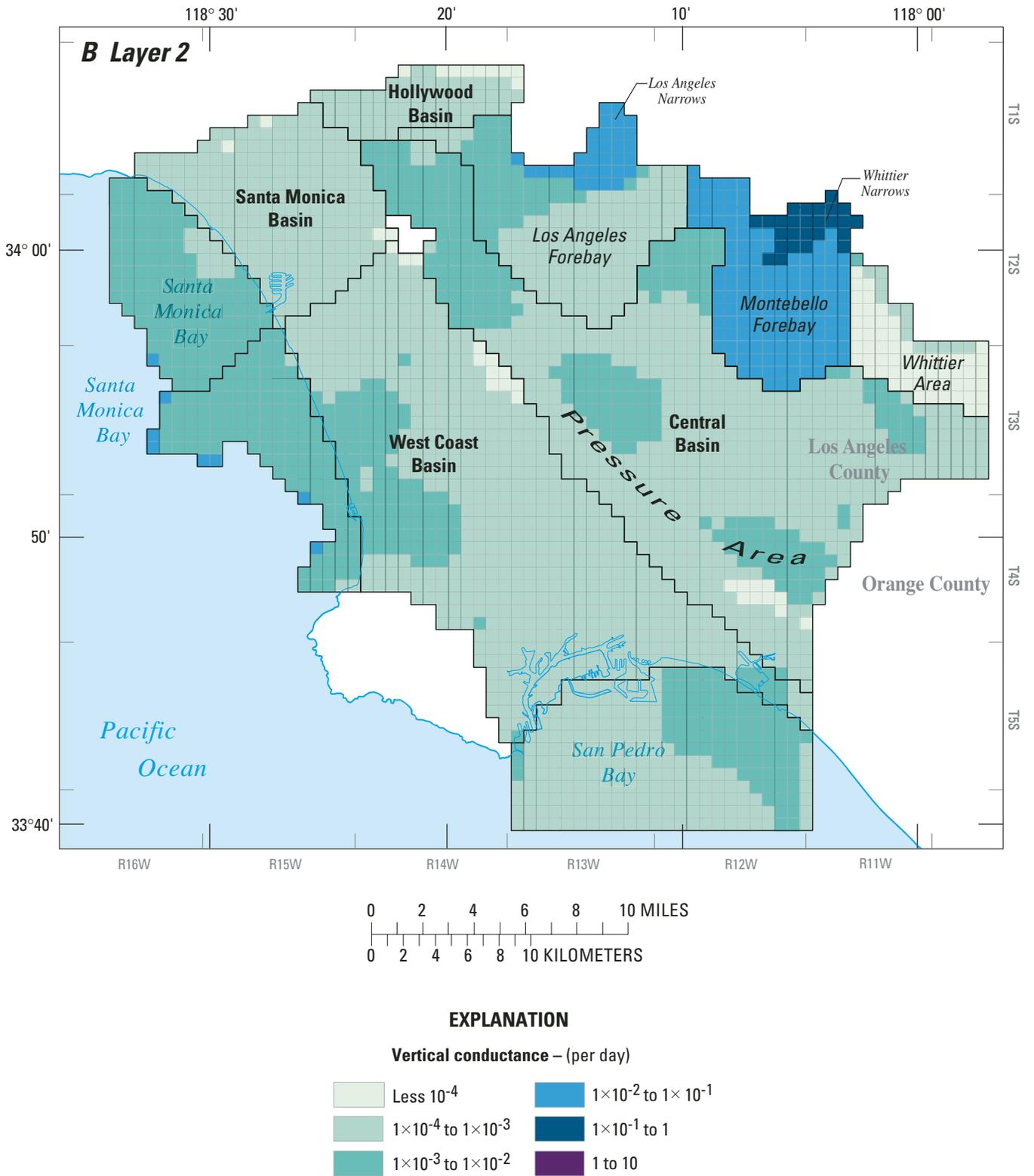
Figure 26.—Continued.
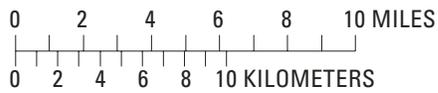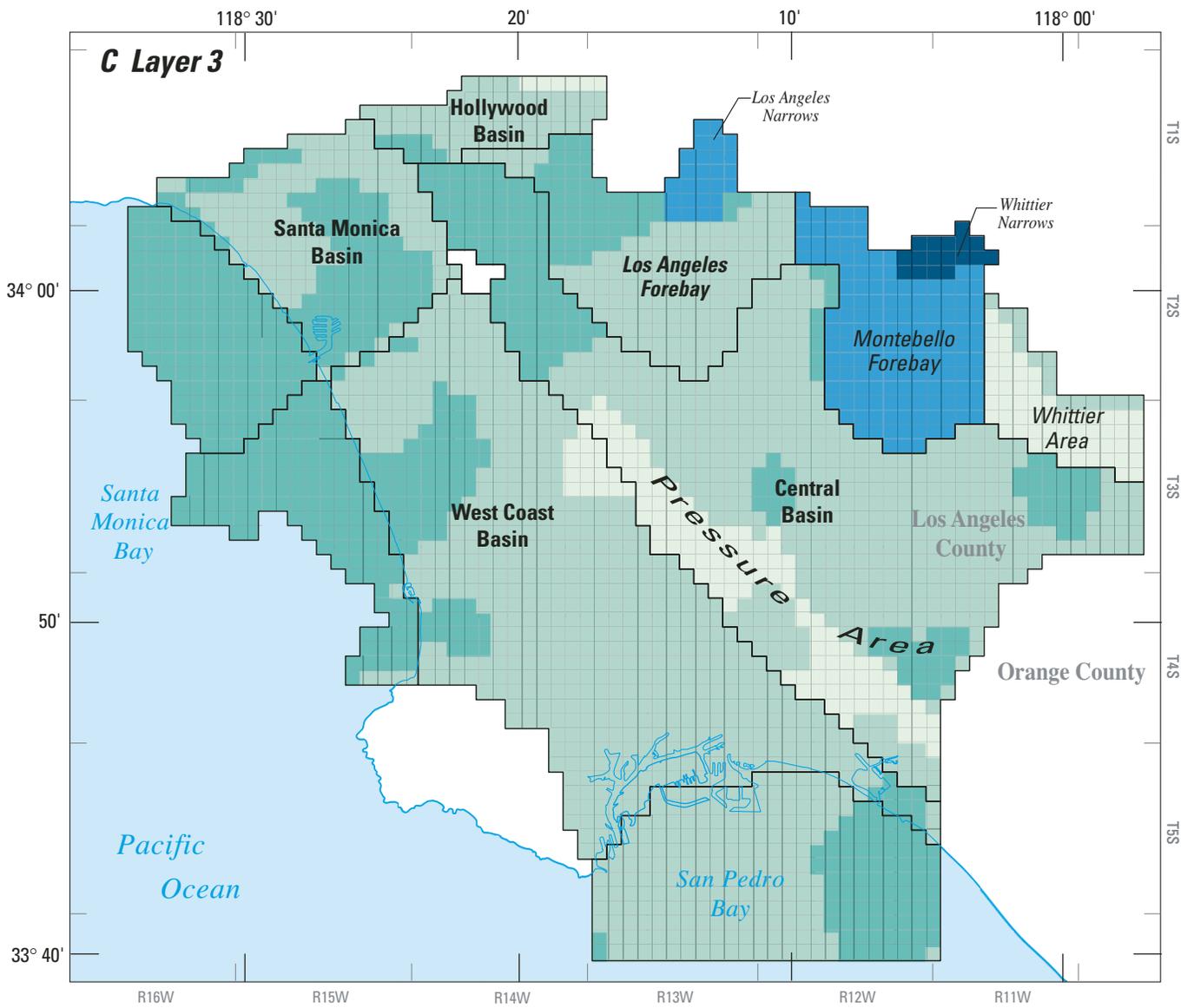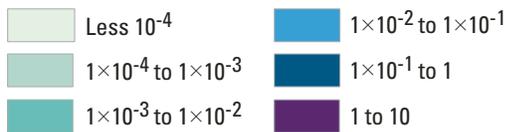
Figure 26.—Continued.
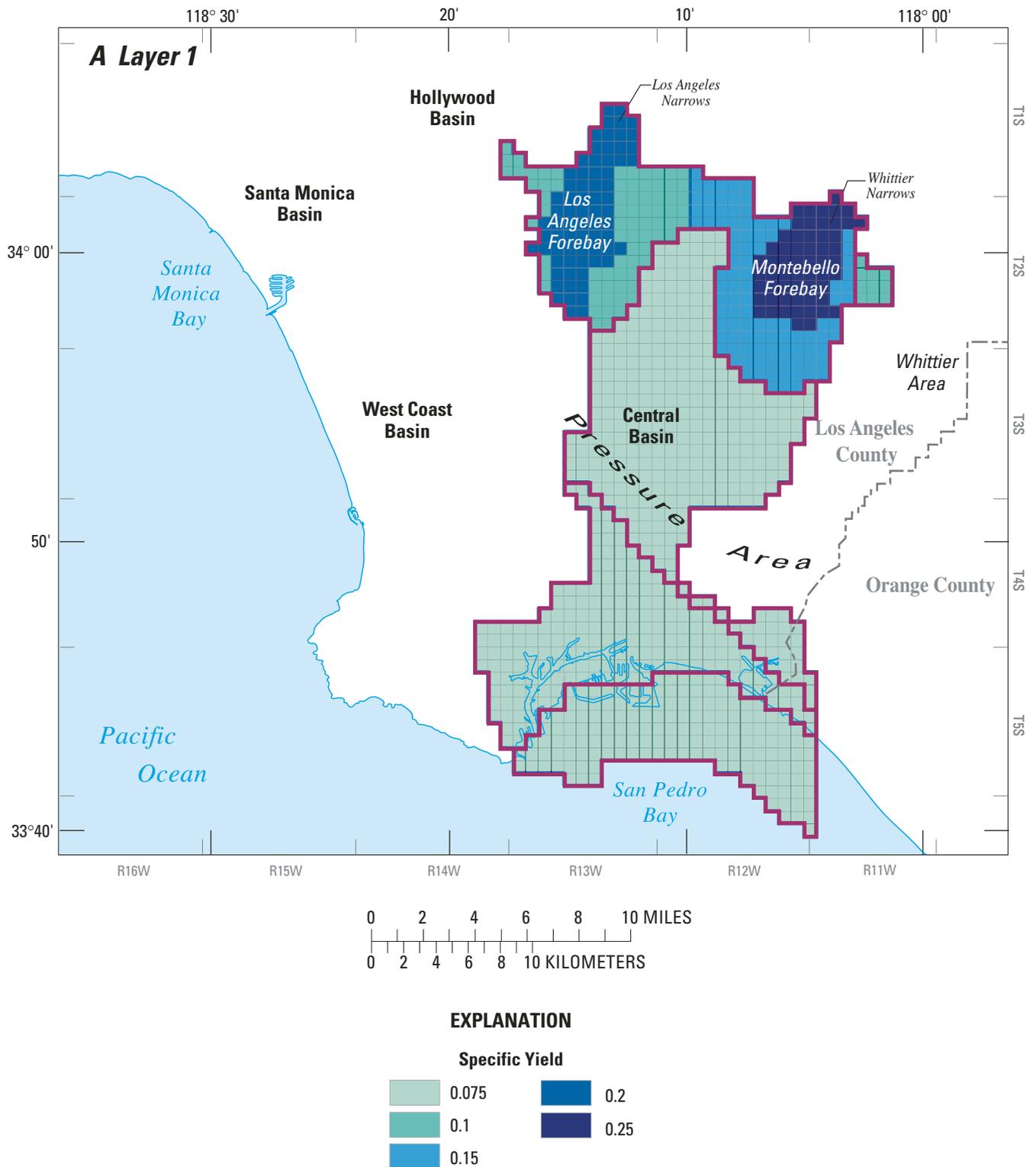
Figure 27. Specific yield for layer 1 and storage coefficients for layers 2–4 of the ground-water simulation model: Recent aquifer system (*A*), Lakewood aquifer system (*B*), Upper San Pedro aquifer system (*C*), and Lower San Pedro aquifer system (*D*), Los Angeles County, California.

Figure 27.—Continued.

C Layer 3

118° 30'   20'   10'   118° 00'

Hollywood
Basin

Los Angeles
Narrows

Santa Monica
Basin

Whittier
Narrows

34° 00'

Los Angeles
Forebay

Montebello
Forebay

Whittier
Area

Central
Basin

Santa
Monica
Bay

West Coast
Basin

Pressure

Los Angeles
County

50'

Area

Orange County

Pacific

Ocean

San Pedro
Bay

33° 40'

R16W   R15W   R14W   R13W   R12W   R11W

T1S
T2S
T3S
T4S
T5S

0   2   4   6   8   10 MILES

0   2   4   6   8   10 KILOMETERS
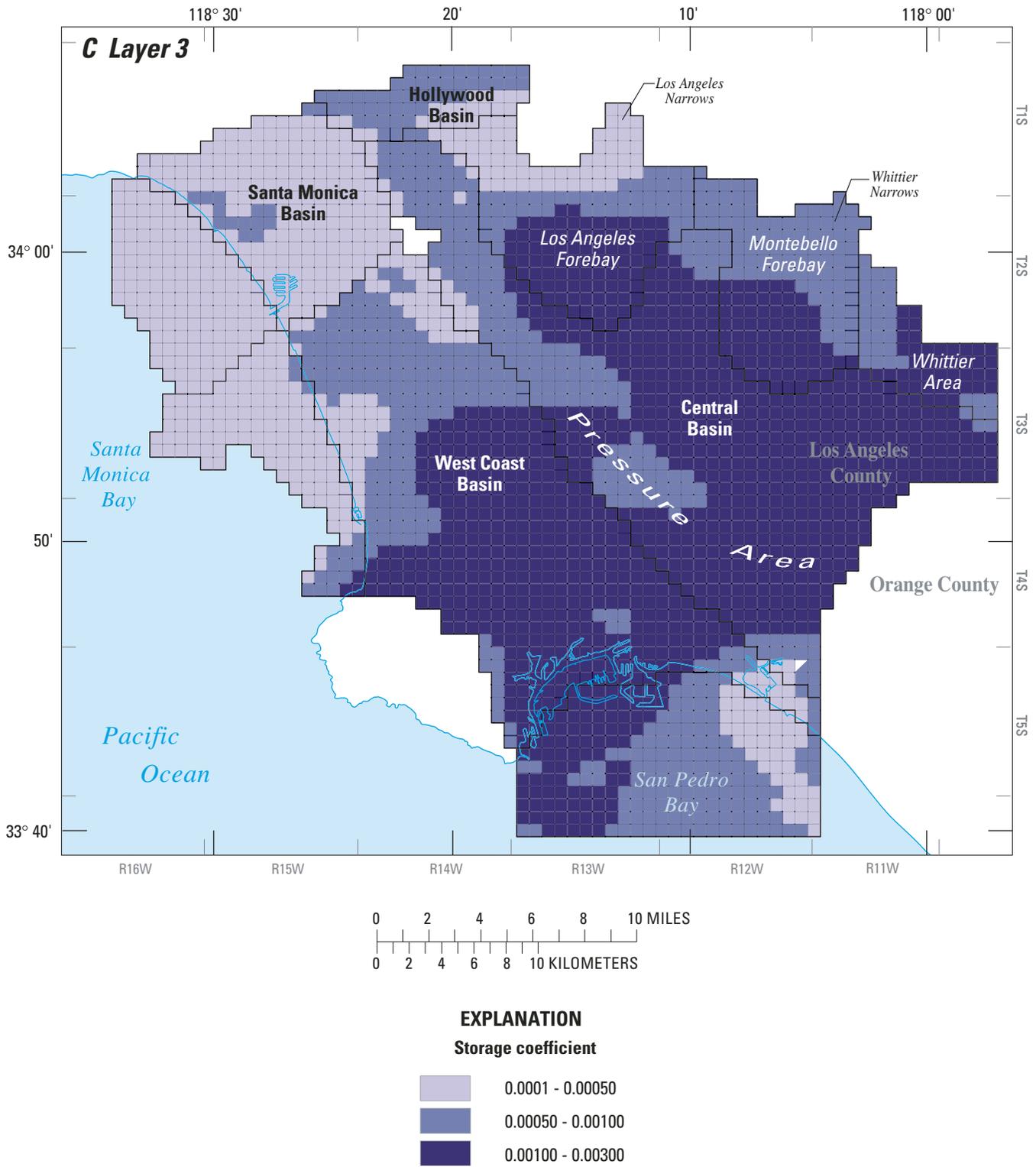
EXPLANATION

Storage coefficient

0.0001 - 0.00050

0.00050 - 0.00100

0.00100 - 0.00300

Figure 27.—Continued.

Figure 27.—Continued.

Table 4. Hydraulic characteristic values used in the ground-water simulation model

Fault name	Model layer(s)	Fault hydraulic characteristic (per second)
Avalon-Compton	2	1×10^{-7}
Avalon-Compton	3, 4	1×10^{-9}
Baldwin Hills faults	2	1×10^{-9}
Baldwin Hills faults	3, 4	5×10^{-10}
Cabrillo	2, 3, 4	1×10^{-6}
Charnock	2	1×10^{-7}
Charnock	3, 4	1×10^{-8}
Cherry Hill	2, 3, 4	5×10^{-10}
Dominguez anticline	2	1×10^{-7}
Dominguez anticline	3, 4	1×10^{-9}
Elysian Hills	2, 3, 4	1×10^{-5}
Inglewood	2, 3, 4	5×10^{-10}
Long Beach	2	1×10^{-8}
Long Beach	3, 4	1×10^{-9}
Los Alamitos	2	1×10^{-5}
Los Alamitos	3, 4	1×10^{-7}
Northeast Flank	2, 3, 4	5×10^{-10}
Norwalk	2, 3, 4	1×10^{-8}
Offshore faults	2, 3, 4	1×10^{-5}
Overland	2, 3, 4	1×10^{-8}
Palos Verdes	2, 3, 4	1×10^{-5}
Pico	2, 3, 4	1×10^{-5}
Poretero Canyon	2, 3, 4	5×10^{-10}
Portero	2, 3, 4	5×10^{-10}
Railroad Grade	2, 3, 4	5×10^{-10}
Reservoir Hill	2, 3, 4	5×10^{-10}
Rio Hondo	2, 3, 4	1×10^{-5}
Roscrans anticline and faults	2	1×10^{-7}
Roscrans anticline and faults	3, 4	1×10^{-8}
Santa Monica	2, 3, 4	1×10^{-7}
Santa Monica, unnamed	2, 3, 4	1×10^{-5}
Seal Beach	2, 3, 4	5×10^{-10}

Mountain-front recharge is simulated on the model perimeter along the foothills bounding the model area to the north, northeast, and southwest (fig. 28). Estimated values for steady state (1971) mountain-front recharge were computed by applying a modified version of the Maxey and Eakin (1949) method. A description of the approach and steps taken to estimate the mountain-front recharge is presented in Appendix V. As emphasized in Appendix V, this is a very simplified approach with many important assumptions.

For distributed interior recharge in the model for the steady state simulation (1971), a value of 1.5 in/yr was applied throughout the model domain, except the Montebello Forebay where a value of 2 in/yr was applied. These very simple estimates of recharge in the model interior were based on the measured precipitation within the model domain (ranging from 9 to 16 inches in 1971), along with the likely effects of irrigation, pipe leakage, evapotranspiration, and amount of impervious area.

For the transient simulation, the steady-state values used in the model for mountain-front recharge on the perimeter of the model area and for distributed interior recharge were varied annually as a function of precipitation. Precipitation station 107*D*, operated by the LACDPW, in Downey was used as an indicator station (fig. 1 in Appendix V). Precipitation at station 107*D* was normalized by the total precipitation in water year 1971 (table 5). For each year of the transient simulation, mountain-front and distributed interior recharge values were set equal to the steady-state values multiplied by the normalized precipitation for that year. An upper bound of 1.3 (determined by calibration) was placed on the normalized precipitation value to reflect the fact that there is a limit to the amount of additional precipitation and runoff that will replenish the ground-water system. Values used for mountain-front recharge and distributed interior recharge are summarized in table 5. This recharge is incorporated into MODFLOW using the recharge package. As is discussed later, there are significant limitations in the data and methodology used to estimate these recharge values.
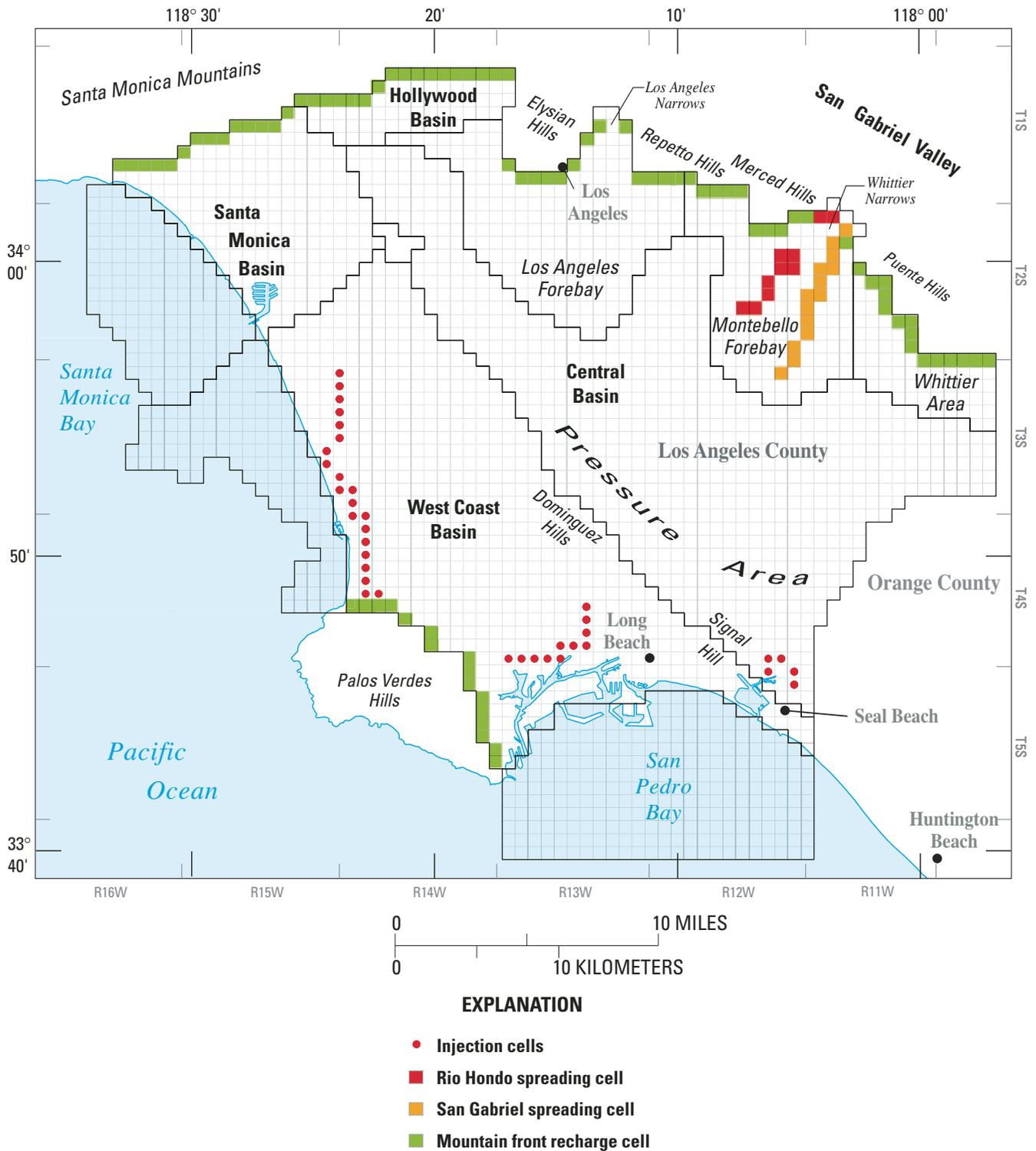
Figure 28. Injection, spreading, and mountain-front recharge cells for the ground-water simulation model, Los Angeles County, California.

Table 5. Annual precipitation at LACDPW Downey Station 107D and recharge and pumpage used in ground-water simulation model

[Acre-ft/yr, acre-feet per year]

Water year	Precipitation (inches)	Normalized precipitation	Mountain front and interior recharge (acre-ft/yr)	Spreading (acre-ft/yr)	Injection (acre-ft/yr)	Pumpage (acre-ft/yr)
1971	11.46	1	64,400	121,700	36,200	278,300
1972	6.4	.56	36,100	62,900	41,000	289,300
1973	18.63	1.63	83,700	147,100	41,800	272,300
1974	14.55	1.27	81,800	123,900	42,700	274,000
1975	15.01	1.31	83,700	105,700	36,900	278,500
1976	9.58	.84	54,100	81,900	44,800	283,200
1977	11.24	.98	63,100	69,900	49,300	279,000
1978	33.86	2.95	83,700	170,700	40,200	259,600
1979	18.69	1.63	83,700	151,800	34,500	270,700
1980	28.29	2.47	83,700	137,100	37,200	272,300
1981	8.74	.76	48,900	128,400	34,400	275,800
1982	13.41	1.17	75,300	110,100	34,300	276,500
1983	30.32	2.65	83,700	165,200	45,200	261,400
1984	11.99	1.05	67,600	114,500	39,500	258,300
1985	12.45	1.09	70,200	110,200	37,500	256,900
1986	19.47	1.7	83,700	117,400	31,700	264,600
1987	6.49	.57	36,700	101,000	39,400	254,000
1988	11.47	1	64,400	100,300	37,500	254,300
1989	7.82	.68	43,800	123,900	33,500	252,100
1990	7.87	.69	44,400	132,700	32,100	245,200
1991	12.22	1.07	68,900	138,700	29,700	247,900
1992	16.07	1.4	83,700	152,800	34,800	260,500
1993	26.56	2.23	83,700	174,500	31,300	226,800
1994	9.26	.81	52,200	113,600	25,100	181,100
1995	26.17	2.28	83,700	151,700	23,200	235,300
1996	10.68	.93	59,900	130,500	23,300	238,800
1997	13.95	1.22	78,600	128,300	29,300	243,800
1998	32.45	2.83	83,700	133,200	25,400	244,500
1999	7.29	.64	41,200	80,400	27,300	259,700
2000	9.21	.8	51,500	108,900	30,400	254,200
Mean	15.39	1.34	67,500	123,000	35,000	258,300

Pumpage, Spreading, and Injection

The model incorporates data on pumpage, spreading, and injection provided by the WRDSC, Los Angeles County Department of Public Works (LACDPW), the city of Santa Monica, and the California Department of Water Resources. Pumpage records for the West Coast and Central Basins have been maintained since the early 1960s by the California Department of Water Resources, which has served as water master. These pumpage data, along with data from the Santa Monica Basin (provided by the city of Santa Monica), were used in the model. Pumpage for wells perforated in more than one layer was divided between layers on the basis of perforation information and hydraulic conductivities and elevations of each model layer. Where perforation data were not available for a given well, water in that well was distributed between model layers on the basis of the average distribution for other wells in that area in that year. This dividing of pumpage between layers was done iteratively during calibration as hydraulic-conductivity values were adjusted. Model cells with pumpage in at least one stress period are shown in figure 29. Pumpage was incorporated into MODFLOW using the well package. Note that the well package does not have the capability of reapportioning pumpage between layers when a cell in a layer becomes dry during the simulation. Annual values input for pumpage are given in table 5.

Artificial recharge in the model includes spreading in the Montebello Forebay and direct injection at the three barrier projects: the West Basin Barrier and the Dominguez Gap Barrier in the West Coast Basin and the Alamitos Barrier in the Central Basin (fig. 28). Annual values for spreading and injection are given in table 5. Reported total annual spreading rates for the Rio Hondo and San Gabriel spreading facilities are incorporated into the model as recharge to layer 1 in the cells shown in figure 28 using the recharge package in MODFLOW. Total amounts of injection are reported for each of the three barrier projects. These injection totals are prorated among individual wells based on periodic well measurements.

As was done with pumpage, injected water was distributed between model layers on the basis of the perforations of the injection well and the aquifer conductivities and elevations. Injection was incorporated into MODFLOW using the well package.

Model Calibration

The steady-state and transient calibrations were done in a coupled, iterative manner. Water year 1971 (October, 1970 to September, 1971) was chosen as an approximate representation of steady-state conditions. The goal was to identify an interval during the modern period (after the basins were adjudicated) when accurate pumpage data were available and ground-water levels were relatively constant. Analysis of long-term hydrographs indicated that water year 1971 was the most appropriate choice. It was the earliest year after the dramatic water-level recovery resulting from adjudication in which water levels had somewhat stabilized at many wells. However, it is certain that ground-water conditions were not at a true equilibrium in 1971 (fig. 7), nor at any other time after the initiation of ground-water development in the area. The 30-year transient simulation period was considered adequate to minimize most residual effects of the initial conditions. Water-level data for calibrating the model were compiled from LACDPW, the WRDSC, and the city of Santa Monica, and from USGS monitoring wells. The locations of the wells used for model calibration are shown in figure 23.

Shown in figure 30 are simulated steady-state ground-water levels for water year 1971, along with average measured water levels for the water year in the four model layers representing the four aquifer systems. Note that most measured water-level data for 1971 is for layer 3. The transient calibration used the simulated 1971 water levels as initial conditions.

Transient hydrographs for the 1971–2000 transient simulation are shown in Appendix VI. Contours of simulated and average measured water levels for water year 2000 are shown in figure 31.
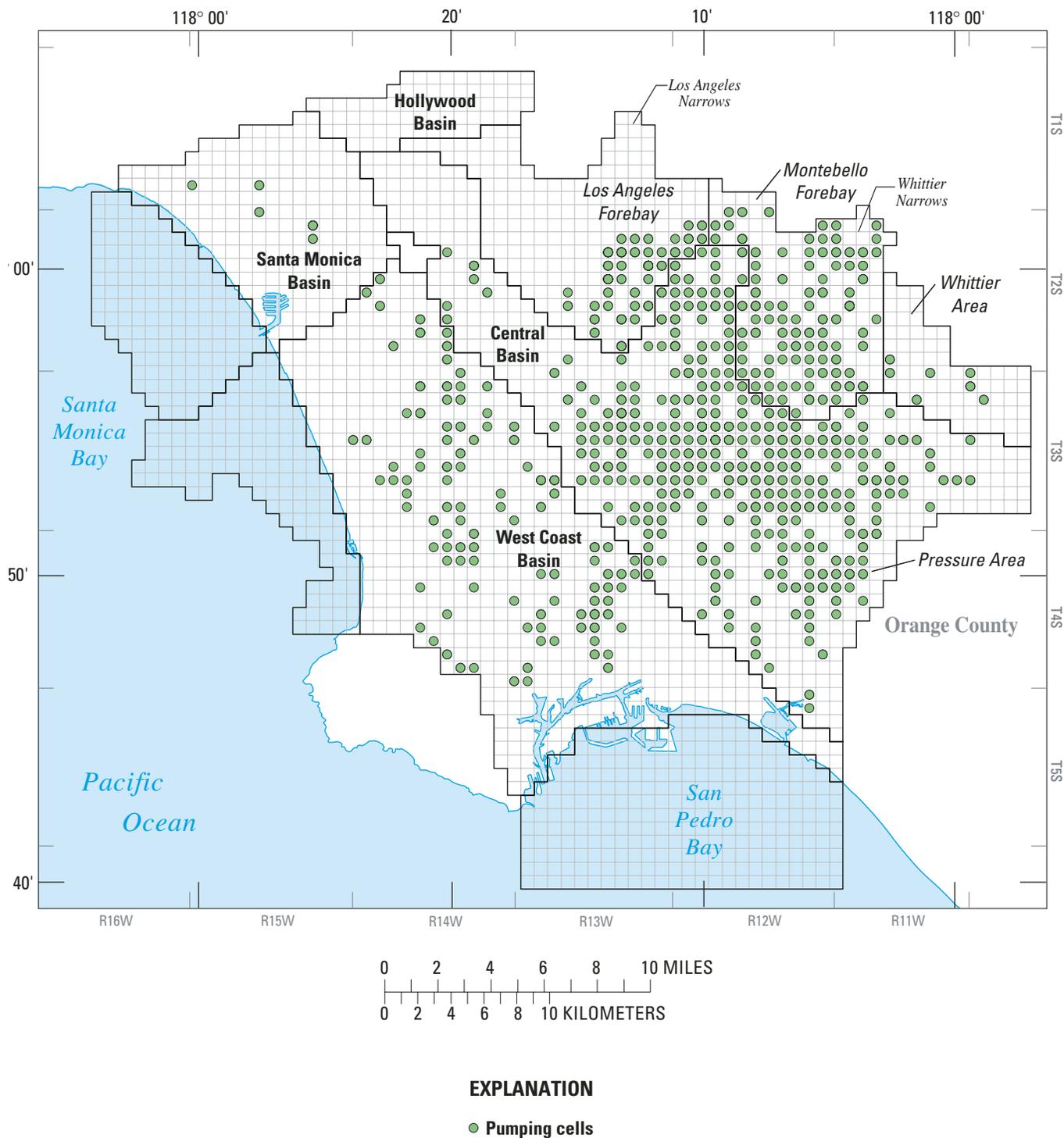
Figure 29. Pumping cells for years 1971–2000 in ground-water simulation model, Los Angeles County, California.
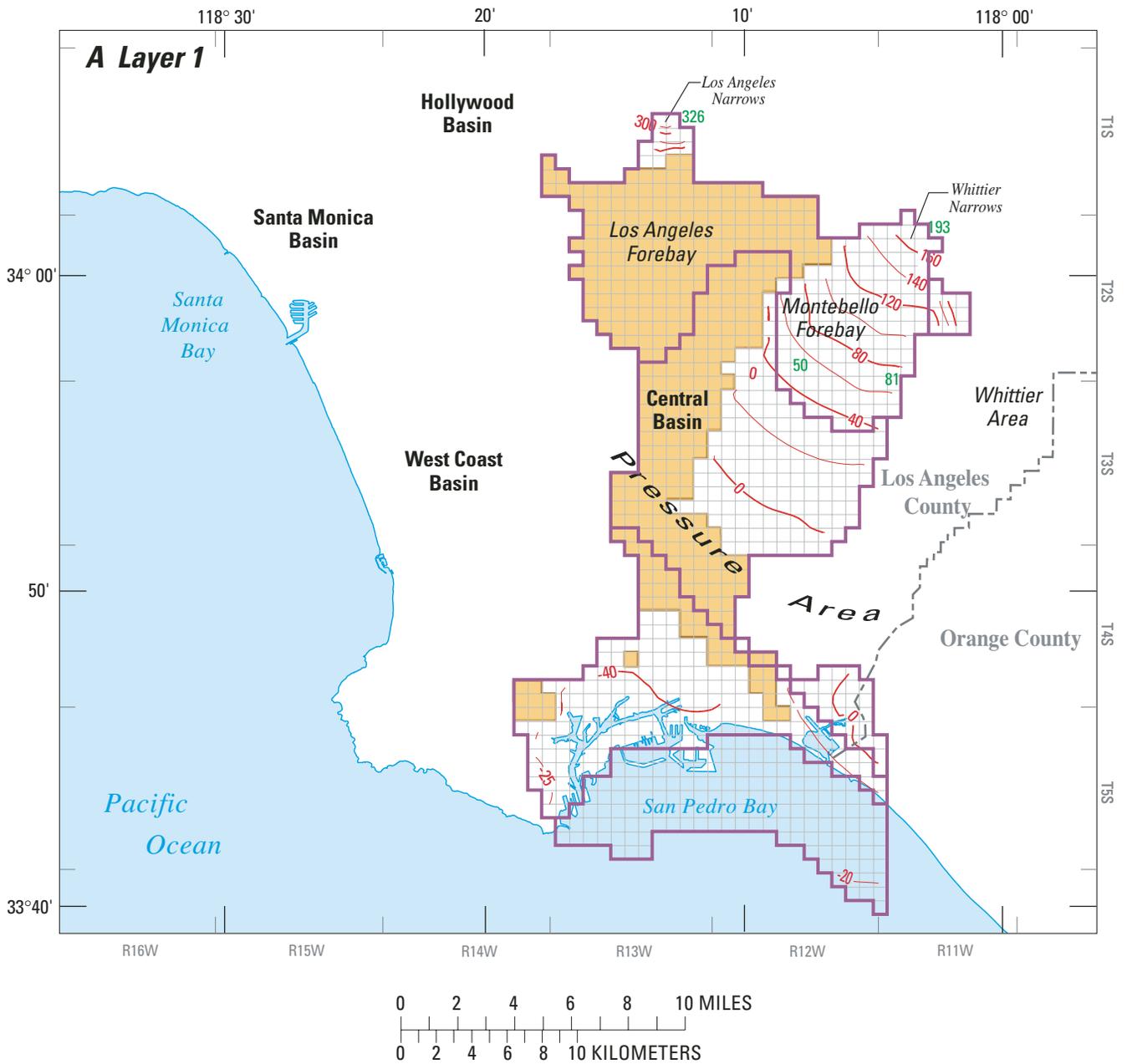
Figure 30. Model-simulated and average measured water levels, 1971, for layers 1–4 of the ground-water simulation model: Layer 1, Recent aquifer system (*A*); Layer 2, Lakewood aquifer system (*B*); *Layer* 3, Upper San Pedro aquifer system (*C*); and Layer 4, Lower San Pedro aquifer system (*D*), Los Angeles County, California.

B Layer 2

34° 00'

50'

33°40'

Hollywood Basin

Los Angeles Narrows

Whittier Narrows

Santa Monica Basin

Santa Monica Bay

Los Angeles Forebay

Montebello Forebay

Whittier Area

Central Basin

West Coast Basin

Pressure Area

Los Angeles County

Orange County

Pacific Ocean

San Pedro Bay

0   2   4   6   8   10 MILES

0   2   4   6   8   10 KILOMETERS

EXPLANATION

——⌐_   **Model Boundary**

☐   **Grid cell**

▨   **Dry cells**

50   **Water-level measurement -** In feet above sea level

—130—   **Simulated water-level contour -** Shows water level in feet above sea level. Contour interval 20 feet

Figure 30.—Continued.

C Layer 3

EXPLANATION

⌐ Model Boundary

☐ Grid cell

▨ Dry cells

50 **Water-level measurement -** In feet above sea level

—130— **Simulated water-level contour -** Shows water level in feet above sea level. Contour interval 20 feet

Figure 30.—Continued.

Figure 30.—Continued.

Figure 31. Model-simulated and average measured water levels, 2000, for layers 1–4 of the ground-water simulation model: Layer 1, Recent aquifer system (*A*); Layer 2, Lakewood aquifer system (*B*); *Layer* 3, Upper San Pedro aquifer system (*C*); and Layer 4, Lower San Pedro aquifer system (*D*), Los Angeles County, California.

B Layer 2
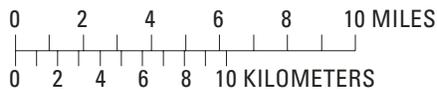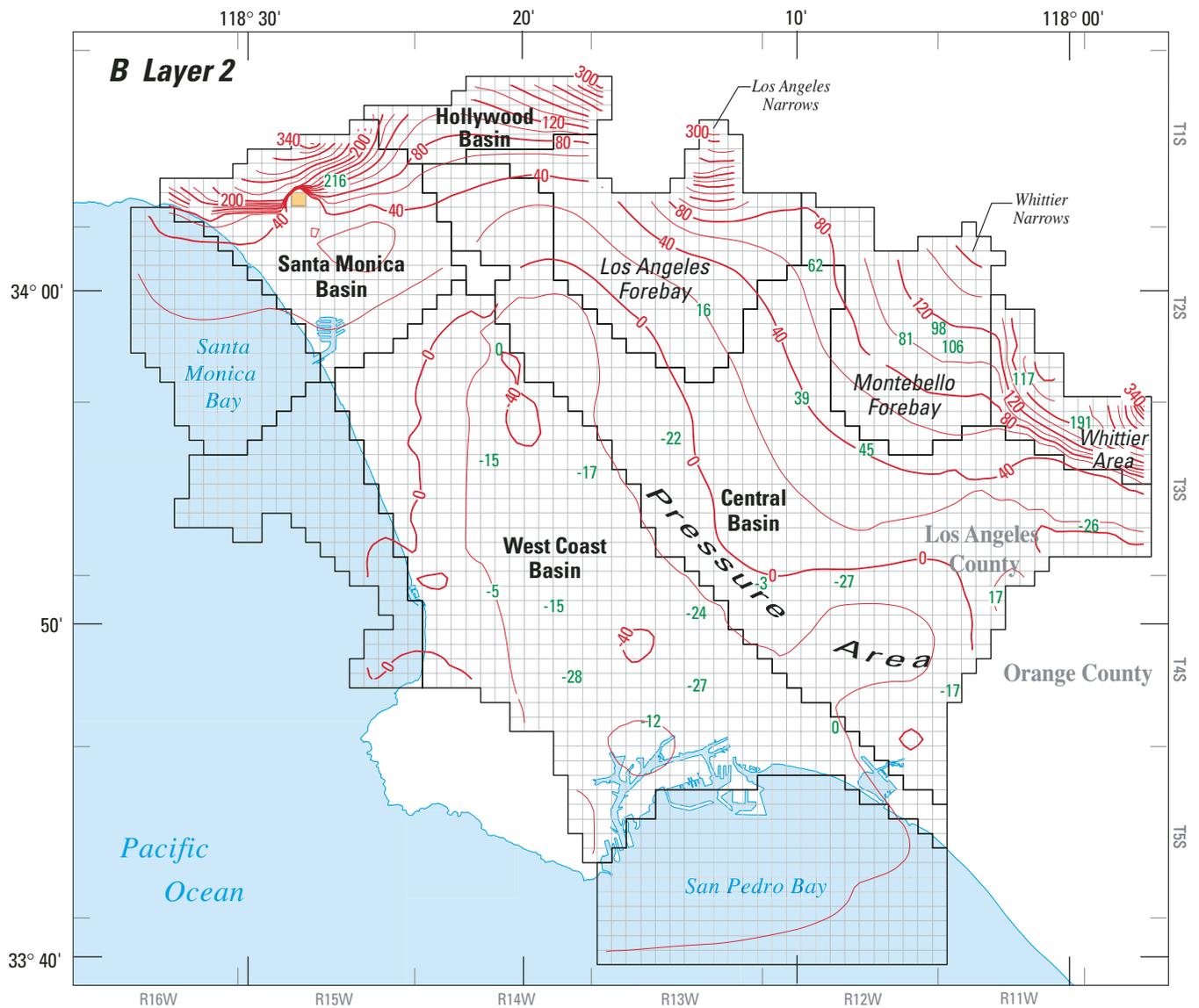
EXPLANATION

☐   **Grid cell**

▧   **Dry cells**

50   **Water-level measurement -** In feet above sea level

—130—   **Simulated water-level contour -** Shows water level
in feet above sea level. Contour interval 20 feet

Figure 31.—Continued.

Figure 31.—Continued.

Figure 31.—Continued.

The strategy for calibration was to achieve the best possible match to measured water levels at the USGS multiple-well monitoring sites drilled for this study and at selected long-term monitoring wells used by local agencies. Parameters varied as part of the calibration included hydraulic conductivity, vertical-to-horizontal hydraulic-conductivity ratios, specific yield, and selected hydraulic characteristics.

Hydraulic conductivities in the Montebello Forebay were increased from their initial values (by factors of 2.5 and 1.5 for layers 1–3 and 4, respectively) in order to match measured water levels, given the large quantities of artificially recharged water moving out through that area. Initial values of hydraulic conductivity in layers 1 and 2 in the Los Angeles Forebay also were increased by a factor of 2.0 near the Los Angeles Narrows and 1.5 elsewhere. Initial values of hydraulic conductivity in layers 3 and 4 in the Los Angeles Forebay were decreased to 0.15 times their initial values in order to simulate the depressed water levels in the lower aquifers in that area. In the Central Basin Pressure Area downgradient from the forebays, hydraulic conductivities in layers 1 and 3 were increased from their initial values by factors of 1.5 and 2.0, respectively. As in the Montebello Forebay, this increase was necessary to match water levels given the large flows of water flowing into the Central Basin Pressure Area from the Montebello Forebay. Hydraulic conductivities in the southwestern part of the Central Basin Pressure Area adjacent to the NIU were reduced to about 0.20 times their initial values in layers 3 and 4. This was required to simulate the depressed water levels in this region. Hydraulic conductivities also were reduced from their initial values in all active layers of the Whittier area (0.5 and 0.05 times initial values in layers 1 and 2-4, respectively), Hollywood subbasin (0.50 times initial values), Santa Monica Basin (0.25 times initial values), and West Coast Basin (0.30 times initial values in the area between the Charnock Fault and the NIU and 0.65 times initial values elsewhere).

Modification of hydraulic characteristics in the MODFLOW horizontal-flow-barrier package focused on a small subset of the faults included in the model. The initial hydraulic characteristics of the faults and folds making up the NIU were reduced to match the overall regional gradient across the NIU between the Central and West Coast Basins (fig. 2A, table 4). The hydraulic characteristics of the Santa Monica and Portrero Canyon Faults (fig. 2A, table 4) were reduced to improve the simulation of water-level gradients across the Santa Monica Basin. The hydraulic characteristics of the Norwalk Fault were reduced to improve the simulation of water levels in and downgradient from the Whittier area. The hydraulic characteristics of the Charnock and Overland Faults also were reduced to provide better simulation of water levels in the area between these faults and the NIU.

Vertical-conductance values were modified (by modifying the vertical-to-horizontal hydraulic conductivity ratios) to match the vertical differences in water levels measured at the USGS monitoring sites. High vertical-conductance values were required in the upgradient part of the Montebello Forebay area; these values are consistent with the lack of confining layers between the aquifers in that area. The greatest reduction in vertical- conductance values was required between layer 2 (the Lakewood aquifer system) and layer 3 (the Upper San Pedro aquifer system) in the eastern (inland) part of the West Coast Basin to better simulate the vertical discontinuity in water levels observed at USGS monitoring sites at Inglewood-1 (2S/14W-28M5–7), Carson-1(4S/13W-9H9–12), and Gardena-1(3S/14W-13J6–8) (fig. 23)(note that the model still underestimates the vertical gradients between layers 2 and 3 at these sites).

Specific yield in layer 1 was varied by zones (4 zones for the Montebello Forebay, 2 zones for the Los Angeles Forebay, and 1 zone for all non-forebay areas). As stated earlier, a single value of specific yield was applied to layers 2–4 for the entire model area. The model was somewhat sensitive to values of specific yield in the Montebello Forebay area. The maximum specific-yield value in the Montebello Forebay was set at 0.25. When this value was lowered, the model overestimated transient water level responses to annual changes in spreading quantities. The amplitude of annual water-level fluctuations also was sensitive to the non-forebay specific yield in layer 1 and to the specific yield specified for layers 2-4. Values for specific storage were modified little during the calibration.

In general, results shown in figures 30, 31, and Appendix VI indicate that the simulation model provides a reasonable representation of the regional ground-water system. Vertical differences between water levels in the four aquifer systems are generally simulated well (see the USGS multiple-well monitoring sites in Appendix VI). The model also matches the historical transient changes in water levels over the 30-year simulation period well. There undoubtedly are local features that are not captured by the model. The sum-of-squared errors (SS) was computed by

$$SS = \sum_{k=1}^{nwl} (\hat{h}_k - h_k)^2 \qquad (1)$$

where

nwl = the total number of water-level comparisons

$\hat{h}_k$ = the kth *simulated* water level, in feet, and

h_k = the kth measured water level, in feet

Root-mean-square error is related to the sum-of-squared error by

$$RMSE = \sqrt{\frac{SS}{nwl}} \qquad (2)$$

The average error (*AE*) is:

$$AE = (1/nwl) \sum_{k=1}^{nwl} (\hat{h}_k - h_k) \qquad (3)$$

A total of 942 measurements of water levels in the Central and West Coast Basins were used (fig. 23) (the six wells in the Hollywood and Santa Monica Basins were excluded). These are average annual water levels that range from 109 ft below mean sea level to 158 above mean sea level, a range of 267 ft. The

RMSE for the model is 16.4 ft. The average error is 1.2 ft. A plot of simulated and measured water levels for the calibration wells is shown in figure 32.

When interpreting the model results, applying the model, and considering future modifications of the model, it is important to keep in mind several features that are less accurately simulated by the model. These features are summarized below and can be seen from examining Appendix VI and figures 30–31. See figure 23 for well locations.

Water levels are overestimated in parts of Montebello Forebay. (for example, USGS monitoring sites Rio Hondo-1 (layers 2–4, wells 2S/12W-26D9–13) and Pico Rivera-2 (layer 4, well 2S/12W-25G3) and the Los Angeles Forebay (layer 3, well 2S/13W-10A1). On the boundary of the Whittier area, the model underestimates water levels in layer 4 at the USGS Santa Fe Springs-1 monitoring site (3S/11W-9D2). Note that at this site, measured water levels in layer 4 are significantly above those in layer 3 (3S/11W-9D3–4) and are similar to those measured in the deepest piezometer at this site (which is considered to be in the Pico unit). Pressurized gas was encountered in this deepest piezometer.

In the northwest part of the Central Basin Pressure Area the model overestimates water levels in layer 4 in well 2S/14W-14F2. This well is included as a calibration well because it has been used as a long-term monitoring well. There is no perforation information for the well, but based on its depth (954 ft) it is assumed to represent layer 4. At the USGS Inglewood-2 monitoring site (2S/14W-26N5–6), also located in the northwest part of the Central Basin Pressure Area, the model underestimates water levels in layer 3. This monitoring site is located very close to the NIU.

In the southern part of the Central Basin Pressure Area, the model underestimates water levels in layer 4 at 4S/12W-25E1. At the USGS Lakewood-1 monitoring site, the model does not match the extreme decline in water levels in layers 3 and 4 at the very end of the simulation period (4S/12W-5H5–7). This drawdown is the result of a new production well, located within 100 ft of the monitoring wells, going online in water year 1998. Such pumping well effects cannot be simulated in a regional model such as this.
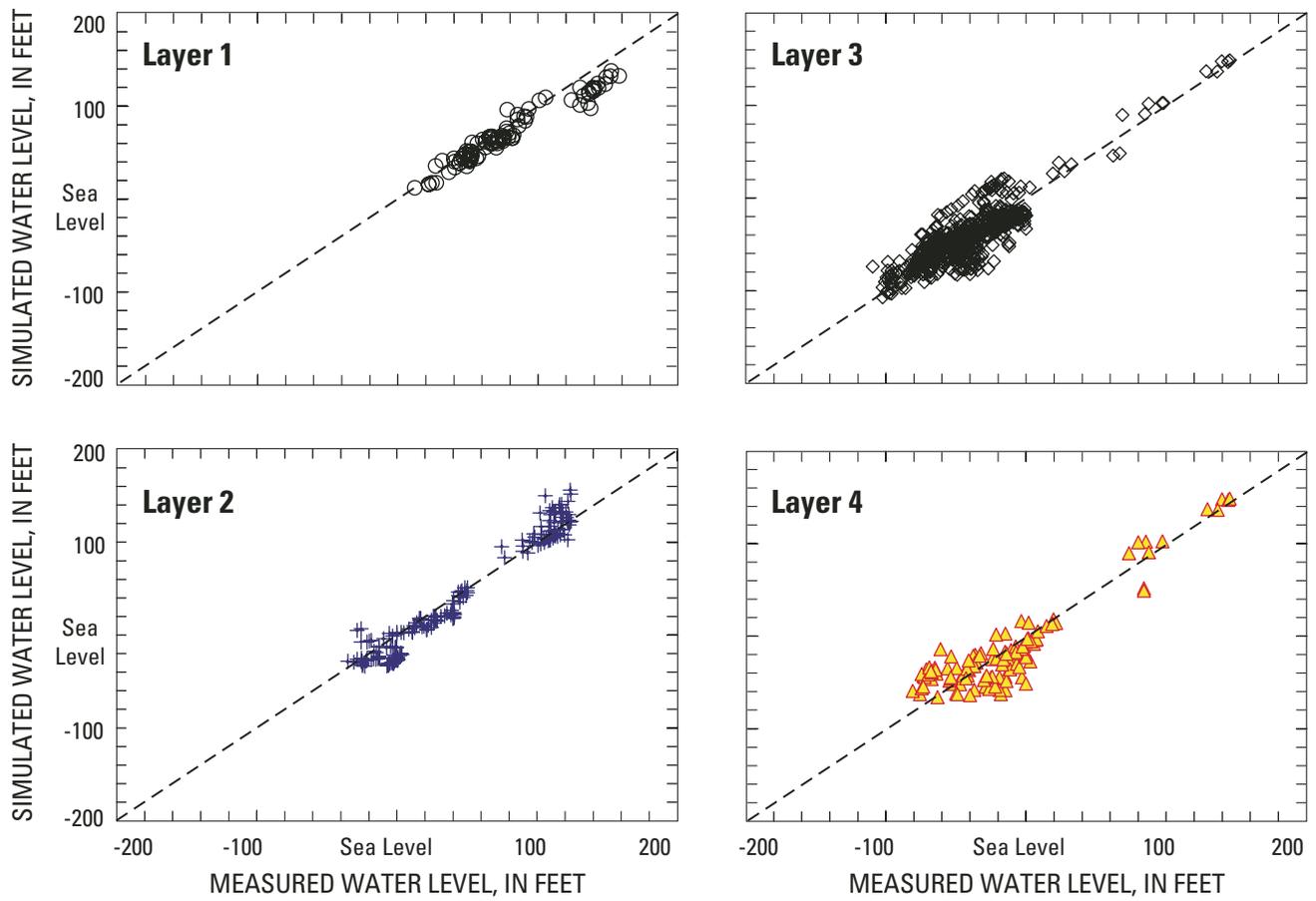
Figure 32. Simulated water levels as a function of measured water levels at calibration wells, model layers 1–4, Los Angeles County, California.

In the inland part of the West Coast Basin, adjacent to the NIU, water levels are slightly underestimated in layer 2 [for example, USGS monitoring sites at Inglewood-1 (2S/14W-28M7), Carson-1(4S/13W-9H12), and Gardena-1 (3S/14W-13J8)]. In the southern part of the West Coast Basin, near the Dominguez Gap Barrier project, water levels are slightly underestimated in layer 2 at USGS monitoring site at Wilmington-2 (4S/13W-32F5) and overestimated in layer 4 at USGS monitoring site Wilmington-1 (4S/13W-28A3–4). In the middle of the West Coast Basin, the model slightly underestimates water levels in layer 3 at monitoring wells PM-3 Madrid and PM-4 Mariner.

Although the primary goal of the model is to simulate water levels in the Central and West Coast Basins, water levels in the Santa Monica Basin also were compared. In the Santa Monica Basin, comparing simulated and measured water levels is complicated by the fact that most of the reported water levels were measured under pumped conditions. Pumping ceased in the Charnock well field in 1996. Post-1996 model-simulated water levels are slightly higher than the measured water levels for recent years in well 2S/15W-11A1 (Charnock -18). There has been very little pumpage from the ARC well field in recent years. The model appears to underestimate recent water levels at 1S/15W-32A5 (ARC-4). Active pumping continues at wells 2S/15W-4C2 (SM3) and 1S/15W-31E1 (SM1).

In addition to identifying areas where there are differences between simulated and measured water levels in particular model layers, it is also important to identify areas where there are differences between different measured water levels within the same model layer. Most of the USGS monitoring sites have multiple wells within layer 3—the Upper San Pedro aquifer system. In several of these—Carson-1 (4S/13W-9H9–11), Wilmington-1 (4S/13W-28A5–6), Inglewood-1(2S/14W-28M5–6), and Long-Beach-2(4S/13W-1N5–6)—there is a noticeable difference in measured water levels in layer 3 wells (Appendix VI). This indicates that in these parts of the study area, the shallower part of the upper San Pedro aquifer system (the Lynwood aquifer) has a hydraulic response that is different from that of the deeper part of the Upper San Pedro aquifer system (the Silverado aquifer) (fig. 3). At two monitoring sites, Downey-1

(3S/12W-9J4–5) and Hawthorne-1 (3S/14W-17G7–8), there are differences between measured water levels in layer 2 wells.

Model-Parameter Sensitivity

A sensitivity analysis was done by independently varying 74 parameters to determine how parameter estimates affected simulation results. Model sensitivity was described in terms of RMSE. Parameter values were multiplied by 0.2 to 5 times the calibrated estimates. Changes in RMSE for all 74 parameters at 0.2 and 5 times the calibrated estimate are summarized in table 6. Although 74 parameters are presented in this sensitivity analysis, a much more limited number of parameters were systematically varied as part of the model calibration (see previous discussion). Variations in computed RMSE for a range of factors for selected model parameters are shown in figure 33.

Hydraulic conductivities of layer 3 in the West Coast Basin, layers 1 and 3 in the Montebello Forebay, and layer 3 of the Central Basin Pressure Area were among the most sensitive parameters (table 6). The model was sensitive to hydraulic conductivity of layer 3 in the West Coast Basin and Central Basin Pressure Area because most pumpage is drawn from layer 3 (Upper San Pedro Aquifer system) in these two areally extensive zones that include many of the available observations. The model was sensitive to hydraulic conductivities in the Montebello forebay because these parameters controlled the availability of water to all downgradient areas.

The model was fairly sensitive to changes in all of the recharge parameters (table 6). Other than adjusting the bound set on maximum rates, recharge was not treated as a model calibration parameter. Model sensitivity to individual parameter changes was asymmetric about the calibrated value for almost all the parameters that were evaluated (fig. 33, table 6). For example, increases in recharge affected RMSE much more than decreases in recharge. As shown in table 6, the RMSE is relatively insensitive to the hydraulic characteristics of faults over the range of values tested. Among the four fault sets tested, the model is most sensitive to large reductions in the hydraulic characteristic of the Charnock and Overland Faults

Table 6. Sensitivity of model parameters

[RMSE, root mean squared error, in feet]
times calibrated value—than other parameters).

Table 6. Sensitivity of model parameters—Continued

Parameter name	Change in RMSE from calibrated estimate		Maximum absolute change
	0.2 X	5 X	
Hydraulic conductivity of layer 3 in the West Coast Basin	20.22	4.49	20.22
Hydraulic conductivity of layer 1 in the Montebello Forebay	5.34	18.15	18.15
Hydraulic conductivity of layer 3 in the Montebello Forebay	6.83	17.32	17.32
Recharge of layer 2 in the Los Angeles Forebay	1.53	13.66	13.66
Recharge of layer 2 in the Central Basin Pressure area	1.10	13.22	13.22
Hydraulic conductivity of layer 3 in the Central Basin Pressure area	12.61	7.60	12.61
Recharge of layer 2 in the Hollywood Basin	1.02	11.41	11.41
Recharge of layer 2 in the West Coast Basin	1.91	11.17	11.17
Recharge of layer 2 in the Santa Monica Basin	.90	10.15	10.15
Specific Yield	4.90	1.07	4.90
Hydraulic conductivity of layer 3 in the Los Angeles Forebay	4.64	.07	4.64
Hydraulic conductivity of layer 2 in the Los Angeles Forebay	1.48	4.52	4.52
Hydraulic conductivity of layer 4 in the Montebello Forebay	.70	3.76	3.76
Vertical leakance (V_{cont}) of layer 2 in the Whittier area	3.09	−.29	3.09
Hydraulic conductivity of layer 2 in the Montebello Forebay	.68	2.92	2.92
Recharge of layer 2 in the Montebello Forebay	.15	2.26	2.26
Hydraulic conductivity of layer 4 in the Central Basin Pressure area	1.98	1.41	1.98
Hydraulic conductivity of layer 2 in the Whittier area	1.53	−.31	1.53
Vertical leakance (V_{cont}) of layer 2 in the Central Basin Pressure area	1.32	.67	1.32
Recharge of layer 2 in the Whittier area	.13	1.16	1.16
Hydraulic conductivity of layer 1 in the Central Basin Pressure area	.81	1.07	1.07
Hydraulic conductivity of layer 3 in the Whittier area	.92	−.19	.92
Hydraulic conductivity of layer 2 in the Central Basin Pressure area	.29	.84	.84
Vertical leakance (V_{cont}) of layer 2 in the West Coast Basin	.75	.62	.75
Hydraulic conductivity of layer 4 in the West Coast Basin	.05	.44	.44
Hydraulic conductivity of layer 4 in the Los Angeles Forebay	.32	.10	.32
Vertical leakance (V_{cont}) of layer 2 in the Montebello Forebay	−.28	.15	.28
Vertical leakance (V_{cont}) of layer 3 in the Central Basin Pressure area	.25	−.17	.25
Vertical leakance (V_{cont}) of layer 3 in the Los Angeles Forebay	.25	.00	.25
Hydraulic conductivity of layer 3 in the Santa Monica Basin	−.25	−.10	.25
Vertical leakance (V_{cont}) of layer 1 in the West Coast Basin	.24	−.04	.24
Hydraulic conductivity of layer 3 in the offshore-San Pedro Bay	.20	−.03	.20
Vertical leakance (V_{cont}) of layer 2 in the Los Angeles Forebay	.20	−.07	.20
Hydraulic conductivity of layer 4 in the Whittier area	.17	−.13	.17
Hydraulic conductivity of layer 2 in the West Coast Basin	.12	.17	.17
Vertical leakance (V_{cont}) of layer 1 in the Montebello Forebay	−.13	.03	.13
Vertical leakance (V_{cont}) of layer 3 in the Whittier area	.11	.00	.11

Table 6. Sensitivity of model parameters—Continued

Parameter name	Change in RMSE from calibrated estimate		Maximum absolute change
	0.2 X	5 X	
Hydraulic conductivity of layer 1 in the West Coast Basin	−.01	−.10	.10
Vertical leakance (V_{cont}) of layer 1 in the Central Basin Pressure area	.07	−.02	.07
Storage coefficient in Layer 3	.03	−.06	.06
Hydraulic conductivity of layer 4 in the Santa Monica Basin	.06	−.06	.06
Vertical leakance (V_{cont}) of layer 3 in the West Coast Basin	.06	.01	.06
Hydraulic characteristic of Charnock and Overland Faults	−.05	.06	.06
Vertical leakance (V_{cont}) of layer 1 in the Los Angeles Forebay	−.05	−.01	.05
Hydraulic characteristic of faults along Newport-Inglewood uplift	0.03	−0.05	0.05
Storage coefficient in Layer 2	.01	−.05	.05
Hydraulic conductivity of layer 2 in the Hollywood Basin	−.04	.04	.04
Hydraulic conductivity of layer 4 in the offshore-San Pedro Bay	.04	−.03	.04
Hydraulic conductivity of layer 3 in the Hollywood Basin	−.03	.04	.04
Hydraulic conductivity of layer 4 in the offshore-North Santa Monica Bay	.04	−.01	.04
Hydraulic characteristic of Norwalk fault	.03	.03	.03
Hydraulic conductivity of layer 2 in the Santa Monica Basin	−.01	−.03	.03
Vertical leakance (V_{cont}) of layer 3 in the Montebello Forebay	−.03	.01	.03
Storage coefficient in Layer 4	.01	−.03	.03
Conductance of South Monica and Portero Canyon Faults	−.03	−.02	.03
Vertical leakance (V_{cont}) of layer 2 in the Hollywood Basin	.03	−.01	.03
Hydraulic conductivity of layer 4 in the Hollywood Basin	−.01	.03	.03
Hydraulic conductivity of layer 2 in the offshore-San Pedro Bay	.01	−.03	.03
Vertical leakance (V_{cont}) of layer 2 in the Santa Monica Basin	.022	.011	.022
Vertical leakance (V_{cont}) of layer 2 in the offshore-San Pedro Bay	.020	.002	.020
Hydraulic conductivity of layer 3 in the offshore-North Santa Monica Bay	.018	−.014	.018
Vertical leakance (V_{cont}) of layer 1 in the offshore-San Pedro Bay	.018	.000	.018
Hydraulic conductivity of layer 3 in the offshore-South Santa Monica Bay	.006	−.015	.015
Vertical leakance (V_{cont}) of layer 3 in the Santa Monica Basin	−.010	.011	.011
Hydraulic conductivity of layer 4 in the offshore-South Santa Monica Bay	.010	−.004	.010
Vertical leakance (V_{cont}) of layer 2 in the offshore-North Santa Monica Bay	−.009	−.003	.009
Hydraulic conductivity of layer 2 in the offshore-South Santa Monica Bay	.001	−.007	.007
Vertical leakance (V_{cont}) of layer 3 in the offshore-South Santa Monica Bay	.006	.000	.006
Vertical leakance (V_{cont}) of layer 2 in the offshore-South Santa Monica Bay	.001	−.005	.005
Vertical leakance (V_{cont}) of layer 3 in the offshore-San Pedro Bay	−.004	.002	.004
Vertical leakance (V_{cont}) of layer 1 in the Whittier area	.003	.003	.003
Hydraulic conductivity of layer 2 in the offshore-North Santa Monica Bay	.002	−.003	.003
Vertical leakance (V_{cont}) of layer 3 in the offshore-North Santa Monica Bay	.000	−.002	.002
Vertical leakance (V_{cont}) of layer 3 in the Hollywood Basin	−.001	−.001	.001
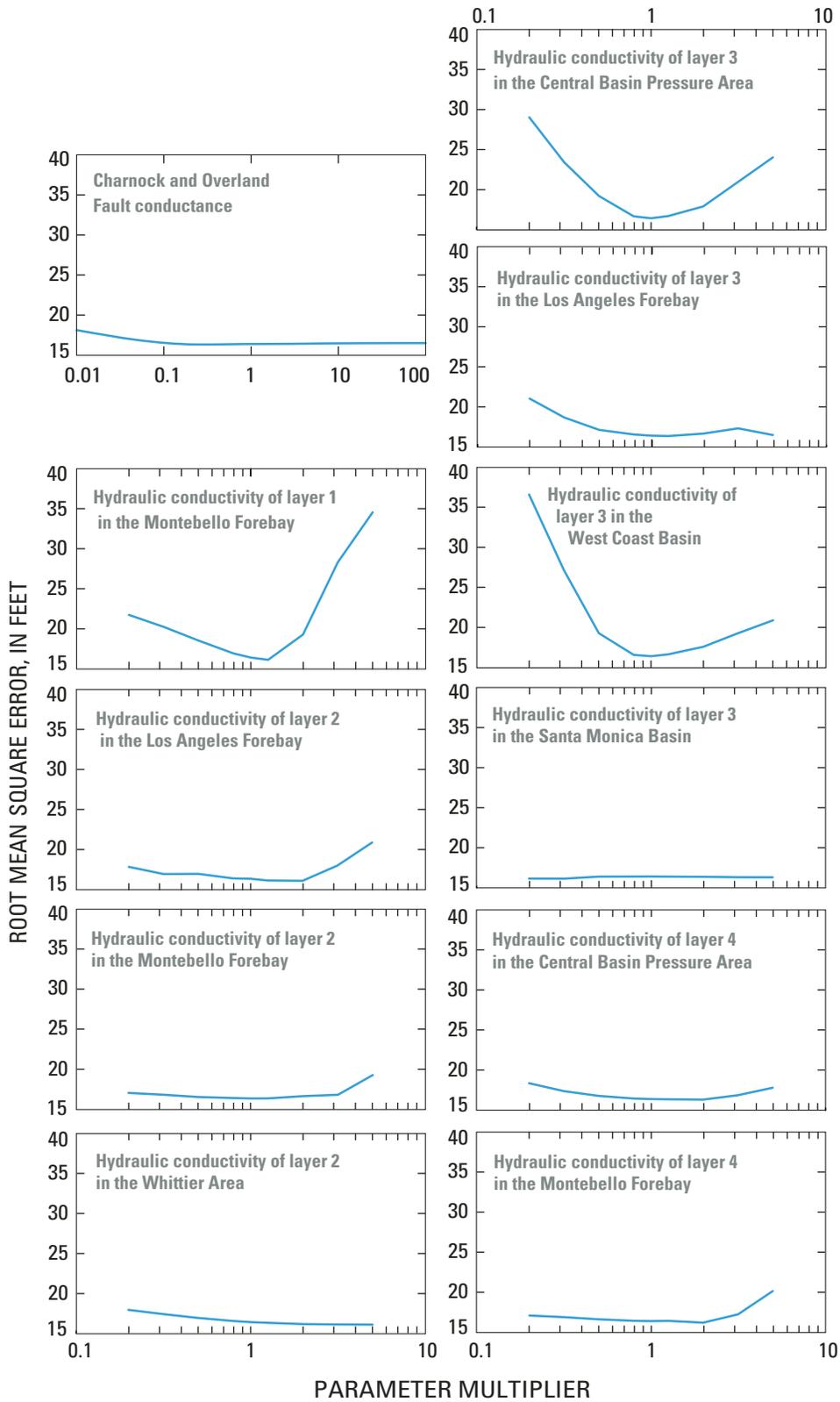
Figure 33. Sensitivity graphs for selected model parameters.
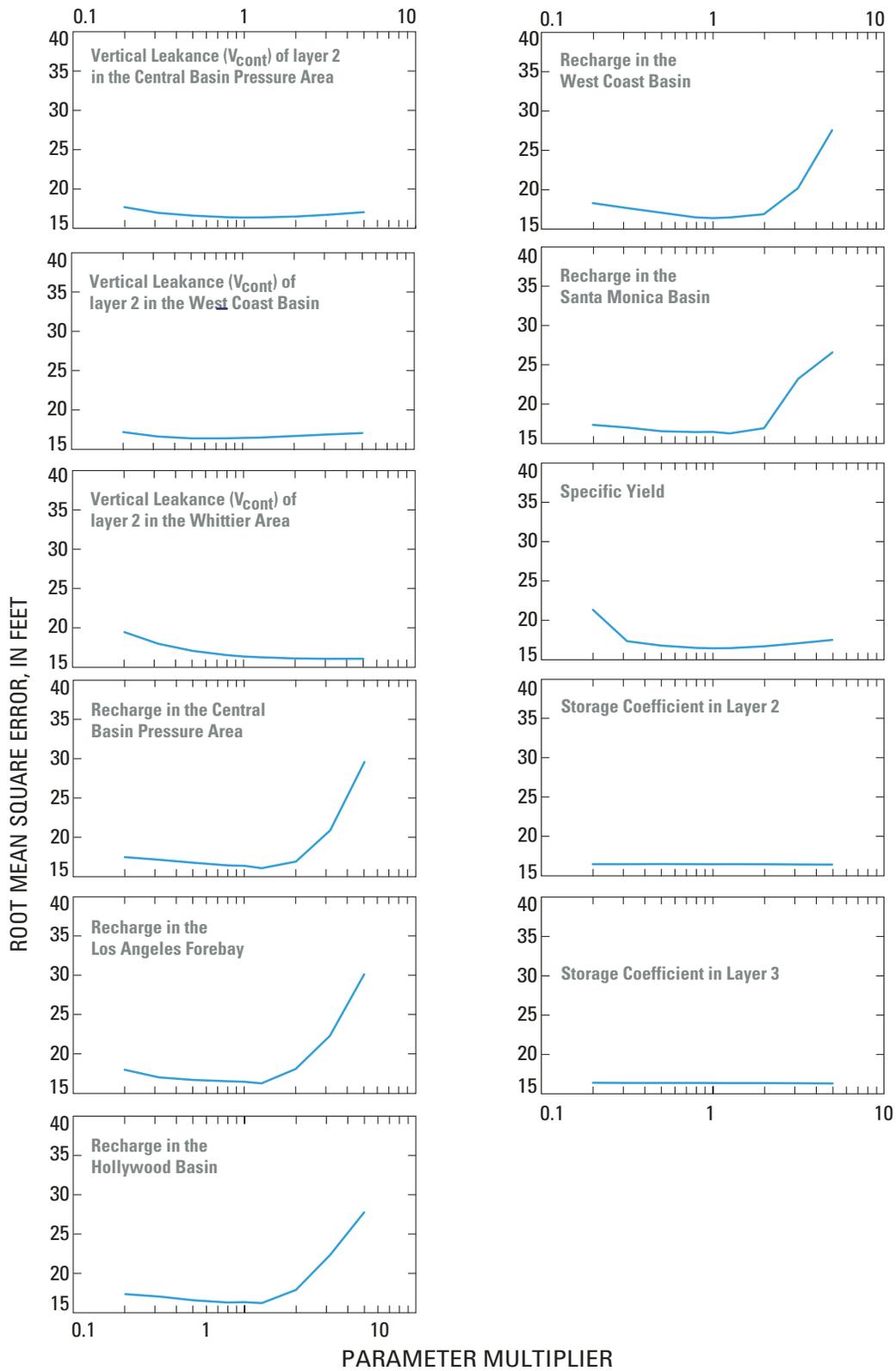
Figure 33.—Continued.

Many parameters were important to model calibration in particular areas despite being relatively insensitive as measured by the RMSE. For example, as described above, vertical leakance (V_{cont}) in layer 2 in the West Coast Basin was important for matching vertical water-level gradients at monitoring wells Inglewood 1 (2S/14W-28M5-7), Carson-1 (4S/13W-9H9-12) and Gardena-1 (3S/14W-13J6-8), although it did not have a large impact on the total RMSE (table 6).

Results from a sensitivity analysis are affected by location of observation wells, parameter definition, and boundary conditions. Parameter sensitivity tends to increase as the number of observations near that parameter increases. Areally extensive parameters tend to be more sensitive than more localized parameters because more observations can be affected directly. Areas within layers that are heavily stressed tend to have higher sensitivities.

Analysis of Regional Ground-Water Budget with Ground-Water Simulation Model

The ground-water simulation just described was used to quantify the three-dimensional regional ground-water budget. Shown in tables 7 and 8 are ground-water budget components for the 30-year simulation period from 1971 to 2000 and for the last five years of the simulation (1996–2000). The components include pumpage, spreading, injection, mountain-front and interior recharge, boundary flows, and change in storage. The values for these components are output directly from the model. For the few cells that contain both pumping and injection wells, the model outputs a net amount.

As shown in tables 7 and 8, the spreading in the Montebello Forebay and injection at the seawater barrier projects are the main sources of recharge. Also shown is the fact that about 80-percent of total pumpage comes from model layer 3, the Upper San

Pedro aquifer system, and that there has been an increase in water in storage over the 30-year simulation period in all subareas. Note that there has been a net decrease in storage from 1996 to 2000. The small differences between simulated total net flow (row G on tables 7 and 8) and the simulated total net change in storage (row H on tables 7 and 8) are due to rounding and the fact that the multi-year averages in tables 7 and 8 are computed using the rates at a single time step (the midpoint) of each stress period to represent the average rates during that stress period (it was infeasible to have the model save all the flows for all time steps in each stress period).

Average model-calculated lateral flows between subareas and vertical flows between the four model layers are shown in figure 34. The model results show the large horizontal and vertical movements of water emanating from the Montebello Forebay. These results also indicate relatively small average simulated flows of ground water moving across the NIU between the Central and West Coast Basins (the simulated average net flow over all four model layers is about 3,200 acre-ft/yr for 1971–2000 and 5,900 acre-ft/yr for 1996–2000).

Model-calculated flows between onshore and offshore zones provide an indication of seawater intrusion. In the West Coast Basin, the model-computed average flows are moving onshore in layers 3 and 4 (representing the Upper and Lower San Pedro aquifer systems) and offshore in layers 1 and 2 (representing the Recent and Lakewood aquifer systems)(fig. 34). The simulated average net flow from San Pedro Bay to all four model layers is about 6,100 acre-ft/yr for 1971–2000 and 5,900 acre-ft/yr for 1996–2000. The simulated average net flow from Santa Monica Bay to the West Coast Basin over all four model layers is about 1,000 acre-ft/yr for 1971–2000 and 2,000 acre-ft/yr for 1996–2000. The model simulates average flows moving offshore in all model layers in the Santa Monica Basin.

Table 7. Average 30-year water budget for historic ground-water simulation, 1971–2000

Budget item and model layer	Montebello Forebay	Los Angeles Forebay	Whittier Area	Central Basin	Hollywood Basin	West Coast Basin	Santa Monica Basin	Total
				In acre feet per year				
Pumpage								
—Layer1	−1,600	0	0	−1,200	0	−90	0	−2890
—Layer2	−8,100	−600	0	−6,500	0	−1,700	−60	−16,960
—Layer3	−33,100	−11,600	−1,300	−108,900	0	−49,400	−5,100	−209,400
—Layer4	−1,400	−9,100	−200	−13,900	0	−1,900	−1,600	−28,100
A. TOTAL	**−44,200**	**−21,300**	**−1,500**	**−130,500**	**0**	**−53,090**	**−6,760**	**−257,350**
Net flow from adjacent inland zones								
—Layer1	−132,000	−3,700	−1,400	−900	0	−5,000	0	−143,000
—Layer2	−100	−5,700	−3,700	−11,900	−5,700	−11,900	−10,600	−49,600
—Layer3	26,200	10,700	1,300	108,500	0	22,200	7,000	175,900
—Layer4	−4,800	8,800	200	11,500	0	−1,400	2,300	16,600
B. TOTAL	**−110,700**	**10,100**	**−3,600**	**107,200**	**−5,700**	**3,900**	**−1,300**	**−100**
C. Spreading	**122,900**	**0**	**0**	**0**	**0**	**0**	**0**	**122,900**
Injection								
—Layer1	0	0	0	400	0	3,000	0	3,400
—Layer2	0	0	0	3,200	0	4,600	0	7,800
—Layer3	0	0	0	1,700	0	21,200	0	22900
—Layer4	0	0	0	0	0	500	0	500
D. TOTAL	**0**	**0**	**0**	**5,300**	**0**	**29,300**	**0**	**34,600**
E. Mountain front and interior recharge	**5,700**	**7,200**	**5,100**	**14,300**	**5,900**	**15,600**	**13,100**	**66,900**
Net flow from ocean and adjacent basins								
—Layer1	7,200	2,800	0	0	0	−900	0	9,100
—Layer2	6,900	2,200	0	6,900	0	−1,000	−1,600	13,400
—Layer3	6,900	900	0	−1,200	0	6,100	−1,800	10,900
—Layer4	6,200	300	0	2,300	0	2,800	−700	10,900
F. TOTAL	**27,200**	**6,200**	**0**	**8,000**	**0**	**7,000**	**−4,100**	**44,300**
G. Total net flow, (A+B+C+D+E+F)	**900**	**2,200**	**0**	**4,300**	**200**	**2,710**	**940**	**11,250**
Change in storage								
—Layer1	740	10	20	2,200	0	1600	0	4570
—Layer2	220	2,100	40	1,900	210	1200	740	6,410
—Layer3	10	30	10	60	0	40	40	190
—Layer4	0	10	0	40	0	30	0	80
H. TOTAL	**970**	**2,150**	**70**	**4,200**	**210**	**2,870**	**780**	**11,250**

Table 8. Average 5-year water budget for historic ground-water simulation, 1996–2000

Budget item and model layer	Montebello Forebay	Los Angeles Forebay	Whittier Area	Central Basin	Hollywood Basin	West Coast Basin	Santa Monica Basin	Total
				In acre-feet per year				
Pumpage								
—Layer1	−2,200	0	0	−1,100	0	0	0	−3,300
—Layer2	−7,100	−230	0	−4,800	0	−1,100	−70	−13,300
—Layer3	−33,800	−11,400	−20	−107,200	0	−48,000	−2,100	−202,520
—Layer4	−1,700	−9,500	−10	−14,000	0	−2,300	−1,200	−28,710
A. TOTAL	**−44,800**	**−21,130**	**−30**	**−127,100**	**0**	**−51,400**	**−3,370**	**−247,830**
Net flow from adjacent inland zones								
—Layer1	−134,800	−3,700	−1,500	−4,000	0	−5,400	0	−149,400
—Layer2	−500	−6,500	−2,900	−11,600	−5,300	−12,100	−8,600	−47,500
—Layer3	27,800	10,500	10	109,700	10	25,600	4,100	177,720
—Layer4	−3,700	9,100	10	12,700	0	−900	2,100	19,310
B. TOTAL	**−111,200**	**9,400**	**−4,380**	**106,800**	**−5,290**	**7,200**	**−2,400**	**130**
C. Spreading	**116,200**	**0**	**0**	**0**	**0**	**0**	**0**	**116,200**
Injection								
—Layer1	0	0	0	290	0	2,400	0	2,690
—Layer2	0	0	0	3,100	0	3,200	0	6,300
—Layer3	0	0	0	2,000	0	15,100	0	17,100
—Layer4	0	0	0	0	0	540	0	540
D. TOTAL	**0**	**0**	**0**	**5,390**	**0**	**21,240**	**0**	**26,630**
E. Mountain front and interior recharge	**5,300**	**6,800**	**4,800**	**13,500**	**5,500**	**14,500**	**12,300**	**62,700**
Net flow from ocean and adjacent basins								
—Layer1	6,200	2,800	0	0	0	−1,100	0	7,900
—Layer2	6,000	2,200	0	5,500	0	−900	−1,700	11,100
—Layer3	6,000	900	0	−4,700	0	7,200	−2,000	7,400
—Layer4	5,400	300	0	1,200	0	2,700	−800	8,800
F. TOTAL	**23,600**	**6,200**	**0**	**2,000**	**0**	**7,900**	**−4,500**	**35,200**
G. Total net flow, (A+B+C+D+E+F)	**−10,900**	**1,270**	**390**	**590**	**210**	**−560**	**2,030**	**−6,970**
Change in storage								
—Layer1	−10,500	−50	−220	0	0	320	0	−10,450
—Layer2	−380	1,300	490	810	210	−720	1,900	3,610
—Layer3	−60	10	−10	−150	10	−40	110	−130
—Layer4	−30	0	−10	−100	0	−40	10	−170
H. TOTAL	**−10,970**	**1,260**	**250**	**560**	**220**	**−480**	**2,020**	**−7,140**
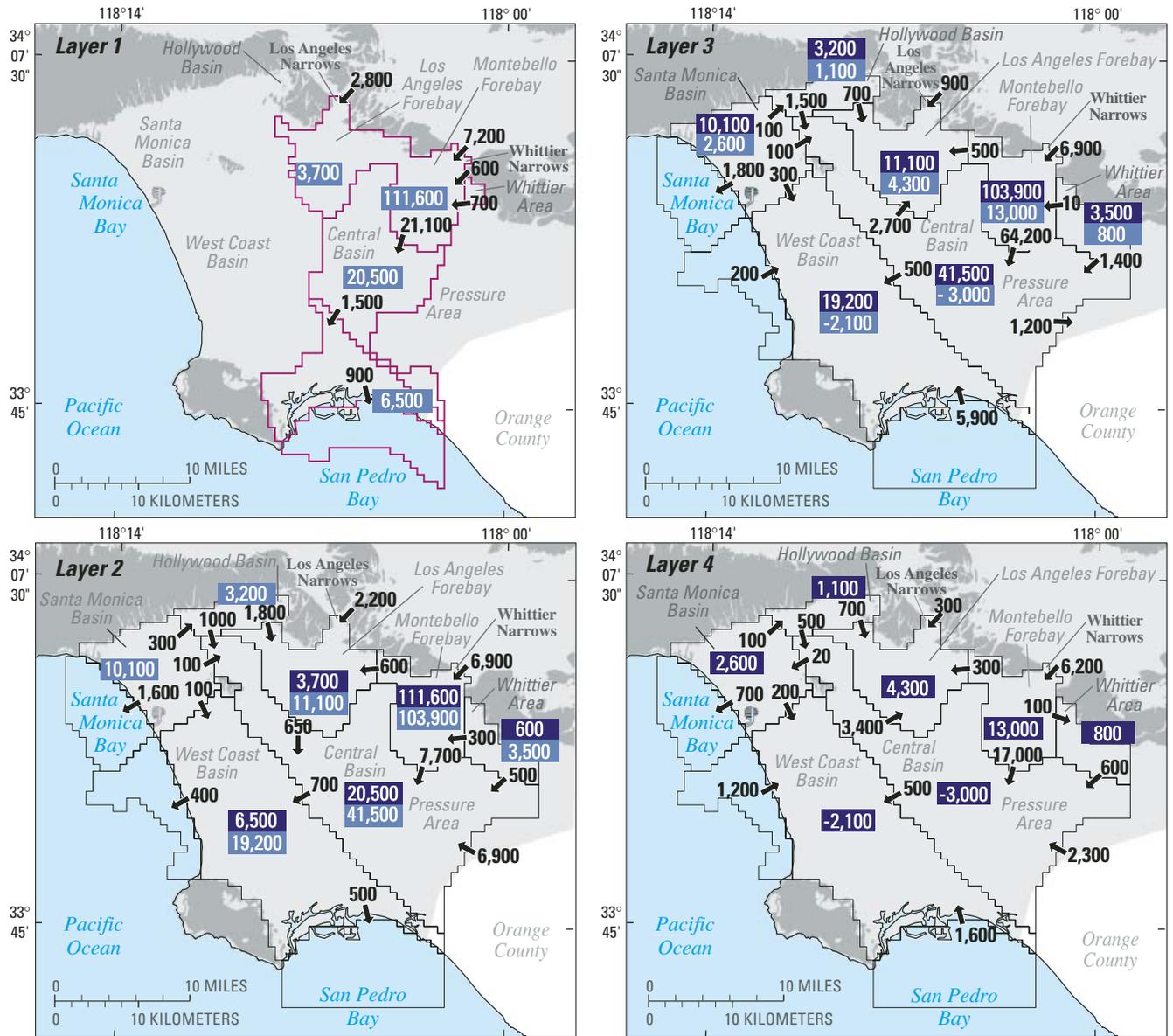
Figure 34. Average model-simulated inter-zone flows for layers 1–4 for 1971–2000 (*A*) and 1996–2000 (*B*), Los Angeles County, California.

B 1996–2000
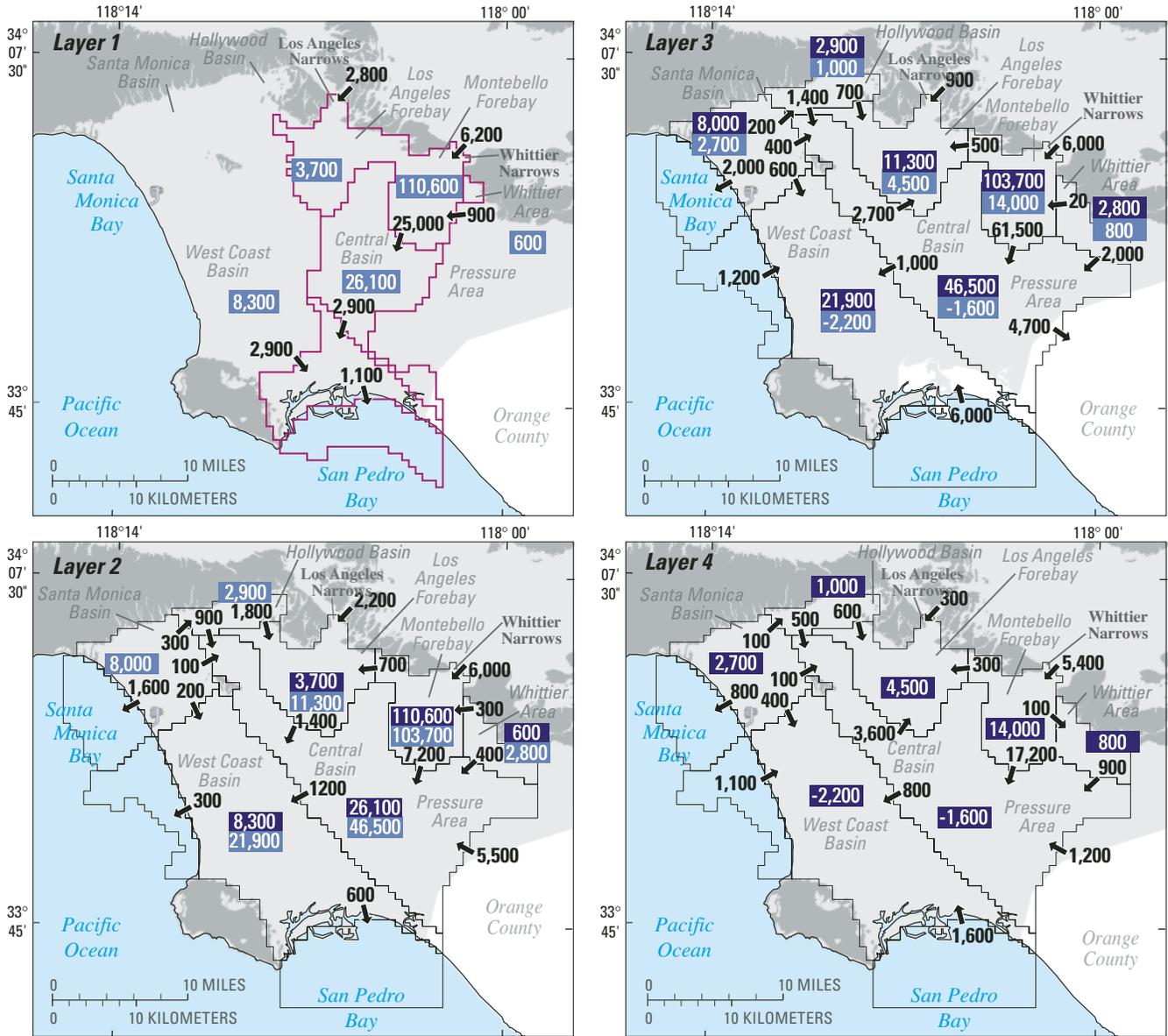
Figure 34.—Continued.

Model-computed average net flow through the Los Angeles Narrows (from the San Fernando Valley) through all layers is 6,200 acre-ft/yr for both 1971–2000 and for 1996–2000 (fig. 34). Model-computed average net flow through the Whittier Narrows (from the San Gabriel Valley) is 27,200 acre-ft/yr for 1971–2000 and 23,600 acre-ft/yr for 1996–2000. Model-computed average net flow from Orange County is 8,000 acre-ft/yr for 1971–2000 and 2,000 acre-ft/yr for 1996–2000. For these computed flows at head-dependent boundaries, the total simulated flow for all layers is considered to be a reasonable estimate. How the model apportions these flows among the layers is probably not significant, as it is very dependent on the assumptions used to define the boundary head value in each layer. The computed flows at the Orange County boundary are similar in magnitude to those computed from a three-layer model of the Orange County Basin developed by the Orange County Water District, which has a specified head boundary located about five miles into Los Angeles County. In that model, the average simulated flow across the County line for the period 1990–99 was 9,300 acre-ft/yr; the average simulated flow for the period 1996–99 was 8,200 acre-ft/yr (Tim Sovich, Orange County Water District, oral commun., 2002).

In addition to these mean simulated flows, it is instructive to consider temporal trends. These are shown in figure 35. For example, simulated flows through the Whittier Narrows vary considerably year-to-year depending on the water levels in the upper part of the Montebello Forebay, which are, in turn, mostly a function of the amount of spreading. Simulated net flows into the model area from Orange County generally decrease through the model period, showing a significant shift in flow beginning about 1984. The average total simulated flow from 1971 to 1983 across the Orange County boundary is 14,000 acre-ft/yr. The average total simulated flow from 1984 to 2000 is 3,300 acre-ft/yr.

Simulated flows from San Pedro Bay into the West Coast Basin show a slightly decreasing trend during the model period (fig. 35). This is consistent with the general rise in water levels in the southern part of the West Coast Basin (for example, wells 4S/13W-21H5 and -23B2 and -30G1 in Appendix VI). Note in figure 35 that the model shows small flows to the San Pedro Bay in layers 1 and 2, and significantly

larger flows from the Bay in layers 3 and 4. Simulated flows across the NIU from the Central to the West Coast Basin were higher in the last 6 years of the simulation period.

Model Sensitivity to Orange County Boundary Condition

To test the model sensitivity to the assumed time-varying specified head along the Orange County boundary, the historical model simulation was rerun replacing the time-varying specified-head boundary with a specified- flow boundary. This flow boundary was specified along the segment of the specified-head boundary that runs north-south (figs. 22B, C); the north-most segment of the specified head boundary, running east-west, was re-specified as no flow. Constant flows of 14,000 and 3,300 acre-ft/yr were specified for the periods 1971–83 and 1984–2000, respectively (see discussion of fig. 35 in previous section). Each flow was apportioned by putting 50 percent in layer 2, 25 percent in layer 3, and 25 percent in layer 4. Resulting simulated water levels for 2000 are shown in figure 36. As can be seen from comparing these results with those in figure 31, the model results change little except for selected areas extending 2–4 model cells from the boundary. Using the model to draw conclusions about activities in these areas near the boundary—operations of the Alamitos Gap Barrier Project, for example—is not appropriate. The sensitivity to this boundary condition of simulations of potential future scenarios and of optimization analyses is discussed later.

Model Limitations

Areal recharge—mountain-front recharge and distributed interior recharge—rates in the model are estimated and applied in a simplified manner. An important area for additional work would be to develop more processed-based, spatially distributed estimates of natural recharge. This would require rigorous analysis and integration of rainfall/runoff relations, infiltration properties, land use (and associated applied water), pipeline leakage, unsaturated flow properties, and chemical isotope indicators.
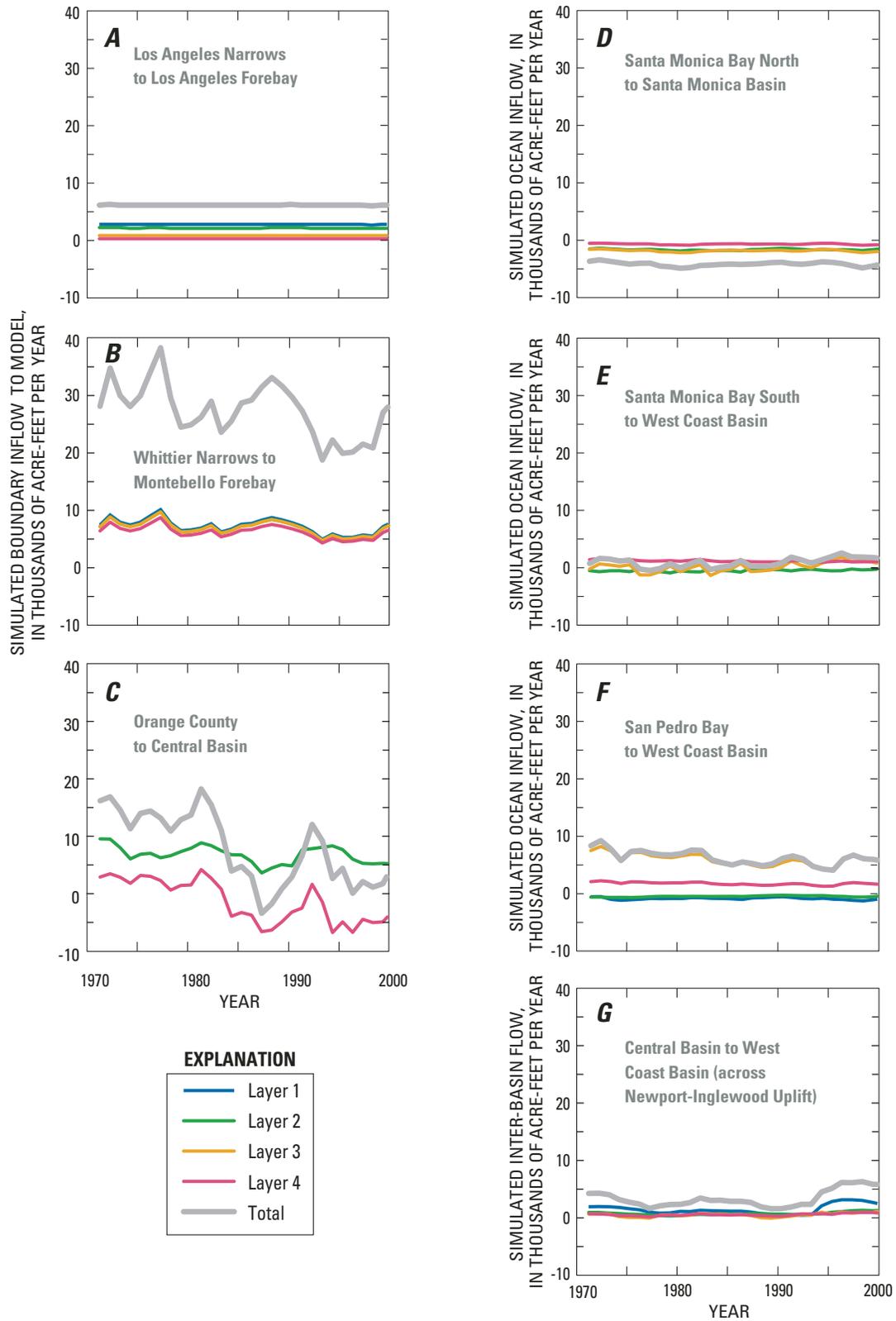
Figure 35. Annual model-simulated flows between zones and from basins outside model area, 1971–2000, Los Angeles County, California.

Figure 36. Model-simulated and measured water levels, 2000, with specified flow boundary at Orange County for layers 1–4 of the ground-water simulation model: Layer 1, Recent aquifer system (A); Layer 2, Lakewood aquifer system (B); Layer 3, Upper San Pedro aquifer system (C); and Layer 4, Lower San Pedro aquifer system (D), Los Angeles County, California.

B Layer 2

118° 30' 20' 10' 118° 00'

Los Angeles Narrows

T1S

Hollywood Basin

Whittier Narrows

T2S

Santa Monica Basin

Los Angeles Forebay

34° 00'

Santa Monica Bay

Montebello Forebay

Whittier Area

T3S

West Coast Basin

Central Basin

Los Angeles County

50'

Orange County

T4S

Pacific Ocean

T5S

San Pedro Bay

33° 40'

R16W R15W R14W R13W R12W R11W

0 2 4 6 8 10 MILES

0 2 4 6 8 10 KILOMETERS
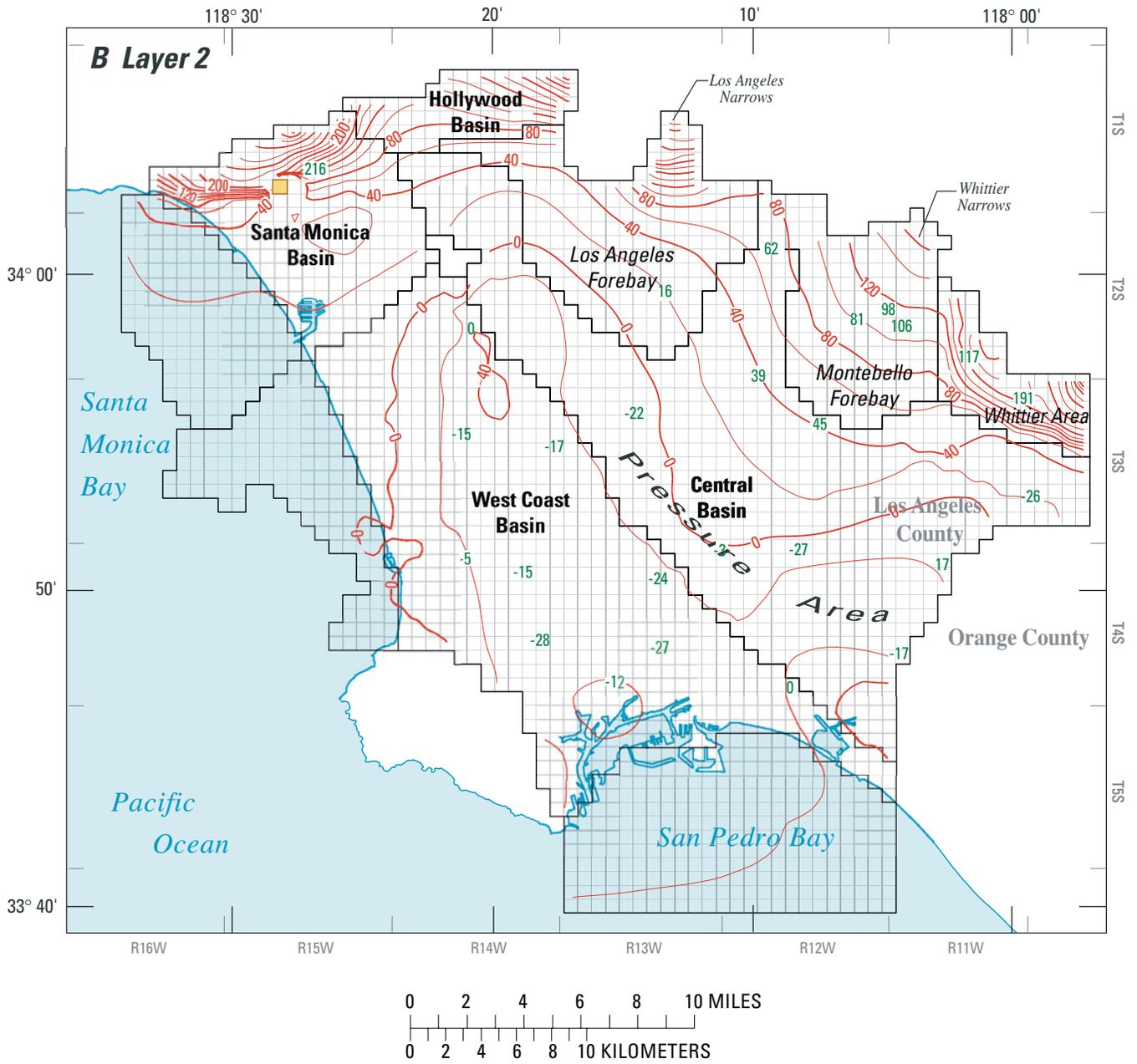
EXPLANATION

☐ **Grid Cell**

▨ **Dry cells**

50 **Measured water-level** (in feet above sea level).

—130— **Simulated water-level contour -** shows simulated water-level in feet above sea level. Contour interval 20 feet.

Figure 36.—Continued.

Figure 36.—Continued.

D Layer 4

118° 30'   20'   10'   118° 00'

Hollywood Basin

Los Angeles Narrows

Whittier Narrows

Los Angeles Forebay

Santa Monica Basin

34° 00'

Santa Monica Bay

Montebello Forebay

Whittier Area

Central Basin

Pressure

Los Angeles County

West Coast Basin

50'

Area

Orange County

Pacific Ocean

33° 40'

San Pedro Bay

R16W   R15W   R14W   R13W   R12W   R11W

T1S   T2S   T3S   T4S   T5S

0   2   4   6   8   10 MILES
0   2   4   6   8   10 KILOMETERS
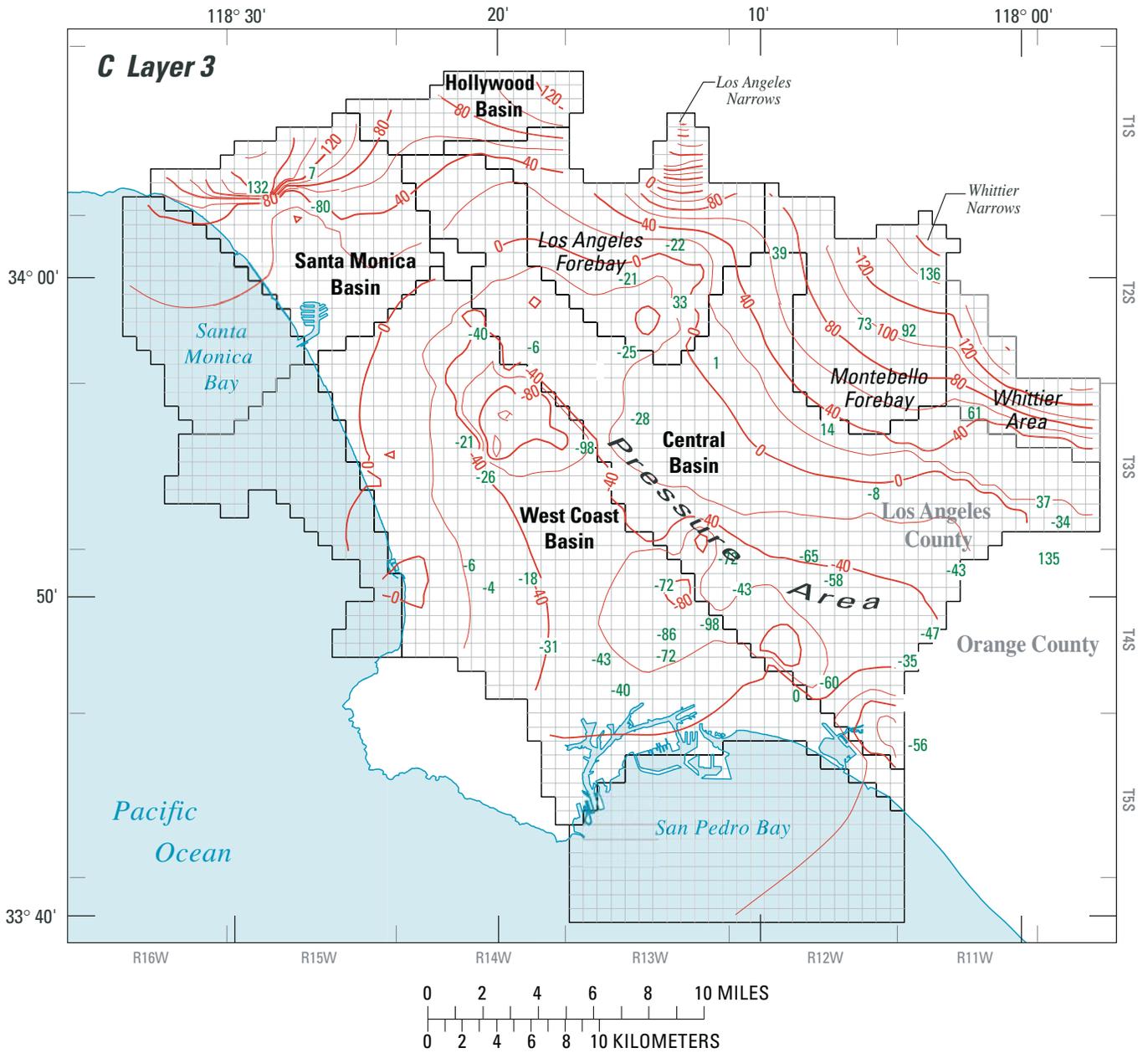
EXPLANATION

☐   **Grid Cell**

50   **Measured water-level** (in feet above sea level).

—130—   **Simulated water-level contour** - shows simulated water-level in feet above sea level. Contour interval 20 feet.

Figure 36.—Continued.

Offshore-boundary conditions also are treated in a very simplified manner, extrapolating aquifer surfaces offshore and applying equivalent freshwater heads and conductance values as general-head boundaries. Increased understanding of the offshore hydrostratigraphy and the location(s) of the freshwater/seawater interface(s) are needed to more accurately simulate ground-water flow at and near the ocean boundaries.

The eastern boundary with Orange County is treated as a time-varying specified-head boundary. In fact, the Orange County Basin and the basins considered in this report—Central, West Coast, Santa Monica, and Hollywood Basins—are part of the same geohydrologic system. Coordinated use of this model and the model of the Orange County Basin developed by the Orange County Water District will help reduce geohydrologic uncertainties along the Orange County—Los Angeles County boundary. In the future, developing an integrated model of the combined Orange-Los Angeles County coastal ground-water basins may be beneficial.

The model represents the regional ground-water system with four layers. In at least some parts of the study area, water levels in the upper and lower parts of layer 3 respond differently. This points to the potential of subdividing layer 3 into at least two separate layers. As is discussed below in the section on particle tracking, further subdivision of model layers would be necessary to simulate solute transport.

The model uses annual stress periods for the historical simulations. It does not simulate seasonal changes in water levels. In some locations (for example, wells 4S/12W-28H9, 4S/13W-12K1, and USGS monitoring sites La Mirada-1, Long Beach-1, and Lakewood-1 in Appendix VI) seasonal water-level changes are significant. Incorporating shorter stress periods into the model would allow representation of these seasonal changes. Note that in the simulations of future scenarios and in the optimization analyses described later, 6-month stress-periods are used.

The model does not incorporate simulation of subsidence, because virtually all measured water levels during the simulation period, 1971–2000, were above historic low values (fig. 7). However, during the late

1990s, some seasonal low water levels in the Long Beach area (well 4S/12W-28H9 in figure 7) are at or just below the historic low levels that occurred around 1960. To accurately simulate the effects of continuing drawdowns in this area would require incorporating the Interbed Storage Package for MODFLOW (Leake and Prudic, 1988).

The model calibration focused on matching water levels at USGS multiple-well monitoring sites and a set of long term historical water levels. Incorporating additional depth-dependent water-level data in areas of current data gaps would reduce model uncertainty (figure 23 shows location of USGS multiple-well monitoring sites used in model calibration). Formal parameter-estimation techniques were not used in the calibration of this model. Applying such techniques could provide improved estimates of parameter values and statistical measures of the correlation between parameters.

APPLICATIONS OF THE GROUND-WATER SIMULATION MODEL

Particle Tracking Analyses

The MODFLOW ground-water flow model just described was coupled with MODPATH, a particle-tracking routine developed by the USGS to simulate advective transport. Details on the algorithm and assumptions in MODPATH are given by Pollock (1994). The particle-tracking analysis was used in this study to evaluate the historical movement of water from the spreading grounds in the Montebello Forebay and to estimate the net advective movement of water from the coastline and from injection wells during the model period.

MODPATH requires selected MODFLOW input data sets and output files, including cell-by-cell flows for each time step. Additional required inputs include porosity (n), top and bottom elevations of layers, and particle-starting locations. Initially, a porosity of 0.25 was assumed for all model layers.

As noted earlier, tritium data collected as part of this study showed the highest tritium value for well 3 at Downey-1 monitoring site (3S/12W-9J3) (fig. 18), suggesting that this water was recharged near the time of peak tritium concentrations in the atmosphere. Tritium/helium age dating of samples collected in 1998 provided an estimated age for water collected at Downey-1 well 3 (3S/12W-9J3) of 30 years and for water from Downey-1 well 2 (3S/12W-9J2) of 34 years (Robert Anders, U.S. Geological Survey, San Diego, written commun., 2001). This is consistent with the results of Schroeder and others (1993) and Michel and Schroeder (1994) showing the highest tritium concentration in water delivered from the Colorado River occurred in 1967.

The first particle tracking application consisted of placing particles at the tops and bottoms of perforations of Downey-1 wells 2 and 3 (both in model layer 3) in 1998 and backward tracking the particles to their point of entry in the system in the area of the spreading grounds. Because the simulation period began in October 1970, it was assumed for this analysis that prior water levels were constant at the initial steady-state conditions.

Using the initial assumed 0.25 porosity for all model layers, backward particle-tracking simulations from Downey-1 wells 2 and 3 resulted in computed ages of 103 and 54 years, respectively. This is far older than the tritium--helium computed ages (34 and 30 years, respectively).

This overestimate in age is likely explained by the fact that MODPATH uses average hydraulic conductivity within each layer to compute advective velocities. In reality, most transport probably occurs preferentially within high-permeability zones within each aquifer system. To truly model this transport requires much more detailed vertical discretization—that is, discretely modeling these higher conductivity zones. In the context of the four-layer regional flow model, it is possible to crudely estimate the fraction of the layer thickness in which most flow is actually occurring by artificially reducing the porosity value input into the model. This has the same result as reducing the aquifer thickness while maintaining the same effective aquifer transmissivity (hydraulic conductivity times thickness) calibrated for the flow model. In order to get rates of advective particle movement that are consistent with the tritium/helium age estimates, it was necessary to reduce the model porosity value for layer 3 to 0.05, which is 20 percent of the originally assumed porosity value of 0.25. Flow paths of water particles are shown in figure 37. The thickness of model layer 3 (the Upper San Pedro aquifer system) in cells within the flow paths shown in figure 37 ranges from about 570 to 760 ft (fig. 24). This implies that high-conductivity zones that dominate flow in layer 3 are between 110 and 150 ft in cumulative thickness. However, since the actual hydraulic gradient prior to 1970 was steeper than is simulated in this simplified analysis; at least a small part of the artificial reduction, in porosity in the model is accounting for this steeper gradient.

This backward particle-tracking simulation indicates that the apparent location of the tritium peak (and the tritium/helium age estimates) at the USGS Downey-1 well 3 is generally consistent with the geohydrologic conceptualization as incorporated into the regional flow model, if one assumes that most flow within the Upper San Pedro aquifer system (model layer 3) occurs within about 20 percent of the total aquifer-system thickness.

The second application of particle tracking involved forward-tracking of water from the spreading grounds from the time of the tritium peak in water imported from the Colorado River, 1967 to 2000, using the reduced porosity of 0.05 for layer 3. Particles were placed in each of the 24 cells representing spreading ponds (25 particles in each cell for a total of 600 particles). Results shown in figure 38 provide an estimate of the extent of advective movement of artificial recharge. Most (66 percent, or 396 particles, including 34 particles that ended in pumping wells) of the recharged particles were in layer 3 by 2000, about 22 percent (129 particles) were in layer 2, about 12 percent (73 particles, including 4 that ended in pumping wells) were in layer 4, and less than 1 percent (2 particles) were in layer 1.
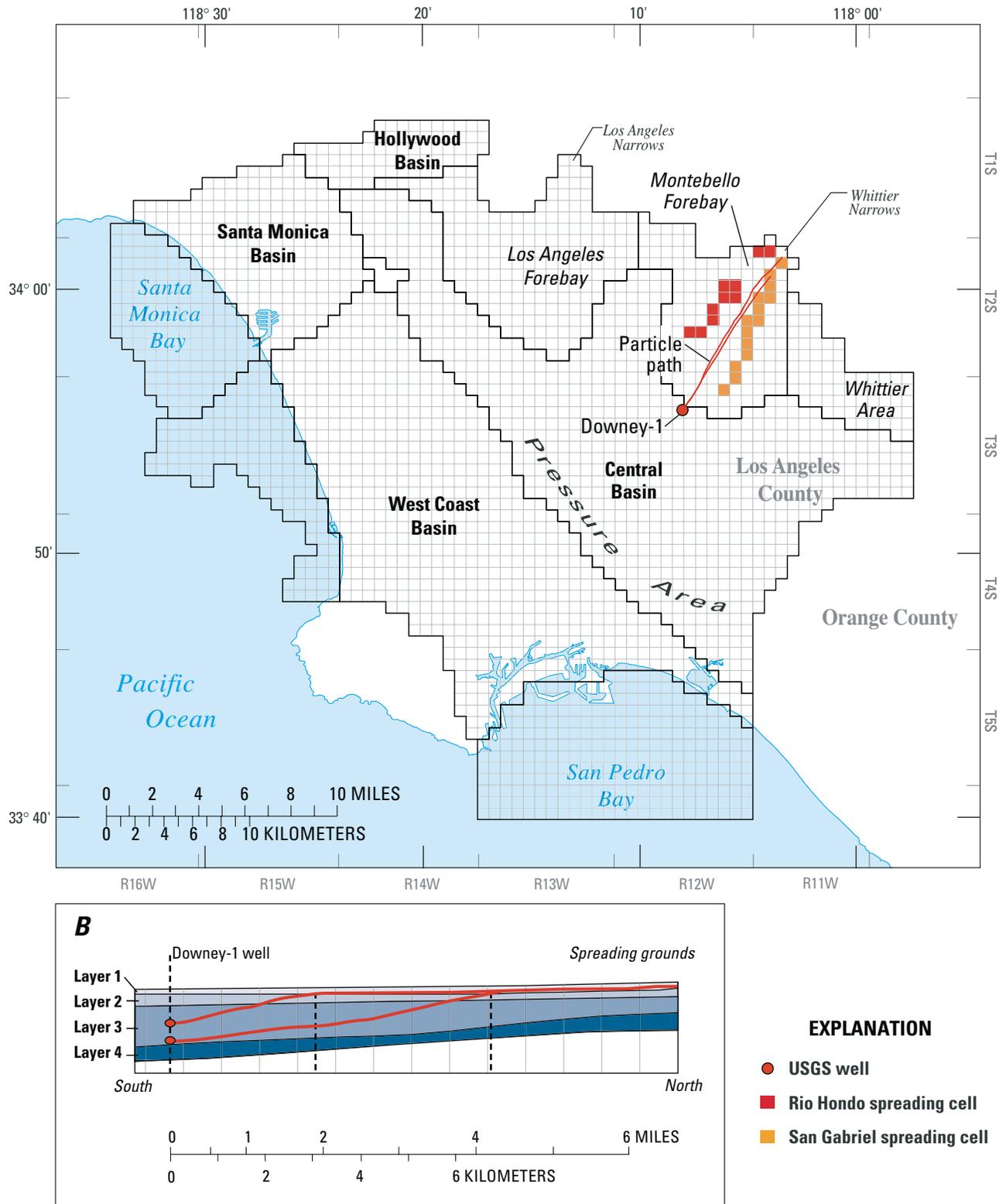
Figure 37. Model-simulated backward tracking of advective flow paths of water particles from U.S. Geological Survey Downey-1 monitoring site in 1998 to their time of entry into the simulation model, Los Angeles County, California (*A*, aerial view; *B*, cross-sectional view).
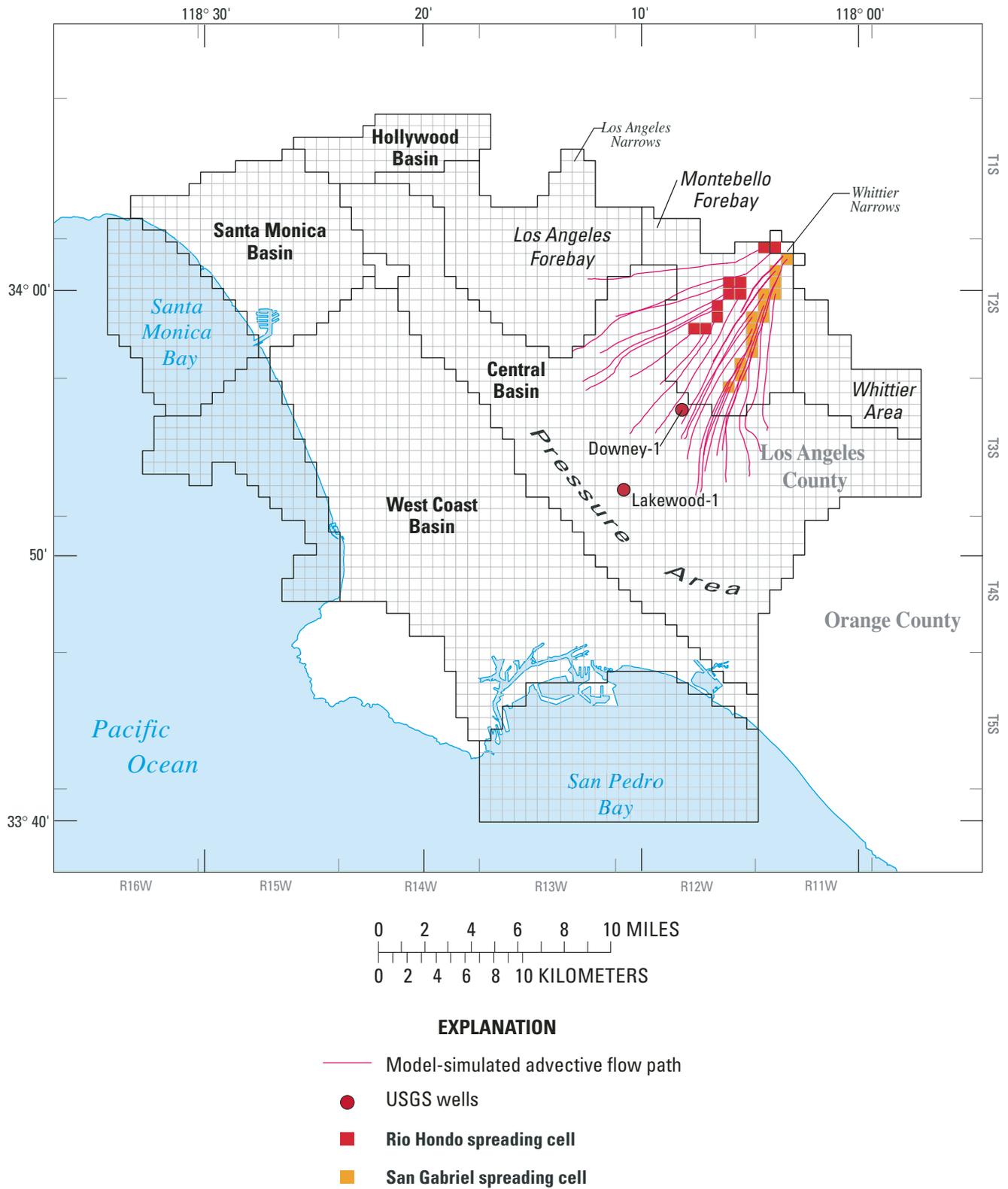
Figure 38. Model-simulated forward tracking of advective flow paths of water particles from spreading grounds, 1967–2000, Los Angeles County, California.

The third application of the particle-tracking analysis involved the tracking of particles with initial starting locations in layer 3 along the coast in the West Coast Basin, again using the same parameters, including the artificial 0.05 value of porosity in model layer 3. The path of particle movement over the model period, 1971–2000, is shown in figure 39A. The average velocities of the particles over the 30-year period ranged from 0.1 to 2.1 ft/d (mean of 0.6 ft/d) along the Santa Monica Bay and from 0.1 to 1.0 ft/d (mean of 0.5 ft/d) along the San Pedro Bay. Of note in figure 39A is the large inland distance traveled by particles that originate just north of Redondo Canyon, apparently as a result of limited simulated injection in layer 3 in that area. Historical data on injection rates at individual wells are limited; more accurate estimates of the actual amount of water injected in each well in the barrier projects is needed to validate the particle-tracking results in this region.

A fourth and final particle-tracking simulation was conducted to estimate how much of the injected water moves inland, recharging the West Coast Basin aquifers. To conduct this simulation, 10 particles were placed in each injection well at the beginning of each of the 30 stress periods (a total of 24,497 particles over the simulation period; an average of 817 particles per stress period). Results show that nearly all particles move inland (that is, few move toward the ocean) (fig. 39B). About 15 percent of the particles injected were eventually captured by pumped wells during the simulation period. The simulated 30-year advective paths of water injected in 1971 are shown in figure 39B.

The particle-tracking analyses provide insight into the pathways, travel times, and velocities of water spread in the Montebello Forebay, water from offshore, and water injected in barrier wells. However, the significant limitations of particle tracking must be reiterated. First, particle tracking considers only advective transport (dispersion is not considered). Second, reasonable results from the particle tracking can be achieved only if it is assumed that most of the flow in the Upper San Pedro aquifer system (model layer 3) is transmitted within about 20 percent of the total thickness. More rigorous simulation of transport of recharge water or of seawater requires a true solute-transport model with more detailed vertical discretization.

Simulation of Future Water-Management Scenarios

The ground-water simulation model was used to evaluate two possible future water-management scenarios being considered by local water managers. The inputs used for the scenarios are presented in table 9. The two scenarios differ only in that scenario 2 incorporates increased pumpage in the Central Basin.

These future scenarios were evaluated in the following way. Model-simulated water levels for 2000 (fig. 31) were used as initial conditions. The future simulation period was 25 years, 2001–25. Instead of the annual stress periods used in the historical transient simulations described above, 6-month model stress periods were used. Specified heads along the Orange County boundary initially were set to vary seasonally, based on average high (October–March) and low (April–September) water levels during recent years (1996–2000). The same total annual values of interior areal recharge and mountain-front recharge used for 1971–95 in the historical simulation were used, but were prorated into the 6-month stress periods on the basis of the fraction of total annual precipitation during each 6-month period. Six-month values of historical spreading for 1971–95 were used for the future simulations.

Injection rates were set as follows. Injection at the West Coast Basin Barrier Project was set equal to the 2000 rate of 18,700 acre-ft/yr. Injection at the Dominguez Gap Barrier Project was set equal to the 2000 rate of 6000 acre-ft/yr plus an additional 2,900 from a first set of planned new wells in April 2002 and 4,350 from a second set of planned new wells in October 2003 (an ultimate total of 13,250 acre-ft/yr). Injection at the Alamitos Gap Barrier Project was set equal to the 2000 rate of 5,800 acre-ft/yr with an increase of 1,300 acre-ft/yr from planned new wells starting in April 2002 (an ultimate total of 7,000 acre-ft/yr). Operation of a newly installed desalination well in the Torrance area was incorporated, pumping at a constant rate of 3,045 acre-ft/yr from layer 3. In future scenario 1, pumping rates were set equal to the average 6-month rates over the period 1997-2000. In future scenario 2, pumpage from all wells in the Central Basin (with the exception of wells operated by the City of Los Angeles) were increased 25 percent from the 1997–2000 rates over the simulation period (in 5-percent increments every 5 years) (table 9).
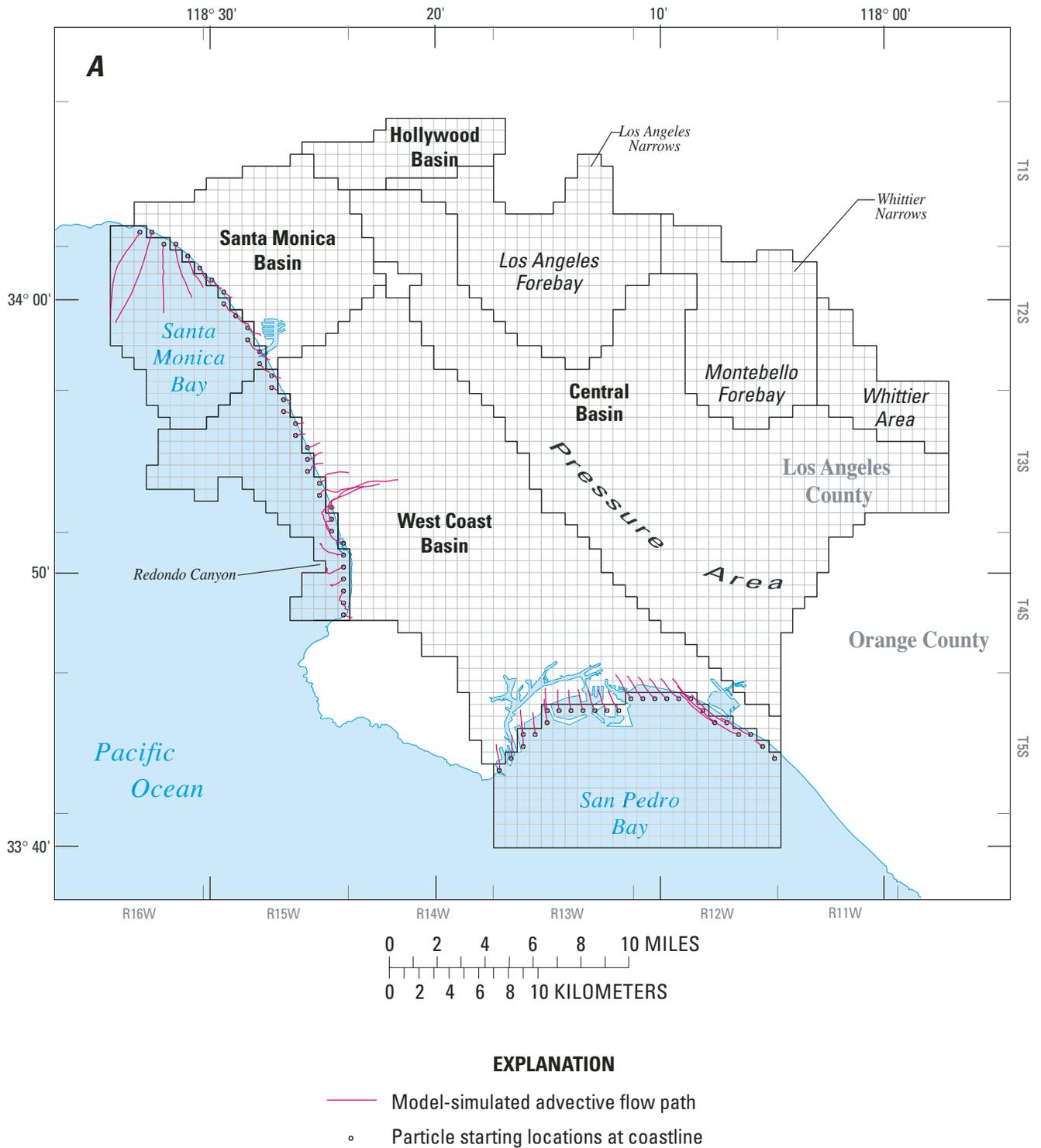
Figure 39. Model-simulated advective flow paths of water particles from coastline, Layer 3, 1971–2000 (*A*) and from injection wells, 1971–2000 (*B*), Los Angeles County, California.
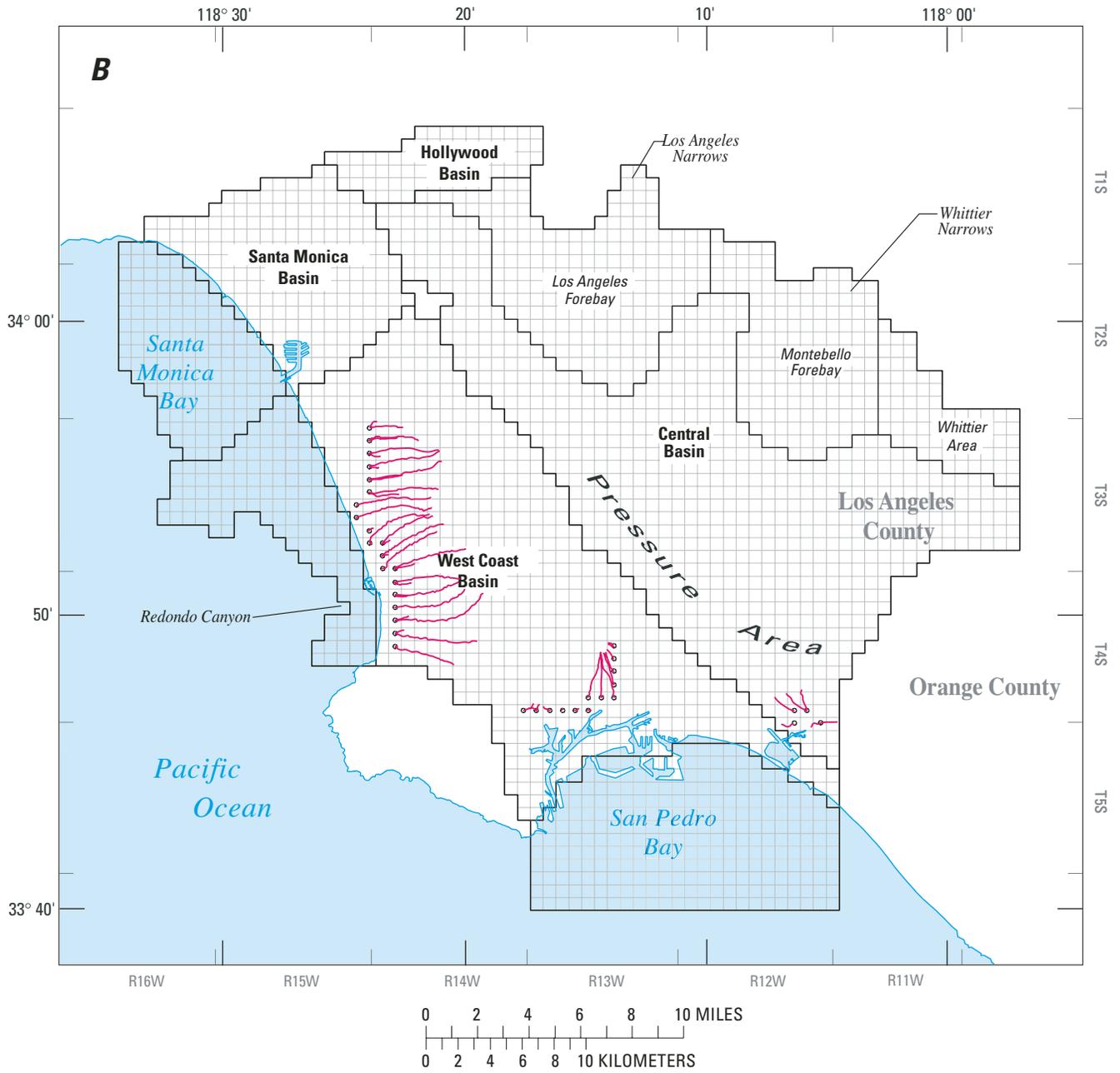
Figure 39.—Continued.

Table 9. Inputs used for future model scenarios (2001–25)

Model input	Scenario 1	Scenario 2
Recharge (spreading, mountain front, and interior)	1971–95 values (divided into 6 month stress periods)	Same as scenario 1
Injection	**West Coast Basin Barrier Project:** —2000 rate (18,700 acre-ft/yr)	Same as scenario 1
	Dominguez Gap Barrier Project: —Oct. 2000– March 2002: 2000 rate (6,000 acre-ft/yr) —April 2002–Sept, 2003: additional 2,900 acre-ft/yr —Oct. 2003–Sept, 2025: additional 4,350 acre-ft/yr	Same as scenario 1
	Alamitos Gap Barrier Project: —Oct. 2000– March 2002: 2000 rate (5,800 acre-ft/yr) —April 2002–Sept, 2025: additional 1,300 acre-ft/yr	Same as scenario 1
Desalination pumping	3,045 acre-ft/yr	Same as scenario 1
Pumpage	Average 1997–2000 6-month values	Increase Central Basin pumpage (excluding City of Los Angeles wells) 25-percent over future simulation periods (in 5-percent increments every 5 years)

The values for the flow components in tables 10 and 11 are output directly from the model. As noted for tables 7 and 8, the model outputs a net pumpage or injection for the small number of cells that contain both pumping and injection wells.

Shown in figures 40 and 41 are the simulated drawdowns for layer 3 and hydrographs for selected wells for 2001 to 2025 for scenario 1 and scenario 2 (in figs. 40A and 41A positive drawdowns represent water level declines and negative drawdowns represent water level rises). For scenario 1, water levels throughout most of the model area are generally constant or slightly increasing throughout the 25-year simulation period. (Note that the apparent water-level declines in the southeast part of the Central Basin Pressure Area shown in figure 40A reflect seasonal drawdown from the average annual 2000 water levels used as initial conditions; long term trends can be seen in the hydrographs shown in figure 40B). The simulation results for scenario 2 (fig. 41) show water levels decreasing by 25 to 50 ft in much of the Central Basin. Simulation results for scenario 1 indicate that there is an average increase in storage in the onshore areas of about 8,000 acre-ft/yr (table 10). For scenario 2, there is an average decrease in storage of about 9,000 acre-ft/yr (table 11).

Average model-calculated ground-water flows laterally between basins and subareas and vertically between the four model layers for future scenarios 1 and 2 are shown in figures 42 and 43. The simulated flows for future scenario 1 (fig. 42) are generally similar to those for 30-year historical simulation (fig. 34A). The increased pumpage in the Central Basin in scenario 2 results in additional water being drawn from the Whittier Narrows boundary to the Montebello forebay and from the Orange County Boundary into the Central Basin Pressure area. Note that there also is a very slight increase in flows from offshore into the West Coast Basin (figs. 42, 43).

An important issue in testing future scenarios is the assumption made about the Orange County boundary condition. As with the historical simulations, the two future scenarios were re-run with a constant flow specified along the Orange County boundary. A flow of 3,700 acre-ft/yr, prorated 50 percent to layer 2 and 25 percent each to layers 3 and 4, was applied. The results for scenario 1 with the constant-flow boundary, which are shown in figure 44, do not differ greatly from the results for the specified head-case shown in figure 40. In contrast, the results for scenario 2 with the constant-flow Orange County boundary, which are shown in figure 45, show more drawdown throughout the Central Basin than the results for the specified-head case shown in figure 41.

These potential future water-management strategies are just two of many possible scenarios that the model can be used to evaluate. Other scenarios could incorporate alternative assumptions regarding future water demand, availability of surface-water supplies, development of new projects, and the impacts of climatic variability.

Table 10. Average water budget for future scenario 1, 2001–2025

Budget item and model layer	Montebello Forebay	Los Angeles Forebay	Whittier Area	Central Basin	Hollywood Basin	West Coast Basin	Santa Monica Basin	Total
				In acre-feet per year				
Pumpage								
—Layer1	−2,500	0	0	−2,100	0	0	0	−4,600
—Layer2	−6,600	−240	0	−4,300	0	−1,200	−60	−12,400
—Layer3	−33,800	−11,500	−20	−108,000	0	−51,200	−1,800	−206,320
—Layer4	−1,800	−9,600	−10	−16,400	0	−2,400	−1,200	−31,410
A. TOTAL	**−44,700**	**−21,340**	**−30**	**−130,800**	**0**	**−54,800**	**−3,060**	**−254,730**
Net flow from adjacent inland zones								
—Layer1	−131,700	−3,700	−1,400	−3,700	0	−5,200	0	−145,700
—Layer2	−1,300	−7,800	−3,600	−10,100	−5,500	−14,000	−10,100	−52,400
—Layer3	27,200	10,700	30	109,600	0	25,100	4,200	176,830
—Layer4	−4,100	9,200	10	14,200	0	-500	2,300	21,110
B. TOTAL	**−109,900**	**8,400**	**−4,960**	**110,000**	**−5,500**	**5,400**	**−3,600**	**−160**
C. Spreading	**124,300**	**0**	**0**	**0**	**0**	**0**	**0**	**124,300**
Injection								
—Layer1	0	0	0	400	0	3,200	0	3,600
—Layer2	0	0	0	3,800	0	5,900	0	9,700
—Layer3	0	0	0	2,300	0	20,400	0	22,700
—Layer4	0	0	0	0	0	500	0	500
D. TOTAL	**0**	**0**	**0**	**6,500**	**0**	**30,000**	**0**	**36,500**
E. Mountain front and interior recharge	**5,600**	**7,400**	**5,200**	**14,500**	**6,000**	**15,700**	**13,300**	**67,700**
Net flow from ocean and adjacent basins								
—Layer1	6,800	2,800	0	0	0	−1,600	0	8,000
—Layer2	6,600	2,200	0	3,600	0	−1,000	−1,800	9,600
—Layer3	6,600	900	0	−4,100	0	5,700	−2,400	6,700
—Layer4	5,900	300	0	2,300	0	2,400	−1,100	9,800
F. TOTAL	**25,900**	**6,200**	**0**	**1,800**	**0**	**5,500**	**−5,300**	**34,100**
G. Total net flow (A+B+C+D+E+F)	**1,200**	**660**	**210**	**2,000**	**500**	**1,800**	**1,340**	**7,710**
Change in storage								
—Layer1	1,300	10	30	-20	0	1,200	0	2,520
—Layer2	60	510	160	2,000	510	670	1,400	5,310
—Layer3	10	0	10	−170	0	60	10	-80
—Layer4	0	0	0	80	0	20	0	100
H. TOTAL	**1,370**	**520**	**200**	**1,890**	**510**	**1,950**	**1,410**	**7,850**

Table 11. Average water budget for future scenario 2, 2001–2025

Budget item and model layer	Montebello Forebay	Los Angeles Forebay	Whittier Area	Central Basin	Hollywood Basin	West Coast Basin	Santa Monica Basin	Total
				In acre-feet per year				
Pumpage								
—Layer1	−2,900	0	0	−2,400	0	0	0	−5,300
—Layer2	−7,800	−280	0	−5,000	0	−1,200	−60	−14,340
—Layer3	−39,700	−13,600	−20	−126,900	0	−51,200	−1,800	−233,220
—Layer4	−2,200	−11,200	−20	−19,300	0	−2,400	−1,200	−36,320
A. TOTAL	**−52,600**	**−25,080**	**−40**	**−153,600**	**0**	**−54,800**	**−3,060**	**−289,180**
Net flow from adjacent inland zones								
—Layer1	−135,900	−3,700	−1,400	−7,200	0	−6,000	0	−154,200
—Layer2	−1,500	−10,400	−3,700	−15,400	−5,700	−14,900	−10,300	−61,900
—Layer3	32,000	12,700	20	120,500	0	24,500	4,200	193,920
—Layer4	−4,700	10,900	20	14,400	0	−700	2,200	22,120
B. TOTAL	**−110,100**	**9,500**	**−5,060**	**112,300**	**−5,700**	**2,900**	**−3,900**	**−60**
C. Spreading	**124,300**	**0**	**0**	**0**	**0**	**0**	**0**	**124,300**
Injection								
—Layer1	0	0	0	400	0	3,200	0	3,600
—Layer2	0	0	0	3,800	0	5,900	0	9,700
—Layer3	0	0	0	2,300	0	20,400	0	22,700
—Layer4	0	0	0	0	0	500	0	500
D. TOTAL	**0**	**0**	**0**	**6,500**	**0**	**30,000**	**0**	**36,500**
E. Mountain front and interior recharge	**5,600**	**7,400**	**5,200**	**14,500**	**6,000**	**15,700**	**13,300**	**67,700**
Net flow from ocean and adjacent basins								
—Layer1	8,000	2,800	0	0	0	−1,500	0	9,300
—Layer2	7,700	2,200	0	4,900	0	-900	−1,700	12,200
—Layer3	7,700	900	0	3,900	0	6,300	−2,400	16,400
—Layer4	6,900	300	0	4,900	0	2,600	−1,000	13,700
F. TOTAL	**30,300**	**6,200**	**0**	**13,700**	**0**	**6,500**	**−5,100**	**51,600**
G. Total net flow (A+B+C+D+E+F)	**−2,500**	**−1,980**	**100**	**−6,600**	**300**	**300**	**1,240**	**−9,140**
Change in storage								
—Layer1	−2,200	−10	−20	−3,900	0	520	0	−5,610
—Layer2	−250	−2,000	40	−2,500	280	−240	1,200	−3,470
—Layer3	−20	−30	0	−200	0	40	10	−200
—Layer4	−10	−10	0	20	0	−10	0	−10
H. TOTAL	**−2,480**	**−2,050**	**20**	**−6,580**	**280**	**310**	**1,210**	**−9,290**

Figure 40. Model-simulated drawdowns, layer 3 (*A*) and selected model-simulated hydrographs (*B*) for future scenario 1, 2001–25, Los Angeles County, California.

B

Figure 40.—Continued.

Figure 41. Model-simulated drawdowns, layer 3(*A*) and selected model-simulated hydrographs (*B*) for future scenario 2, 2001–25, Los Angeles County, California.

B

Figure 41.—Continued.

Figure 42. Average model-simulated inter-zone flows for layers 1–4 for future scenario 1, 2001–25, Los Angeles County, California.

Figure 43. Average model-simulated inter-zone flows for layers 1–4 for future scenario 2, 2001–25, Los Angeles County, California.

Figure 44. Model-simulated drawdowns, layer 3 (*A*) and selected model-simulated hydrographs (*B*) for future scenario 1 with constant flow at the Orange County boundary, 2001–25.

B
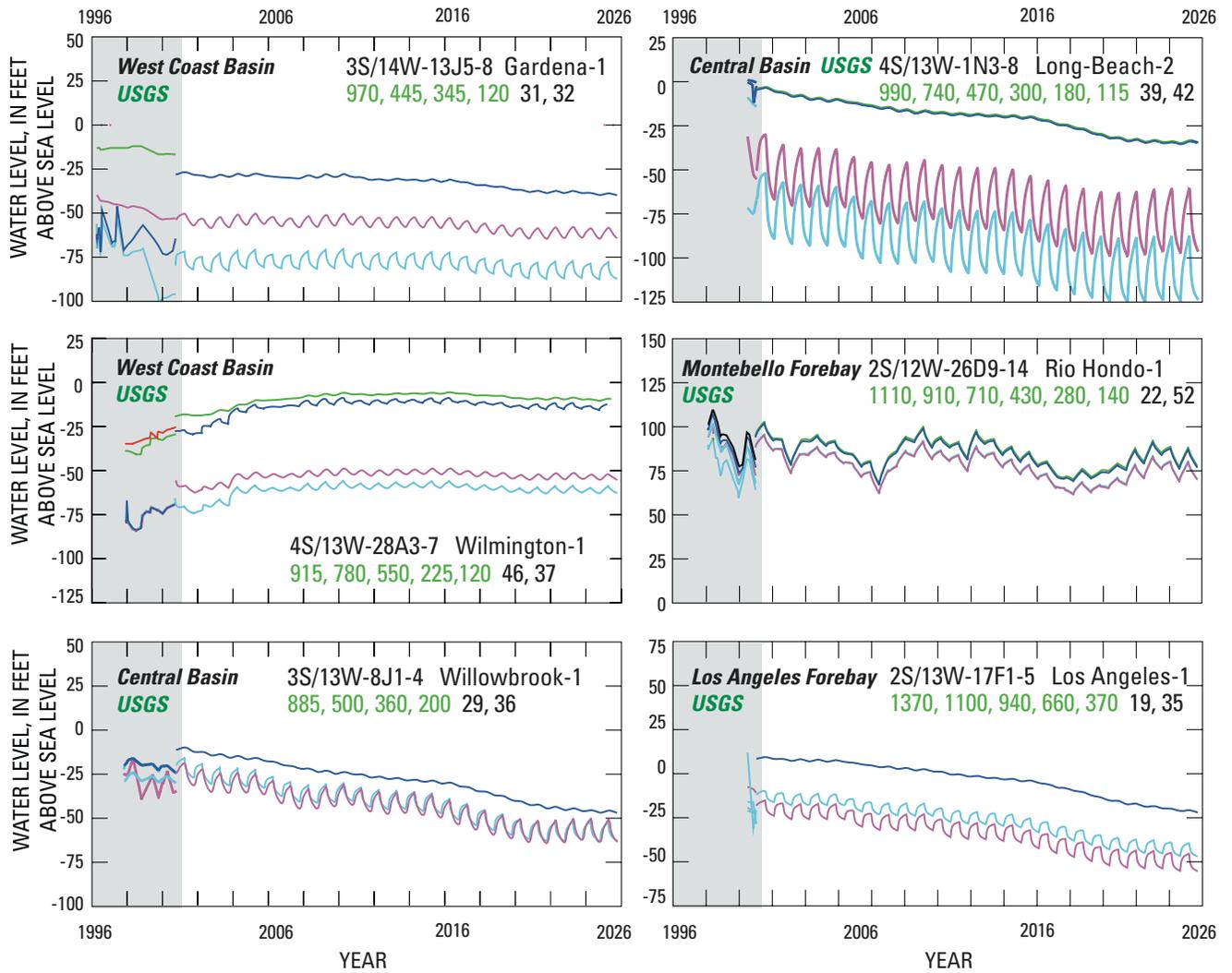
EXPLANATION

Historical measured
water levels

Simulated future
water levels

Layer 1

Layer 2

Layer 3

Layer 4

31, 32   Model row and column

885, 500, 360, 200   Well depths

Figure 44.—Continued.
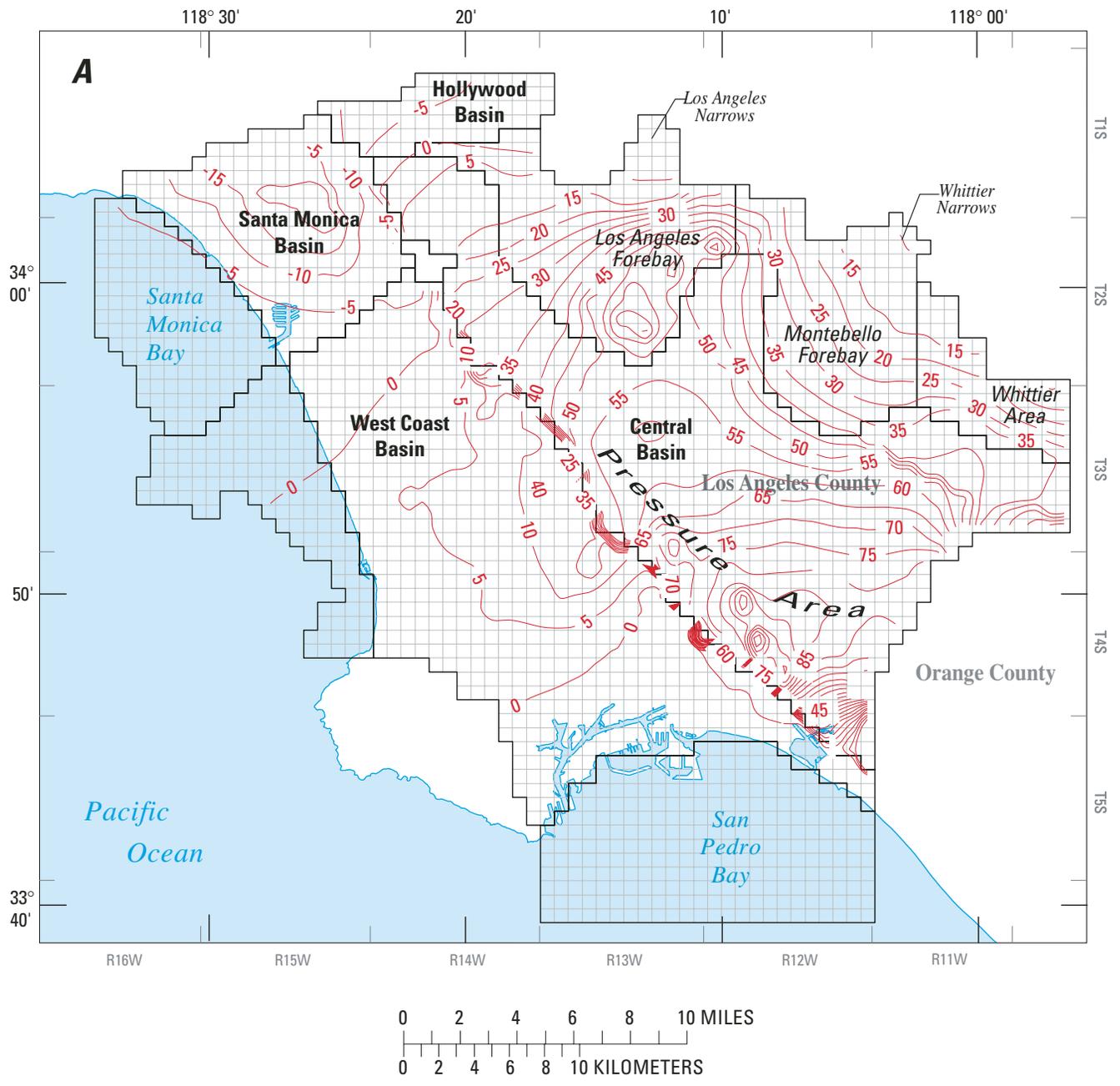
EXPLANATION

— 130 — **Simulated drawdown 2001-2025 in model layer 3.**
Countour interval 5 feet. (Note: negative drawdowns
represent water-level rises)

Figure 45. Model-simulated drawdowns, layer 3 (*A*) and selected model-simulated hydrographs (*B*) for future scenario 2 with constant flow at the Orange County boundary, 2001–25.

B

EXPLANATION

(gray box)	**Historical measured water levels**
(white box)	**Simulated future water levels**
—— (green)	**Layer 1**
—— (dark blue)	**Layer 2**
—— (light blue)	**Layer 3**
—— (magenta)	**Layer 4**
31, 32	**Model row and column**
885, 500, 360, 200	**Well depths**

Figure 45.—Continued.

SIMULATION-OPTIMIZATION ANALYSIS

The simulation model was coupled with mathematical optimization algorithms to identify least-cost solutions for improving control of seawater intrusion. Initial development of simulation-optimization methods for ground-water management was done by Bredehoeft and Young (1970), Deninger (1970), Maddock (1972), and Aguado and Remson (1974). Literature reviews of simulation-optimization research can be found in Gorelick (1983), Yeh (1992), Wagner (1995), and Ahfeld and Mulligan (2000). Specific applications that utilize optimization methods to address issues of seawater intrusion include Shamir and others (1984), Willis and Finney (1988), Reichard (1995), Nishikawa (1998), Emch and Yeh (1998), Chang and others (2000), and Gordon and others (2001).

The base case optimization analysis utilizes future scenario 1 presented in the previous section. Model- simulated 2025 water levels in layer 3 (Upper San Pedro aquifer system) for scenario 1 are shown in figure 46. Note that simulated water levels are below sea level. The goal of the analysis is to determine the most cost effective way to raise water levels along the coast, either by increasing injection or reducing pumpage through in-lieu delivery of surface water, so as to better control seawater intrusion. Sensitivity to several factors—restrictiveness of water-level constraints, cost structures, and assumed future scenario—is evaluated.

Shown in figure 46 are locations of injection in cells where additional injection is considered, in lieu cells where in lieu delivery of surface water is considered (based on information provided by WRDSC), and control cells where water-level constraints are imposed.
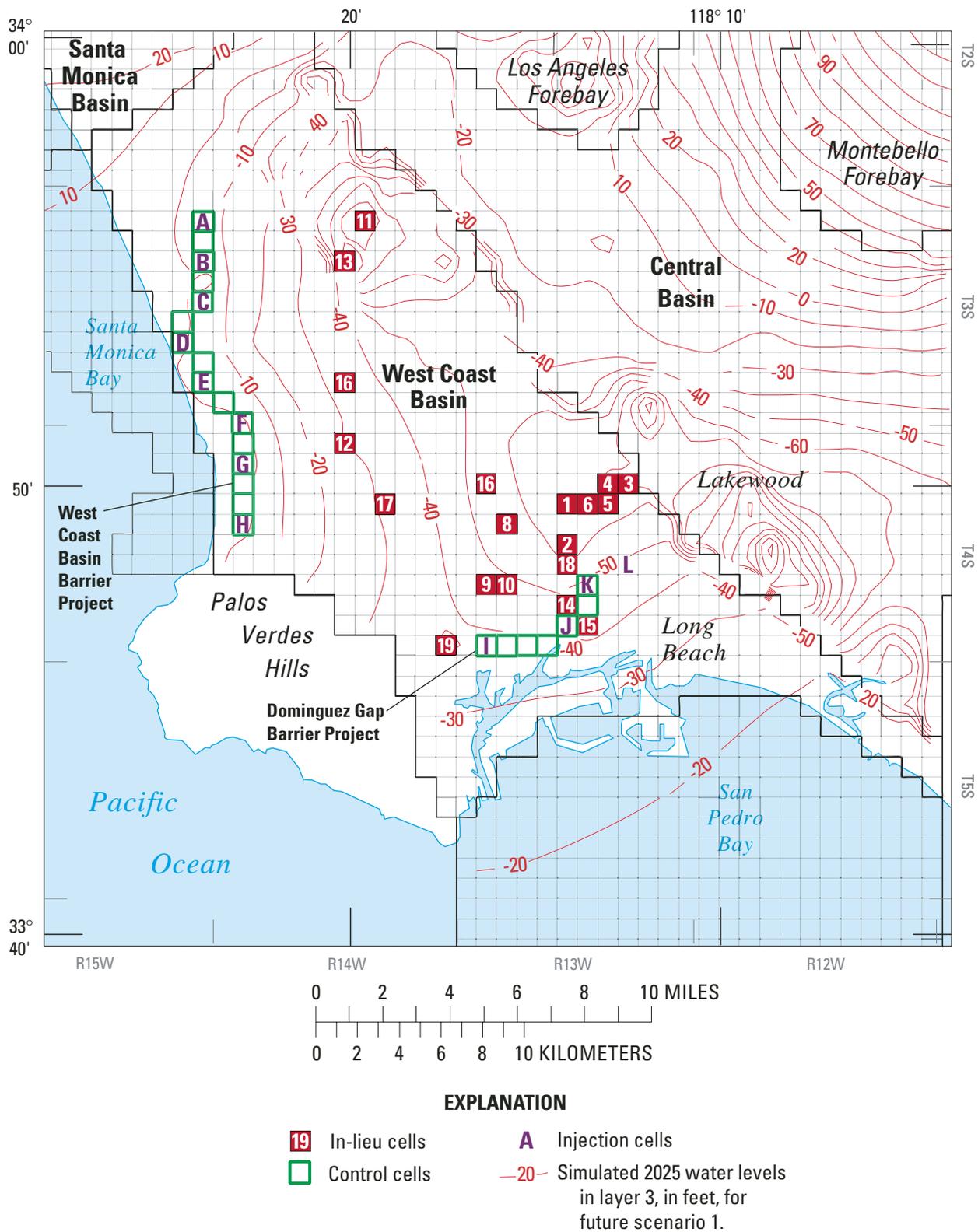
Figure 46. In-lieu and injection cells for the ground-water simulation model-optimization analysis, Los Angeles County, California.

The optimization problem is the following:
Minimize:

$$\sum_{t=1}^{T}\left[\sum_{i=1}^{I}(c_{il}\cdot Il_{it}) + \sum_{j=1}^{J}(cinj\cdot Inj_{jt})\right] \qquad (1)$$

subject to:

$$h_{kt} = h_{ko} + du_{kt} + $$

$$\sum_{\tau=1}^{t}\left[\sum_{i=1}^{I}(\alpha_{i\tau kt}\cdot Il_{it}) + \sum_{j=1}^{J}(\beta_{j\tau kt}\cdot Inj_{it})\right] t = 1, T(2)$$

$$1/T\cdot\sum_{t=1}^{I} h_{kt} \geq H_{\text{min-avg}} \qquad k = 1, K \qquad (3)$$

$$h_{kt} > h_{min} \qquad k = 1, K \qquad (4)$$

$$h_{kt} < h_{max} \qquad k = 1, K \qquad (5)$$

$$Il_{it} < Il\text{–}max_{j} \qquad i = 1, I \qquad (6)$$

$$Inj_{jt} < Inj\text{–}max_{j} \qquad j = 1, J \qquad (7)$$

where:

c_{il} = cost of water for in-lieu delivery ($168 per acre-ft for base case);

Il_{it} = in-lieu delivery at location i in time period t;

c_{inj} = cost for injection water ($528 per acre-ft for base case);

Inj_{jt} = additional injection at injection cell j in time period t;

h_{kt} = head at control location k in time period t;

h_{k0} = head at control location k in time step 0;

du_{kt} = drawdown at control location k in time step t due to initial and boundary conditions and unmanaged stresses;

$\alpha_{i\tau kt}$ = water-level response at control location k at time step t resulting from unit in-lieu delivery to location i at time τ;

$\beta_{j\tau kt}$ = water-level response at control location k at time step t resulting from unit injection at location j at time τ;

$H_{\text{min-avg}}$ = lower bound on average water level at all control locations (set at 0 ft for base case);

h_{min} = lower bound on water level at control locations during each stress period (−30 ft);

h_{max} = upper bound for water level at control locations during each stress period (30 ft);

$Il\text{-}max_i$ = upper bound on in-lieu delivery for location i (based on average October–March, 1997–2000, pumping at that location);

$Inj\text{-}max_j$ = upper bound on additional injection at injection location j (set at 7,200 acre-ft/yr for all cells);

T = management period (fifty 6-month periods);

I = in-lieu locations (locations where ground-water pumpage can be replaced by delivery of surface water) (19);

J = injection locations (12); and

K = water-level control locations (23).

The objective function of the model, equation 4, is to minimize the undiscounted sum of the water costs of in lieu delivery (Il) and additional injection (Inj). Any additional operational or capital costs are not considered. The current (2002) costs for injection (c_{inj}) and in-lieu (c_{il}) water, as reported by WRDSC, are $528/acre-ft and $168/acre-ft, respectively. The costs differ because water delivered for injection must be non-interruptible and the in-lieu costs incorporate the cost savings resulting from reduced pumpage. The implications of this cost differential are explored in the sensitivity analysis.

Equation 5 incorporates the hydraulics of the ground-water flow system. Water levels at control location k at time t (h_{kt}) are a function of the initial water levels at that location (h_{k0}), unmanaged drawdown (du_{kt}), and the sums of all in-lieu deliveries (Il_{it}) and injections (Inj_{it}) up through time t multiplied by their appropriate response coefficients ($\alpha_{i\tau kt}$ and $\beta_{j\tau kt}$). The response coefficients, $\alpha_{i\tau kt}$ and $\beta_{j\tau kt}$, are generated by repeated runs of the simulation model using the processing program MODMAN (Greenwald, 1998). Each simulation run involves applying a unit stress (representing injection or reduced pumpage resulting from in-lieu delivery) at one of the 31 in-lieu and injection cells shown in <u>figure 46</u>. Response coefficients are computed by subtracting the simulated changes in water levels at the 23 control locations in each of the 50 management periods from the unmanaged drawdown.

Equations 6–8 represent head constraints at the control locations. Equation 6 constrains average water levels (averaged over all 50 management periods) to be greater than a specified value, $H_{min-avg}$. Constraining water levels in this manner allows levels to be below $H_{min-avg}$ in some periods, as long as this is offset by water levels above $H_{min-avg}$ in other periods. The implicit assumption in applying this constraint is that average water levels are the determining factor in long-term seawater intrusion. For the base-case optimization run, the minimum water level allowed at the control locations, $H_{min-avg}$, was set equal to 0 (sea level). It is recognized that this value is not completely protective for seawater intrusion because of the density effects. This is addressed in the sensitivity analysis. Equations 7 and 8 constrain the minimum (h_{min}) and maximum (h_{max}) water levels allowed at the control locations in each period. In the optimization runs described below, h_{min} and h_{max} are set at –30 ft and 30 ft, respectively.

Equations 9 and 10 represent upper bounds on the amount of in-lieu delivery (reduced pumpage) and injection at each location. Upper bounds in-lieu delivery (Il-max) were determined from 1997–2000 average winter (October–March) pumpage at the in-lieu cells and are listed in <u>table 12</u>. Upper bounds on injection (Inj-max) were set at 7,200 acre-ft/yr.

The optimization model represented by equations 4–10 was solved as a linear program using the software LINDO (Schrage 1993, 1997). The optimization model includes a total of 1,550 decision variables and 1,173 constraints (note that equations 7–10 are represented in LINDO as bounds rather than explicit constraints).

The response matrix approach assumes linear conditions. Because unconfined (non-linear) conditions are considered in the simulation model, it was necessary to solve the optimizations in an iterative fashion (Danskin and Freckleton, 1992; Greenwald, 1998). The iterative solution involves setting the calculated pumpage and injection rates from the previous optimization solution as fixed rates and regenerating the response matrix. The optimization is then rerun with the new response matrix, appropriately adjusting the bounds on the decision variables. The output from the new optimization run is a change in rates and objective values from the previous solution. The process is repeated until the change in the objective function is considered acceptably small (less than 0.5 percent). Three to six such iterations were required in the optimizations presented below.

Table 12. Summary of optimization results

[All in-lieu and injection amounts in acre-feet/year; $H_{min-avg}$ in feet above sea level; upper bound, maximum rate allowed in optimization; because of rounding, all values may not add to totals; *, total cost not listed for runs with varied injection/in-lieu cost ratios]

Optimization run		1 (base)	2	3	4	5	6	7	8	9
Future scenario		1	1	1	1	1	1	1	2	2, constant flow
$H_{min-avg}$		0	5	10	0	0	0	0	0	0
Injection/in-lieu cost ratio		3.3	3.3	3.3	2.5	2	1.5	1	3.3	3.3
In lieu cells	Upper bound									
1	2,138	1,026	1,069	681	1,069	1,033	556	0	1,171	1,186
2	3,683	2,910	2,818	2,472	2,838	2,988	2,620	294	3,031	3,142
3	2,108	893	1,181	1,007	859	878	464	0	1,070	1,032
4	3,950	1,456	2,115	1,501	1,417	1,452	790	0	1,623	1,732
5	998	547	643	554	540	542	300	0	670	620
6	1,274	663	806	614	670	663	349	0	816	768
7	1,442	0	288	134	173	144	58	0	173	144
8	1,330	320	533	320	320	320	213	0	453	425
9	1,404	941	960	816	928	843	990	169	1,083	984
10	0	0	0	0	0	0	0	0	0	0
11	3,128	0	0	0	0	0	0	0	0	0
12	1,472	0	0	0	0	0	0	0	0	0
13	1,888	0	0	0	0	0	0	0	0	0
14	2,028	2,000	1,880	1,812	1,988	1,997	1,907	812	1,998	2,007
15	2,530	2,327	2,361	2,362	2,328	2,237	2,100	150	2,276	2,280
16	1,782	0	0	0	0	0	0	0	0	0
17	1,432	0	57	57	0	0	0	0	0	0
18	2,208	2,092	1,822	1,734	2,149	2,122	1,825	354	2,099	2,117
19	3,522	2,756	2,547	1,984	2,719	2,442	2,070	414	2,799	2,781
Total	34,795	17,931	19,080	16,048	17,999	17,661	14,240	2,193	19,263	19,219
Injection cells										
A	7,200	0	0	200	0	0	0	0	0	0
B	7,200	0	0	40	0	0	0	0	0	0
C	7,200	0	0	0	0	0	0	0	0	0
D	7,200	0	0	0	0	0	0	0	0	0
E	7,200	0	0	0	0	0	0	0	0	0
F	7,200	0	0	0	0	0	0	0	0	0
G	7,200	0	0	0	0	0	0	0	0	0
H	7,200	0	0	0	0	0	0	0	0	0
I	7,200	0	0	4	0	0	0	0	0	0
J	7,200	0	271	1,149	0	8	1,271	4,449	0	0
K	7,200	0	0	1,810	0	0	17	4,268	0	0
L	7,200	0	774	1,995	0	154	841	3,392	0	0
Total	108,000	0	1,044	5,197	0	162	2,129	12,109	0	0
Total cost (million dollars per year)		2.870	3.604	5.311	*	*	*	*	3.082	3.075

The results of the base case optimization run are shown in table 12 (optimization run 1). The optimization model yields individual rates for each injection and in-lieu cell for all fifty 6-month stress periods; however, it is the average results that are useful for practical implementation of a management strategy. An example sequence of the iterative solution is shown in table 13. In the final solution, the average annual cost is $2.87 million. The average annual in-lieu delivery is about 18,000 acre-ft and there is no additional injection. Although injection is more hydraulically efficient (that is, injecting water is directly at the control locations rather than reducing pumpage several miles inland), this is outweighed by the lower unit cost of in-lieu water.

The optimization results can be analyzed to determine relative priorities for in-lieu delivery. One way to do this is by looking at the average reduced cost associated with the in-lieu delivery for each possible in-lieu well. Reduced cost can be defined as the change in the objective function resulting from a small change in the value of the variable (Schrage, 1997; Ahfeld and Mulligan, 2000). If computed in-lieu delivery at a given location and time period (Il_{it}) is at its upper bound ($Il\text{-}max_i$), then the reduced cost is negative. In this case, the reduced cost is the same as the dual price associated with the upper bound constraint on in-lieu delivery (equation 9) and represents the cost reduction that would result from increasing $Il\text{-}max_i$. If Il_{it} is greater than 0 but less than $Il\text{-}max_i$, then the reduced cost is 0. If Il_{it} equals 0, the reduced cost is positive. In this case, increasing Il_{it} from 0 has a detrimental effect on the objective function (equation 4). The average annual reduced cost for each in-lieu cell is shown in table 14. The more negative the average reduced cost,

the greater the cost reduction resulting from increasing the upper bound on in-lieu delivery to that well. Based on these criteria, it can be seen from table 13 that the most benefit would be yielded by additional in-lieu delivery to wells 2, 9, 10, 14, 15, 18, and 19, all located close to the Dominguez Gap Barrier Project.

The first sensitivity analysis tests the impact of changing the imposed average water-level constraint (changing $H_{min\text{-}avg}$ in equation 6) on the optimization results. The water-level constraint is first tightened to require minimum average heads to be greater than or equal to 5 ft above sea level. As shown in figure 47 and table 12 (optimization run 2), the average annual cost is $3.60 million, with average in-lieu delivery of about 19,000 acre-ft/yr and average additional injection of about 1,000 acre-ft/yr. This additional injection occurs in cells J and L (table 12) the eastern part of the Dominguez Gap Barrier Project (fig. 46). The cost increase from the initial optimization for $H_{min\text{-}avg}$ equal to 0 ft indicates that the annual cost of additional hydraulic protection from seawater intrusion is about $150,000 per foot. If equation 6 is tightened further to require average heads at control locations to be greater than or equal to 10 ft above sea level, then the average annual cost is $5.31 million, with average in-lieu delivery of about 16,000 acre-ft/yr and average additional injection of 5,200 acre-ft/yr (virtually all in the eastern part of the Dominguez Gap Barrier Project) (fig. 47; optimization run 3 in table 12). The additional annual cost of increasing the level of hydraulic protection from 5 ft to 10 ft is about $340,000 per foot. In other words, the additional costs of increasing hydraulic protection from 5 to 10 ft are greater than those for increasing from 0 to 5 ft.

Table 13. Results from iterative solution for optimization run 1 (base case)

Iteration	Cost (million dollars per year)	Percentage change	In lieu (acre-feet per year)	Percentage change
1	2.843		17,770	
2	2.904	2.14	18,160	2.19
3	2.882	−.73	18,020	−.77
4	2.870	−.45	17,930	−.50

Table 14. Average reduced cost for in lieu cells, for optimization run 1 (base case)

In lieu cells	Average reduced cost (dollars per acre-foot per year)
1	50
2	−430
3	80
4	110
5	−50
6	−20
7	940
8	300
9	−320
10	−450
11	2,920
12	2,660
13	2,880
14	−970
15	−670
16	2,750
17	2,020
18	−790
19	−520

In the second sensitivity analysis, the effects of the cost structure are evaluated. In the initial optimization, the ratio of unit costs of injection to in lieu is 3.30 ($528/acre-ft versus $168/acre-ft). The optimization model was run repeatedly, incrementally reducing that ratio (reducing the costs of injection relative to in-lieu delivery). As shown in figure 48 and table 12 (optimization runs 1, 4–7), small reductions in the ratio have little impact on the amounts of injection in comparison with in-lieu delivery. However, when that ratio becomes less than 2.0, the solution switches from in lieu to injection. Figure 48 is a tradeoff curve

between relative costs and quantities of injection and in-lieu. At a cost ratio of 2.0 or greater, the lower unit costs of in-lieu delivery dominate the solution; at cost ratios of 1.5 or less, the hydraulic efficiency of injection becomes significant. When the costs of in lieu delivery and injection are equal (cost ratio of 1.0), the optimization results show average in-lieu delivery of about 2,200 acre-ft/yr and average additional injection (all in the eastern part of the Dominguez Gap Barrier) of about 12,100 acre-ft/yr (table 12). The base costs used in this analysis are provided by WRDSC. The tradeoff curve shown in figure 48 provides a means to evaluate the impacts of different unit costs on the optimization solutions.

For the third sensitivity analysis, the optimization was run using future scenario 2, rather than future scenario 1. The original cost structure was maintained and the minimum average head ($H_{min-avg}$) was set to 0 in equation 6. As shown in table 12 (optimization run 8), total annual costs are $3.08 million per year (about $200,000, or 7 percent, greater than those of the base case optimization). In-lieu delivery is 19,300 acre-ft/yr (about 1,000 acre-ft more than in the base case optimization) with no additional injection. Although scenario 2 involves only changes (increases in pumpage) in the Central Basin, it has some effect on these optimization results for seawater-intrusion management in the West Coast Basin. The optimization also was rerun using scenario 2 with a constant-flow boundary for Orange County. The optimization results were essentially unchanged (table 12, optimization run 9). This is consistent with the fact that the different boundary-condition assumptions for Orange County have little effect on future simulated water levels in the West Coast Basin (compare figs. 41 and 45).
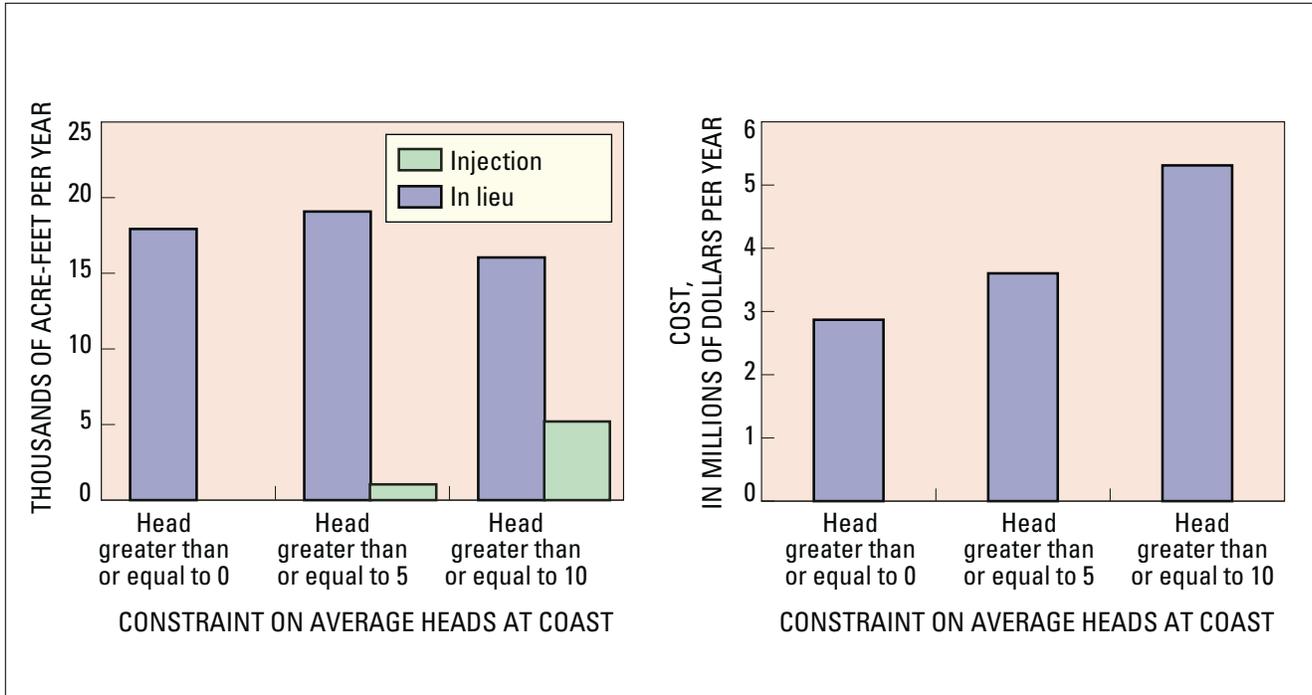
Figure 47. Sensitivity of optimization results (injection rates, in lieu rates and total cost) to average head constraint, Los Angeles County, California.
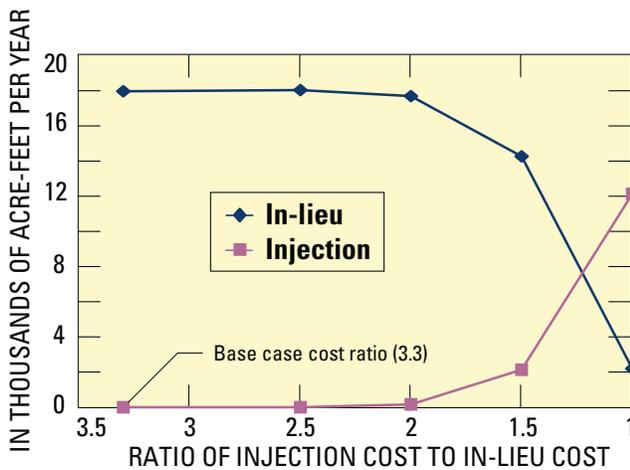
Figure 48. Sensitivity of optimization reslts to relative cost of injection and in-lieu water, Los Angeles County, California.

SUMMARY

Nearly one-hundred years after Mendenhall (1905a,b,c) first described the ground-water resources of the Los Angeles area, there is a continuing need to improve the scientific basis for regional ground-water management. To help address this need in the Central and West Coast Basins, the USGS has compiled existing data, collected extensive new data, conducted new characterizations of the regional geohydrology and geochemistry, and developed and applied ground-water flow simulation and optimization models.

The data compilation centered on development of a GIS. The new data collected in this study focused on collecting hydraulic, geologic, and chemical data

from newly installed multiple-well monitoring sites. Chemical data also were collected from existing production and observation wells in the study area. All the new data collected as part of this study are included in a companion report by Land and others (2002).

The geohydrologic and geochemical characterizations of the study were based on the compiled and newly collected data. The geohydrologic analyses build on the important previous studies of Poland and his co-workers and the California Department of Water Resources. In this study, the complex three-dimensional aquifer system was divided into four aquifer systems—Recent, Lakewood, Upper San Pedro, and Lower San Pedro. A set of geohydrologic sections were developed and surfaces for the aquifer systems were generated by evaluating geophysical logs, drill cuttings, geochemistry, and other supplementary information.

The geochemical analyses focused on developing a three-dimensional conceptualization of the regional geochemistry in order to better understand the ground-water flow system. Analyses of major ions, the stables isotopes of oxygen and hydrogen, and tritium and carbon-14 provided information on the sources of recharge and the movement and age of ground water in the study area.

Dissolved-solids concentrations in many parts of the basin are low (less than 500 mg/L), and generally decrease with increasing depth and with increasing distance from the forebays. The chemical composition of most water grades from calcium-bicarbonate/sulfate to sodium-bicarbonate with increasing residence time in the aquifer system. Near the coast, several wells yielded sodium-chloride water high in dissolved solids.

Stable-isotope data reveal a distinct composition for natural recharge from the San Fernando Valley (about −47 per mil δD), San Gabriel Valley (about −55 δD per mil), and locally along the coastal plain and surrounding hills (greater than −43 per mil δD). Stable-isotope data suggest that recharge to several wells located in and downgradient from the Montebello Forebay and near the seawater-barrier projects is attributable to a significant proportion of imported

water. Generally, these wells also contain water with tritium greater than 8 TU, indicating that recharge occurred within the last 50 years.

Water with less than measurable tritium is found in and downgradient from the Los Angeles Forebay and in most wells in the West Coast Basin, indicating an age for recharge exceeding 50 years. For these wells, uncorrected estimates of age from carbon-14 measurements show that water in the West Coast Basin (56 pmc; 9,500 years before present) is much older than water in the Central Basin (28 pmc; 3,900 years before present).

The ground-water simulation model was developed to integrate the information on the geohydrology and the ground-water flow system, quantify the three-dimensional ground-water budget, test alternative geohydrologic hypotheses about the basin, and assess the hydraulic effects of alternative ground-water-management scenarios. Development of the model required defining of boundary conditions, delineating aquifer elevations and hydraulic properties, compiling pumpage, spreading, and injection rates, and estimating areal recharge. The four-layer MODFLOW model was run for a steady-state simulation to approximate conditions in 1971 and for a transient simulation for the period 1971–2000. The model is generally effective in reproducing the spatial and temporal dynamics of the regional ground-water flow system over the simulation period. Specific areas where water levels or vertical gradients are not well reproduced by the model and important model assumptions and limitations were identified. Sensitivity of model results to hydraulic parameters and to the assumed conditions along the Orange County boundary were quantified.

The model was used to analyze the three-dimensional ground-water budget. The model simulates large flows of water from the Montebello Forebay and relatively small flows across the NIU. The model simulates average 1971–2000 net inflow to the West Coast Basin of about 7,000 acre-ft/yr from the ocean (San Pedro and Santa Monica Bay). The model simulates average 1971-2000 net inflow to the Central Basin of about 6,000 acre-ft/yr through the Los Angeles Narrows, 24,000 acre-ft/yr through the

Whittier Narrows, and 8,000 acre-ft/yr from Orange County. The historical transient simulation indicates that there has been a net increase in ground-water storage throughout the study area from 1971-2000. There has been a net decrease in storage in the last five years of the simulation (1996–2000).

Particle tracking was applied to simulate advective transport of water from the spreading grounds, from offshore, and from injection wells. The particle tracking from the spreading grounds yielded results that were consistent with tritium-based estimates of ground-water travel times from the Montebello Forebay if it was assumed that most transport within the Upper San Pedro aquifer system occurs within about 20 percent of the total aquifer thickness. This particle tracking indicates that most of the spread water reaches the Upper San Pedro aquifer system (model layer 3). The particle tracking of water from the coastline provides estimates of average advective velocities of landward flow. Particle tracking of injection water indicates that nearly all injected water has moved inland, providing recharge to the West Coast Basin.

The simulation model also was used to evaluate two alternative future (2001–2025) ground-water-management scenarios for the Central and West Coast Basins. Scenario 1 assumes continued pumping at average current rates; scenario 2 assumes that pumpage at most wells in the Central Basin will increase by 25 percent over the management period. For scenario 1, water levels are generally constant or slightly increasing throughout the management period. For scenario 2, water levels decline by 25 to 50 ft in the Central Basin. If flows from Orange County are fixed in the model, simulated water-level declines in the Central Basin for scenario 2 are larger.

A final application of the simulation model was to link it with an optimization algorithm to identify efficient strategies for hydraulic control of seawater intrusion. Future scenario 1 was assumed for background conditions for the base case. The optimization analysis considered the tradeoffs between increased injection and increased in-lieu delivery for maintaining hydraulic barriers to seawater intrusion. Given the current cost structure (the cost for injection water is more than three times that of in-lieu water), the optimization solution is to put all resources into purchase of additional in-lieu water. Preferential locations for in-lieu delivery near the Dominguez Gap Barrier Project were identified.

Several sensitivity analyses were conducted with the optimization model. The sensitivity of the solution to the water-level constraints was tested by modifying the required lower bound on average water levels at control locations. As the required average water level was increased from 0 to 5 to 10 ft, the costs increased nonlinearly. The sensitivity of the solution to the cost structure also was tested by varying the relative costs of injection versus in-lieu water. When the cost of injection water relative to in-lieu water decreases below about 2, the solution shifts to injection water. Changing the assumed Orange County boundary condition did not affect the optimization results. Changing the assumed future conditions from scenario 1 to scenario 2 resulted in a slight increase in in-lieu delivery.

REFERENCES CITED

Aguado, E. and Remson, I., 1974, Groundwater hydraulics in aquifer management: Journal of Hydraulics Division, American Society of Civil Engineers, v. 100 (HY1), p. 103–118.

Ahfeld, D.P. and Mulligan, A.E., 2000, Optimal management of flow in groundwater systems: San Diego, Academic Press, 185 p.

Bawden, G.W., Thatcher, Wayne, Stein, R.S., Hudnut, K.W., and Peltzer, Gilles, 2001, Tectonic contraction across Los Angeles after removal of groundwater pumping effects, Nature, p. 812–815.

Berner, R.A., 1981, A new geochemical classification of sedimentary environments: Journal of Sedimentary Petrology, v. 51, no. 2, p. 359–365.

Biddle, K.T., 1991, The Los Angeles Basin: An overview, in Biddle, K.T., ed., Active margin basins, AAPG Memoir 52: Tulsa, Oklahoma, American Association of Petroleum Geologists, p. 5–24.

Blake, G.H., 1991, Review of the neogene biostratigraphy and stratigraphy of the Los Angeles Basin and implications for basin evolution, in Biddle, K.T., ed., Active margin basins, AAPG Memoir 52: Tulsa, Oklahoma, American Association of Petroleum Geologists, p. 135–184.

Bredehoeft, J.D., and Young, R.A., 1970, The temporal allocation of groundwater: A simulation approach: Water Resources Research, v. 6, no. 1, p. 3–21.

California Department of Health Services, 1998, California Drinking Water Data: Statewide Drinking-Water Monitoring Database.

California Department of Water Resources, 1961, Planned utilization of the ground water basins of the coastal plain of Los Angeles Country, Appendix A, Ground water geology: California Department of Water Resources Bulletin 104, 191 p.

_____ 1962, Planned utilization of the ground water basins of the coastal plain of Los Angeles Country, Appendix B, Safe yield determinations: California Department of Water Resources Bulletin 104, 129 p.

_____ 1966, Planned utilization of the ground water basins of the coastal plain of Los Angeles Country, Appendix C, Operation and economics: California Department of Water Resources Bulletin 104, 435 p.

California Division of Water Resources, 1934, South coastal basin investigation, Geology and ground water storage capacity of valley fill: Bulletin 45, 279 p.

Chang, A.H-D., Halhal, D., Naji, A., and Ouazar, D., 2000, Pumping optimization in saltwater-intruded coastal aquifers: Water Resources Research, v. 36, no.8, p. 2155–2165.

Clark, I.D., Fritz, P., 1997, Environmental isotopes in hydrogeology: New York, Lewis Publishers, 328 p.

Craig, H., 1961, Isotopic variations in meteoric waters: Science, v. 133, p. 1702–1703.

D'Agnese, F.A., Faunt, C.C., Turner, A.K., and Hill, M.C., 1997, Hydrogeologic Evaluation and numerical simulation of the Death Valley Regional Ground-Water Flow System, Nevada and California: U.S. Department of the Interior Geological Survey: Water-Resources Investigations Report 96-4300, 131 p.

Danskin. W.R., and Freckleton, J.R., 1992, Ground-water flow modeling and optimization techniques applied to high ground-water problems in San Bernardino, California: in S. Subitzky, ed., Selected papers in hydrologic sciences: U.S. Geological Survey Water-Supply Paper 2340, p. 165–177.

Davis, T.L., Namson, J., and Yerkes, R.F., 1989, A cross section of the Los Angeles area: seismically active fold and thrust belt, the 1987 Whittier Narrows earthquake and earthquake hazard: Journal of Geophysical Research, v. 94, no. B7, p. 9644–9664.

Deninger, R.A., 1970, Systems analysis of water supply systems: Water Resources Bulletin, v. 6, no. 4, p. 573–579.

Drever, J.I., 1988, The geochemistry of natural waters (2d ed): New Jersey, Prentice Hall, 327 p.

Emch, P.G., and Yeh, W. W-G, 1998, Management model for conjunctive use of coastal surface water and ground water: Journal of Water Resources Planning and Management, v. 124, no. 3, p. 129–139.

Fontes, J.C., 1985, Some considerations on ground water dating using environmental isotopes: Memoires of the 18th Congress of the International Association of Hydrogeologists: Cambridge, p. 118-154.

Gat, J.R., and Gonfiantini, R., 1981, Stable isotope hydrology—Deuterium and oxygen-18 in the water cycle: International Atomic Energy Agency, Vienna, 337 p.

Golden Software, 1999, Surfer 7 User's Guide: Golden Colo., Golden Software, Inc., 619 p.

Gonfiantini, R., 1984, Advisory group meeting on stable isotope reference samples for geochemical and hydrological investigations, Vienna, September 19–21, 1983. Report to the Director General: Vienna, International Atomic Energy Agency, 77 p.

Gordon, Ekaterina, Shamir, Uri, and Bensabat, Jacob, 2001, Optimal extraction of water from regional aquifer under salinization: Journal of Water Resources Planning and Management, v. 127, no. 2, p. 71–77.

Gorelick, S.M., 1983, A review of distributed parameter groundwater management modeling methods: Water Resources Research, v. 19, no, 2, p. 305–319.

Greenwald, R.M. 1998, Modman4.0, Windows-based preprocessor: Freehold, NJ., HIS Geotrans, 125 p.

Harbaugh, A.W., and McDonald, M.G., 1996, User's documentation for MODFLOW-96, an update to the U.S. Geological Survey Modular Finite-Difference Ground-Water Flow Model: U.S. Geological Survey Open-File Report 96-485, 56 p.

Harding, T.P., 1973, Newport-Inglewood trend, California–an example of wrenching style of deformation: American Association of Petroleum Geologists Bulletin, v. 57, no. 1, p. 97–116.

Hecker, S., Kendrick, K.J., Ponti, D.J., and Hamilton, J.C., 1998, Cigital fault and fold map and database for southern California: Phase 1—Faults of the Long Beach 30' X 60' quadrangle: U.S. Geological Survey Open-file Report 98-129, 300p. plus plates.

Hem, J.D., 1992, Study and interpretation of the chemical characteristics of natural water [4th ed.]: U.S. Geological Survey Water-Supply Paper 2254, 264 p.

Hevesi, J.A., Flint, A.L., and Istok, J.D., 1991, Precipitation estimation in mountain terrains using multivariate geostatistics: II. Isohyetal maps: Journal of Applied Meteorology, v. 31, no. 7., p. 677−688.

Hill, M.L., 1971, Newport-Inglewood zone and Mesozoic subduction: Geological Society of America Bulletin, v. 82, no. 10, p. 2957–2962.

Hsieh, P.A., and Freckleton, J.R., 1993, Documentation of a computer program to simulate horizontal-flow barriers using the U.S. Geological Survey's modular three-dimensional finite difference ground-water flow model: U.S. Geological Survey Open-File Report 92-477, 32 p.

Izbicki, J.A., 1991, Chloride sources in a California coastal aquifer: American Society of Civil Engineers, IR Div/ASCE, Proceedings, p. 7177.

Izbicki, J.A., 1996, Source, movement, and age of ground water in a coastal California aquifer: U.S. Geological Survey Fact Sheet FS 126-96, 4 p.

Izbicki, J.A., Danskin, W.R., and Mendez, G.O., 1998, Chemistry and isotopic composition of ground water along a section near the Newmark area, San Bernadino County, California: U.S. Geological Survey Water-Resources Investigations Report 97-4179, 27 p.

Kendall, C., and McDonnell, J.J., 1998, Isotope tracers in catchment hydrology: Amsterdam, Elsevier, 839 p.

Knobel, L.L., Chapelle, F.H., and Meisler, Harold, 1988, Geochemistry of the northern Atlantic Coastal Plain Aquifer System: U.S. Geological Survey Professional Paper 1404-L, 57 p.

Land, Michael, Everett, R.R., and Crawford, S.M., 2002, Geologic, hydrologic, and water-quality data from multiple-well monitoring sites in the Central and West Coast Basins, Los Angeles, County, California, 1995–2000: U.S. Geological Survey Open-File Report 01-277, 178 p.

Leake, S.A., and Prudic, D.E., 1988, Documentation of a computer program to simulate aquifer-system compaction using the modular finite-difference ground-water flow model: U.S. Geological Survey Open-File Report 88-482, 80 p.

Leenheer, J.A., Rostad, C.E., Barber, L.B., Schroeder, R.A., Anders, Robert, and Davisson, M.L., 2001, Nature and chlorine activity reactivity of organic constituents from reclaimed water in groundwater, Los Angeles County, California: Environmental Science and Technology, v. 35, p. 3869–2876.

Los Angeles County Department of Public Works, 1998, Hydrologic Report 1996-1997, Los Angeles County Department of Public Works, Hydraulic/Water Conservation Division, 8 p.

Maddock. T., III, 1972, Algebraic technological function from a simulation model: Water Resources Research, v. 8, no. 1, p. 129–134.

Maidment, D., and Djokic, D., 2000, Hydrologic and hydraulic modeling support with Geographic Information Systems: ESRI Press, Redlands California, 216 p.

Maxey, G.B., and Eakin, T.E., 1949, Ground water in White River Valley, White Pine, NYE, and Lincoln Counties, Nevada: State of Nevada Office of the State Engineer, in cooperation with the U.S. Department of the Interior Geological Survey.

Mazor, Emmanuel, 1991, Applied chemical and isotopic groundwater hydrology: Buckingham, U.K., Open University Press, 274 p.

McDonald, M.G., and Harbaugh, A.W., 1988, A modular three-dimensional finite-difference ground-water flow model: U.S. Geological Survey Techniques of Water-Resources Investigations, book 6, chap. A1, 586 p.

Mendenhall, W.D., 1905a, Development of underground waters in the eastern coastal plain region of southern California: U.S. Geological Survey Water Supply Paper 137, 140 p.

_____1905b, Development of underground waters in the central coastal plain region of southern California: U.S. Geological Survey Water Supply Paper 138, 162 p.

_____1905c, Development of underground waters in the western coastal plain region of southern California: U.S. Geological Survey Water Supply Paper 139, 103 p.

Michel, R.L., 1989, Tritium deposition in the continental United States, 1953-1989: U.S. Geological Survey Water-Resources Investigations Report 89-4072, 46 p.

Michel, R.L., and Schroeder, R.A., 1994, Use of long-term tritium records from the Colorado River to determine timescales for hydrologic processes associated with irrigation in the Imperial Valley, California: Applied Geochemistry, v. 9, p. 387–401.

Miller, G. A., 1977, Appraisal of the Water Resources of Death Valley, California-Nevada: U.S. Department of the Interior Geological Survey, in cooperation with the National Park Service, Open-File Report 77-728.

Montgomery Watson, 1993, Summary of subsurface water supplies to the West Coast Basin: Pasadena, Calif., Montgomery Watson, 7 p.

Nishikawa, Tracy, 1998, Water resources optimization model for Santa Barbara, California: Journal of Water Resources Planning and Management, v. 124, no. 5, p. 252–263.

Piper, A.M., 1944, A graphic procedure in the geochemical interpretation of water analyses: American Geophysical Union Transactions, v. 25, p. 914–923.

Piper, A.M., and Garrett, A.A., 1953, Native and contaminated ground waters in the Long Beach–Santa Ana Area, California: U.S. Geological Survey Water-Supply Paper 1136, 320 p.

Poland, J.F., Garrett, A.A., and Sinnot, A., 1959, Geology, hydrology, and chemical character of ground waters in the Torrance-Santa Monica area, California: U.S. Geological Survey Water Supply Paper 1461, 425 p.

Poland, J.F., Piper, A.M., and others, 1956, Ground water geology of the coastal zone, Long Beach–Santa Ana area, California: U.S. Geological Survey Water-Supply Paper 1109, 162 p.

Pollock, D.W., 1994, User's guide for modpath/modpath-plot, version 3: a particle tracking post-processing package for modflow, the U.S. Geological Survey finite difference ground-water flow model: U.S. Geological Survey Open-File Report 94-464.

Ponti, D.J., 1989, Aminostratigraphy and chronostratigraphy of Pleistocene marine sediments, southwestern Los Angeles basin, California: University of Colorado, unpublished Ph.D. thesis, 409 p.

Pratt, T.L., Dolan, J.F., Odun, K.K., Stephenson, W.J., Williams, R.A., and Templeton, M.E., 1998, Multiscale seismic imaging of active fault zones for hazard assessment: A case study of the Santa Monica Fault Zone, Los Angeles, California: Geophysics, v. 63, no. 2, p. 479–489.

Reichard, E.G., 1995, Groundwater-surface water management with stochastic surface water supplies: A simulation-optimization approach: Water Resources Research, v. 31, no. 11, p. 2845–2865.

Schrage, Linus, 1993, User's manual for linear, integer, and quadratic programming with LINDO, Release 5.3: Danvers, Mass., Boyd and Fraser Publishing Company, 132 p.

Schrage, Linus, 1997, Optimization modeling with LINDO, Fifth Edition: Pacific Grove, Calif., Brooks/Cole Publishing Company, 470 p.

Schroeder, R.A., Rivera, M.R., Redfield, B.J., Densmore, J.N., Michel, R.L., Norton, D.R., Audet, D.J., Setmire, J.G., and Goodbread, S.L., 1993, Physical, chemical, and biological data for detailed study of irrigation drainage in the Salton Sea area, 1988–90: U.S. Geological Survey Open-file Report 93-83.

Schroeder, R.A., Anders, R., Bohlke, J.K., Michel, R.L., and Metge, D.W., 1997, Water quality at production wells near artificial-recharge basins in Montebello Forebay, Los Angeles County, in Kendall, D.R., ed., Conjunctive use of water resources: Aquifer storage and recovery: Proceedings, American Water Resources Association, October 1997, p. 273–284.

Shamir, Uri, Bear, Jacob, and Gamliel, Amir, 1984, Optimal operation of a coastal aquifer: Water Resources Research, v. 20, no. 4, p. 435–444.

Tinsley, J.C. and Fumal, T.E., 1985, Mapping Quarternary sedimentary deposits for areal variations in shaking response, in Ziony,m J.I. (ed.), Evaluating earthquake hazards in the Los Angeles Region—An earth science perspective: U. S. Geological Survey Professional Paper 1360, p. 101–125.

U.S. Environmental Protection Agency, 1996, Drinking water regulations and health advisories: U.S. Environmental Protection Agency, Office of Water, EPA 822-R-96-001, 11 p.

Wagner, B.J., 1995, Recent advances in simulation-optimization groundwater management modeling: Reviews of Geophysics, Supplement, 33, p. 1021–1028.

Water Replenishment District of Southern California, 2000, Regional groundwater monitoring report Water Year 1998–99: Cerritos, Calif., 123 p. total.

Williams, A.E., and Rodini, D.P., 1997, Regional isotopic effects and application to hydrologic investigations in southwestern California: Water Resources Research, v. 33, no. 7, p. 1721–1729.

Willis, Robert., and Finney, B.A., 1988, Planning model for optimal control of seawater intrusion: Journal of Water Resources Planning and Management, v. 114, no. 2, p. 163–178.

Woodring, W.P., Bramlette, M.N., and Kew, W.S.W., 1946, Geology and paleontology of Palos Verdes Hills, California: U.S. Geological Survey Professional Paper 207, 145 p.

Wright, T.L., 1991, Structural geology and tectonic evolution of the Los Angeles Basin, California, in Biddle, K.T., ed., Active margin basins, AAPG Memoir 52: Tulsa, Oklahoma, American Association of Petroleum Geologists, p. 35–134.

Yeats, R.S., 1973, Newport-Inglewood fault zone, Los Angeles Basin, California: American Association of Petroleum Geologists Bulletin, v. 57, no. 1, p. 117–135.

Yeh, W. W-G., 1992, Systems analysis in ground-water planning and management: Journal of Water Resources Planning and Management, v. 118, no. 3, p. 224–237.

Yerkes, R.F., McCulloh, T.H., Schoellhamer, J.E., and Vedder, J.G., 1965, Geology of the Los Angeles basin, California—An Introduction: U.S. Geological Survey Professional Paper 420-A, 57 p.

Zielbaur, A.E., Kues, H.A., Burnham, W.L., and Keene, A.G., 1962, Coastal basins barrier and replenishment investigation: Dominguez Gap Barrier Project geologic investigation: Los Angeles County Flood Control District, 29 p.

APPENDIXES

The GIS contains spatial data layers, databases, and other data files. Spatial data layers consist of COVERAGEs (points, lines, or polygons), GRIDs (raster data), and TINs (triangulated irregular network) created with ESRI's (Environmental Systems Research Institute) ArcGIS 8.1 and ArcView 3.2 software. Databases are maintained using Microsoft Access 2000, along with other data files stored in Microsoft Excel, dbase and in INFO tables. The current platforms used include UNIX and NT servers, and Windows 2000 workstations. Metadata for the spatial data layers are documented to Federal Geographic Data Center (FGDC) standards, easily searchable by extent, keyword, or other parameters.

The GIS structure consists of spatial data files related to tabular data files by common items. For example, a State well number from the wells coverage can be related to a set of water-quality records from the water- quality Access database. Databases are linked, sharing tables.

All the spatial data layers in the GIS are projected in the Universal Transverse Mercator (UTM) projection, zone 11, using the North American Datum of 1927 (NAD27). The UTM projection was chosen because a single UTM zone encompasses the entire study area, and because all distances, directions, shapes, and areas are reasonably accurate within that zone. The units of the projection are in meters. The coordinates of the spatial layers are stored as single-precision values that allow as many as seven significant digits for each coordinate. Because of the distance from the equator north to the study area, the Y-direction coordinates are large (over 3 million). To maintain the positional integrity of the spatial layers, a value of 3.5 million meters was subtracted from all Y coordinates during the projection process.

Data files and spatial layers for this study were acquired and created in a variety of ways from public sources. Data files were created from ASCII files imported into an INFO database within ArcInfo or directly into Access. Several coverage-creation methods were used—including transforming page coordinates to projected coordinates from DXF files, importing ArcInfo coverages, and digitizing from paper or Mylar maps. In the case of wells or other point coverages, latitude and longitude were the primary location reference items. Where latitude and longitude were absent, the State well identification number was used as an estimate to plot wells within 1/8 mile using the Public Land Survey System (PLSS).

The spatial data layers in the GIS for this study include cultural, hydrologic, and geologic features. Cultural features include city centers, roads, and land use/land cover. Hydrologic features include wells, precipitation stations, and streams. Geologic features include faults, folds, and geology.

An essential component of the GIS, for the geohydrologic and geochemical analysis described in this report, is well information. Specific well data include water levels, water quality, pumpage, and injection. Almost all well files were created from existing digital data, spreadsheets, or other applications from cooperators, and USGS measurements. In addition to well information, streamflow and precipitation data also were compiled.

Appendix II. Well identification, Model Layer, and Aquifer-Systems information for U.S. Geological Survey Multiple-well Monitoring Sites, Los Angeles, California

[Location of sites shown in figure 2*A*; state well Nos., see well-numbering diagram in text; Model Layer, see section on "Development of ground-water simulation model" in text and fig. 3; Aquifer Systems, see section on "Geochemical analysis in text and fig. 3; well depth and perforated interval, in feet below land surface; —, not included in model]

State well No.	Local designation	Well depth	Perforated interval	Model layer	Aquifer systems
4S/13W-9H9	Carson-1 #1	1,010	990–1,010	3	Lower
4S/13W-9H10	Carson-1 #2	760	740–760	3	Lower
4S/13W-9H11	Carson-1 #3	480	460–480	3	Lower
4S/13W-9H12	Carson-1 #4	270	250–270	2	Lower
4S/11W-5P9	Cerritos-1 #1	1,215	1,155–1,175	4	Lower
4S/11W-5P10	Cerritos-1 #2	1,020	1,000–1,020	4	Lower
4S/11W-5P11	Cerritos-1 #3	630	610–630	3	Lower
4S/11W-5P12	Cerritos-1 #4	290	270–290	3	Lower
4S/11W-5P13	Cerritos-1 #5	200	180–200	2	Upper
4S/11W-5P14	Cerritos-1 #6	135	125–135	2	Upper
2S/12W-7J1	Commerce-1 #1	1,390	1,330–1,390	—	Pico Unit
2S/12W-7J2	Commerce-1 #2	960	940–960	4	Lower
2S/12W-7J3	Commerce-1 #3	780	760–780	4	Lower
2S/12W-7J4	Commerce-1 #4	590	570–590	3	Lower
2S/12W-7J5	Commerce-1 #5	345	325–345	3	Lower
2S/12W-7J6	Commerce-1 #6	225	205–225	2	Upper
3S/12W-9J1	Downey-1 #1	1,190	1,170–1,190	3	Lower
3S/12W-9J2	Downey-1 #2	960	940– 960	3	Lower
3S/12W-9J3	Downey-1 #3	600	580–600	3	Lower
3S/12W-9J4	Downey-1 #4	390	370–390	2	Upper
3S/12W-9J5	Downey-1 #5	270	250–270	2	Upper
3S/12W-9J6	Downey-1 #6	110	90–110	1	Upper
3S/14W-13J5	Gardena-1 #1	990	970–990	4	Lower
3S/14W-13J6	Gardena-1 #2	465	445–465	3	Lower
3S/14W-13J7	Gardena-1 #3	365	345–365	3	Lower
3S/14W-13J8	Gardena-1 #4	140	120–140	2	Upper
3S/14W-17G3	Hawthorne-1 #1	990	910– 950	—	Pico Unit
3S/14W-17G4	Hawthorne-1 #2	730	710–730	4	Lower
3S/14W-17G5	Hawthorne-1 #3	540	520–540	3	Lower
3S/14W-17G6	Hawthorne-1 #4	420	400–420	3	Lower

Appendix II. Well identification, Model Layer, and Aquifer-Systems information for U.S. Geological Survey Multiple-well Monitoring Sites, Los Angeles, California—Continued

State well No.	Local designation	Well depth	Perforated interval	Model layer	Aquifer systems
3S/14W-17G7	Hawthorne-1 #5	260	240–260	2	Upper
3S/14W-17G8	Hawthorne-1 #6	130	110–130	2	Upper
2S/13W-22C1	Huntington Park-1 #1	910	890–910	3	Lower
2S/13W-22C2	Huntington Park-1 #2	710	690–710	3	Lower
2S/13W-22C3	Huntington Park-1 #3	440	420–440	3	Lower
2S/13W-22C4	Huntington Park-1 #4	295	275–295	2	Upper
2S/13W-22C5	Huntington Park-1 #5	134	114–134	1	Upper
2S/14W-28M3	Inglewood-1 #1	1,400	1,380–1,400	—	Pico Unit
2S/14W-28M4	Inglewood-1 #2	885	865–885	—	Pico Unit
2S/14W-28M5	Inglewood-1 #3	450	430–450	3	Lower
2S/14W-28M6	Inglewood-1 #4	300	280–300	3	Lower
2S/14W-28M7	Inglewood-1 #5	170	150–170	2	Upper
2S/14W-26N3	Inglewood-2 #1	860	800–840	—	Pico Unit
2S/14W-26N4	Inglewood-2 #2	470	450–470	—	Pico Unit
2S/14W-26N5	Inglewood-2 #3	350	330–350	3	Lower
2S/14W-26N6	Inglewood-2 #4	245	225–245	3	Lower
3S/11W-26E2	La Mirada-1 #1	1,150	1,130–1,150	4	Lower
3S/11W-26E3	La Mirada-1 #2	985	965–985	4	Lower
3S/11W-26E4	La Mirada-1 #3	710	690–710	3	Lower
3S/11W-26E5	La Mirada-1 #4	490	470–490	3	Lower
3S/11W-26E6	La Mirada-1 #5	245	225–245	2	Upper
4S/12W-05H5	Lakewood-1 #1	1,009	989–1,009	4	Lower
4S/12W-5H6	Lakewood-1 #2	660	640– 660	3	Lower
4S/12W-5H7	Lakewood-1 #3	470	450–470	3	Lower
4S/12W-5H8	Lakewood-1 #4	300	280–300	2	Upper
4S/12W-5H9	Lakewood-1 #5	160	140–160	2	Upper
4S/12W-5H1	Lakewood-1 #6	90	70–90	1	Upper
4S/14W-26A2	Lomita-1 #1	1,340	1,240–1,260	4	Lower
4S/14W-26A3	Lomita-1 #2	720	700–720	3	Lower
4S/14W-26A4	Lomita-1 #3	570	550–570	3	Lower
4S/14W-26A5	Lomita-1 #4	420	400–420	3	Lower

State well No.	Local designation	Well depth	Perforated interval	Model layer	Aquifer systems
4S/14W-26A6	Lomita-1 #5	240	220–240	2	Upper
4S/14W-26A7	Lomita-1 #6	120	100–120	2	Upper
4S/12W-25G1	Long Beach-1 #1	1,470	1,430–1,450	4	Lower
4S/12W-25G2	Long Beach-1 #2	1,250	1,230–1,250	4	Lower
4S/12W-25G3	Long Beach-1 #3	990	970–990	3	Lower
4S/12W-25G4	Long Beach-1 #4	619	599–619	3	Lower
4S/12W-25G5	Long Beach-1 #5	420	400–420	3	Lower
4S/12W-25G6	Long Beach-1 #6	175	155–175	2	Upper
4S/13W-1N3	Long Beach-2 #1	1,090	970–990	—	Pico Unit
4S/13W-1N4	Long Beach-2 #2	740	720–740	4	Lower
4S/13W-1N5	Long Beach-2 #3	470	450–470	3	Lower
4S/13W-1N6	Long Beach-2 #4	300	280–300	3	Lower
4S/13W-1N7	Long Beach-2 #5	180	160–180	2	Upper
4S/13W-1N8	Long Beach-2 #6	115	95–115	2	Upper
2S/13W-17F1	Los Angeles-1 #1	1,370	1,350–1,370	4	Lower
2S/13W-17F2	Los Angeles-1 #2	1,100	1,080–1,100	3	Lower
2S/13W-17F3	Los Angeles-1 #3	940	920–940	3	Lower
2S/13W-17F4	Los Angeles-1 #4	660	640–660	3	Lower
2S/13W-17F5	Los Angeles-1 #5	370	350–370	3	Lower
2S/11W-18C4	Pico Rivera-1 #1	900	860–900	—	Pico Unit
2S/11W-18C5	Pico Rivera-1 #2	480	460–480	4	Lower
2S/11W-18C6	Pico Rivera-1 #3	400	380–400	3	Lower
2S/11W-18C7	Pico Rivera-1 #4	190	170–190	3	Lower
2S/12W-25G3	Pico Rivera-2 #1	1,200	1,180–1,200	4	Lower
2S/12W-25G4	Pico Rivera-2 #2	850	830–850	3	Lower
2S/12W-25G5	Pico Rivera-2 #3	580	560–580	3	Lower
2S/12W-25G6	Pico Rivera-2 #4	340	320–340	3	Lower
2S/12W-25G7	Pico Rivera-2 #5	255	235–255	2	Upper
2S/12W-25G8	Pico Rivera-2 #6	120	100-120	1	Upper
2S/12W-26D9	Rio Hondo-1 #1	1,150	1,110-1,130	4	Lower
2S/12W-26D10	Rio Hondo-1 #2	930	910–930	3	Lower

Appendix II. Well identification, Model Layer, and Aquifer-Systems information for U.S. Geological Survey Multiple-well Monitoring Sites, Los Angeles, California—Continued

State well No.	Local designation	Well depth	Perforated interval	Model layer	Aquifer systems
2S/12W-26D11	Rio Hondo-1 #3	730	710–730	3	Lower
2S/12W-26D12	Rio Hondo-1 #4	450	430–450	3	Lower
2S/12W-26D13	Rio Hondo-1 #5	300	280–300	2	Upper
2S/12W-26D14	Rio Hondo-1 #6	160	140–160	1	Upper
3S/11W-9D1	Santa Fe Springs-1 #1	1,410	1,290–1,310	—	Pico Unit
3S/11W-9D2	Santa Fe Springs-1 #2	845	825–845	4	Lower
3S/11W-9D3	Santa Fe Springs-1 #3	560	540–560	3	Lower
3S/11W-9D4	Santa Fe Springs-1 #4	285	265–285	3	Lower
3S/12W-6B4	South Gate-1 #1	1,460	1,440–1,460	4	Lower
3S/12W-6B5	South Gate-1 #2	1,340	1,320–1,340	3	Lower
3S/12W-6B6	South Gate-1 #3	930	910–930	3	Lower
3S/12W-6B7	South Gate-1 #4	585	565–585	3	Lower
3S/12W-6B8	South Gate-1 #5	250	220–240	2	Upper
3S/11W-2K4	Whittier-1 #1	1,280	1,180–1,200	3	Lower
3S/11W-2K5	Whittier-1 #2	940	920–940	3	Lower
3S/11W-2K8	Whittier-1 #3	620	600–620	3	Lower
3S/11W-2K6	Whittier-1 #4	470	450–470	3	Lower
3S/11W-2K7	Whittier-1 #5	220	200–220	2	Upper
3S/13W-8J1	Willowbrook-1 #1	905	885–905	4	Lower
3S/13W-8J2	Willowbrook-1 #2	520	500–520	3	Lower
3S/13W-8J3	Willowbrook-1 #3	380	360–380	3	Lower
3S/13W-8J4	Willowbrook-1 #4	220	200–220	2	Upper
4S/13W-28A3	Wilmington-1 #1	1,035	915–935	4	Lower
4S/13W-28A4	Wilmington-1 #2	800	780–800	4	Lower
4S/13W-28A5	Wilmington-1 #3	570	550–570	3	Lower
4S/13W-28A6	Wilmington-1 #4	245	225–245	3	Lower
4S/13W-28A7	Wilmington-1 #5	140	120–140	2	Upper
4S/13W-32F1	Wilmington-2 #1	1,030	950–970	4	Lower
4S/13W-32F2	Wilmington-2 #2	775	755–775	3	Lower
4S/13W-32F3	Wilmington-2 #3	560	540–560	3	Lower
4S/13W-32F4	Wilmington-2 #4	410	390–410	3	Lower
4S/13W-32F5	Wilmington-2 #5	140	120–140	2	Upper

Appendix III. Correlation between Specific Conductance and Dissolved-Solids Concentration

Dissolved-solids concentrations (DSC), commonly referred to as total dissolved solids (TDS), is a measure of the total amount of dissolved ions in a water, and give an indication as to the overall quality of water. TDS concentrations are commonly determined by weighing the residue of a known volume of water following evaporation at 180 degrees Celsius.

Dissolved-solids concentrations discussed in this report are calculated values, computed by summing all major (Ca, Mg, Na, Cl, SO_4, alk, Si) and minor (K, Fe, Mn, Sr, B, F, NO_3) constituents. For a few samples (for which a complete chemical analysis was not available), dissolved solids concentrations were estimated from measurements of specific conductance taken in the field.

The relation between TDS and specific conductance (SC) is nearly linear, but the slope of this line varies according to the chemical composition of a particular water (Hem, 1992). The regression of dissolved-solids and specific-conductance measurements taken as part of this study yield a slope of 0.59 with a correlation coefficient of 0.99 ($r^2 = 0.99$). This is similar to the slope computed during earlier work in the basin (Piper and Garrett, 1953).

Appendix IV. Parameters used to generate model layer elevation surfaces

[NA, not applicable; nugget effect and sill are expressed in terms of variance of elevation (feet squared); correlation length is expressed in terms of X–Y space measured in UTM coordinates (meters); anisotropy, expressed as a ratio of variability between two axes; the angle is measured from the positive x-axis to the first axis; nested spherical model requires specification two values for both sill and correlation length; the gridding program, Surfer 7 (Golden Software, 1999) was used to generate the surfaces]

Layer	Aquifer system	Function type used	Description of model used	Nugget effect (in feet squared)	Sill (in feet squared)	Correlation length (meters)	Slope	Anisotropy
1	Recent	Radial basis function interpolation	Multiquadratic kernal	NA	NA	NA	NA	No
2	Lakewood	Block kriging	Nested spherical models with nugget	2,000	8,000 7,000	10,000 24,000	NA	No
3	Upper San Pedro	Block kriging	Gaussian model with nugget	16,200	66,200	5,000	NA	Yes[1]
4	Lower San Pedro	Block kriging	Linear model with nugget	37,400	NA	NA	8.03	No

[1]1.238 ratio at 178.2 degrees

The areas contributing to mountain-front recharge range in elevation from sea level to 2,100 ft with a mean of about 560 ft. The active onshore model area averages about 170 feet in comparison. The specific geographic areas are the Santa Monica Mountains and Elysian Hills to the north, the Repetto Hills, Merced Hills and Puente Hills to the northeast, and the Palos Verdes Hills to the southwest (fig. 1 in Appendix V).

Contributing watersheds were delineated for the entire basin using a 30-meter USGS digital elevation model (DEM) and various ArcInfo hydrologic functions. Delineation steps included clipping the DEM to the study area; filling in the DEM sinks (imperfections in the DEM); creating a flow direction model to determine the steepest down-slope direction of flow; creating a flow accumulation model to find areas where water congregates, such as in a stream course; and creating a stream network to simulate possible stream locations. These steps are standard hydrologic functions performed in ArcInfo for delineating a watershed (Maidment and Djokic, 2000).

Once the individual watersheds were delineated for the entire study area, the domain of the ground-water model was overlaid to clip out the areas that extend beyond the model. Areas already accounted for with head-dependent boundary conditions at the Los Angeles Narrows, the Whittier Narrows, and the Orange County boundary were excluded. The watersheds were labeled according to the zone of the ground-water model into which the water flowed (fig. 1 in Appendix V). The areas of these contributing watersheds are given in table 1 in Appendix V.

A precipitation grid was then constructed using a precipitation station database compiled by the Los Angeles County Department of Public Works. Water-year totals were computed and the stations geo-referenced. Only precipitation stations that were located in the basin model area and the surrounding mountains were used.

Three surface-extrapolation methods were considered for producing the precipitation-grid surface in ArcInfo: inverse distance weighting (IDW), kriging, and a simple regression model. IDW and kriging both weight the data on the basis of their spatial relation to one another. Therefore, with the sparse precipitation data in the mountains, a biased grid reflecting the precipitation amounts of the basin floor would be

created. To illustrate this point, precipitation values in the Puente Hills were more closely related to values in the Santa Monica Mountains 30 mi away than they were to precipitation values on the basin floor 3 mi away. More advanced kriging algorithms, such as co-kriging, may be able to compensate for this and could be considered in the future.

The simple method chosen for this application was regression. The regression method is based on the assumption that as altitude increases, precipitation increases (Hevesi and others, 1991). An equation can be derived that correlates precipitation with elevation. Different equations were tested in fitting the data, including exponential and logarithmic functions. A simple linear regression produced the highest R-squared value and therefore was used (fig. 2 in Appendix V).

By using a clipped USGS 30-meter DEM and applying the regression on a cell-by-cell basis, a precipitation grid was interpolated using a cell size of 100 m (328 ft). The results for water year 1971 are included in table 1 in Appendix V.

Mountain-front recharge for 1970–71 was estimated from this precipitation grid by applying simple percentages of precipitation. In a report on ground water in the Great Basin area of Nevada, Maxey and Eakin (1949) estimated the following percentages to apply for recharge estimation: 0 percent for less than 8 in., 3 percent for 8 to 10 in., 7 percent for 10 to 12 in., 15 percent for 12 to 15 in., and 25 percent for greater than 15 in. By applying the percentages to each cell in the precipitation grid, a recharge grid was produced. Average recharge per watershed can be calculated by using ArcInfo zonal functions. Results are given in table 1 in Appendix V.

The resulting estimated values of mountain-front recharge shown in the last column of the table were applied to represent steady state (1970–71) mountain-front recharge in the model. These values are considered to be reasonable estimates, but there are many limitations to this simple approach that was developed for recharge in the Great Basin (Miller, 1977), especially when applied to a different physiographic area. D'Agnese and others (1997) summarized some important limitations of the Maxey-Eakin method, including the fact that the method does not considering important factors such as slope aspect, interbasin flow, permeabilities of different deposits, soil moisture, and vegetation differences.
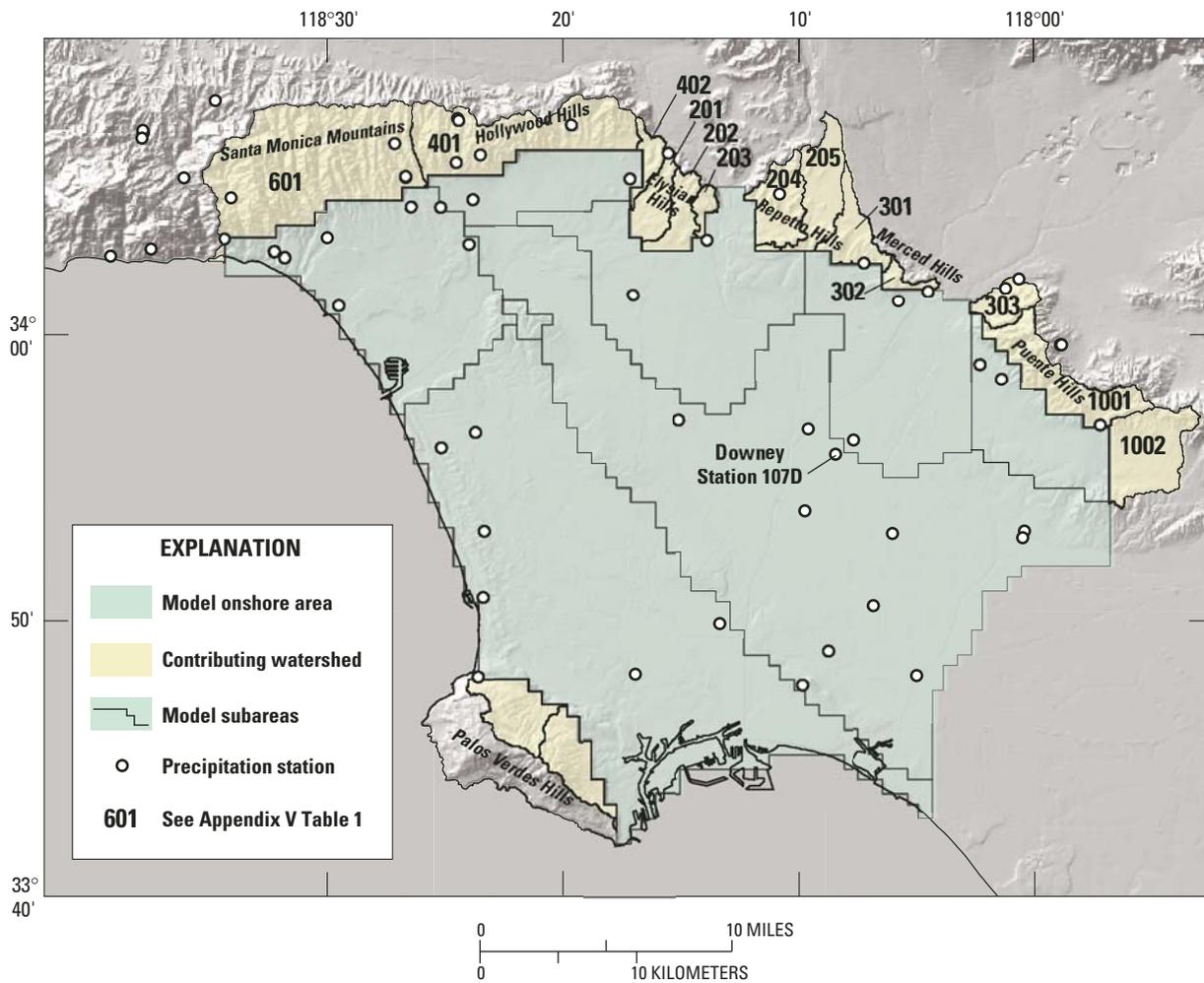
Appendix V Figure 1.Location of precipitation stations and contributing watersheds used for estimating recharge, Los Angeles County, California.

Appendix V, Table 1. Estimated mountain front recharge for water year 1971

Model zone	Contributing watershed	Area of watersheds (meters squared)	Average precipitation, in inches	Recharge. in acre feet
Los Angeles Forebay	201	10,280,000	13.6	440
	202	9,380,000	13.9	440
	203	3,160,000	14.6	170
	204	15,550,000	14.6	840
	205	18,560,000	14.8	1,050
Montebello Forebay	301	11,660,000	14.2	540
	302	2,990,000	13.9	130
	303	8,310,000	13.9	430
Hollywood Basin	401	46,870,000	17.4	4,050
	402	4,870,000	14.4	250
West Coast Basin	501	15,920,000	16.2	1170
	502	15,250,000	15.5	1000
Santa Monica Basin	601	86,800,000	19.3	8,540
Whittier Area	1001	25,960,000	16.5	2,080
	1002	25,620,000	14.4	1,350
TOTAL		**308,660,000**		**22,470**
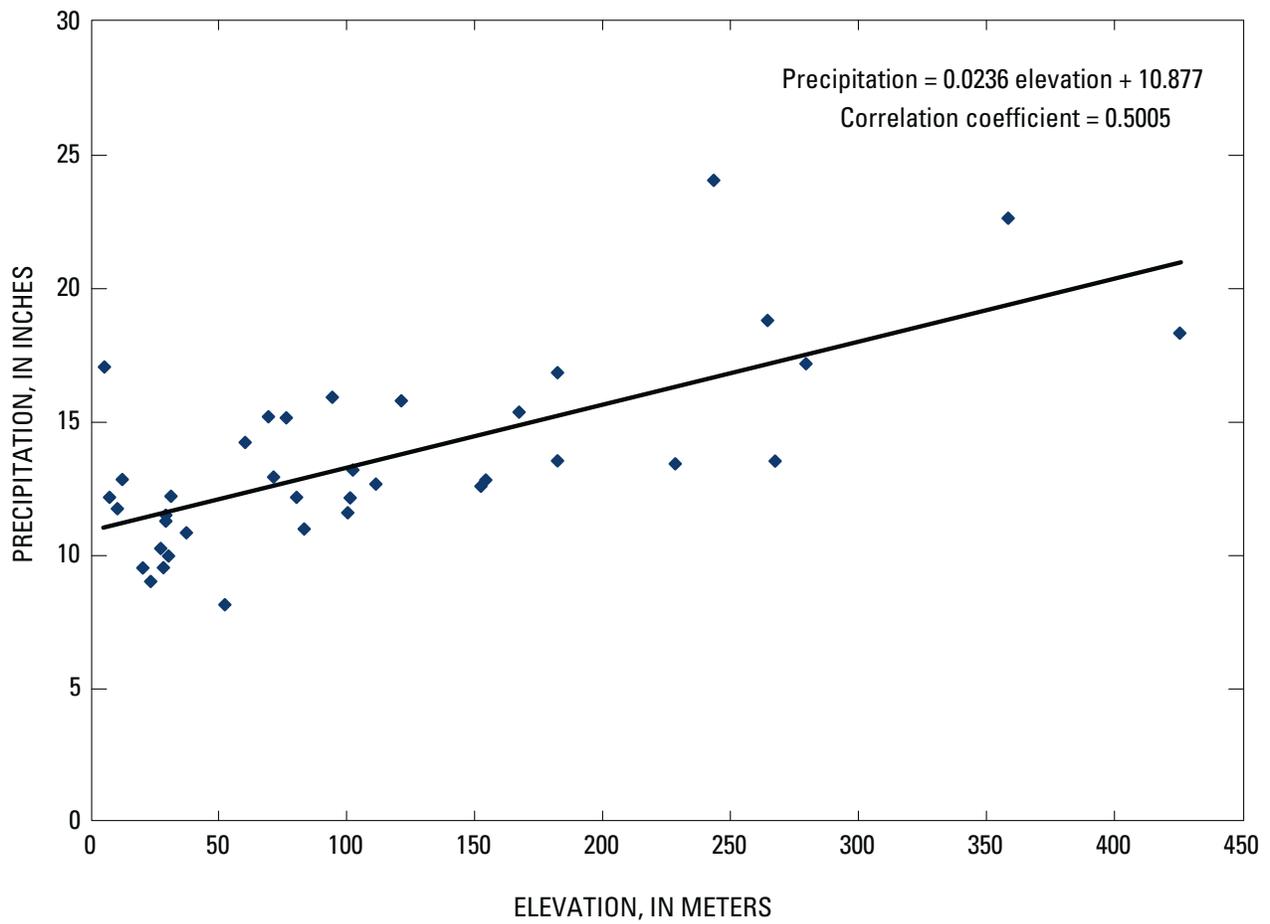
Appendix V Figure 2.Correlation between precipitation and elevation, 1970–71, Los Angeles County, California.

EXPLANATION FOR APPENDIX VI HYDROGRAPHS
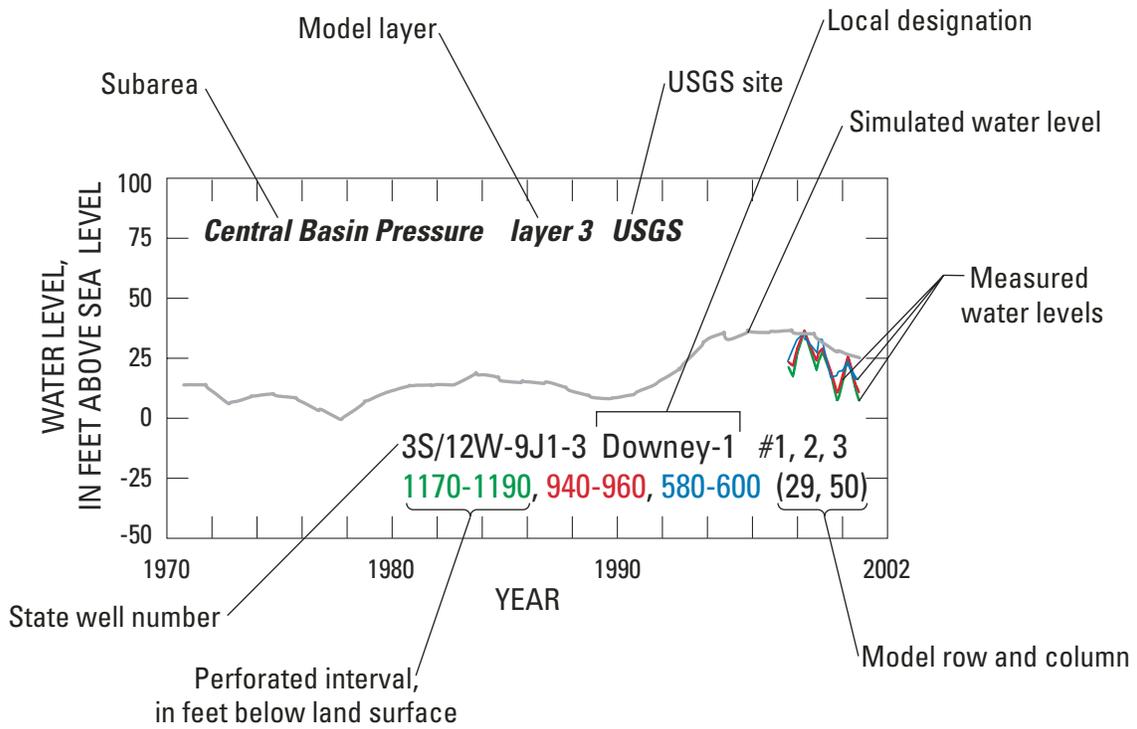
Locations of wells are shown on figure 23

YEAR

WATER LEVEL, IN FEET ABOVE SEA LEVEL

Montebello Forebay   layer 1   USGS

2S/12W-25G8 Pico Rivera-2 #6
100-120 (29, 50)

Montebello Forebay   layer 2   USGS

2S/12W-25G7 Pico Rivera-2 #5
235-255 (29, 50)

Montebello Forebay   layer 1   USGS

2S/12W-26D14 Rio Hondo-1 #6
140-160 (35, 65)

Montebello Forebay   layer 2   USGS

2S/12W-26D13 Rio Hondo-1 #5
280-300 (22, 52)

Montebello Forebay   layer 1

2S/12W-14J1 1590F
35-71 (19, 54)

Montebello Forebay   layer 2

2S/12W-24MO3   1601P/T
154-174 (21, 55)

Montebello Forebay   layer 1

2S/12W-33L3   1554F
80-119   (25, 49)

Montebello Forebay   layer 3   USGS

2S/11W-18C6   Pico Rivera-1 #3
380-400   (18, 57)

Montebello Forebay   layer 2   USGS

2S/11W-18C7   Pico Rivera-1 #4
170-190   (18, 57)

Montebello Forebay   layer 3   USGS

2S/12W-25G4-6   Pico Rivera-2 #2, 3, 4
830-850, 560-580, 320-340   (29, 50)

YEAR

Central Basin Pressure   layer 2   USGS

3S/12W-26E6 La Mirada-1 #5
225-245 (35, 65)

Central Basin Pressure   layer 2   USGS

4S/12W-5H8, 9 Lakewood-1 #4, 5
280-300, 140-160 (38, 48)

Central Basin Pressure   layer 2   USGS

3S/12W-6B8 South Gate-1 #5
220-240 (26, 45)

Central Basin Pressure   layer 2   USGS

4S/12W-25G5-14 Long Beach-1 #6
155-175 (46, 55)

Central Basin Pressure   layer 2   USGS

3S/12W-9J4, 5 Downey-1 #4, 5
370-390, 250-270 (29, 50)

Central Basin Pressure   layer 2   USGS

4S/13W-1N7,8 Long Beach-2 #5, 6
160-180, 95-115 (39, 42)

Central Basin Pressure   layer 2   USGS

3S/13W-8J4 Willowbrook-1 #4
200-220 (29, 36)

Central Basin Pressure   layer 2

3S/12W-8L3 1537A
126-176, 221-236 (30, 49)

Central Basin Pressure   layer 2 USGS

4S/11W-5P13,14 Cerritos-1 #5, 6
180-200, 125-135 (39, 59)

Central Basin Pressure   layer 3 USGS

2S/14W-26N5,6 Inglewood-2 #3, 4
330-350, 225- 245 (23, 29)

WATER LEVEL, IN FEET ABOVE SEA LEVEL

YEAR

YEAR

Central Basin Pressure   layer 3   USGS

3S/11W-26E4, 5   La Mirada-1 #3, 4
690-710, 470- 490 (35, 65)

Central Basin Pressure   layer 3   USGS

4S/12W-5H6, 7 Lakewood-1 #2, 3
640-660, 450-470 (38, 48)

Central Basin Pressure   layer 3   USGS

3S/12W-6B5-7   South Gate-1 #2, 3, 4
1,320-1,340, 910-930, 565-585 (26, 45)

Central Basin Pressure   layer 3   USGS

4S/12W-25G3-5 Long Beach-1   #3, 4, 5
970-990, 599-619, 400-420 (46, 55)

Central Basin Pressure   layer 3   USGS

3S/12W-9J1-3 Downey-1   #1, 2, 3
1,170-1,190, 940-960, 580-600 (29, 50)

Central Basin Pressure   layer 3   USGS

4S/13W-01N5,6 Long Beach-2   #3, 4
450-470, 280-300 (39, 42)

Central Basin Pressure   layer 3   USGS

3S/13W-8J2, 3 Willowbrook-1   #2, 3
500-520, 360-380 (29, 36)

Central Basin Pressure   layer 3

2S/13W-32C4   1434J
604-785 (24, 35)

Central Basin Pressure   layer 3   USGS

4S/11W-5P11,12 Cerritos-1   #3, 4
610-630, 270-290 (39, 59)

Central Basin Pressure   layer 3

2S/14W-22P4   1362P
285-322 (21, 27)

WATER LEVEL, IN FEET ABOVE SEA LEVEL

YEAR

YEAR

YEAR

WATER LEVEL, IN FEET ABOVE SEA LEVEL

Central Basin Pressure layer 4 USGS

4S/12W-5H5 Lakewood-1 #1
989-1,019 (38, 48)

Central Basin Pressure layer 4

4S/12W-25E1 500D
1,124-1,146 (46, 54)

Central Basin Pressure layer 4 USGS

4S/12W-25G1,2 Long Beach-1 #1, 2
1,430-1,450, 1,230-1,250 (46, 55)

West Coast Basin layer 2

4S/12W-32G1 441
120-130 (48, 48)

Central Basin Pressure layer 4 USGS

4S/13W 1N4 Long Beach-2 #2
720-740 (39, 42)

West Coast Basin layer 2 USGS

2S/14W-28M7 Inglewood-1 #5
150-170 (23, 25)

Central Basin Pressure layer 4

2S/13W-36F2 1504C
978-1,276 (24, 43)

West Coast Basin layer 2 USGS

3S/14W-13J8 Gardena-1 #4
120-140 (31, 32)

Central Basin Pressure layer 4

2S/14W-14F2 1380
(19, 29)

West Coast Basin layer 2 USGS

3S/14W-17G7, 8 Hawthorne-1 #5, 6
240-260, 110-130 (30, 24)

YEAR

YEAR

WATER LEVEL, IN FEET ABOVE SEA LEVEL

West Coast Basin   layer 3 USGS

3S/14W-17G5, 6 Hawthorne-1 #3, 4
520-540, 400-420 (30, 24)

West Coast Basin   layer 3

3S/14W-22L1 760C
352-458 (33, 27)

West Coast Basin   layer 3 USGS

4S/13W-9H9-11 Carson-1 #1, 2, 3
990-1,010, 740-760, 460-480 (40, 38)

West Coast Basin   layer 3

4S/13W-21H5 868H
440-709 (44, 38)

West Coast Basin   layer 3 USGS

4S/13W-28A5, 6 Wilmington-1 #3, 4
550-570, 225-245 (46, 37)

West Coast Basin   layer 3

4S/13W-23B2 888F
650-900 (43, 41)

West Coast Basin   layer 3 USGS

4S/13W-32F2-4 Wilmington-2 #2, 3, 4
755-775, 540-560, 390-410 (48, 35)

West Coast Basin   layer 3

4S/14W-01F2 794B
477-540 (38, 31)

West Coast Basin   layer 3 USGS

4S/14W-26A2-4 Lomita-1 #2, 3, 4
700-720, 550-570, 400-420 (45, 29)

West Coast Basin layer 3

4S/14W-2N1, 2 PM-3 Madrid #1, 2
640-680, 480-520 (40, 28)

YEAR   YEAR

West Coast Basin   layer 3

4S/14W-4K PM-4 Mariner #1, 2, 3
670-710, 500-540, 340-380 (39, 24)

West Coast Basin   layer 4 USGS

4S/13W-32F1 Wilmington-2 #1
950-970 (48, 35)

West Coast Basin   layer 3

4S/14W-9Q1 746
241-395 (41, 25)

West Coast Basin   layer 4 USGS

4S/14W-26A2 Lomita-1 #1
1240-1260 (45, 29)

West Coast Basin   layer 4 USGS

3S/14W-13J5 Gardena-1 #1
970-990 (31, 32)

Santa Monica layer 2

2S/15W-22E3 1251T
120-185 (20, 15)

West Coast Basin   layer 4 USGS

3S/14W-17G4 Hawthorne-1 #2
710-730 (30, 24)

Santa Monica layer 3

2S/15W-11A1 Charnock-18
103-438 (16, 17)

West Coast Basin   layer 4 USGS

4S/13W-28A3, 4 Wilmington-1 #1, 2
915-935, 780-800 (46, 37)

Santa Monica   layer 3

1S/15W-31E1SMI
151-250 (12, 8)

WATER LEVEL, IN FEET ABOVE SEA LEVEL

YEAR

YEAR

YEAR

WATER LEVEL, IN FEET ABOVE SEA LEVEL

Santa Monica   layer 3
2S/15W-4C2 SM3
210-530   (14, 13)

Boundary wells layer 3
Orange County
4S/11W-4K1
225-1020 (38, 61)
(nearest cell)

Santa Monica   layer 2
1S/15W-32 A5 ARC4
85-218 (11,13)

Boundary wells layer 3
Orange County
4S/11W-19R1, Q3
266-306, 300-700 (44, 57) (nearest cell)

Boundary wells layer 3
Orange County
5S/11W-C1, C2
548-802, 580-674 (52, 56)

Hollywood Basin   layer 3
1S/14W-20M2 1380
108-438 (9,23)

Boundary wells layer 1
Whittier Narrows
2S/11W-5L1   6M1
48-97 (16, 59)

Boundary wells layer 3
Orange County
3S/11W-35J3
373-678 (36, 66)
(nearest cell)

Boundary wells layer 1
Whittier Narrows
2S/11W-6G2 SM3
44-51   (16, 58) (nearest cell)

YEAR

YEAR

Boundary wells layer 1
LA Narrows

1S/13W-14E3
(7, 41) (nearest cell)